Predicting the Capacity of Pulse Piles

Anton Dmitriev

Submitted in accordance with the requirements for the degree of
Doctor of Philosophy

The University of Leeds
School of Civil Engineering

September 2018

The candidate confirms that the work submitted is his own and that appropriate credit has been given where reference has been made to the work of others.

Acknowledgements

First of all, I would like to thank my supervisor professor Barry Clarke for giving me the opportunity to work on the subject of this research. Only with his guidance, support and patience this thesis could have been completed.

I would like to thank Echo-Tech Ltd Moscow for their assistance with the collection of the field test results and a wealth of knowledge and expertise they were sharing with me over the years.

I wish to acknowledge the help provided by Ivor King Ltd with my research and training.

Finally, I am very grateful to my parents, brothers, family and friends, for their support and encouragement throughout my study.

Abstract

Pulse piles have been successfully used in geotechnical construction for last 25 years. This type of mini piles has proved to be very useful on the restricted access sites and provide a cost effective solution in comparison to the conventional piling techniques.

The shockwave created by an electric arc discharge in wet grout reaching the walls of a borehole provides enough pressure to create local failure of the ground surrounding the point of discharge. This phenomenon known as Electrohydraulic effect applied along the shaft of a pile increases the diameter of a pre-bored hole, changes shape of pile-soil interface and improves shaft friction and end-bearing of the resultant pulse pile.

The design approach is based on calculation of shaft friction and end bearing of the bored pile using empirical coefficients obtained from the load testing. Pulse discharge technology has been used in Russia and South Korea, therefore additional work was required to provide theoretical basis for design procedure in accordance with Eurocodes and British Standards.

This research focuses on prediction of capacity of a pulse pile in coarse and fine grained soils. A finite element 2D axisymmetric model was developed to simulate construction sequence of a bored pile in Plaxis software. The calculated settlement from a vertical load applied at the top of pile has been compared to the results of semi-empirical calculations of pile performance. Full-scale field test results were used to validate methodology of both calculation methods.

Table of Contents

List of Tables

List of Figures

List of Symbols

γ_b	partial resistance base factor
γ_s	partial resistance shaft factor
ε	available dynamic soil densification
η	coefficient of mechanical action of an explosive
μ	empirical coefficient
ρ_0	density of liquid
c_0	acoustic wave speed in liquid
C	electric capacitance
CFA	continuous flight auger [piling method]
D	density of soil
d_0	initial diameter of borehole
$d(n)$	diameter of the borehole after discharges impact
e	porosity
E	energy of one discharge
g	pressure
k	empirical coefficient
K_p	efficiency of discharge
n	number of discharges
$N_{ев}$	specific energy per unit weight of the explosive
P	pressure on the front of a shockwave in a discharge
P_0	isotropic pressure of a gas-vapor cavity
P^{max}	maximum pressure at the surface of system mortar - soil
$p(x)$	pressure in the soil at a distance x from the borehole wall
p_0	pressure on the borehole wall
PDT	pulse discharge technology
R_0	initial radius of the well
R_u^i	radius of the well expansion after i-th discharge
$R_{Пmax}$	maximum radius of the gas bubble
$u(l)$	radial displacement of the borehole wall from a single discharge
V	voltage
W	energy
W_n	effective discharge energy
K_0	coefficient of lateral earth pressure
φ'	angle of friction
OCR	overconsolidation ratio
E'	stiffness modulus
γ	unit weight

v	poisson's ratio
c_u	undrained shear strength
D^e	elastic material stiffness matrix
$\underline{\varepsilon}^e$	elastic strain rate
$\underline{\dot{\sigma}}'$	stress rate
τ	shear strength
σ	normal stress
σ_1	major principle stress
σ_3	minor principle stress
$\dot{\varepsilon}^p$	plastic strain
$g(\sigma)$	plastic potential function
λ	scalar multiplier
ψ	dilatancy angle
FEM	finite element method
E_{50}	secant stiffness modulus depending on σ_3
E_{oed}	tangent stiffness modulus depending on σ_1
E_{ur}	unloading/reloading stiffness modulus depending on σ_3
m	power for stress- level dependency of stiffness
c'_{ref}	effective cohesion
γ^{ps}	state parameter that defines the opening of the cone
p_p	state parameter that remembers the position of the cap
p^{ref}	reference stress
G_0	initial shear modulus
$\gamma_{0.7}$	the shear strain level at 70% of G_0
e	current void ratio
e_{max}	maximum void ratio
e_{min}	minimum void ratio
RD	relative density
I_p	plasticity index
P	applied load
U_s	ultimate shaft friction
Δ_s	settlement at the top of the pile
K_s	inverse function of ultimate shaft friction
U_B	ultimate base load
M_S	flexibility factor
r_m	radius at which soil deflections become negligible
r_c	pile radius
E_B	modulus of the soil under the tip of the pile
q	applied base pressure

f_1	standard settlement reduction factor
P_T	total load
Q_p	ultimate resistance of a pile
Q_b	ultimate resistance of the base
Q_s	ultimate resistance of the shaft
W_p	weight of the pile
A_b	base area
A_s	shaft area of layer i
q_b	unit base resistance
q_s	unit shaft resistance
δ_i	effective interface angle of friction
$K_{s;i}$	earth pressure coefficient
$\sigma'_{v;i}$	average vertical effective stress of soil layer i
σ'_{vb}	vertical effective stress at pile base level
N_q	empirical bearing capacity factor
N_c	bearing capacity factor
$RMSE$	root mean square error
$\Delta_{T,Fleming,i}$	settlement from i-th applied load calculated by Fleming't method
$\Delta_{T,Plaxis,i}$	settlement from i-th applied load calculated using Plaxis
γ_{cF}	shaft capacity factor
γ_{cR}	end bearing capacity factor

Chapter 1
Introduction

1.1 Overview

Pulse Discharge Technology (PDT) is a technique that can be used to increase the radius of a bored pile over a defined length using a series of high voltage electric discharges in a wet concrete in a preformed borehole. The electric discharge effectively expands the cavity formed during installation of the pile creating an increased surface area and consolidating/compacting soil around the pile. PDT in geotechnical construction is known only in Russia and South Korea. Its effectiveness has been confirmed by numerous successful projects.

1.1 Pulse Discharge Technology

PDT is an electro hydraulic effect in which electric energy created by an electric arc discharge is converted to mechanical energy. The discharge vaporizes the liquid creating a shockwave which applies pressure to the surrounding soil causing the borehole to expand. It has been known for more than 60 years and successfully applied in mechanical engineering, metal forming, mining, rock defragmentation, chemical industry, and the agro-industrial sector. Application of the electro-hydraulic effect in construction became possible with development of appropriate PDT by researchers and construction companies in Russia. PDT is a series of explosive pulses in a concrete liquid mortar using an electrical discharge. Electrical energy is converted into mechanical energy through the formation of high-pressure gas vapor. As a result, the preformed hole is forced to expand and the soils around the borehole compact if granular or consolidate if cohesive (see Figure 1-1).

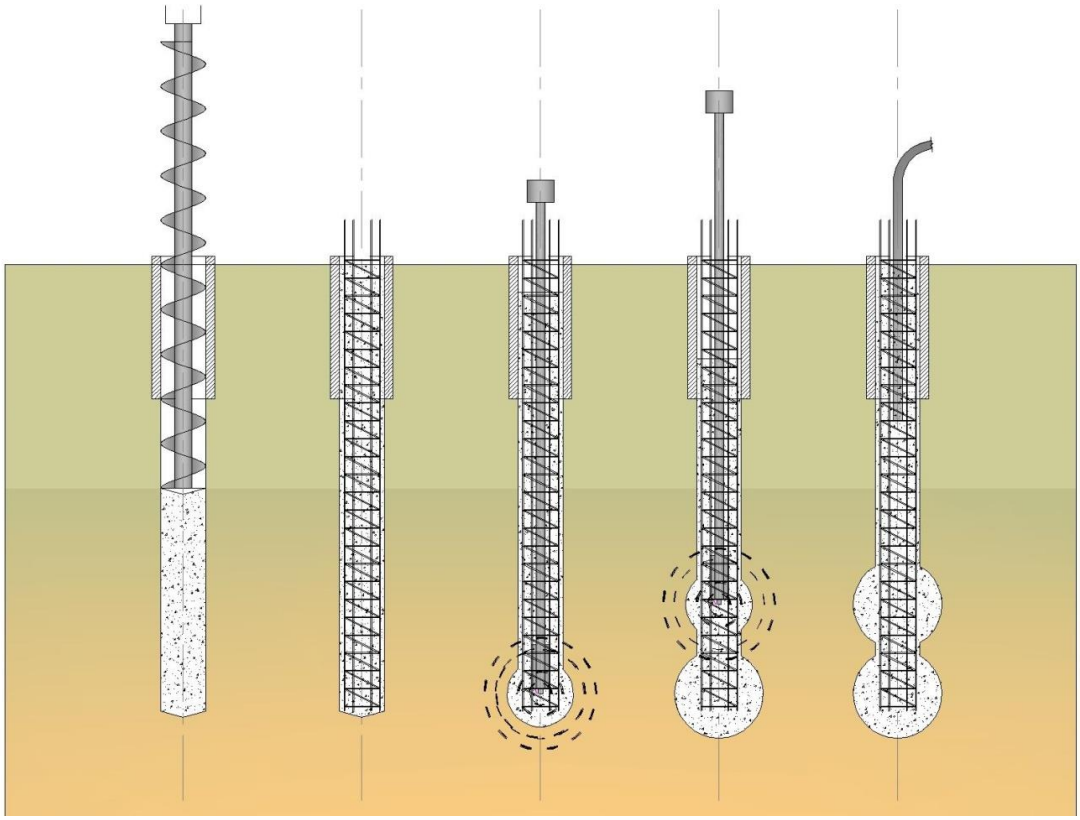

Figure 1-1 – PDT construction sequence: (a) Create a mortar filled borehole; (b) insert casing; (c) insert probe to create an electric discharge at the base of the pile; (d) withdraw probe to create a second discharge; (e) withdraw the probe and allow the mortar to set

1.1.1 Application of PDT

In 1960‘s Soviet scientists Gilman & Lomize (1962) started their research into soil densification using the electro-hydraulic effect. The electro-spark method had been used during the construction of Hydro Power Plants in Saratov and Kiev. At the same time the technology of under reaming by detonation of explosives at a pile toe to increase the load capacity was being developed. However, explosives are dangerous, require a special permit, can be performed just once for a pile and have low reliability due to failed detonations. Thus, another solution to increase pile capacity was required.

In 1978-1981, in the Soviet Union, the electro-hydraulic effect was developed to compact surrounding soils and increase a pile shaft diameter. In 1990’s, in Moscow and S.-Petersburg, several private companies started using the PDT with bored piles. Some of them still exist and have developed PDT for different soil conditions: coarse-grained, fine-grained or fill, saturated to partially saturated; and for different

construction processes: soil reinforcement, soil grouting, production of bored and CFA piles, bored anchors and piled walls.

In 2000‘s Korean scientists Kim & Cha (2008) undertook research into PDT and means of predicting the behaviour of electric pulse technology in pile and anchor construction in their laboratories and in field tests in different soil conditions.

1.2 Major Issues Associated with PDT

A PDT pile is a form of under reamed pile such that the capacity of a bored pile can be doubled using PDT. The first series of discharges is carried out at the base of the pile creating an under ream which increases the base capacity. The probe is raised and a second series of discharges is carried out above the first thus increasing the diameter the pile which increases the shaft capacity over the length of the expanded section. This is repeated at several levels to increase the pile diameter over the required length to produce the overall increase in capacity. This will depend on the soil type and density, degree of saturation, the concrete composition, the pile geometry and the electric discharge. An electric discharge is a function of electric capacitance, voltage, current, inter-electrode gap, resistance of circuit, time of pulse and inductance.

1.2.1 Health and Safety Regulations

There are a number of health and safety issues specific to PDT because of the voltages involved. The generator should be as close to the pile as possible to restrict the area affected by the process. This area is prohibited to all personal other than those operating the PDT. There has to be least two people experienced in PDT on site.

1.2.2 Engineering Calculation Approach

Predicting the capacity of a pile treated by PDT is difficult because the final diameter is unknown. There is no known relationship between the electric discharge and the soil conditions and the final geometry of the pile will depend on the positions of the discharge. For example, a discharge near the base of a pile will, in effect, create an under reamed pile; the diameter of the under ream being a function of the discharge and soil conditions. It is also possible to increase the diameter of the shaft by setting off the discharge at different levels in the pile. This will create a non-uniform pile diameter, which means there will be a component of increase of end bearing and friction along the full length of the pile. This is further compounded in layered soils.

Field trials and laboratory tests have been used to develop empirical methods of estimating capacity but the actual capacity has to be assessed by pile tests. This is expensive and time consuming.

Korean engineers Park et al. (2011) have used the ABAQUS and the UNDEX shockwave model to simulate expansion of the borehole by PDT. They have obtained good agreement between predicted and measured values of expansion in clay and sand deposits.

1.3 Aims and objectives

The following aims and the corresponding objectives have been specified for this research:

a) To review existing information in regard to the PDT to increase pile capacity (Chapter 2)
    - A critical review of literature relating to PDT including the methodology, the design process and the application (Chapter 2)
    - Identify the gaps in the knowledge and the research to be undertaken (Chapter 2)

b) Development of the finite element model of a single Pulse pile (Chapters 3 & 4)
    - To create 2D model and produce a sensitivity analysis (Chapter 3)
    - To explore Plaxis 2D software to create reference models in a range of coarse and fine grained soils (Chapter 4)
    - To find the way to simulate pulse treatment (Chapters 3 & 4)

c) Validation of the results of finite element modelling (Chapters 5 & 6)
    - To explore alternative analytical methods to predict pulse pile performance (Chapter 5)
    - To obtain field test results to compare with predicted pile capacity (Chapter 6)

Chapter 2
Literature Review

2.1 Introduction

This research analyses PDT application to pile construction, its advantages and weaknesses. This chapter reviews the historical background, the PDT process and the development of technology. The electro-hydraulic effect is triggered by an electric discharge which converts to mechanical energy causing an expansion within the soil. The principles of the electric discharge will be described and the types of energy created explained. There are a number of applications of PDT in geotechnics but this study will focus on piles, the most developed of the applications. The study will cover safety problems relevant to PDT and the impact of PDT on adjacent structures. The aim is to produce a set of design curves that will be applicable to under ream piles and enhanced shaft capacity in layered soils. The zone of influence in different soil conditions will be investigated.

2.2 Theoretical Approach

2.2.1 The electrical discharge as a source of mechanical work

Frungel (1948) showed that an electric discharge in liquid would produce mechanical work. This phenomenon was called the electro-hydraulic effect. Yutkin (1986) suggested many applications of the electro-hydraulic effect. The most common areas of electro-hydraulic application have been in the processing of solids, hydraulic punching, beading, fettling a casting, fracturing of rock to name but a few.

Figure 2-1 shows the application to hole punching.

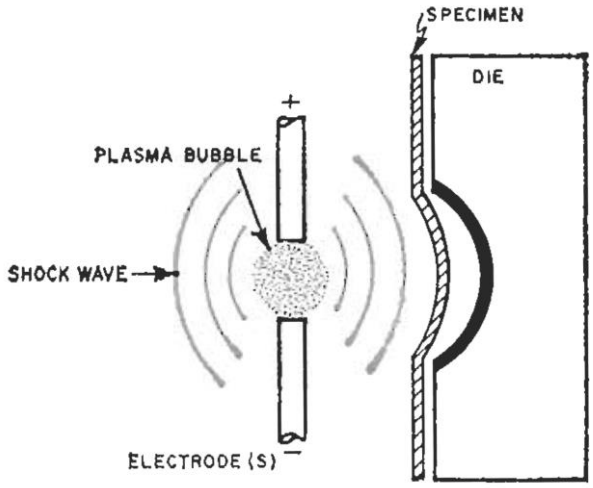

Figure 2-1 – **Application of electro-hydraulic effect (Lawrence (1969))**

The electro-hydraulic effect is a rapid means of converting electrical energy into mechanical energy through an electric discharge in a liquid medium. The energy, *W*, of the electric discharge is determined from the (1):

$$W = \frac{V^2 C}{2} \tag{1}$$

where *V* = voltage, *C* = discharge capacitance.

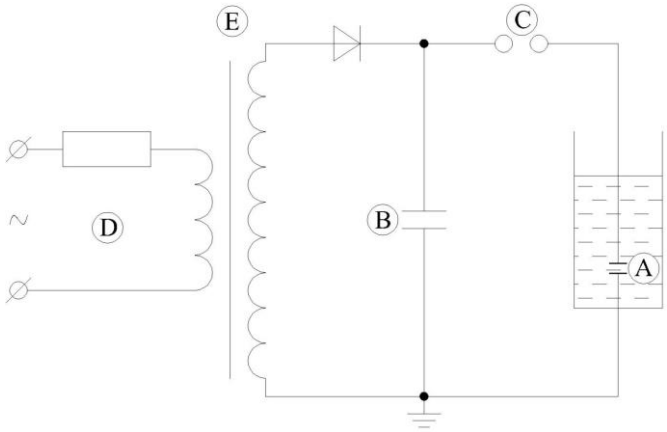

Figure 2-2 – Schematic diagram of the electric circuit used to create the electro hydraulic effect.

The electro-hydraulic effect is a result of an electric arc forming between two electrodes (A) in a liquid. Depending on electrical field strength between the electrodes thermal or leader, electrical breakdown occurs in liquid. The electrodes plasma channel has a temperature of the order of $4x10^4$ °C (Yutkin (1986)) which evaporates the liquid between the electrodes creating a gas-vapour cavity. The energy

discharge through the plasma channel transforms to a shockwave with a high pressure on a shock front. This phenomenon is described in more details in section 2.2.3.

The resistance of most liquids is normally too high to allow the electric current to flow. However, if the voltage is increased there comes a point when the electrical field strength exceeds the electrical resistance causing an electric arc to form.

Figure 2-2 shows schematic diagram of the electric circuit used to create the electro-hydraulic effect. The electrical energy is built up in a capacitor (B) using direct current. The energy release is controlled by a spark gap (C). A power source (D) generates an alternate current in the primary circuit. This creates a magnetic flux in the transformer (E) core, which, in turn, generates an alternate current in the secondary circuit at a higher voltage. A rectifier is used to convert the alternate current to a direct current, which supplies the voltage to the capacitor.

This circuit ensures a high pulse of energy to the liquid. The discharge produces a plasma channel in the liquid, which raises the temperature and pressure. A shockwave is created. The plasma channel forms within a gas cavity, which is a result of evaporation and electrolysis of the liquid. The gas cavity expands due to the pressure. This lasts microseconds. A high pressure wave of about $10^9 – 10^{10}$ Pa acts for a short time t ($t \sim 10^{-6}$ sec.) according to Samarin (2005) who conducted studies on underwater electric blasts. Such a shockwave is one of the main sources of mechanical impact on the boundary of the borehole wall in a pile. A gas-vapor cavity is formed and expanded by merging of bubbles of dissolved gases caused by the electric breakdown of the liquid between the electrodes. This cavity is a further source of mechanical stress on the borehole wall.

The energy potential of the gas-vapor cavity and the shockwave depends on the voltage, V, and capacitance, C, of the capacitor. The energy, W, stored in the capacitor is $0.5\ CV^2$ (equation 1). Varying these parameters at a constant energy, W, of the discharge results in a redistribution of energy between the gas-vapor cavity and the shockwave. In cohesive soils, a higher capacitance extends the time of treatment thus giving more time for the gas cavity to expand. In granular soils, the shockwave has more impact (Samarin (2005)). Increasing the voltage increases the shockwave.

2.2.2 Application of PDT for soil densification.

In 1960, Lomize and Gilman suggested the use of the electro-hydraulic phenomenon for soil densification. Later, in 1961, the same researchers undertook laboratory experiments to compact saturated soils using electric discharge. The research results showed a decrease in porosity of saturated sands. They investigated compaction of partially saturated sands. Experiments have shown that the porosity of partially saturated sand decreases almost by 20% Gilman & Lomize (1962).

This led Lomize and Gilman to propose a new approach to produce foundations called the electro spark soil densification method, an electro-hydraulic effect. The sequence of this method was as follows. Referring to Figure 2-2, the electrodes (A) are placed in the soil to be densified. The subsequent shockwave changes the soil structure resulting in a compaction of soil (Lomize, et al. (1963)). During 1963 and 1964, the spark method for soil densification was used on industrial construction sites in Russia.

Experimental studies of densification of saturated sandy soils and loess clayey soils using electric discharge also showed that the method was effective in these soils. It was found that the process of densification of loess soils destroys the soil structure; that is it remoulds the soils. The physical processes occurring in the soil when subject to electrical discharges were studied by Khlyupina (1967), Semushkina (1968), Gilman (1963) and Lomize et al (1963).

According to Khlyupina (1967), Gilman (1963) and others, the main cause of the destruction of the soil structure during its densification by means of electro-hydraulic effect is the effect of the shockwave. They suggested an electric discharge in sandy soil creates dynamic short-term shockwave load. The outcome of the discharge in a fluid environment is qualitatively similar to the effect of a chemical blast of explosives. The action of the gas-vapor cavity has only a minor effect on the break-down of the soil structure.

A feature of compaction of saturated sandy soils by the power of electric discharges is the possibility of direct and repeated discharge at a given point. The increase of the pulse energy leads to greater efficiency of soil densification (Figure 2-3-6). Figure 2-3 shows the variation of void ratio and density with stress created for different energy levels. Lomize & Khlyupina (1965) obtained results from a series of experiments in saturated sandy soils with an initial void ratio of 0.72. The number of pulses, *N*, was

80 and the frequency of discharges, *f*, 0.07Hz. The changes of void ratio *e* and relative density *D* at a constant energy *W* of 350 (A), 770 (B) and 1460 (C) J in relation to earth passive pressure *g* are shown on Figure 2-3. Figure 2-4 shows the variation in void ratio and density with energy for measured earth passive pressure applied to the soil around the expanding cavity (0.5kg/cm^2, 1kg/cm^2 and 1.5kg/cm^2).

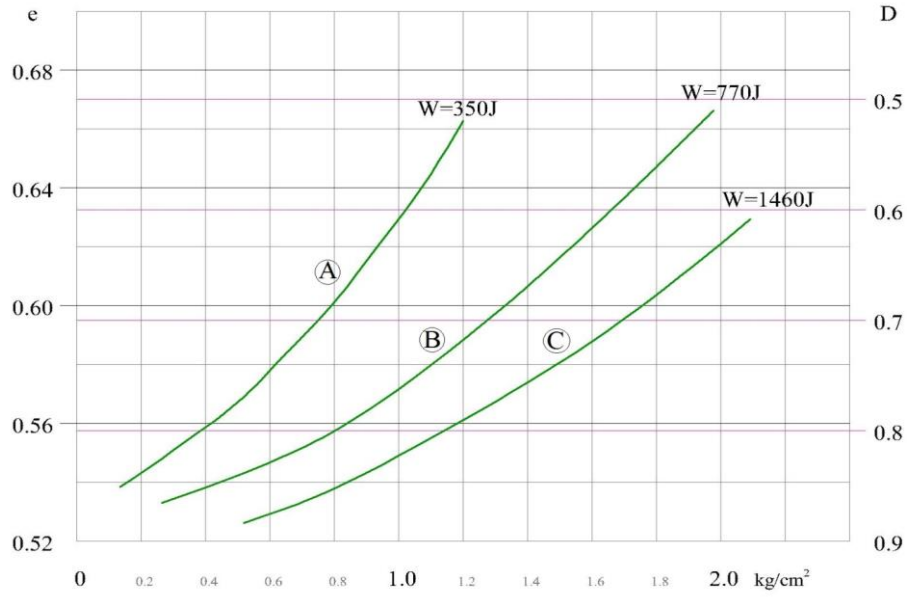

Figure 2-3 – Curves of void ratio and relative density dependent on earth passive pressure at constant discharge energy (Lomize & Khlyupina (1965))

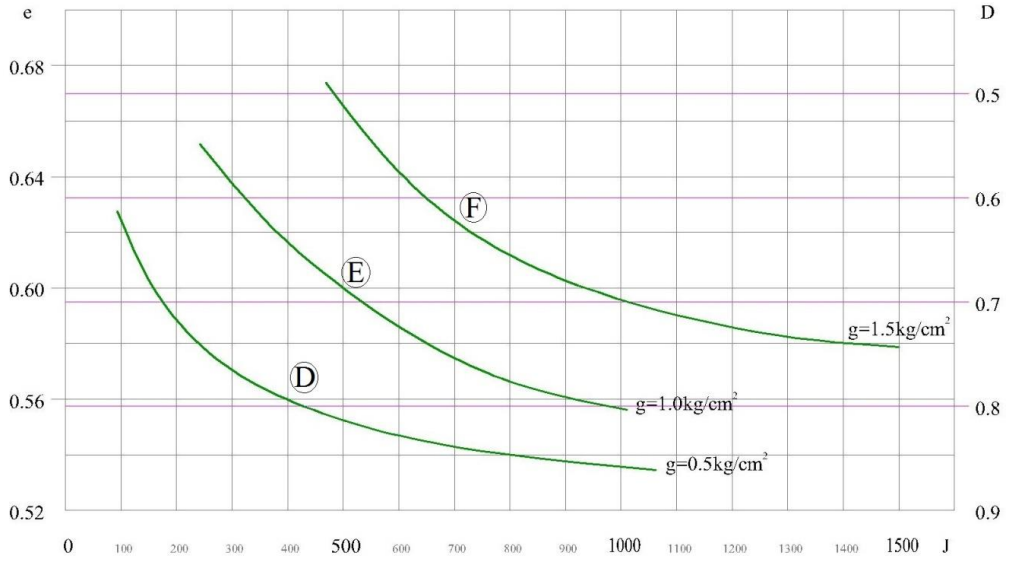

Figure 2-4 – Curves of void ratio and relative density dependent on discharge energy at constant earth passive pressure (Lomize & Khlyupina (1965))

Khlyupina (1967) proposed to evaluate the energy of the discharge, *W*, as the sum of the energy of the shockwave and the energy of radial motion of the gas-vapor cavity:

$$W = S\frac{1}{\rho_0 c_0}\int_0^{\tau} P^2\,dt + \frac{4}{3}P_0 R_{\Pi max}^3 \qquad (2)$$

where S = the area of the sphere, $\rho_0 c_0$ – shockwave (acoustic) impedance of the liquid (ρ_0 is the density; c_0 is the acoustic wave speed in the liquid) , P = the pressure on the front of a shockwave in a discharge, P_0 = isotropic pressure of a gas-vapor cavity, $R_{\Pi max}$ = the maximum radius of the gas bubble.

The contribution of the gas-vapor bubble expansion and the shockwave energy are, respectively, 20 - 30% and 70 - 80% of the energy of the discharge (Khlyupina (1967)).

The dynamic action of the electric discharge and the explosion of chemical explosives create a similar effect from the mechanical point of view. Therefore, it is possible to replace the pulse discharge with an equivalent amount of explosives and to assess the pressure, P, at the front of the shockwave caused by the discharge, using the empirical formula for the blast of chemical explosives (Lyakhov (1982))

$$P = k_1 \frac{\sqrt[3]{C^{\mu}}}{r} \qquad (3)$$

where C = the mass of explosives, k_1 and μ = empirical coefficients depending on the percentage of air in the soil.

Gilman (1963) transformed the formula for electrical discharge in saturated soil to the form:

$$\mathrm{P} = \frac{\mathrm{k}}{\mathrm{r}^{\mu}}\left(\sqrt[3]{\frac{0{,}102\mathrm{K_P CV^2}}{2\eta \mathrm{N_{вв}}}}\right)^{\mu} \qquad (4)$$

Here, k and μ are empirical coefficients (Lyakhov (1964)), η = 0,1 = coefficient of mechanical action of an explosive, $N_{вв}$ = specific energy per unit weight of the explosive, C = discharge capacitance, V = voltage, $K_p = W_n/w$ (K_p =0,3) = efficiency of discharge, W_n - the effective discharge energy allowing for energy losses, $W = CV^2/2$ = full discharge energy.

The formula relates the pressure, P, at the front of a shockwave with the energy of discharge, W, and distance r from the discharge channel.

The radius of densification can be estimated as (Lomize et al. (1963)):

$$r = \left(\frac{k}{P}\right)^{\frac{1}{\mu}} \sqrt[3]{\frac{0{,}102 K_p C U^2}{2\eta N_{\text{вв}}}} \qquad (5)$$

where P = the minimum amount of pressure that can cause damage of the soil structure.

Further development of the studies presented in the work of Lomize & Khlupina (1965), and others showed that the mechanical work of the shockwaves depends on the distance between the discharge electrodes in soil, and the ratio between the discharge voltage and capacitance at constant energy. Since $W = CV^2/2$, the same energy W can be obtained by increasing the voltage V at a constant discharge capacitance C or increasing the capacitance C at a constant voltage V. The resulting energy W in both cases will be equal. Semushkina (1968) found that when the voltage reduced at a constant discharge energy W the amount of power wasted increases. Studies by Semushkina (1968) showed that a voltage drop from 50 to 10 kV at a constant discharge energy (W = 1,5 kJ) does not create a pulsed load on the soil and, therefore, does not densify it. Hence, for a constant W the most important mechanical effect of the discharge occurs at the highest voltage. It was found (Semushkina (1968)) that discharge performance depends on the ratio of voltage and capacitance at constant energy level. Increasing the discharge capacitance when decreasing the voltage leads to a reduction of impact force.

According to Khlyupina (1967), reducing the voltage from 60 to 18 kV causes a decrease in the level of destruction of the soil structure by a factor of 1.4, and the densification effect by 1.2. Increasing the voltage on the contrary, increases the impact of the discharge since the energy released much faster. The amplitude of the pressure on the front of a shockwave and effectiveness of mechanical work of discharge increase.

Opposite results were shown by Semushkina (1968). The objectives of her experiments were to clarify the main parameters that affected the process and to develop the technology to densify saturated soils by PDT. While the efficiency of the mechanical work performed by the discharge was higher with a lower voltage, it was found (Semushkina (1968)) that more efficient mechanical work of the discharge occurs at lower amplitudes of pressure generated at the shockwave front. Furthermore,

it was shown that the mechanical work is also connected with the pressure generated by the gas-vapor cavity.

Thus, the experimental results obtained by different authors are contradictory. Some researchers consider the main effect of the mechanical work of the discharge is the shockwave; others show that the gas-vapor cavity has a significant impact on the mechanical work of the discharge. There is no consensus about the impact of the voltage and capacitance with constant energy on the form of mechanical energy (shockwave or gas vapor cavity expansion)

Field tests by Lomize et al. (1963), carried out on saturated sandy soils showed that the production of high-voltage discharges lead to the formation of a crater around the point of blast, which is then filled by water. It is suggested that the discharge increases the pore pressure to such an extent that liquefaction occurs. The soil particles settle (compact) leaving a crater at the surface. Increasing the number and energy of high-voltage discharges results in an increase in the diameter of the crater and its depth. This suggests that the location and magnitude of the discharges affects the amount and extent of the densified zone. Studying the deformation of the soil allowed the shape of densified zone to be established and therefore the design of the electrode layout to achieve the required effect.

Thus, an electrical discharge in a fluid is an effective means of mechanically compacting a soil. This leads to densification of the soil and thus enhancement of its physical-mechanical properties.

The analogy between the electrical discharge and chemical explosives in a liquid medium was used to design the pulse discharge in a concrete grout to produce piles in a densified soil by Park et al (2011). This approach is based on the method of under reaming using explosive energy of chemical explosives.

2.2.3 Theoretical premises of PDT

There are two different ways to generate electric breakdown in a liquid: thermal and leader (spark). At present, most power sets for creating pulse discharges work with voltages from 7 to 10 kV and discharge energy up to 60 kJ. With these energy parameters, an electrical discharge in a concrete grout causes a thermal breakdown between the electrodes.

The level of mechanical impact due to the effects of an electrical pulse in liquids depends on the electrical properties of the liquids and the electrical pulse: of the voltage, the distance between the electrodes, the shape of the electrodes and the time of release of current. A low voltage circuit (6-12V) is enough to obtain simple electrolysis set (Figure 2-5). Increasing the voltage up to 20-30 kV leads to thermal (Figure 2-6) and thereafter leader (Figure 2-8) electric breakdown of the liquid between the electrodes. The created plasma filled cavity that discharges the energy, creates a shockwave and causes the cavity to expand (Figure 2-6 D).

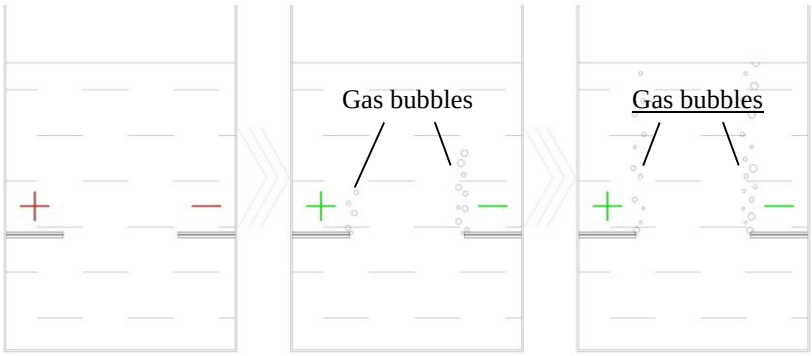

Figure 2-5 – Electrolysis of water showing the formation of gas at the electrodes which increases with time

Figure 2-5 shows the process of electrolysis in water. A low voltage of 6-12V is enough to generate oxygen from the anode and hydrogen from the cathode from the water. These form bubbles rising from the electrodes.

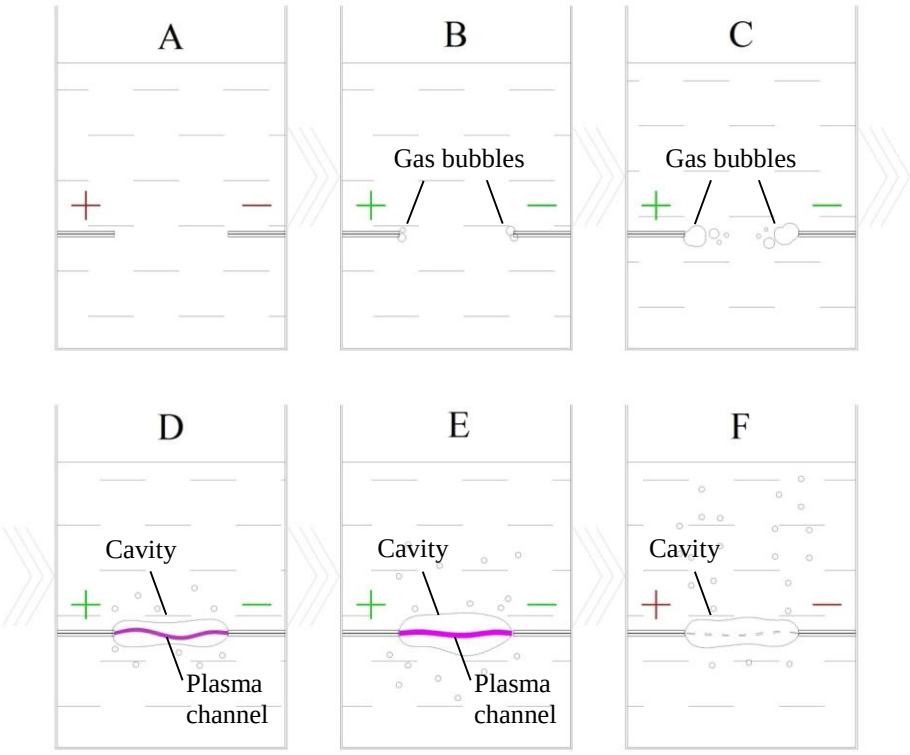

Figure 2-6 – Thermal electric breakdown in water showing the formation of a gas filled cavity: (A) – current off; (B) – current on: formation of gas bubbles; (C) – growth of gas bubbles and temperature; (D) – ionization of gas-vapour cavity and electrical breakdown; (E) – expansion of plasma channel and gas-vapour cavity; (F) – current off.

Figure 2-6 shows the thermal electric breakdown in water (Yutkin (1986), Naugolnykh and Roii (1974)). Voltages of a few kilovolts provide enough electric field strength to implement this type of discharge. Once current is in the circuit gas bubbles (B) gather around electrodes and grow (C). These are bubbles of gas contained in water, formed by heating and evaporation and partially by electrolysis. Bubbles merge and form a gas cavity between the electrodes (D). The electric field between the electrodes is higher than the electrical field strength of the bubbles and gas cavity resulting in electrical breakdown occurs. The electrical breakdown creates a plasma channel by ionization of the neutral gas molecules of gas-vapour cavity subjected to a strong electromagnetic field between the electrodes (D).Ionized gas begin conducting and allows plasma channel to expand increasing temperature and pressure. Plasma can be considered the fourth state of matter that have properties and behave different than the other states. The electrical conductivity of plasma is very high in comparison to that of gas, therefore the accumulated energy is discharged very quickly causing the plasma channel to expand (E) depending on the amount of energy accumulated in the capacitor. The formation of the cavity creates an acoustic

shockwave which passes into the soil. The cavity also expands increasing the pressure in the soil.

In this case, most of the energy is spent on forming the gas connection. These energy costs are unproductive and substantially reduce the mechanical impact of discharge. In strong electrolytes (for example, in concrete grout) energy losses can be significant. Therefore, to create a plasma filled channel in gas-vapor cavity it is necessary to ensure that there is enough energy in excess of that required to form the gas filled cavity. It should be noted that a significant discharge of energy leads to a sharp reduction in the life of the electrodes, which are expected to instantly conduct a high voltage current. This can lead to a breakdown of the insulation between the electrodes. The insulation (C in Figure 2-7) separates the two electrodes. Therefore, it is best to use simple but reliable electrodes, which can be easily maintained and withstand high voltage discharges. Figure 2-7 shows discharger with positive (A) and negative (B) electrodes and the insulation (C).

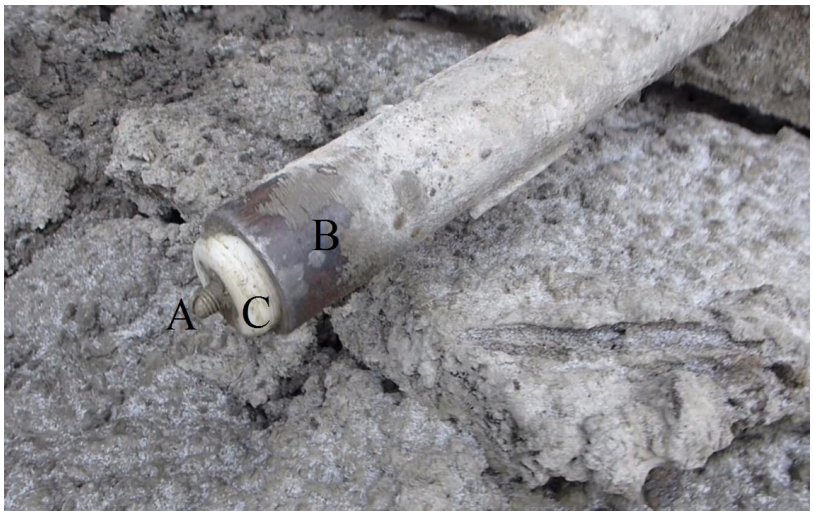

Figure 2-7 – PDT commercial discharger

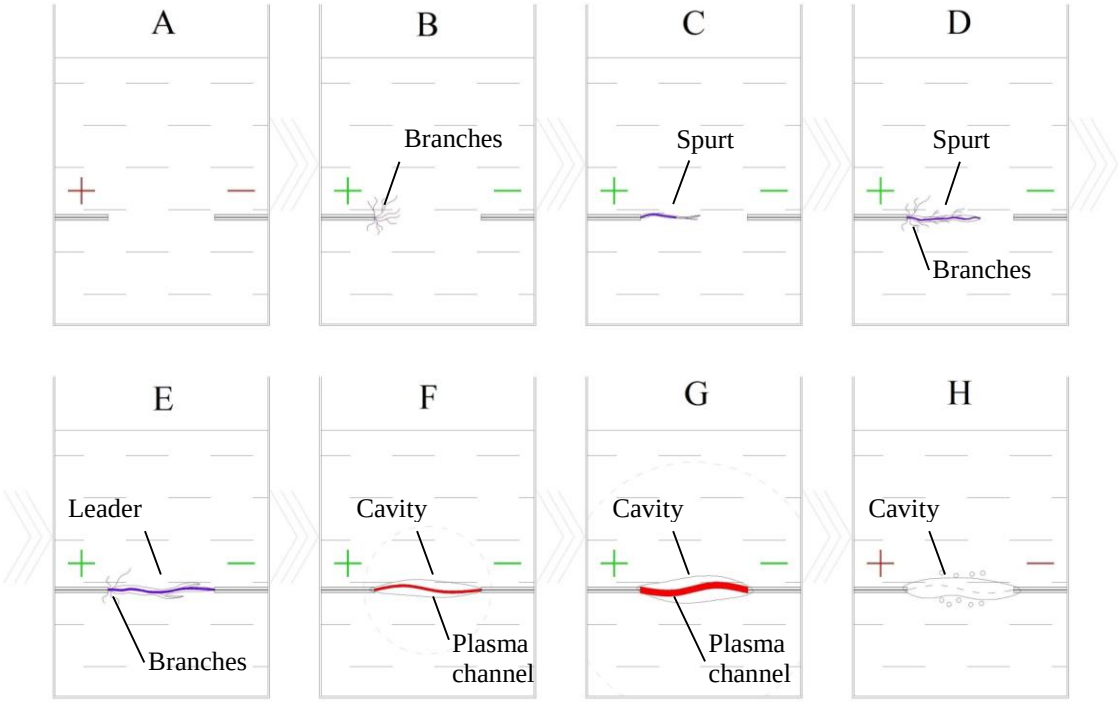

Figure 2-8 – Leader (spark) electric breakdown in water: (A) – current off; (B) – current on: formation of branches; (C) – growth of spurts; (D) – growth of spurts with branches; (E) – leader electrical breakdown with branches; (F) – ionization of gas cavity with plasma channel; (G) – expansion of plasma channel and gas cavity; (H) – current off: collapse of gas cavity

The leader (spark) shown on Figure 2-8 provides an immediate breakdown of the working environment (Yutkin (1986)). A high voltage of several dozens of kilovolts causes an electric breakdown giving rise to electric leaders propagating from the anode to the cathode (B-E). Leaders can be described as channels of ionized gas having high electrical conductivity. The exact form of the leaders depends on the shape of the electrodes (rod-plate, plate-plate, rod-rod), distance between the electrodes, and the resistance of liquid. The generation of leaders can begin from formation of tree-like branches (B) at the tip of cathode, transforming to the spurt (C). The main electric channel is accompanied by branches (D) and the formation of gas envelope around each spurt, which remains for some time after the electric spurts disappear. Once an electric stream bridges the electrode gap (E) all the energy from the capacitor flows to the electrically conducting plasma filled channel causing it to expand (F-G). This in turn expands the gas-vapor cavity. The pressure in the channel reaches a maximum; the plasma channel temperature increases to $4x10^4$ °C; the first shockwave is formed. The pressure generated depends on the energy accumulated in the capacitor. Once all the current has passed through the channel, the gas-vapor cavity collapses (H), its electrical field strength increases and the process damps due

to energy loss oscillating from reverberation of the waves from the chamber walls. It happens due to deionizing of the cooling plasma channel.

Naugolnykh and Roii (1974) noticed that conductivity of liquids, the polarity of electrodes of different shape and the gap between electrodes are critical in streamer growth. They described experiments of leader and thermal electrical breakdown in tap water. Electrical breakdown was obtained using different types of electrodes, point (rod) and plate, varying positive and negative charge on each electrodes. A minimum value of electric field strength required for a leader type electrical breakdown was obtained with 8mm diameter rod shape cathode with conical tip and plate shape anode. At 36 kV/cm it was already possible to obtain leader electrical breakdown in tap water. It has been specified that the minimum value of electric field strength in different conditions was unknown and depends on shape and finish of electrodes, properties of liquid and other factors. The experiments suggested that a relationship can be developed between the voltage density and discharge.

It is difficult to observe high voltage electric discharges in soil, due to the high pressure which can destroy measuring equipment and the opacity for video capturing in soil. However, there are some results of research by Rytov (2009) which shows the formation of electric breakdown in a chamber filled with saturated sand.

Photos (A) and (B) in Figure 2-9 show the start of the electric breakdown, which induces the first shockwave, justified by pressure sensor diagram (Figure 2-10 (P)). At 16 μs (C) there is no current flowing between the electrodes due to the reduced conductivity of the micro-drip medium. The high voltage between the drips of the evaporating medium increase the field density and active current (D)-(E) and full electric breakdown occurs. It causes a second high pressure shockwave. The electrically conductive plasma channel expands and evaporates the surrounding liquid. The gas-vapor cavity around the plasma channel expands (F)-(H). Figure 2-10 shows curves obtained by Rytov (2009) during his experiments. Curve (a) shows the variation of current with time. The labels refer to the time of the images in Figure 2-9. Curve (b) shows the current impulse variation with time. The current (a) at 16 μs (C) is followed by a rapid variation in current at 25 μs (D) shown on Figure 2-10 b. This causes a second shockwave (Q). Curve (c) shows the variation of pressure 195mm from the source of discharge with time. There is a time delay of 147 μs (O)

for the acoustic wave to reach the pressure sensor. The gas-vapor cavity pressure was observed 200 μs after the second shockwave (Q). Diagram (d) shows the variation in resistance in the plasma filled channel with time. Diagram (e) shows the build-up of energy with time, which reaches a maximum of about 2.8 kJ and remains constant during the duration of the discharge.

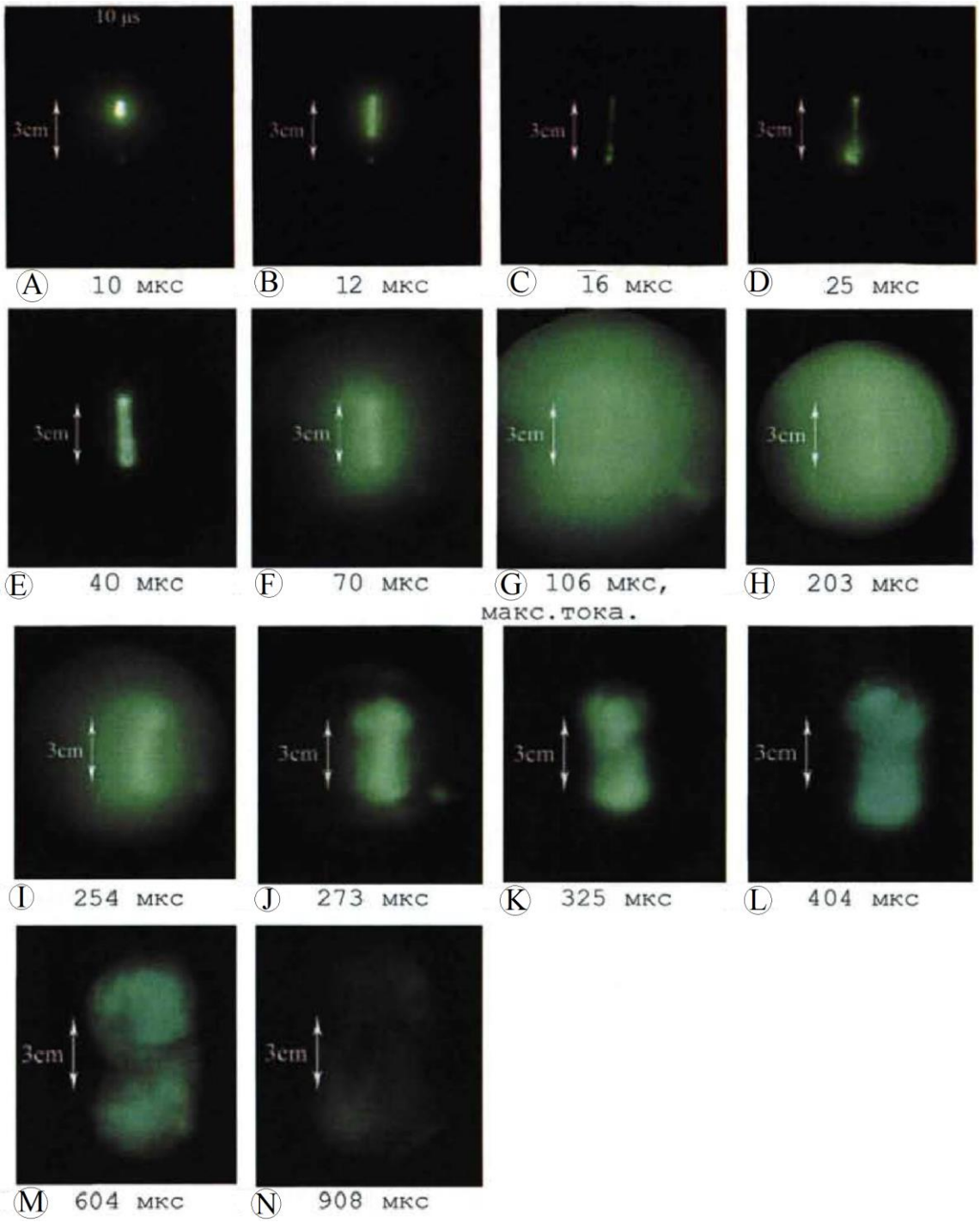

Figure 2-9 – High-speed camera shots of electric discharge in saturated sand. Energy of discharge 5kJ, interelectrode gap – 40 mm. Pressure sensors installed 195mm from the electrodes (Rytov (2009)).

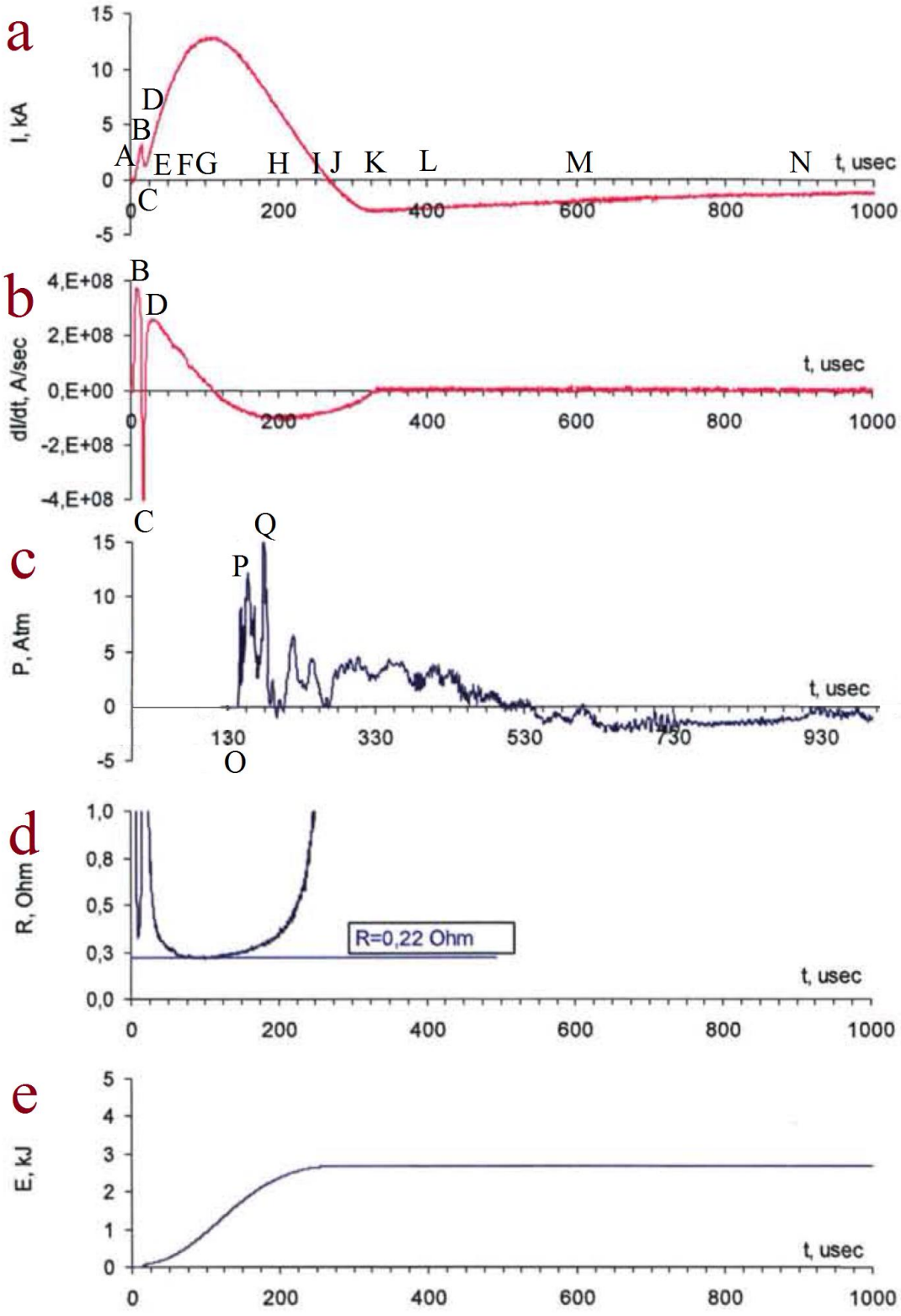

Figure 2-10 – Curves of current, current impulse, pressure on a pressure sensor, resistance and energy (Rytov (2009))

Increasing the voltage reduces the operational reliability of the equipment. Therefore, the use of PDT in piles requires the use of as low as possible a practicable voltage. In order to optimize the process it is necessary to determine the minimum voltage at

which there remains the possibility of an electric discharge occurring. However, increasing the discharge energy can boost the duration of the impulse load thus increasing the pressure on the soil thus having a greater impact on partially saturated soils or liquefiable soils (e.g. loose sand, micaceous sand, etc.)

2.2.4 Application of PDT for bored pile construction

Under reaming of piles using chemical explosives was developed in the 50-60's in the Soviet Union. Most of the borehole is protected by pipe casing to ensure that the explosive energy is focused at the base of the pile. A package of explosive with an electric fuse is placed on the base of the pile. The pile bore is filled with a grout, and the explosive detonated. The explosion of several kilograms of explosives (TNT usually) generates a shockwave and creates an expanding cavity of resultant gases. The walls at the bottom of the borehole expand; a cavity is formed and the soil is densified. The expanded volume of the borehole is backfilled by the wet grout. Thus an under ream is formed thus increasing the capacity of the piles.

This approach has significant shortcomings (Dzhantimirov et al. (2005)), which restricts its use, especially in urban areas. The powerful dynamic impact on the soil can affect the foundations and communications of adjacent buildings and structures. There is also a risk of theft of explosives and the risk of leaving unexploded ordnance in the grout. The use of explosives requires specialized operators. Therefore, this technology is limited in use.

An alternative to chemical explosives is to use the explosive force of an electric discharge (Evdokimov et al. (1991)). In 1977 - 1981 Ulitsky & Shashkin (1999), Yassievich (1977) and Golovchenko (1977) developed technology for producing piles using the electro hydraulic effect. The technology densifies the soil increasing the diameter of the pile shaft. Unlike chemical explosives, there is no risk of theft or handling of dangerous materials.

There are different installation schemes for boring piles with PDT treatment. Bentonite or grout can be used; the reinforcement cage can be installed before or after PDT treatment.

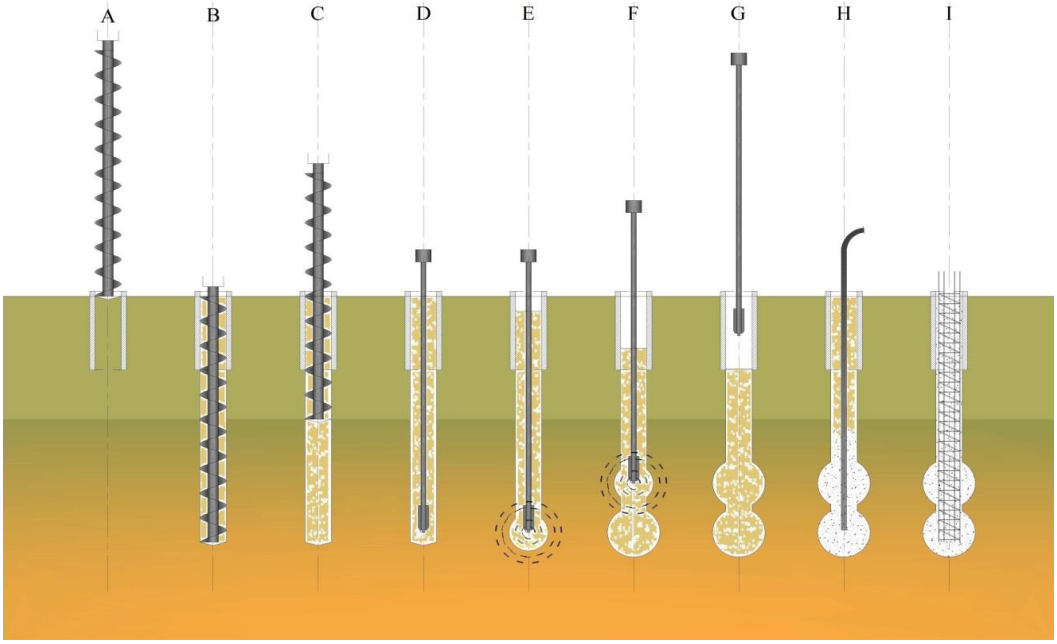

Figure 2-11 – Installation of pile with PDT treatment of bentonite drilling mud

The pile installation starts with drilling the borehole (A-B), using bentonite suspension (C) to stabilize the excavation and as a liquid medium for the electric discharge treatment. After boring a hole to the required depth, the discharge electrodes are plunged into the bentonite mud (D) and a series of electric pulses are initiated at a predetermined level (E-F) of a soil layer, which requires densification. After finishing treatment (G) the bentonite is replaced by grout (H) or concrete and reinforcement inserted (I).

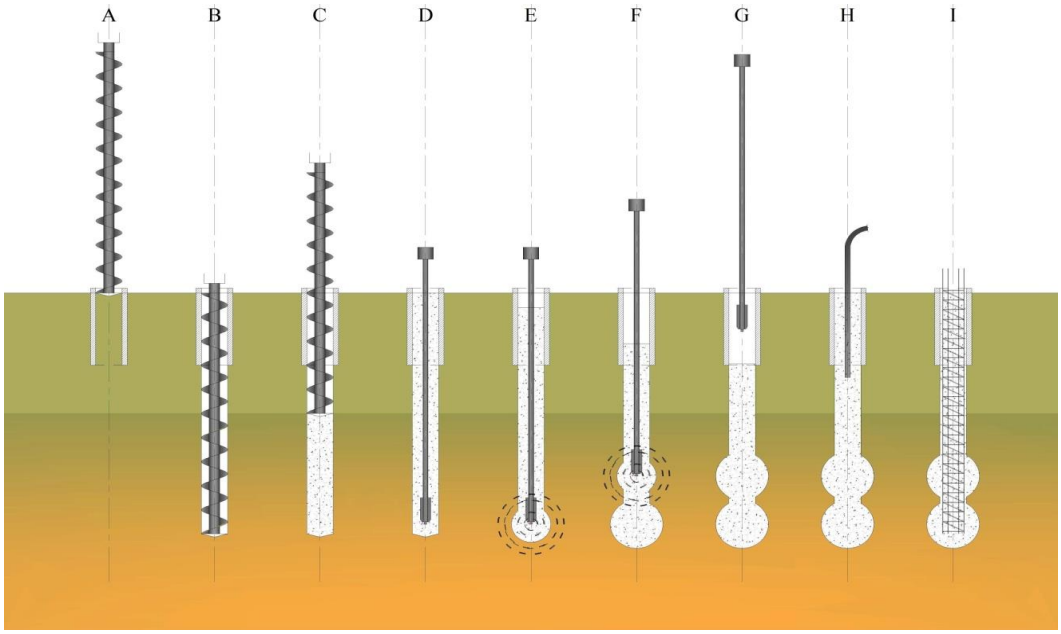

Figure 2-12 – Installation of pile with PDT treatment of mortar

It is possible to implement electric discharges in grout or concrete mortar (Bakholdin & Dzhantimirov (1998)). The borehole is created using a standard CFA process leaving a borehole filled with mortar (C). A series of pulses expand (E-F) it at the required depth. Due to enlargement of the borehole volume (G) by electric discharges it is necessary to refill (H) the borehole after treatment.

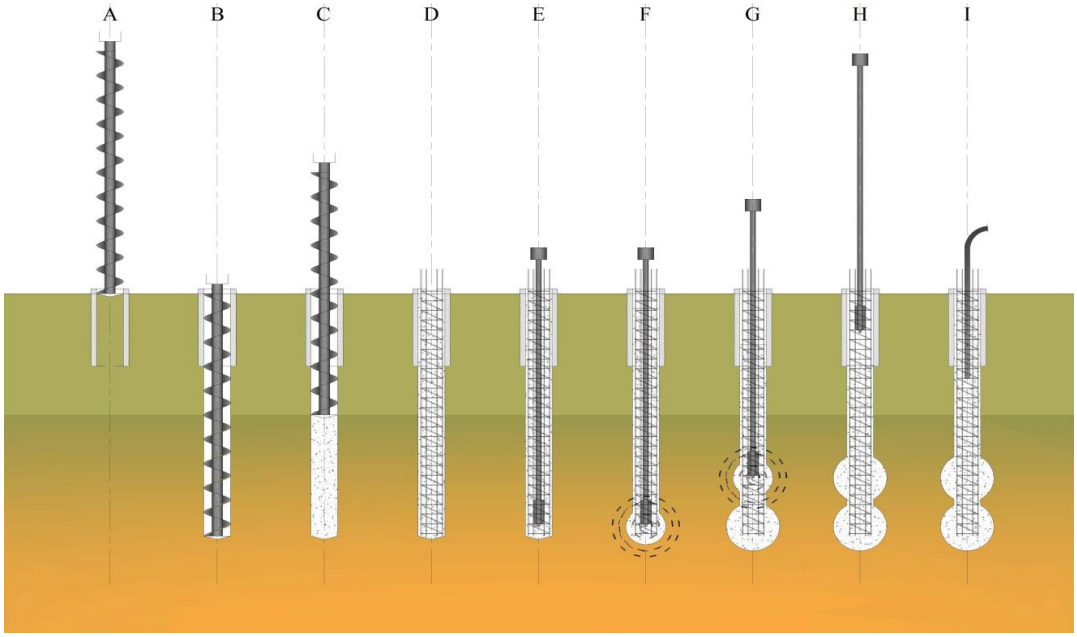

Figure 2-13 – Installation of pile with PDT treatment with inserted reinforcing cage

To reduce the possibility of disturbance of borehole walls a reinforcing cage can be inserted before PDT treatment (D). Although there is wide experience to treat piles with and without a reinforcing cage, the impact of the reinforcing cage on the PDT process has not been analysed. A temperature of 4000°C would have a significant effect on the reinforcing steel but the temperature only occurs in a small zone between the electrodes.

Shelyapin et al (1976) studied the densification of sand and sandy loam in a pile using electrical discharges in cement mortar. They found that the use of electrical discharges created an expanded cavity in the soil and improved soil properties. They assumed that the expansion is determined mainly by the impact of the first shockwave. According to experimental data of Golovchenko (1977), the mechanical impact on the soil due to chemical explosives and electrical discharges are identical and the dynamic impact of the discharge takes place in microseconds.

During the first experiments in grout it was difficult to get discharges strong enough to provide impulse load. Golovchenko (1977) recommended the use of a single discharge initiated by a disposable thin conductor to expand the grout filled borehole. The conductor was used to initiate an electric breakdown between the electrodes. A theoretical solution for the determination of the cavity expansion in the soil was obtained. It was found that a single electric discharge of 700 - 1000 kJ at a voltage, *V*, of 30 - 50 kV, with a capacitance $C = 2.0 – 2.5$ μF was sufficient to increase the base of the pile.

Brovin (1994) showed that the main difference, and an advantage, of the pulsed discharge method compared to the use of explosives is the ability to create a series of discharges with a small amount of energy in each. In this way, the impact of the discharge can be controlled providing a more precise control over the final pile geometry. If the energy in the discharge channel is equivalent to the energy of explosives of a few kilojoules, expansion of diameter of piles will be few centimetres (for saturated sandy soils). This allows the required number of discharges to be calculated to achieve the required pile diameter.

Ulitsky et al. (1995) presented a formula (equation (6)) for the evaluation of the resulting expansion of pile shaft with multi-pulse impact of discharges. This formula is based on an appraisal of cavities formed in the soil during the explosion of explosives. According to this method, each discharge expands the borehole according to the formula:

$$R_u^i = R_0 \left[1 + \sqrt{\frac{P^{max}}{\rho c^2} \left(\sqrt[3]{1+\varepsilon} - 1 \right)'} \right] \qquad (6)$$

where $i = 1, 2, ...$, R_u^i - radius of the well expansion after i-th discharge, R_0 - initial radius of the well, P^{max} - maximum pressure at the pile-soil interface, ρ - density, c - acoustic speed in soil, ε - the available dynamic soil densification.

It is assumed that the shockwave is a main factor of the mechanical work on the formation of the expansion of the pile shaft.

Yassievich (1988) studied the effects of electrical discharges on the strength of grout used in the piles. The experiments showed a significant increase in the strength of concrete with increasing of number of discharges. This may be due to the

densification of the grout due to the electric discharge. They found that to increase the diameter of the pile shaft and densification of soil with a voltage of 30 - 50 kV, relatively small discharge energy was required W = 6-9 kJ.

Brovin (1994) presented results of field tests of piles in saturated soils constructed with PDT. They showed that the use of PDT in the piles can achieve substantial increase in the diameter of the pile shaft thus increasing its load capacity. The pile was excavated to determine the diameter. For example, when the voltage was 30 - 40 kV, the discharge capacitance C = 18 μF (W=8-14 kJ), the electrode gap of 50 mm and with 150 discharges, the diameter of the pile shaft increased by about 40 - 80 mm (initial piles diameter ~ 140 mm). Based on the results of static tests, the bearing capacity of these piles, increased, on average, by 31%. They found that the optimal number of discharges, required for increasing the diameter of the pile shaft is in the range of 10 to 30.

In the 90's, in St. Petersburg and Moscow, laboratory and field piles were installed using the PDT in saturated sands and soft clays (Evdokimov et al. (1991), Bakholdin & Dzhantimirov (1998)). The voltage was varied from 5 to 9 kV; energy of the discharge - from 8 to 60 kJ. The results showed that it is possible to increase the diameter up to 3 times. The values of the bearing capacity of piles were 2 - 4 times higher than those of untreated piles. The costs of PDT piles were 20 - 30% more than untreated piles. For example, 3 m long piles (diameter of borehole was 135 mm; diameter of the treated pile 400-500mm) were compared with untreated piles of the same length and diameter of 181 mm. The bearing capacity of piles was 600kN to 850kN, for the untreated pile it was only 150kN.

For PDT the value of grout plasticity is significant. Experiments conducted on a grout with water-cement ratio of 0.3, showed that it was not possible to generate pulsed loads because of dehydration of grout which prevent the collapse of the gas-vapor cavity.

PDT was applied in Moscow by commercial contractors since 1992. Their experience shows high efficiency of PDT in saturated sand and soft clay soils (Dzhantimirov et al. (2003)). This is due to the fact that these types of soil react to the impact of impulse loads. The impact of the pulse discharges in boreholes filled with grout can cause

cavity expansion by weakening of clayey soils and local loosening of saturated sands with the application of slight pressure. As a result, the pile shaft diameter is increased.

The effectiveness of PDT in soils which do not liquefy, such as the partially saturated sandy soils, is reduced. One of the crucial factors here is the duration of the pulse load, which is not enough to increase the pile shaft diameter. Research by Dzhantimirov et al. (2005) of piles in clayey soils using electrochemical explosions showed that a significant increase in diameter of the pile shaft occurred if the pulse load was applied in milliseconds range. This may be explained by inefficient energy discharge parameters (Semkin et al. (1995)). According to Naugolnykh and Roii (1974), the time of pressure of the discharge is dependent on the energy of the discharge. However, the experience of PDT shows that even significant increase of discharge energy (up to 60 kJ) does not lead to a significant increase in the duration of the pulse load. Studies in various industrial sectors show that the duration of the discharge pressure is determined not only by its energy, but also depends on the ratio of the voltage and discharge capacitance.

Currently, the increase in pile shaft diameter is determined in a similar manner to the evaluation of size of the cavity formed by explosives, where the mechanical work is produced by a shockwave. The dimensions of a pile shaft is a function of energy and does not depend on the ratio of energy parameters of the discharge (Brovin (1994), Gavrilov et al. (1991), Lee et al. (2011)).

It is known (Semushkina (1968), Lomize & Khlyupina (1965)) that by varying the energy parameters of the discharge (voltage and discharge capacitance) at constant energy the effect of the impact varies.

To date, the experimenters do not agree as to how the shockwave and gas-vapor cavity affect the pile shaft. Dzhantimirov et al (2010) showed that the formation of the pile shaft in certain soils (soils with low potential to liquefy) the duration of the impulse is important. According to those studies, it is in the millisecond range. Based on industrial application of PDT the impact of pulse treatment depends on the duration of combined action of the shockwave and expansion of gas-vapour cavity. The microsecond range of duration of the shockwave action is considerably lower than of gas-vapour cavity expansion, therefore, the determining factor in enlarging the

diameter of piles in partially saturated soils is the impact of the gas-vapour cavity expansion.

Semushkina (1968) showed, in saturated granular soils that the energy content of the shockwave can be increased by increasing the voltage at constant discharge capacitance and the gas-vapor cavity increased by increasing of discharge capacitance at a constant voltage. Thus the increase in the energy content of the gas-vapor cavity is possible at a constant voltage, which enhances the discharge.

Reducing energy loss and increasing the intensity of the force impact of the discharge does not solve all problems arising in the process of increasing the pile shaft in partially saturated soils using PDT. One such problem is the interaction of the grout and soil (Brovin (1994), Bakholdin & Dzhantimirov (1998)). During PDT treatment, water can migrate from the grout into the soil. The grout becomes dehydrated, its properties change, and the amplitude of the pressure sharply attenuates away from the discharge. The grout cannot transmit sufficient force on the borehole wall, which significantly affects the deformation of the soil. The change in fluid (grout) parameters can lead to a complete halt of the process of pile production.

Thus, the grout parameters vary during PDT treatment and could influence the formation of the pile shaft. Issues associated with the influence of changes of the properties of grout on the process of creating piles require research and selection of required composition of the grout mix, which provide the required plasticity properties of the mixture over the entire period of the pile construction process.

A rather difficult task is to predict the geometrical dimensions of the pile shaft after PDT treatment. The static pile tests have shown the pile capacity increases after PDT. The processes that occur during the formation of the PDT pile under the impact of discharges in the grout have not been studied, so methods of determining the amount of pressure and its distribution in pile – soil system is not widely applied.

The review of the literature shows that previous attempts to establish the relationship between the energy of the discharge and expansion formed in the soil due to the action of a single discharge have had no success. Summary of experiments and soil types tested in the literature can be found in Table 2-1. Currently the capacity of PDT piles is based on an analogy with piles created using chemical explosions. They do not

take into account the effect of the shockwave and cavity expansion and the soil type, porosity and water content.

2.3 Evaluation of the impact of PDT treatment on adjacent buildings and structures.

Quite often CFA piles are chosen to underpin the foundations of existing buildings and structures in urban areas. At the same time, strengthening work has to be carried without stopping the operation of existing buildings and structures. Sometimes works for reinforcement of the foundations leads to additional settlement of adjacent structures due to weak soils or excessive impact of the PDT. In this regard, it is necessary to ensure the safety of buildings and structures during construction works. Therefore, it is important to analyze soil reactions to such action, to appraise area of possible soil movement and assess the possibility of “resonance" phenomenon.

Aptikaev (2001) undertook experimental work showing the formation of typical wave oscillations of the soil surface near to a PDT power setup (with energy of 40 kJ). The soil of the top layer was comprised of made ground. Figure 2-14 shows a cross section of a vibration monitoring layout for (a) - PDT treatment of a pile at 1m below ground level and (b) - impact driving of a precast pile to 6m below ground level.

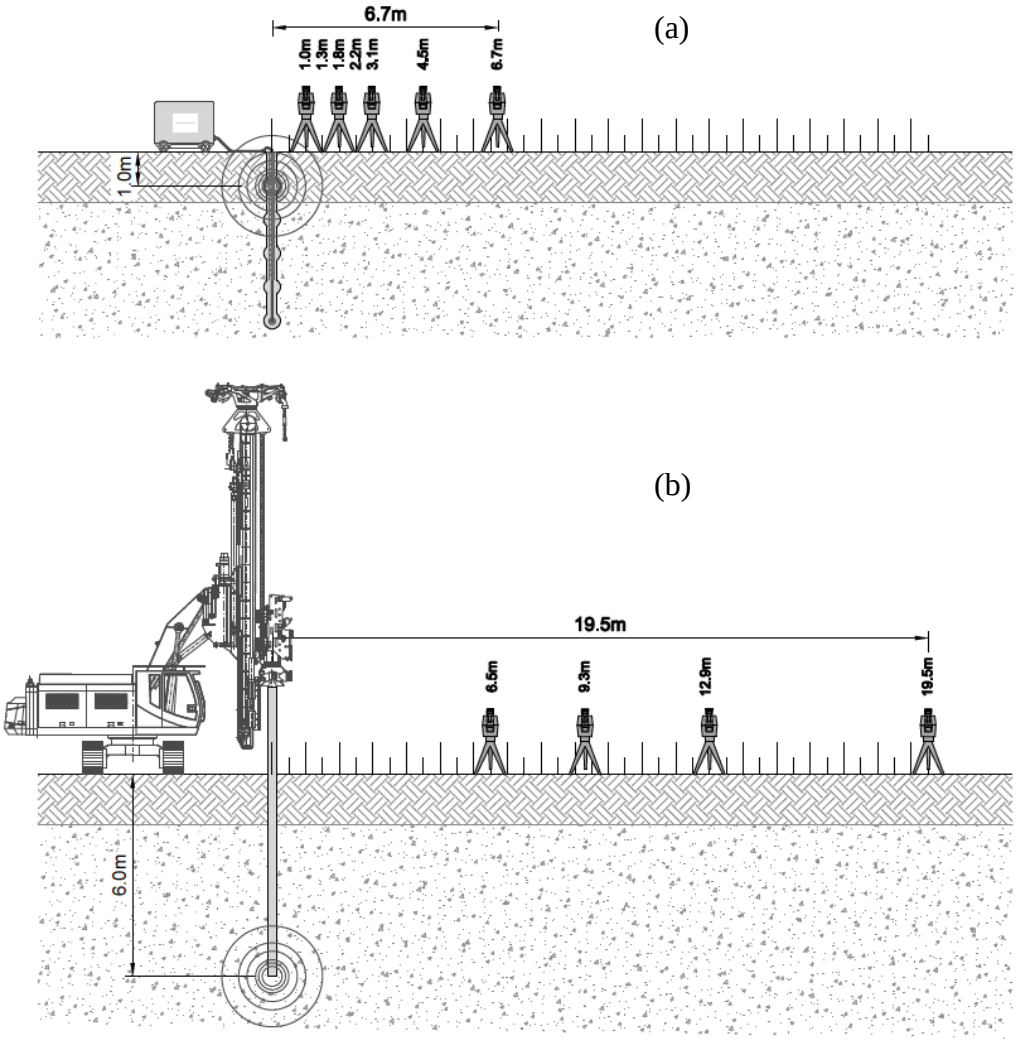

Figure 2-14 - Testing layout of the vibration monitoring of a PDT pile and impact driving of a precast pile (Aptikaev (2001))

A seismogram (Figure 2-15) recorded at existing ground level shows the effect of a discharge of 40 kJ in a 250 mm diameter borehole, filled with grout mortar (Aptikaev (2001)). The graphs show the amplitude (mm) of oscillations at time (s) at fixed distances from the source at a depth of 1m from the surface. Oscillations of up to 0.1 mm were detected up to 0.1 sec after discharge at the distance of 3.1 m from the source. Oscillations were dampened at a distance beyond 3 m from the projection of the source; at a sensor at 6.7 m from the source they are less than 0.025mm. Increasing the energy from 10 to 40 kJ caused no significant change in the wave pattern.

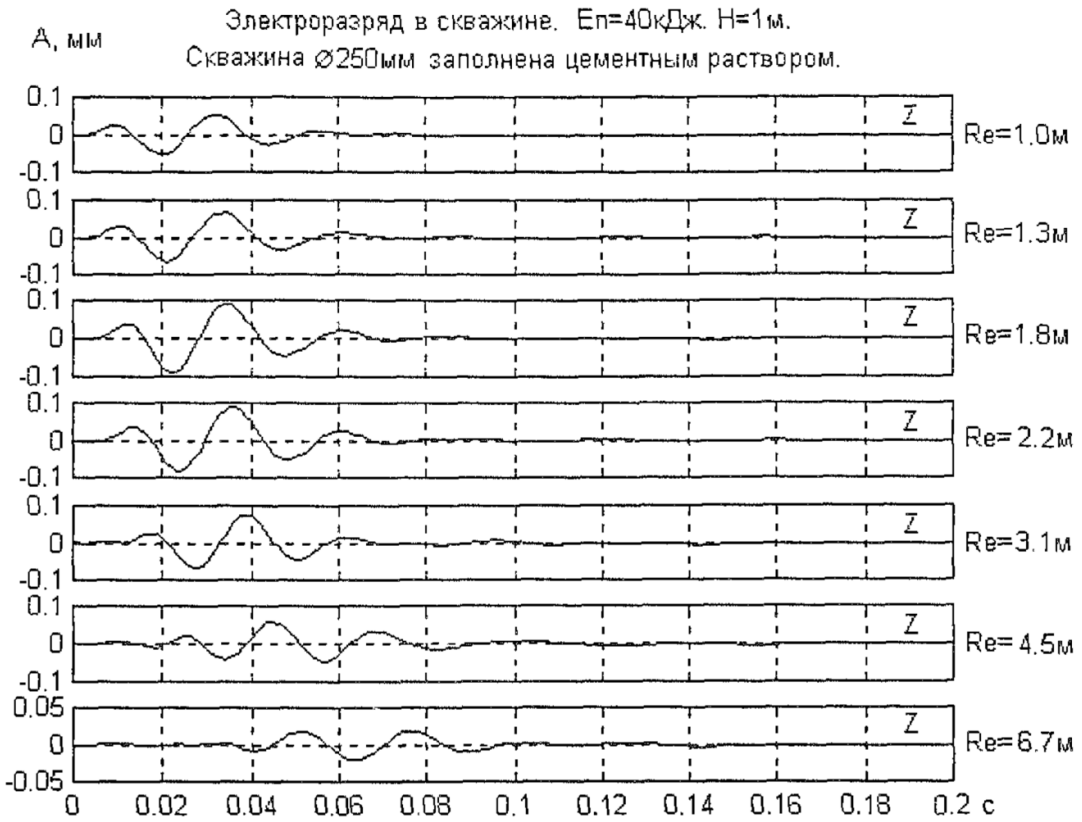

Figure 2-15 – Amplitude (mm) of vibration monitored on the ground surface against the time at distance *Re* from the PDT source. Pulse discharge in a borehole. *E*=40kJ, *H*=1m, *d*=250mm, filled with grout mortar. Soil conditions – made ground. (Aptikaev (2001)).

Figure 2-16 shows a seismogram of a displacement pile driven by hydraulic hammer. Oscillations of up to 0.04 mm amplitude were detected from 6,5m to 9.3 m from the source within 0.2 seconds after discharge. At sensors installed at 12.9 m and 19.5 m the amplitude of oscillations from the pile driving hammer were almost the same amplitude as those of the PDT treatment at distance of 2.2 m from the source. According to Aptikaev (2001), the seismic impact of PDT source is much less than that of a single hammer blow.

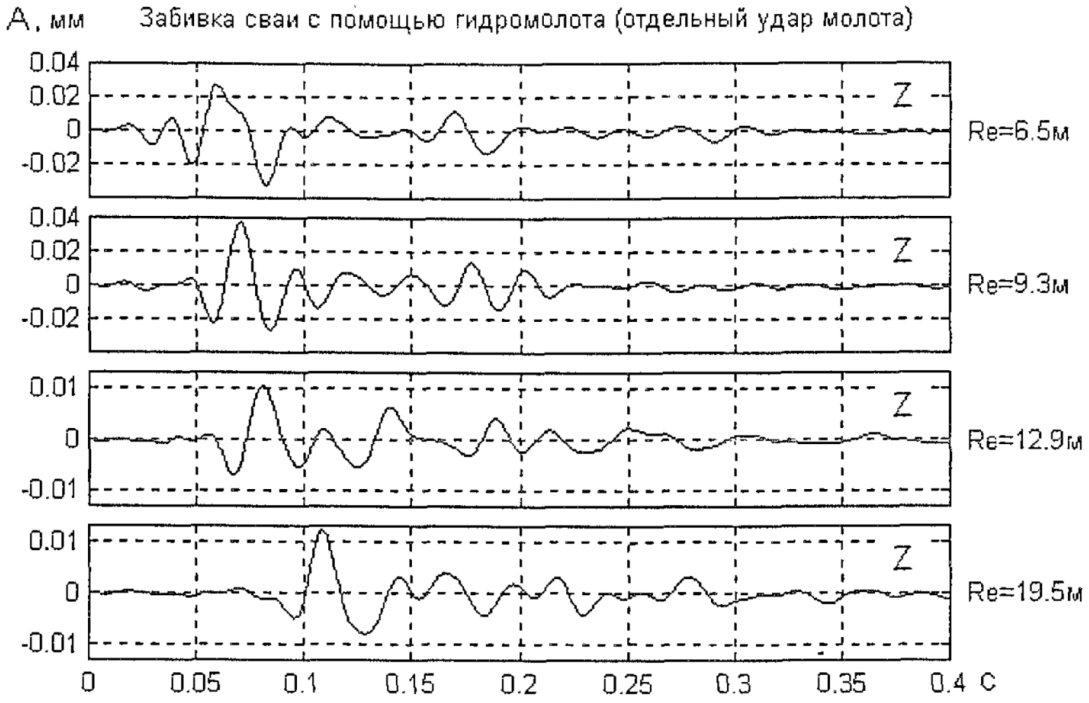

Figure 2-16 – Amplitude (mm) of vibration monitored on the ground surface against the time at distance *Re* from the pile driving source. Pile driving by a hydraulic hammer (single hammer blow). Soil conditions – made ground. (Aptikaev (2001))

The PDT pulse treatment of soils can be compared to vibratory dynamic impact (Rytov (2009)). The differences have been specified as follows:

- The time to release energy in a PDT pile is much less than that for vibration. Hence the impact of PDT is much higher at the same loading amplitude.
- A small number of damping oscillations following the pulse with a peak value of loading compared to a vibratory loading of a lower value.
- 7-10 seconds time gaps between pulses allows unloading/reloading of soil by PDT, whereas vibratory technique provides permanent dynamic loading.

PDT is better at densifying fine grained soils than by vibration. The applicability of PDT is determined by:

- Better local soil compaction by destruction of the soil structure at a given intensity of the source impact;
- Drained behavior of granular soils with no build up of excess pore water pressure;
- consideration of adjacent buildings and structures in terms of possible settlement;

- the size of the impact zone of PDT source in such grounds .

Due to the possibility of liquefaction and subsequent densification of saturated sandy soil at the base of existing foundations, PDT treatment of piles is not recommended in the active zone of the foundation Rytov (2009).

Figure 2-17 shows the variation in pressure with time (Park *et al.* (2011)) for laboratory tests in 110mm diameter chamber filled with fresh cement paste. The shockwave is observed at 0.17 ms, but oscillations of gas-vapor cavity pressure and reflected waves can be seen up to 1 ms. In this case, a short pulse with high peak power is converted to a long pulse with a low peak power during transition from the foundation or embedded pile into the ground.

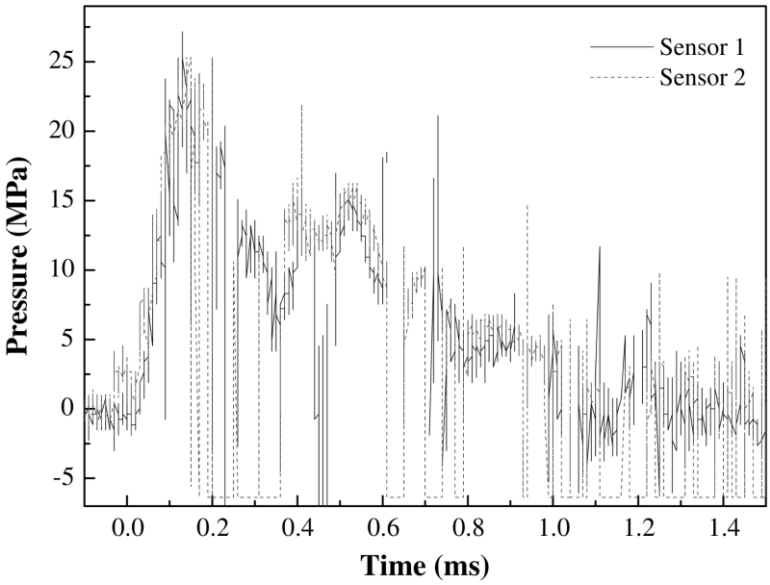

Figure 2-17 – Measured shockwave pressure during PDT test in 110mm diameter chamber filled with fresh cement paste (Park et al. (2011))

An et al. (2011) have studied simulation of soil behaviour under blast loading. They used LS-DYNA software and applied viscoplastic cap model by Tong and Tuan (2007) to simulate responds to shock loading of the three phases of dry and saturated soil. It was found that updated viscoplastic cap model allows for a better prediction of saturated, rather than dry soil behaviour.

2.4 The energy parameters of the PDT for pile installation

To get the leader breakdown in the electrode gap in grout mortar medium a voltage of at least 30 kV is required. This significantly reduces the loss of energy needed to form

the gas-vapor connection between electrodes (thermal electrical breakdown) and increases the intensity of the impulse transmitted to the wall of the borehole through the mortar medium (Samarin (2005)).

The gap between electrodes is an important parameter for the PDT method of pile installation, because it affects the probability of formation of the discharge and the pressure of the pulse loading, transmitted to the wall of the borehole. The gap between the electrodes for pile installation is typically 35 - 40 mm.

The choice of energy needed for the PDT method in partially saturated soil is associated with the duration of the discharge impact. Increasing the time of pressure action generated by electric discharge in a grout mixture is possible by increasing the discharge energy. In this case, it is necessary to get leader (spark) type of breakdown of the inter-electrode gap. Discharge energy is given by equation (1).

Studies (Samarin (2005)) have shown that increasing the time of the pulse can be obtained by increasing the discharge energy of leader (spark) electric breakdown. Thus, in partially saturated coarse grained soils when the discharge energy W = 1.8 kJ , the duration of the pulse loading is 0.002 seconds. Increasing the energy up to 4.5 kJ leads to a sharp increase in the duration of the pulse load up to 0.006 seconds. The pressure on the wall of the borehole is ~ 2 MPa.

The required force on the ground can be obtained at an energy of 4.5 kJ. However, it is now common to use up to 60 kJ for PDT piles.

Samarin (2005) found that treatment of the pile shaft by electric discharges of V = 30 kV and C = 10 microfarads (W = 4.5 kJ) increases the diameter of the borehole from 110 mm to 200 mm (Figure 2-18).

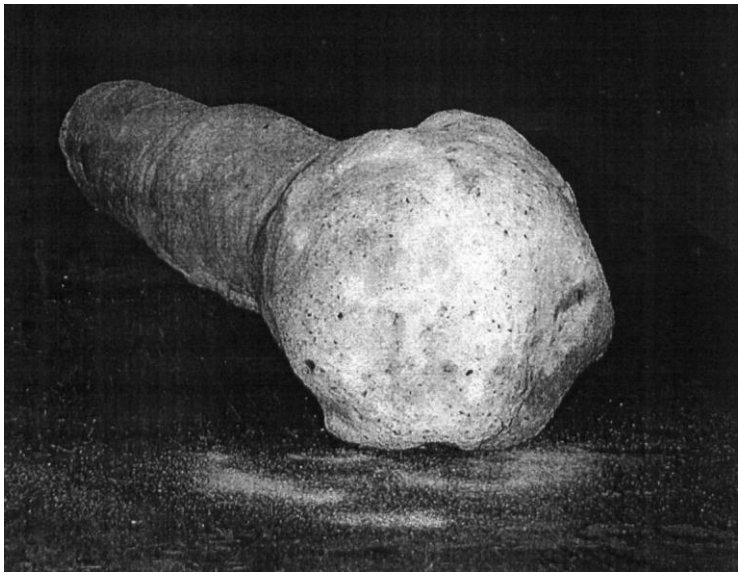

Figure 2-18 – Test pile enlarged by PDT treatment (d=110÷200mm) (Samarin (2005))

Figure 2-19 shows that the diameter of the PDT pile depends on the number of pulses measured in laboratory chamber filled with granular material (φ' = 23-25°, E = 15 – 18MPa). Curve 1 was obtained at frequency of 2 Hz, curve 2 – at 4 Hz. It was found that the increasing the frequency of pulses from 2 Hz to 4 Hz reduces the amount of deformation of the borehole. At a frequency of 4 Hz there is a reduction in the amplitude of pressure; that is the reason for a reduction in soil deformation (Samarin (2005)).

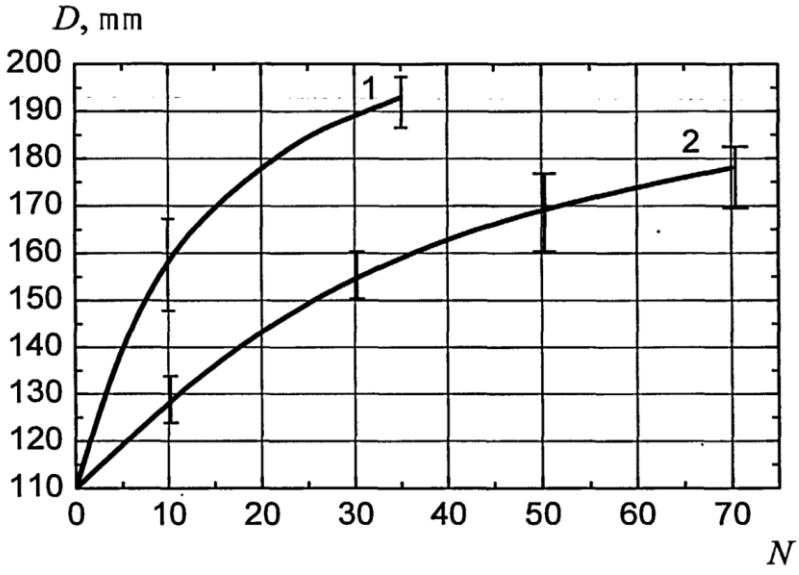

Figure 2-19 – The diameter of the PDT pile depends on the number of pulses and varies with the frequency in granular material measured in laboratory in the chamber (Samarin (2005))

Bakholdin and Dzhantimirov (1998) have shown that PDT treatment causes dewatering of grout mortar. This problem occurs in soils with significant absorption capacity. Dewatering of the grout mortar inevitably leads to a decrease in the amplitude of the pressure exerted on the borehole wall. The process of deformation of the borehole wall has a threshold (Brovin (1994)) below which deformation of the wall will not occur. Dehydration of the grout mortar causes the PDT treatment to stop as the reduced fluidity of the mortar mean that the gas-vapor cavity does not collapse after discharge and blocks the conductivity of inter-electrode gap.

A loss of the liquid component of the grout mixture in between the electrodes practically stops the treatment. This is because subsequent pulses form in a dehydrated local environment which means that thermal breakdown cannot occur. Hence, there is no shockwave or cavity expansion. Thus, the liquid phase must remain in the grout mixture. This ensures efficient transmission of the pulse pressure from the discharge channel to the borehole wall surface.

The problem of grout dewatering during PDT treatment can be solved by using gel-forming additives (Samarin (2005)). Such additives constrain the liquid medium of grout mortar thereby prevent it from extruding into the pores of the surrounding soil and thus maintaining the mixture of grout, which is able to transmit impulse loads to the wall of the borehole.

2.4.1 Analysis of the impact of PDT pulse load on the pile - soil system

During the electrical discharge in a liquid medium a force is generated because of the shockwave and the gas-vapor cavity expansion. Impulse loads from the shockwave and gas-vapor cavity effect different soils in different ways. There is an analogy between PDT and blast of chemical explosives (Khlyupina (1967)). Therefore, most researchers have developed formulas for PDT discharge effects from those for chemical explosives. For example, Ulitsky et al. (1995) proposed to calculate the radius of the expansion from the discharge based on calculation method used for the expansion formed by the blast with the chemical explosives (equation (6)).

To estimate the maximum pressure on the pile-soil interface, Brovin (1994) proposed the formula

$$P^{max}(r) = \frac{k}{r^{\mu}}\left(\sqrt[3]{\eta W}\right)^{\mu} \quad (7)$$

where k,μ - empirical factors, W – energy of the discharge, η – an empirical factor defining the ratio between an electric discharge and a chemical explosive (TNT) blast, r – distance between point of discharge and borehole wall.

Gavrilov & Egorov (1989) proposed the increase in radius of the pile shaft is given by the formula:

$$R = k\sqrt[3]{E} \quad (8)$$

where E - energy of one discharge, k - empirical coefficient based on soil resistance during electric blast.

The deformation in soils from PDT is caused by the sum of pressures from the shockwave and following expansion of gas-vapour cavity. The pressure from shockwave and expanding gas-vapour cavity is a function of the voltage and the time it acts depends on the capacitance. In granular soils the shockwave has a main impact on the value of deformation due to the highest amplitude of a shock front pressure. In fine grained soils the expanding gas-vapour cavity acting in millisecond range is the main source of soil deformation.

2.4.2 Determination of geometrical dimensions of the cross -section of piles after PDT treatment

Alternatively, calculation of the geometry of the PDT piles can be based on analysis of the pressure propagation in the surrounding ground (Samarin (2005)). If the stress properties of soil after treatment are known, it should be possible to assume deformation of the shaft of the pile. Contrary to described in 2.4.1 analogy to chemical explosives, the pressure propagation in the soil depends on the parameters of the electrical discharge energy and can be described as follows:

$$p(x) = p_0\left(1 + \frac{x}{R_0}\right)^{-\mu} \quad (9)$$

where $p(x)$ - pressure in the soil at a distance x from the borehole wall, p_0 – pressure on the borehole wall, μ - approximation coefficient allowing pressure propagation in soil, R_0 – radius of the pile shaft (Samarin (2005)).

Samarin (2005) proposed that elastic-plastic soil models could be used to assess the deformation of foundation soils treated by PDT. He suggested that these models could

be implemented in Plaxis software, which takes into account the mechanical properties of the soil. The deformation of the borehole wall from subsequent discharges can be approximated as follows:

$$d(n) = d_0(1 + \frac{2u(1)}{d_0 ln2} ln(n+1)) \quad (10)$$

where *d(n)* - diameter of the borehole after discharges impact, d_0 – initial diameter of borehole, *u(1)* – radial displacement of the borehole wall from a single discharge, *n* - the number of discharges.

This displacement can be used to model a spherical expansion in a soil. The process starts with the installation of a liquid filled borehole. A number of discharges can be modeled at different levels in the borehole thus creating a simulation of a PDT pile. The constitutive model will depend on the soil type.

2.4.3 Determination of the bearing capacity of CFA piles after PDT treatment

The capacity of displacement piles exceeds that of replacement piles. The zone of influence of displacement piles is about twice the diameter of the pile in granular soil (Samarin (2005)). PDT piles start as replacement piles as a borehole is drilled. The PDT process displaces the soil. The zone of influence after PDT treatment depends on the discharge energy. A study of the displacement piles (Grigoryan & Yuschube (1986), Yuschube (1988)) showed that the density of the transformed soil around a pile was 1.91 g/cm^3. The initial soil density was 1.65 g/cm^3. The dimension of the densified zone was approximately two diameters of the pile suggesting that the PDT treatment has the same impact as full displacement piles. Experimental data (Samarin (2005)) showed that in granular soils with energy parameters V = 30 kV , C = 10 µF, W= 4.5 kJ, after 15 discharges similar results were obtained. Thus, the initial soil density 1.65 g/cm^3, after PDT treatment increased to 1.89 g/cm^3. The dimension of the densified zone was about two pile diameters.

Samarin (2005) recommended the following procedure for assessment of bearing capacity of PDT piles:

1. Assignment of the initial diameter of the pile shaft
2. To assess friction capacity of enlarged pile shaft according to Russian standard (NIIOSP (2001)), PDT treated zone of compacted soil is divided into layers of 0,1 - 0,2 pile diameter. Notional number of layers is 10.

3. Assignment of pressure p_0 in the pile borehole wall, (if diameter of the pile is 110 - 250mm, then p_0 = 1400 - 1800 kPa (Samarin (2005)))
4. Determination of the value of pressure on the pile soil interface of each layer h_i of soil using equation (9)
5. Determination of displacements in each layer h_i in Plaxis
6. Summation of displacements for each layer h_i and determination of cumulative displacement from unit discharge *u(1)*
7. Determination of pile diameter from further discharges. This will provide the dimensions of the enlarged pile.
8. Determination of bearing capacity of pile by a standard method:

- Assumption of calculated resistance of soil below the pile toe
- Assumption of partial resistance base factor γ_b = 1
- Assumption of partial resistance shaft factor γ_s = 1,3
- Assumption of enlarged base area equal to cross-section of maximum pile enlargement

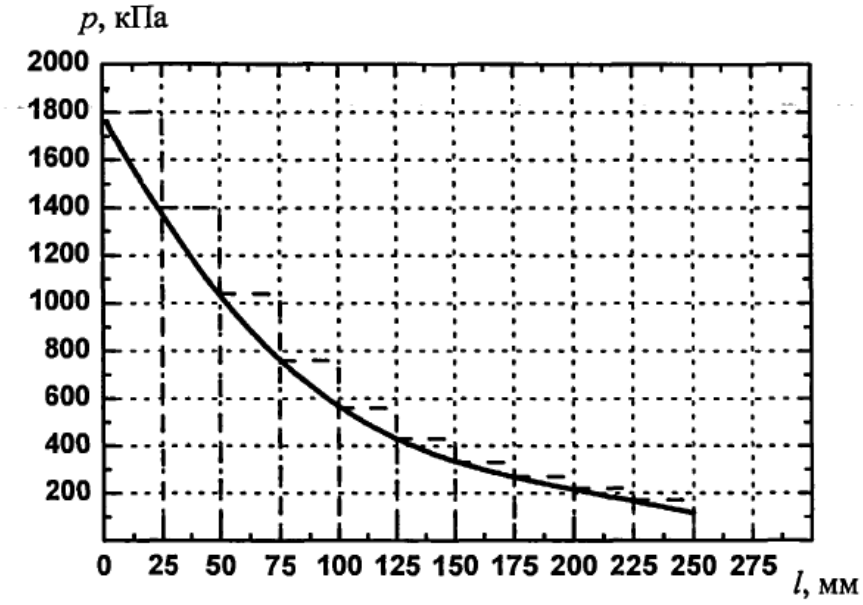

Figure 2-20 Scheme of soil layers for pile capacity calculation (Samarin (2005))

Table 2-1 - Summary of experiments considered in the literature review

Authors	Date	Title	Experiment	Soils	Power	Diameter	Expansion
Samarin, D.	2005	Improving of method of pile installation in partially saturated soils using pulse discharges	Laboratory and field tests of PDT piles	Sandy soil, partially saturated	W=4.5kJ, V=30kV, C=10uF	110mm	200mm
Gilman, Y. & Lomize, G.	1962	Electrospark method of soils compaction	Concept of soil densification with electro-hydraulic effect	Sandy soil, partially saturated			
Lomize, G., Meshcheryakov, A. Gilman, Y. & Fedorov, B.	1963	Compaction of sandy soils by electric discharger	Field tests of densification of soils with PDT	Sandy soil, partially saturated			
Khlyupina, L.	1967	Physical processes in sandy saturated soils by high voltage discharges	Theoretical investigation of PDT in soil densification	Sandy soil, saturated	V=18-60kV		
Semushkina, L.	1968	Experimental justification of the main technological process parameter during impulse achieved stabilization of water saturated soils by construction	Research of densification of saturated soils with PDT	Loose sandy soil, saturated	V=10-50kV, W=1.5kJ		
Gilman, Y.	1963	Stabilizing of saturated soils with the help of electric discharges	Calculation of pressure using equivalent of explosives	Sandy soil, saturated			
Lomize, G. & Khlyupina, L.	1965	Physical processes of electrospark compaction of sandy soils	Field tests of densification of soils with PDT	Sandy soil, saturated	W=300J-1500J;		

Lyakhov, G.	1982	Waves in soils and porous multicomponent materials	Calculation of pressure using equivalent of explosives	Sandy soil, saturated			
Park, H., Lee, S.-R., Kim, T.-H. & Kim, N.-K.	2011	Numerical modelling of ground borehole expansion induced by application of pulse discharge technology	110mm, 250mm chamber	-	W=20kJ, V=6kV		
Naugolnykh, K., & Roii, N.	1974	Electrical discharges in water	Research of thermal and leader breakdown in tap water	-			
Rytov, S.	2009	Installation of bored piles using pulse discharge technology in various soil conditions	Laboratory and field tests of PDT piles	Sandy soils, saturated	W=5kJ		
Yassievich, G.	1977	Research of bored piles installation method via electrohydraulic effect and its' work under vertical load	Field tests of PDT piles	Various	W=6-9kJ, V=30-50kV		
Golovchenko, V.	1977	Research of comprehensive reinforcement of exploded foundation cavities	Comparison of PDT with application of chemical explosives	Sandy and silty soils	W=0.7-1kJ, V=30-50kV, 2-2.5uF		
Shelyapin, R., Golovchenko, V. & Matveev, V.	1976	Spherical compaction of soil by underwater explosion treatment	Field tests of PDT piles	Sandy and silty soils			
Brovin, S.	1994	Performance characteristics of piles injected into pre-augered holes to strengthen a weak soil mass	Field tests of PDT piles	Sandy soil, saturated	V=30-40kV, C=18uF, W=8-14kJ	140mm	180-220mm
Evdokimov, V., Egorov, A. & Borisenkov, V.	1991	Grouted piles installed with application of electric impulse technology	Laboratory and field tests of PDT piles	Weak clayey and sandy soils, saturated	V=5-9kV, W=8-60kJ	135mm	~400mm

Semkin, B., Usov, A. & Kurets, V.	1995	Fundamentals of electric pulse fracturing of materials	Research of electrical parameters of PDT	-	V=7-10kV, W=60kJ		
Lee, S.-R., Park, H., Kim, T.-H., Cha, K.-S.	2011	Numerical analysis of uplift behaviour of ground anchor underreamed by pulse discharge technology	Measurment of PDT pressure on the walls of 250mm chamber	-	W=20kJ, V=4kV		
Aptikaev, S.	2001	Features of soil surface vibration near the man-triggered seismic sources	Vibration monitoring in close proximity of PDT treatment. Vibration from PDT is less than from vibro driving	Made Ground: Sand, gravel size bricks and concrete, GWL @2.8m b.g.l.			
Yuschube. S.	1988	About interaction between single pile and soil	Unit weight increase from 1.65g/cm^3 to 1.89g/cm^3	Sandy soils	V=30kV, C=1-uF, W=4.5kJ		

Chapter 3
Development of approach to model single pulse pile performance in Plaxis 2D

3.1 Introduction

Computer modelling of a pulse pile performance involves simulation of a load test on cast-in-place single pile following its installation, that includes PDT treatment of wet grout mix and curing of the grout to a solid state. The Plaxis 2D programme was used to model the construction sequence:

- Create borehole
- Fill borehole with grout
- PDT treatment of the borehole
- Load test of the pile

PDT treatment has not been simulated in this software before, therefore several methods were considered to simulate the action of the shock wave expanding the walls of the borehole. Dynamic loading applied to the soil-structure surface have been considered as one of the methods. Other methods considered to model the PDT treatment included application of a statically distributed load to the soil-structure surface, volumetric strain in clusters of a pile body and change of properties of the cluster of soil surrounding the treatment zone.

A sensitivity analysis has been performed to justify the set of parameters used in the model. Mesh coarseness and model boundaries options have been compared to evaluate impact on the results. Input parameters of the loading amplitude, number of pulses and length of the shaft treated by the PDT have been specified and compared for different soil types and strata combinations.

This chapter focuses on the initial development of the model for a single pile treated by PDT. The main objective is to build a reliable model of a pulse pile and to obtain sensible results in different soil conditions.

3.2 Model formulation

Laboratory and especially field load testing in geotechnical engineering are quite expensive and the number of test possible means that any experimental investigation will be limited. This is a reason for carrying out a numerical analysis. Results of working and preliminary pulse piles load tests produced in Moscow were available to validate the numerical analysis.

Modelling of soil is different to modelling of solid structures because it is a three phase particulate material whose properties depend on the composition, fabric and structure. Therefore, special constitutive models of soil materials are required. The most developed and internationally recognised software for practitioners that provides required soil models is Plaxis. Parameters and modelling procedure used in this research can be found in the following sections of this chapter.

3.2.1 Model Geometry

A finite element model of a single pile has been simulated in the two-dimensional version of Plaxis software. An axisymmetric system has been chosen for a cylindrical body of soil containing a pile of specified diameter and length. The ratio of the pile to soil boundaries had to be sufficient to ensure that the boundaries had little effect on the results. In static calculation In dynamic calculation to avoid reflection of waves from the model boundaries there is a solution to apply absorbent boundaries as viscous dampers. Although a ratio of 10 to 1 is often recognised as being satisfactory (Dey (2011)) for the size of model geometry, several combinations of vertical and horizontal boundaries have been compared in this chapter to avoid model size impact on calculation results.

3.2.2 Modelling procedure

This section describes the initial development of the Plaxis model of a single pile, including geometry, material properties, calculation sequence sensitivity analysis of model boundaries, mesh coarseness and soil properties.

Once the mesh size and mesh coarseness had been established, further analyses were performed using the following modelling procedure. Basic models were specified for each case to compare different soil properties and their influence on results of computation.

1. An axisymmetric model with 15-noded elements was chosen to simulate a single pile cluster surrounded by a homogeneous soil layer. Single pile is a cylindrical shape structure that can be considered isotropic in horizontal plane. The research is focused on micropiles of a small diameter, therefore to obtain reliable results of modelling it is required to apply detailed meshing and number of nodes and stress point for a fourth order interpolation for displacements as recommended in Plaxis Reference Manual (2017).
2. The material set for the basic model was a coarse grained soil specified as drained sand using the Mohr – Coulomb constitutive model. Unsaturated and saturated unit weights were specified followed by strength and stiffness soil parameters. Default groundwater properties and flow parameters were set as a standard data set for medium soil type. An interface parameter, R_{inter}, of unity was considered for the basic model of a bored cast-in-situ concrete pile. K_0 lateral pressure settings are, by default, determined automatically using Jaky's (1948) formula for normally consolidated soils $K_0 = 1 - \sin\phi'$ or Mayne & Kulhawy (1982) for over-consolidated soils $K_{0(OC)} = K_{0(NC)} * OCR^{\sin\phi'}$.
3. The material of a pile was specified for all construction phases. For the installation phase, the pile material was specified as fresh mortar using a linear elastic constitutive model, with non-porous drainage type. Only unit weight and stiffness parameters have to be specified for this type of soil model. For the pile load testing, in which the fresh mortar is converted to concrete, concrete parameters have been specified using a linear elastic material model.
4. The model geometry was set with the axis along the center line of a pile assuming a single pile as a cluster of elements of 0.15m radius, 10m long (the geometry of the piles used in the field tests) and as a soil cluster of 30m width and 30m height. Mesh coarseness was specified as medium with enhanced mesh refinements. Groundwater level was assumed at 1m below existing ground level because it is typical for many UK soils.
5. The static load test was modelled by applying a uniformly distributed load based on the assumption that forces *act on the boundary of a circle subtending an angle of 1 radian* (Brinkgreve & Broere (2015)). Therefore, the test point load had to be recalculated to a load uniformly distributed over the cross-section of a pile and multiplied by a factor of 2π.

This is the modelling procedure that was used to simulate the basic model of a bearing pile. Parameters of consecutive models can be found in following sections of this chapter.

3.2.3 Material Properties

The soil model consisted of a single layer of soil; either a fine grained or a coarse grained soil. Materials used in the model include those for fine or coarse grained soil, fresh concrete mix for the installation phase and solid concrete for the load test phase. Constitutive models that were used for the materials are as in Table 3-1:

Table 3-1 – Material Models used in Plaxis

Material	Model	Purpose	Input Parameters
Coarse or fine grained soil Fresh concrete mix	Mohr-Coulomb	First approximation of soil behaviour	Effective Young's modulus E', effective Poisson's ratio ν', Effective cohesion c'_{ref}, Effective friction angle φ', Dilatancy angle ψ
Solid concrete	Linear Elastic	Structural Elements	Effective Young's modulus E', effective Poisson's ratio ν'

The Mohr-Coulomb material model has been used for coarse and fine grained soils as a first approximation of soil behaviour. It is a bi-linear elastic perfectly plastic model that requires only five input parameters and provides relatively quick and reliable calculation of the considered problem. More advanced models were not considered at this stage because the challenge was to model the effect of a pulse in expanding the pile.

At the pile installation phase, wet concrete behaves as very weak submerged granular material. Therefore, the fresh concrete mix was modelled using Mohr-Coulomb model. Solid concrete during the load test phase was considered to be linear elastic.

Soil parameters used in Plaxis for a basic single pile model are specified in Tables 3-2 and 3-3.

Table 3-2 – Soil material properties

Parameter	Name	Sand	Clay	Unit
Material Model	Model	Mohr-Coulomb	Mohr-Coulomb	-
Drainage type	Type	Drained	Undrained (C)	-
Soil unit weight above p.l.	γ_{unsat}	18	19	kN/m^3
Soil unit weight below p.l.	γ_{sat}	19	19	kN/m^3
Young's modulus at reference level	E_u	-	60000	kN/m^2
	E'	30000	-	kN/m^2
Undrained shear strength	$s_{u,ref}$	0.1	100	kN/m^2
Friction angle	φ'	33	0	°
Dilatancy angle	ψ	0	0	°
Poisson's ratio	v	0.3	0.495	-
Data set	-	Standard	-	-
Type	-	Coarse	-	-
Set parameters to default	-	Yes	-	-
Horizontal permeability	k_x	0.6	-	m/day
Vertical permeability	k_y	0.6	-	m/day
Interface strength type	Type	Rigid	Rigid	-
Interface strength	R_{inter}	1.0	1.0	-
K_0 determination	-	Automatic	Automatic	-
Lateral earth pressure coefficient	$K_{0,x}$	0.3982	0.5774	-

Material properties of a pile cluster specified in Table 3-3:

Table 3-3 – Pile material properties

Parameter	Name	Mortar	Concrete	Unit
Material Model	Model	Mohr-Coulomb	Linear Elastic	-
Drainage type	Type	Non-porous	Non-porous	-
Soil unit weight above p.l.	γ_{unsat}	24	24	kN/m^3
Soil unit weight below p.l.	γ_{sat}	24	24	kN/m^3
Young's modulus at reference level	E'	2,200,000	21,000,000	kN/m^2
Undrained shear strength	$s_{u,ref}$	5	-	kN/m^2
Friction angle	φ'	5	-	°
Dilatancy angle	ψ	0	-	°
Poisson's ratio	v	0.1	0.15	-
Interface strength type	Type	Rigid	Rigid	-
Interface strength	R_{inter}	1.0	1.0	-
K_0 determination	-	Automatic	Automatic	-
Lateral earth pressure coefficient	$K_{0,x}$	0.9128	1.0	-

For the soil sensitivity analyses, a range of soil parameters have been compared. Sensitivity analysis for soil properties has been based on the material properties specified in Tables 3-2 and 3-3. Sensitivity for soil strength, stiffness and

combinations of these two parameters have been considered. Other parameters have been assumed constant. Material properties for other tests are specified in further sections of this chapter.

3.2.4 Phases of calculation

Calculation phases for the basic and consecutive runs for a static model of a bored pile are as follows:

- Initial phase: calculation type: K0 procedure;
- Phase 1: set pile cluster material as mortar; calculation type: plastic; reset displacements to zero to obtain the relative displacement
- Phase 2: set pile cluster material as cured concrete; calculation type: plastic; reset displacements to zero
- Phase 3: apply uniform distributed load of 5000kN/m/m at the top of the pile; calculation type: plastic;

3.3 Model outputs

3.3.1 Sensitivity of the static model to mesh coarseness

Table 3-4 summarises the results of the model sensitivity to the mesh coarseness. A 20m high 50m diameter soil body was utilised for this comparison. The mesh coarseness ranged from very coarse to very fine. Both prescribed displacement and loading were considered for the pile load testing. Due to the increase in number of elements and nodes in the very fine mesh calculation case, the time required for each run was recorded as well as the size of the file on disk. Enhanced mesh refinement option has been tested for each case.

Table 3-4 – Summary of the mesh coarseness model sensitivity

Calculation case		Elements	Nodes	Running time	Size on disk	Settlement at the top of a pile	Vertical load
				min	Mb	m	kN
Prescribed loading case without enhanced mesh refinement							
mesh1	Very fine	25691	206571	13	610	0.015	412.3
mesh2	Fine	13546	109105	5	356	0.014	412.3
mesh3	Medium	6775	54723	3.5	133	0.012	412.3
mesh4	Coarse	3281	26619	1.5	66	0.01	412.3
mesh5	Very coarse	1704	13893	1	35.6	0.008	412.3
Prescribed loading case with enhanced mesh refinement							
mesh1+	Very fine	30825	47759	15	-	0.017	412.3
mesh2+	Fine	18154	146149	9	356	0.016	412.3
mesh3+	Medium	11014	88841	5	218	0.016	412.3
mesh4+	Coarse	6635	53667	3.5	134	0.016	412.3
mesh5+	Very coarse	4093	33219	2.5	83.5	0.016	412.3
Prescribed displacement case without enhanced mesh refinement							
mesh01	Very fine	25691	206571	-	496	0.025	512.5
mesh02	Fine	13546	109105	-	18.2	0.025	531.1
mesh03	Medium	6775	54723	2.5	134	0.025	569.4
mesh04	Coarse	3281	26619	1.5	134	0.025	605.7
mesh05	Very coarse	1704	13893	1	35.4	0.025	669.1
Prescribed displacement case with enhanced mesh refinement							
mesh01+	Very fine	30825	24759	14.5	609	0.025	494.3
mesh02+	Fine	18154	146149	-	24.8	0.025	497.7
mesh03+	Medium	11014	88841	5.5	218	0.025	498.2
mesh04+	Coarse	6635	53667	3.5	134	0.025	498.2
mesh05+	Very coarse	4093	33219	2.5	83.1	0.025	496.8

On Figure 3-1 images of mesh coarseness tested for model sensitivity can be compared.

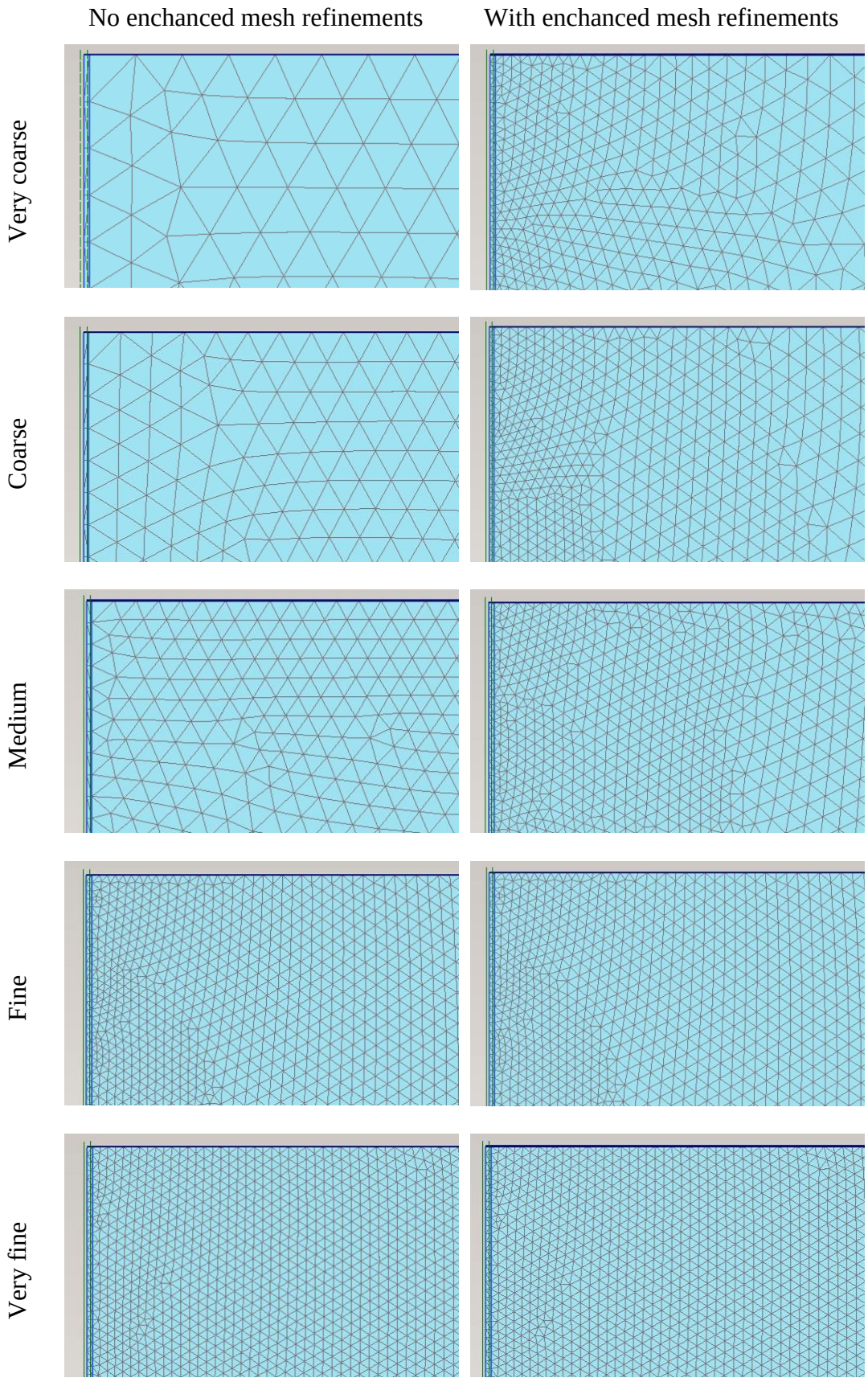

Figure 3-1 - Mesh coarseness tested for model sensitivity

Figure 3-2 is showing the difference between the mesh coarseness with and without local mesh refinements:

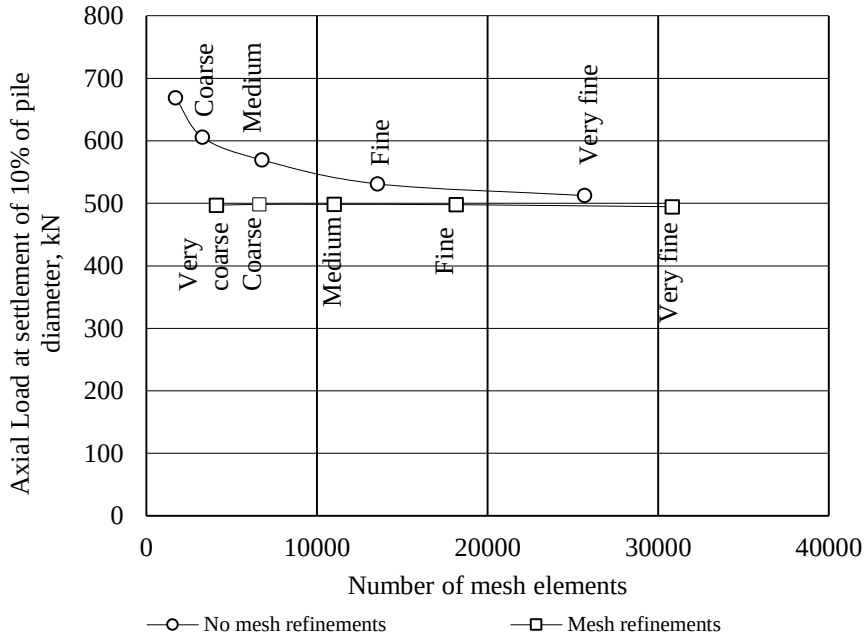

Figure 3-2 – Mesh Coarseness impact on predicted pile capacity

Comparing data for the calculation cases specified in Table 3-4 it can be seen, that number of elements and nodes; and the time of the runs were similar for prescribed loading or displacement. Enhanced mesh refinement increased the number of elements and nodes and time of the computation. Results of all cases show consistent reduction of pile capacity with increased detailing of mesh. However, local mesh refinement (see "Mesh refinements" on Figure 3-2) of the coarse mesh shows comparable results with the very fine mesh without local mesh refinement. It also takes less time to run and uses less space on disk. Therefore, it was decided to use local mesh refinement with medium mesh for the soil cluster.

Additional runs have been performed in Plaxis to study the effect of the mesh size for the PDT pile models using dynamics analysis. On figure 3-3 two load-settlement curves can be compared for a medium and very fine mesh with local refinements. As can be seen the curves for both cases have a very little deviation. It means that local refinement of the mesh allows to obtain reliable results even with the medium coarse mesh. Using local refinement of the mesh makes basic mesh coarseness of the model to have a little effect on the dynamic analysis in Plaxis.

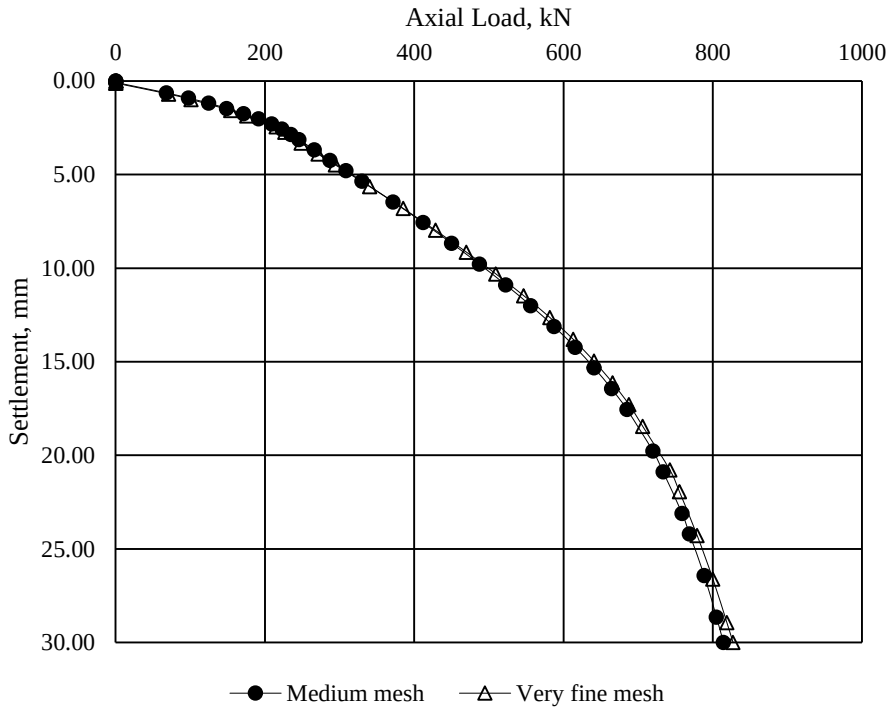

Figure 3-3 - Comparison of load-settlement curves of PDT pile performance for (a) - medium mesh with local refinements; (b) - very fine mesh with local refinements

3.3.2 Sensitivity of the model to the boundaries of the contour

Table 3-5 summarises the results of the model sensitivity to the horizontal and vertical size of the soil body. The dimeter ranged from 5m to 60m, and the depth from 15m to 50m. To determine the optimal size of the model to use in further investigation, the size of the file on disk and the number of nodes were compared as well. Prescribed displacement of 0.025m for the vertical loading were considered for all cases.

Table 3-5 – Summary of soil contour model sensitivity

Calculation case	x	y	Elements	Nodes	Size on disk	Settlement at the top of a pile	Vertical load
	m	m			Mb	m	kN
size 01	20	50	6635	53667	134	0.025	498.2
size 02	20	40	7131	57619	142	0.025	495.3
size 03	20	30	7376	59561	147	0.025	498.2
size 04	20	20	6953	56147	138	0.025	497.7
size 05	20	15	6506	52545	130	0.025	498.7
size 06	5	20	2915	23727	60.5	0.025	495.8
size 07	10	20	5000	40461	102	0.025	495.3
size 08	15	20	6404	51729	128	0.025	490.8
size 09	17	20	6736	54397	136	0.025	494.8
size 10	19	20	6836	55205	136	0.025	495.3
size 11	25	20	7473	60323	150	0.025	497.3
size 12	30	20	7526	60761	146	0.025	501.7
size 13	35	20	7352	59377	146	0.025	501.7
size 14	40	20	7217	58307	144	0.025	504.1
size 15	50	20	6626	53593	132	0.025	505.6
size 16	60	20	6143	49739	123	0.025	506.1
size 17	60	30	8582	69297	172	0.025	502.7
size 18	60	40	9755	78711	196	0.025	500.7
size 19	60	50	10804	87125	214	0.025	502.7
size 20	50	50	10723	86463	212	0.025	503.6
size 21	40	50	9961	80347	197	0.025	502.7
size 22	30	50	8385	67707	167	0.025	499.7
size 23	40	40	10054	81073	199	0.025	503.1
size 24	40	30	8782	70869	174	0.025	504.1
size 25	40	15	5881	47591	119	0.025	504.1
size 26	30	40	9012	72709	179	0.025	501.2
size 27	30	30	8752	70605	174	0.025	503.6
size 28	30	15	6422	51901	128	0.025	494.8
size 29	50	40	10236	82545	203	0.025	501.2
size 30	50	30	8922	72005	177	0.025	505.1
size 31	50	15	5326	43165	109	0.025	506.1
size 32	60	15	4905	-	99.7	0.025	507.1
size 33	10	15	5302	42857	106	0.025	498.7
size 34	10	30	4563	36991	93.8	0.025	489.8
size 35	10	40	4104	33341	85	0.025	489.5
size 36	10	50	3699	30119	77.2	0.025	483.8

Figure 3-4 shows the predicted axial load for a settlement of 10% of the pile diameter with respect to the ratio of the horizontal model dimensions between pile diameter, D, and diameter of the model, x. Curves are plotted for the cases of ratio of vertical dimensions between the length of the pile, L, and depth of the model, y.

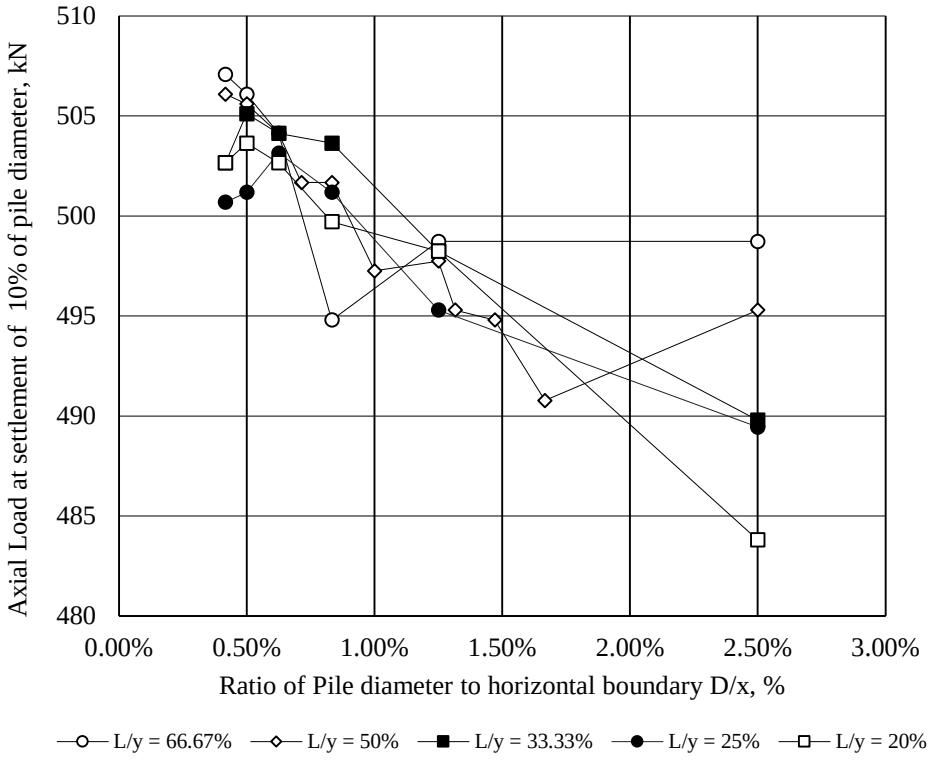

Figure 3-4 – Model boundaries impact on predicted pile capacity

An increase of the horizontal boundary *x* shows consistent improvement of the capacity of the pile at various vertical boundaries *y*. However varying the vertical boundary *y* has no consistent effect. It can be explained by the fact that for specified settlement of the modelled micropile takes place when the shaft friction is mobilised. The end bearing pressure bulb is located above zone of influence of y_{min} boundary. Horizontal ratio of 0.83% and vertical of 33.3% have been chosen for the further analysis as an average reliable boundary conditions. These ratios are relevant to 30m x 30m soil contour.

3.3.3 Sensitivity of the single bored pile model to soil properties

3.3.3.1 Load test model of a single bored pile

Table 3-6 summarises the cases calculated to analyse the sensitivity of the bored pile model to the variation of coarse grained soil strength and stiffness parameters. Settlement at the top of the pile has been measured for each case with a prescribed vertical test load.

Table 3-6 – Sensitivity to coarse grained soil with φ' from 28° to 40°

Bored pile case	Soil properties						Results	
	φ'	γ_{unsat}	γ_{sat}	k_x/k_y	E_{ref}	ν	Settlement at the top of a pile	Vertical load
	°	kN/m^3	kN/m^3	m/day	kN/m^2	-	m	kN
Sensitivity to variation of soil strength – prescribed vertical test load								
sand_phi28	28	18	19	0.1206	30000	0.3	0.08623	353.4
sand_phi29	29	18	19	0.1206	30000	0.3	0.07549	353.4
sand_phi30	30	18	19	0.1206	30000	0.3	0.06722	353.4
sand_phi31	31	18	19	0.1206	30000	0.3	0.06097	353.4
sand_phi32	32	18	19	0.1206	30000	0.3	0.05546	353.4
sand_phi33	33	18	19	0.1206	30000	0.3	0.05061	353.4
sand_phi34	34	18	19	0.1206	30000	0.3	0.04634	353.4
sand_phi35	35	18	19	0.1206	30000	0.3	0.04229	353.4
sand_phi36	36	18	19	0.1206	30000	0.3	0.03893	353.4
sand_phi37	37	18	19	0.1206	30000	0.3	0.03652	353.4
sand_phi38	38	18	19	0.1206	30000	0.3	0.03447	353.4
sand_phi39	39	18	19	0.1206	30000	0.3	0.0326	353.4
sand_phi40	40	18	19	0.1206	30000	0.3	0.03042	353.4

Figure 3-5 shows the load-settlement curves for the models of coarse grained soils with an angle of friction from 28° to 40°. Cut-off have been set on the calculated load of 353.4kN. This value of the axial load has been back-calculated from the axisymmetric distributed vertical load of $5000kN/m^2$ specified in Plaxis model.

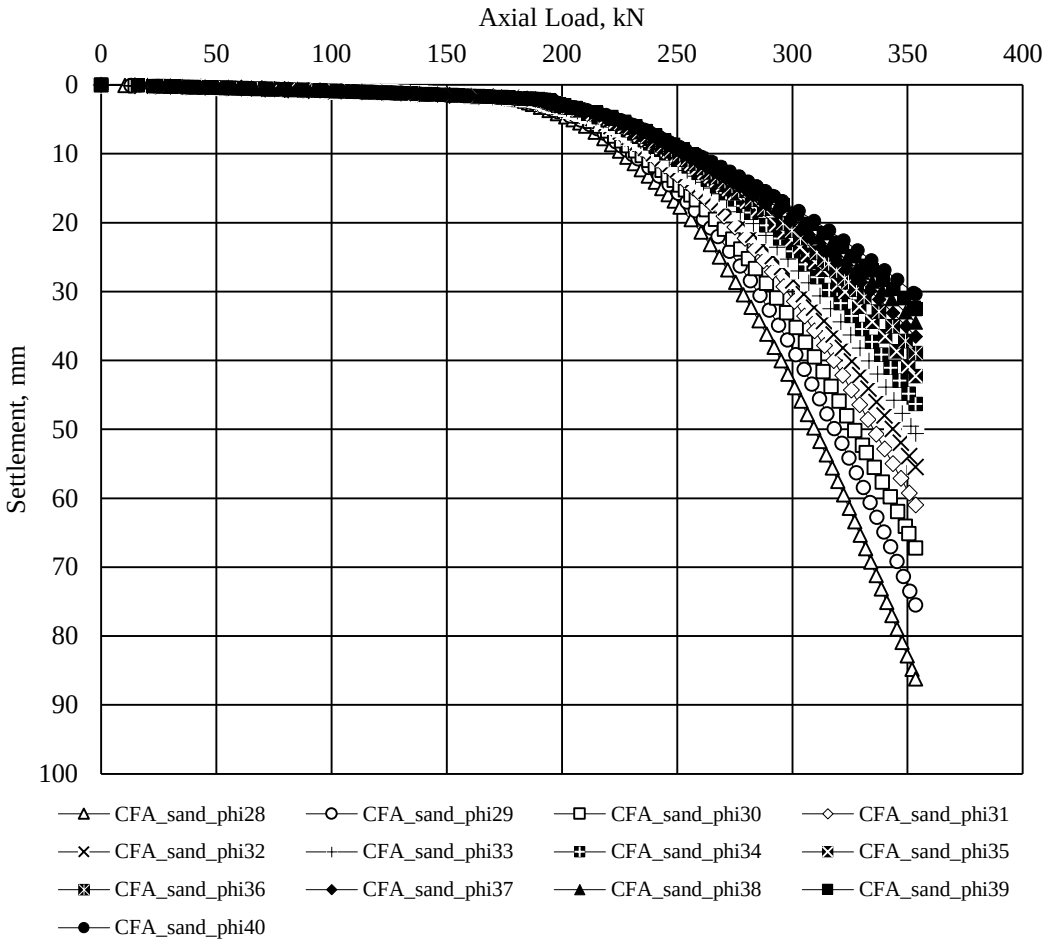

Figure 3-5 – Sensitivity to coarse grained soil with φ' from 28° to 40°

Figure 3-5 shows that increase of a friction angle of a coarse-grained soil reduces the settlement at the top of the pile at constant maximum load at constant stiffness and variable angle of friction. Safe working load at pile settlement of 10% of pile diameter varies from 275kN for φ'=28°, to 353.4kN for φ'=40°.

Stiffness parameters of coarse grained soils have been compared as per Table 3-7:

Table 3-7 – Sensitivity to coarse grained soil with E' from 7500kN/m2 to 65000kN/m2

Bored pile case	Soil properties						Results	
	φ'	γ_{unsat}	γ_{sat}	k_x/k_y	E_{ref}	ν	Pile Settlement	Vertical load
	°	kN/m^3	kN/m^3	m/day	kN/m^2	-	m	kN
Sensitivity to variation of soil stiffness – prescribed vertical test load								
sand_E7500	32	18	19	0.1206	7500	0.3	0.2187	353.4
sand_E13125	32	18	19	0.1206	13125	0.3	0.1253	353.4
sand_E18750	32	18	19	0.1206	18750	0.3	0.08817	353.4
sand_E24375	32	18	19	0.1206	24375	0.3	0.06796	353.4
sand_E30000	32	18	19	0.1206	30000	0.3	0.05546	353.4
sand_E35000	32	18	19	0.1206	35000	0.3	0.04764	353.4
sand_E40000	32	18	19	0.1206	40000	0.3	0.04185	353.4
sand_E45000	32	18	19	0.1206	45000	0.3	0.03719	353.4
sand_E50000	32	18	19	0.1206	50000	0.3	0.03358	353.4
sand_E55000	32	18	19	0.1206	55000	0.3	0.03063	353.4
sand_E60000	32	18	19	0.1206	60000	0.3	0.02809	353.4
sand_E65000	32	18	19	0.1206	65000	0.3	0.02594	353.4

Figure 3-6 shows the load-settlement curves for models of coarse grained soils with drained stiffness from 7,500kN/m^2 to 65,000kN/m^2. The same cut-off as in strength sensitivity analysis have been set on the calculated load of 353.4kN.

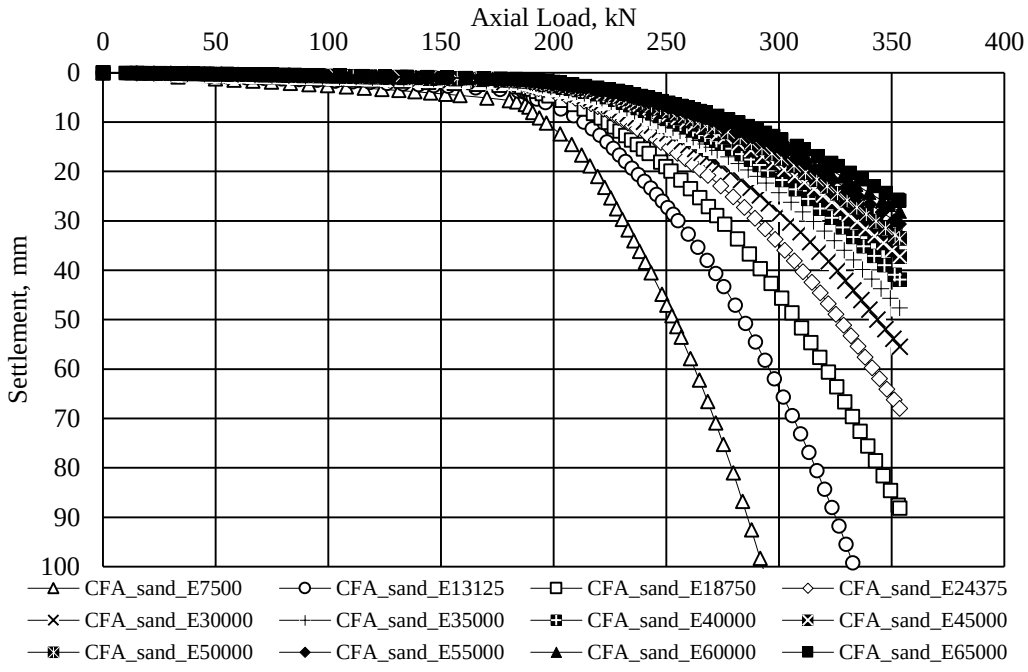

Figure 3-6 – Sensitivity to coarse grained soil with E' from 7,500kN/m^2 to 65,000kN/m^2

Figure 3-6 shows that an increase of a soil stiffness moduli of a coarse-grained soil reduces the settlement at the top of the pile at a constant maximum load. The safe working load at pile settlement of 10% of pile diameter varies from 230kN for E'=7,500kN/m^2, to a projection of approximately 375kN for E'=65,000kN/m^2.

Combination of strength and stiffness parameters of coarse grained soil have been tested as shown in Table 3-8. The relation between strength and stiffness was based on empirical correlations with SPT N values. According to CIRIA C760 (Gaba et al. (2017)) stiffness values of normally consolidated and overconsolidated coarse-grained soils are E'=N_{60} (MPa) and E'=2N_{60} (MPa) respectively. Therefore stiffness modulus for granular soils has been chosen using conservative E' = 1500 x N (kPa)Angles of friction for each value of stiffness modulus were obtained from Peck, Hanson & Thorburn (1974) (see Figure 3-7):

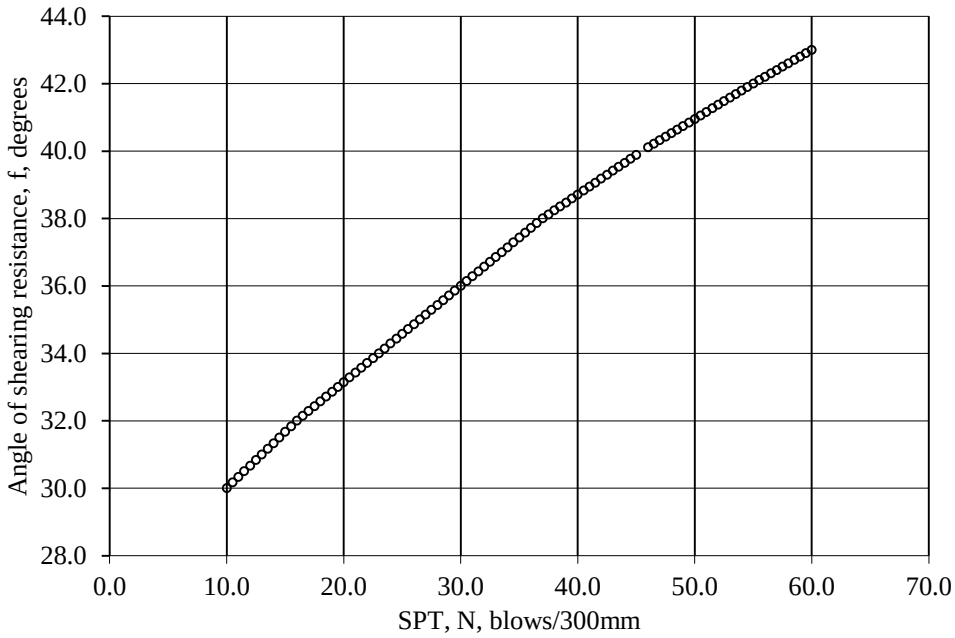

Figure 3-7 – Shearing resistance (Peck et al. (1974))

Table 3-8 – Sensitivity to coarse grained soil with φ' from 29° to 40° and E' from 7,500kN/m^2 to 65,000kN/m^2

Bored pile case	Soil properties						Results	
	φ'	γ_{unsat}	γ_{sat}	k_x/k_y	E_{ref}	ν	Settlement at the top of a pile	Vertical load
	°	kN/m^3	kN/m^3	m/day	kN/m^2	-	m	kN
Sensitivity to variation of strength and stiffness – prescribed vertical test load								
sand_E7500phi29	29	18	19	0.1206	7500	0.3	0.2989	353.4
sand_E13125phi30	30	18	19	0.1206	13125	0.3	0.1527	353.4
sand_E18750phi31	31	18	19	0.1206	18750	0.3	0.09693	353.4
sand_E24375phi32	32	18	19	0.1206	24375	0.3	0.06796	353.4
sand_E30000phi33	33	18	19	0.1206	30000	0.3	0.05061	353.4
sand_E35000phi34	34	18	19	0.1206	35000	0.3	0.03972	353.4
sand_E40000phi35	35	18	19	0.1206	40000	0.3	0.03202	353.4
sand_E45000phi36	36	18	19	0.1206	45000	0.3	0.02645	353.4
sand_E50000phi37	37	18	19	0.1206	50000	0.3	0.02225	353.4
sand_E55000phi38	38	18	19	0.1206	55000	0.3	0.01918	353.4
sand_E60000phi39	39	18	19	0.1206	60000	0.3	0.01676	353.4
sand_E65000phi40	40	18	19	0.1206	65000	0.3	0.01459	353.4

Figure 3-8 shows the load-settlement curves for the models of coarse grained soils with angle of shearing resistance from 28° to 40° and drained stiffness from 7,500kN/m^2 to 65,000kN/m^2. The same cut-off was set for the calculated load of 353.4kN as for the two previous cases.

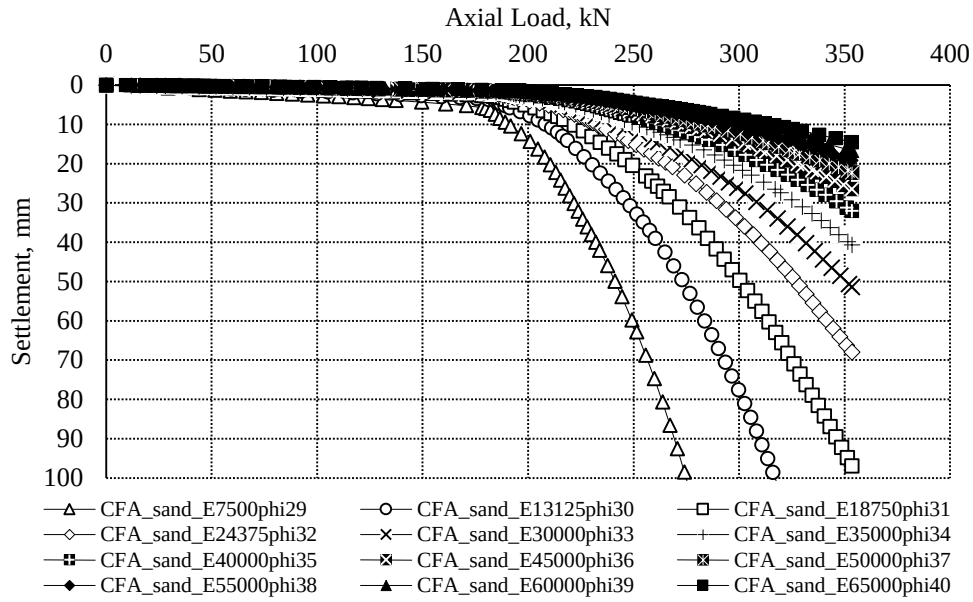

Figure 3-8 – Sensitivity to coarse grained soil with φ' from 29° to 40° and E' from 7,500kN/m^2 to 65,000kN/m^2

Figure 3-8 shows that increase of a soil stiffness moduli of a coarse-grained soil reduces the settlement at the top of the pile at constant maximum load. Safe working load at pile settlement of 10% of pile diameter varies from 221kN for φ'=29° and *E'*=7,500kN/m^2, to a projection of approximately 475kN for φ'=40° and *E'*=65,000kN/m^2.

Additional set of runs were performed with prescribed displacement as listed in Table 3-9.

Table 3-9 – Sensitivity to coarse grained soil with φ' from 29° to 40° and E' from 7500kN/m2 to 65000kN/m2. Case of prescribed displacement of 10% of pile diameter

Bored pile case	Soil properties						Results	
	φ'	γ_{unsat}	γ_{sat}	k_x/k_y	E_{ref}	ν	Settlement at the top of a pile	Vertical load
	°	kN/m^3	kN/m^3	m/day	kN/m^2	-	m	kN
Sensitivity to variation of strength and stiffness – prescribed displacement								
sand_E7500phi29d	29	18	19	0.1206	7500	0.3	0.03	221.5
sand_E13125phi30d	30	18	19	0.1206	13125	0.3	0.03	247.2
sand_E18750phi31d	31	18	19	0.1206	18750	0.3	0.03	269.9
sand_E24375phi32d	32	18	19	0.1206	24375	0.3	0.03	290.3
sand_E30000phi33d	33	18	19	0.1206	30000	0.3	0.03	310.5
sand_E35000phi34d	34	18	19	0.1206	35000	0.3	0.03	328.8
sand_E40000phi35d	35	18	19	0.1206	40000	0.3	0.03	347.6
sand_E45000phi36d	36	18	19	0.1206	45000	0.3	0.03	367.1
sand_E50000phi37d	37	18	19	0.1206	50000	0.3	0.03	386.7
sand_E55000phi38d	38	18	19	0.1206	55000	0.3	0.03	407.4
sand_E60000phi39d	39	18	19	0.1206	60000	0.3	0.03	426.8
sand_E65000phi40d	40	18	19	0.1206	65000	0.3	0.03	446

Figure 3-9 shows the load-settlement curves for the models of coarse grained soils with angle of shearing resistance from 28° to 40° and drained stiffness from 7,500kN/m^2 to 65,000kN/m^2. The cut-off was set at a prescribed displacement of 0.03m equivalent to 10% of pile diameter. The value of load at this settlement is the nominal working load.

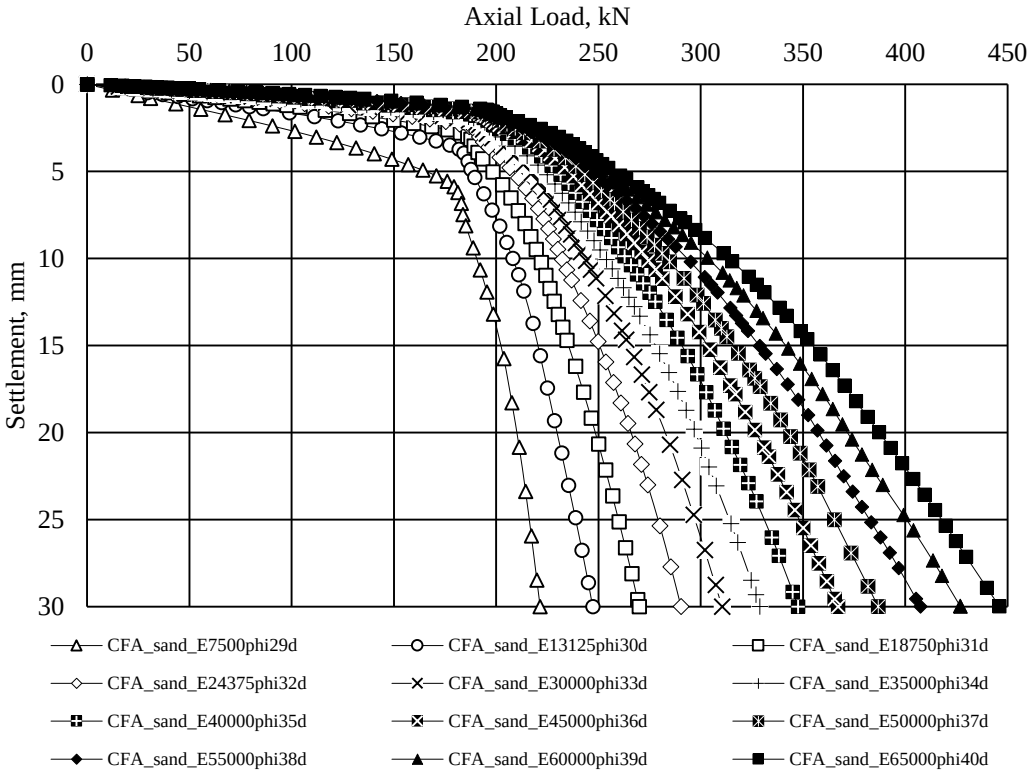

Figure 3-9 – Sensitivity to coarse grained soil with φ' from 29° to 40° and E' from 7500kN/m^2 to 65000kN/m^2. Case of prescribed displacement of 10% of pile diameter

The pile model in coarse grained soil has been analysed for sensitivity to the variable properties of strength and stiffness. To explore the boundaries of results following sets have been considered:

- Variable strength at constant stiffness
- Variable stiffness at constant strength
- Variable strength and stiffness

Figure 3-10 and Figure 3-11 show how settlement is reducing with increase of strength of coarse grained soil. Two curves are showing the difference of approaches for the one with permanent stiffness and combined strength and stiffness sensitivity analysis. Thus stiffness combined with strength at the lower boundary shows much more conservative pile performance due to the constant E' = 30,000kN/m^2 for the sensitivity analysis of a single parameter of friction angle. At the upper boundary, the graph shows more optimistic result, due to increase of both strength and stiffness as opposed to only a friction angle for a single parameter sensitivity calculations.

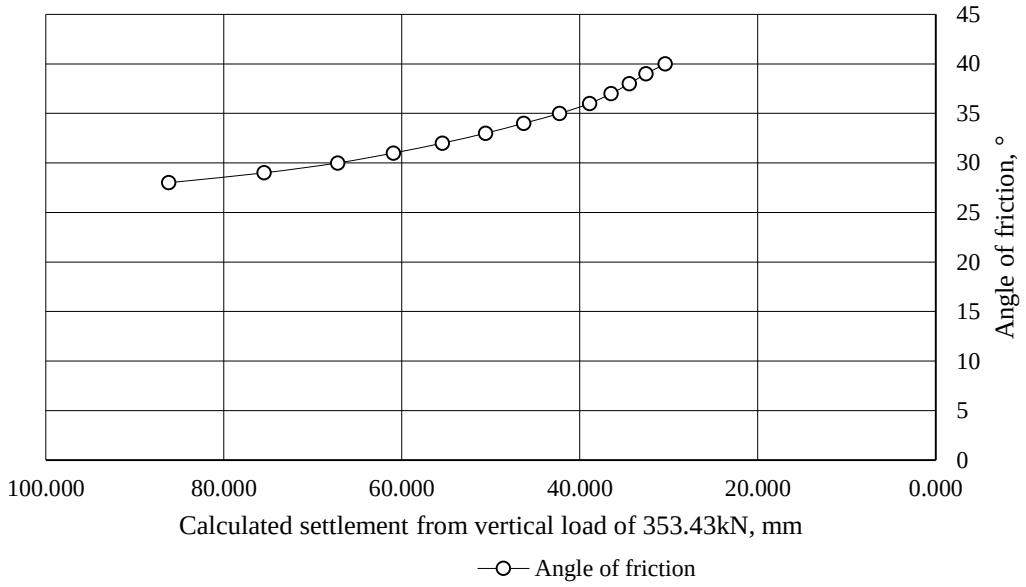

Figure 3-10 – Predicted deflection from strength parameter sensitivity calculation

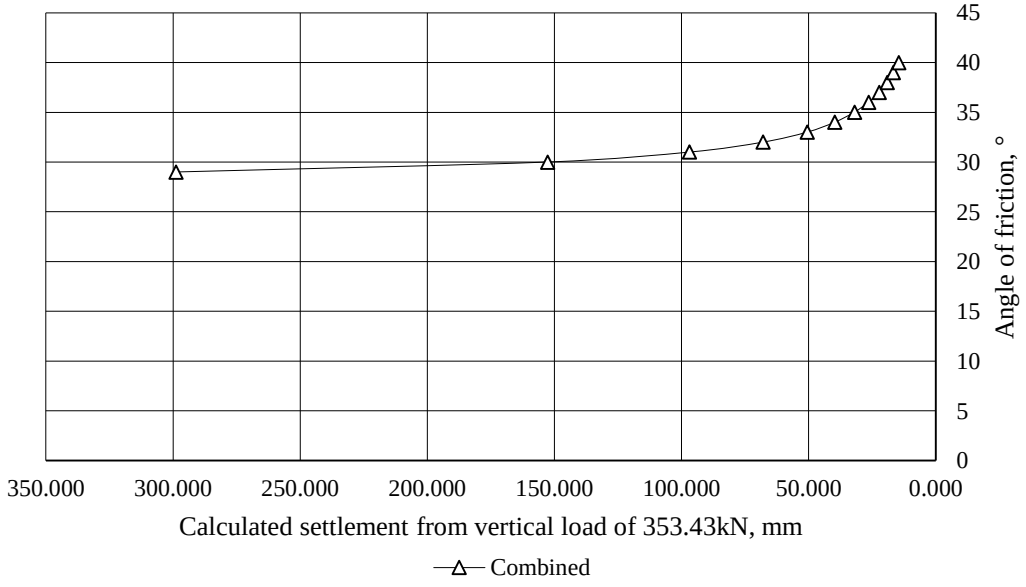

Figure 3-11 – Predicted deflection from strength and stiffness parameters sensitivity calculation

Both curves for strength only and for combined strength and stiffness sensitivity show an improved pile capacity in granular soils with increase of soil properties.

Figure 3-12 summarises sensitivity of the results of a single pile model runs to increase of stiffness parameter of soil with all other parameters being constant. Figure

3-13 summarises sensitivity of the results of a single pile model runs to increase of both strength and stiffness parameters with all remaining parameters being constant.

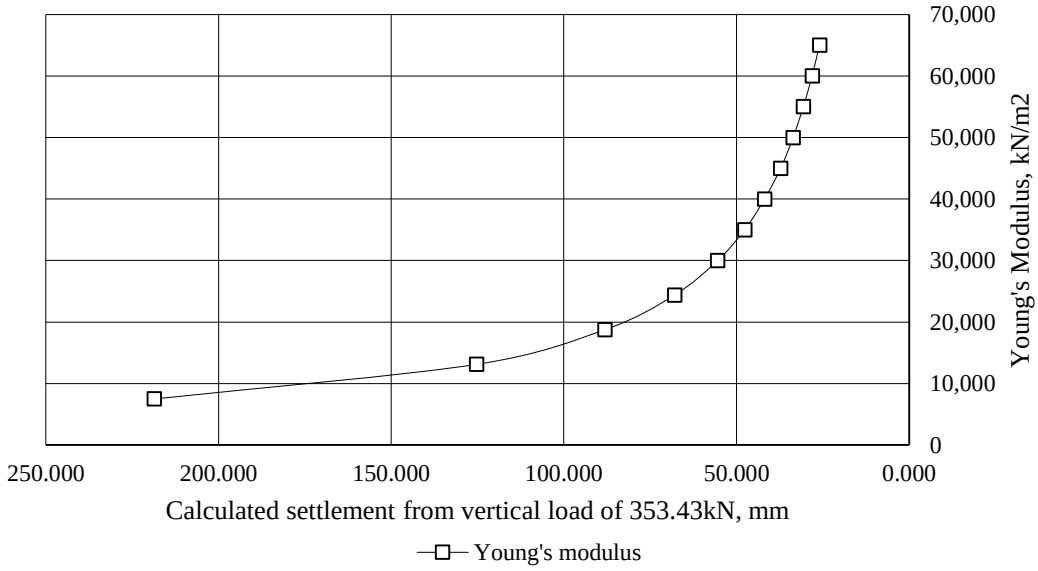

Figure 3-12 – Predicted deflection from stiffness parameter sensitivity calculation

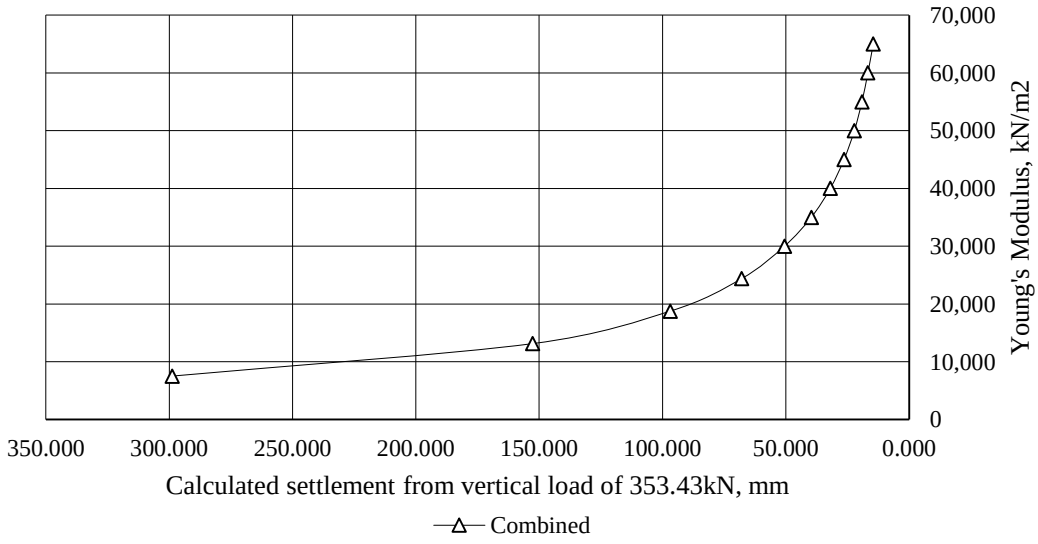

Figure 3-13 – Predicted deflection from strength and stiffness parameters sensitivity calculation

Figure 3-12 and Figure 3-13 show the reduction of settlement by increasing of the stiffness of coarse grained soil. Increasing of soil stiffness reduces settlement at the top of the pile.

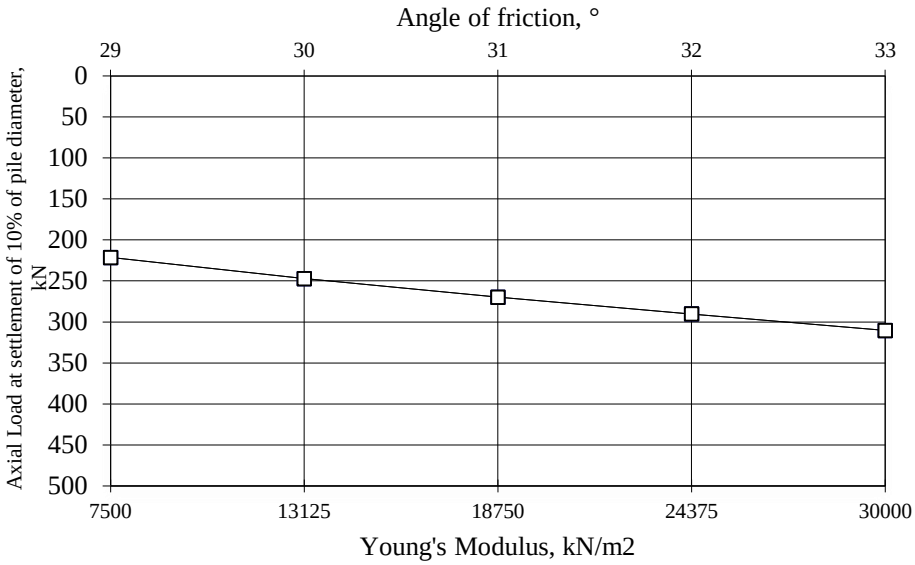

Figure 3-14 and 3-13 show model performance for combined strength and stiffness sensitivity analyses. Increase of angle of friction together with Young's modulus increase pile working load at settlement of 10% of pile diameter. Figure below also summarises relevant values of strength and stiffness considered in the sensitivity analyses.

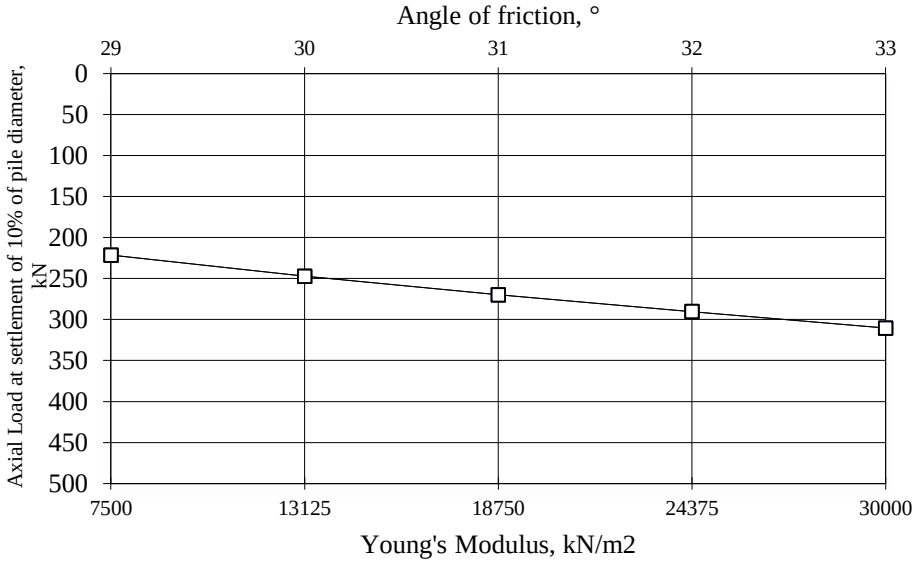

Figure 3-14 – Sensitivity analysis of combined strength and stiffness parameters of coarse grained soils with angle of friction up to 33° and stiffness modulus up to 30000kN/m^2

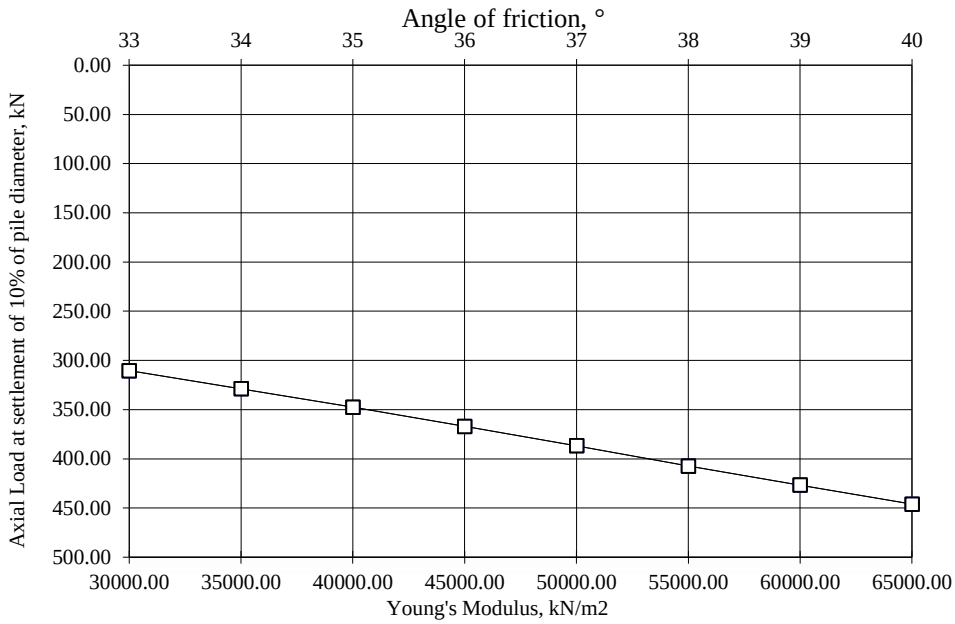

Figure 3-15 - Sensitivity analysis of combined strength and stiffness parameters of coarse grained soils with angle of friction up to 40° and stiffness modulus up to 65000kN/m^2

Results of the sensitivity analysis have proven that an increase of the coarse-grained soil strength, stiffness or combination of those parameters increases pile capacity and decreases settlement. Table 3-10 summarises the results of the sensitivity analysis of fine grained soil properties for a single bored pile model. Fine grained soils have been modelled as undrained cohesive material using Mohr-Coulomb Undrained (C) option. Modelling of undrained soil model in Plaxis is described in detail in Chapter 4. Undrained stiffness has been calculated as $400c_u$ for all fine grained soil cases.

Table 3-10 – Sensitivity to fine grained soil properties of Plaxis 2D model of the bored pile

Bored pile case	Soil properties						Results	
	c_u	γ_{unsat}/ γ_{sat}	Type	k_x/ k_y	E_u	ν	|u|	Vertical load
	kN/m^2	kN/m^3		m/day	kN/m^2	-	m	kN
Sensitivity to variation of strength and stiffness – prescribed displacement								
CFA_clay_u_cu20	20	19	Medium	0	8000	0.495	0.15	243.58
CFA_clay_u_cu40	40	19	Medium	0	16000	0.495	0.15	490.84
CFA_clay_u_cu60	60	19	Medium	0	24000	0.495	0.15	742.20
CFA_clay_u_cu80	80	19	Medium	0	32000	0.495	0.15	989.60
CFA_clay_u_cu100	100	19	Medium	0	40000	0.495	0.15	1245.48
CFA_clay_u_cu120	120	19	Medium	0	48000	0.495	0.15	1496.42
CFA_clay_u_cu140	140	19	Medium	0	56000	0.495	0.15	1747.35
CFA_clay_u_cu160	160	19	Medium	0	64000	0.495	0.15	1998.29
CFA_clay_u_cu180	180	19	Medium	0	72000	0.495	0.15	2249.93
CFA_clay_u_cu200	200	19	Medium	0	80000	0.495	0.15	2500.86
CFA_clay_u_cu220	220	19	Medium	0	88000	0.495	0.15	2751.80

Figure 3-16 shows load-settlement curves for the models of fine grained soils with undrained cohesion from 20 kN/m^2 to 220 kN/m^2 and undrained stiffness from 8,000kN/m^2 to 88,000kN/m^2.

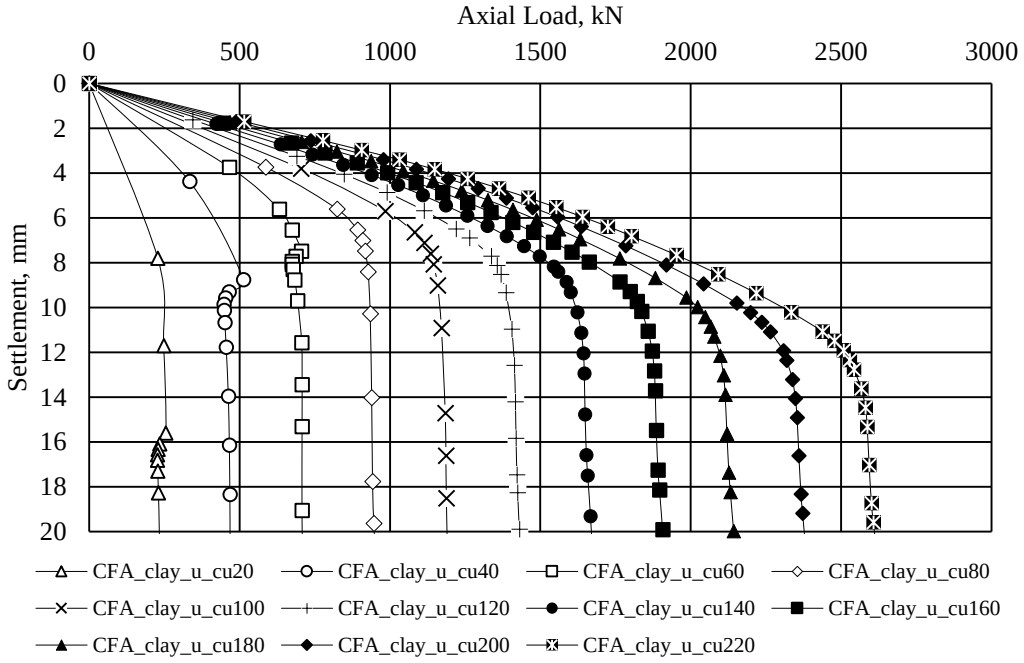

Figure 3-16 – Sensitivity to fine grained soil with cu from 20kN/m^2 to 220kN/m^2 and E_u from 8,000kN/m^2 to 88,000kN/m^2

Figure 3-17 shows the performance for combined strength and stiffness sensitivity analyses. Increase of undrained parameters of undrained shear strength and Young's modulus increase pile capacity at settlement of 10% of pile diameter.

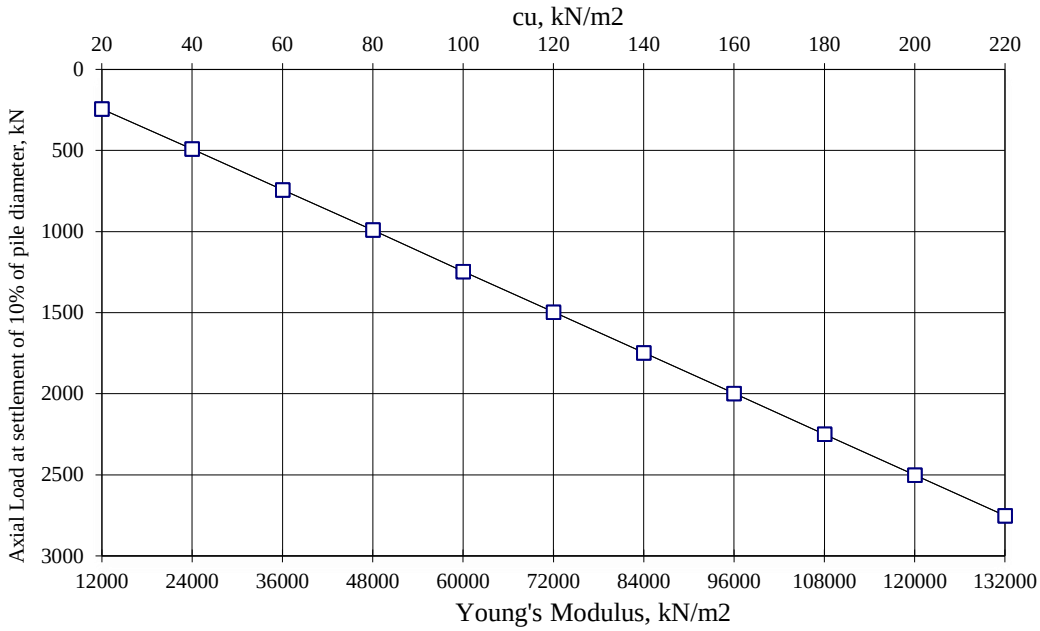

Figure 3-17 – Sensitivity analysis of combined strength and stiffness parameters of fine grained soils

3.3.4 Sensitivity of the model to dynamic inputs

3.3.4.1 Load test model of the pulse pile

There are several options to model in Plaxis a single pile treated by a PDT.

1. Manually change the properties of the soil cluster around the pile
2. Expand the pile cluster using volumetric strain to represent the expansion due to the discharge.
3. Apply a distributed load to the soil cluster to represent the force due to the discharge.
4. Use dynamic loading to model the discharge.

Simulating the impact of pulse discharges, it is possible to change the material properties of a soil cluster surrounding the pile over a treatment zone. It is a simple option that could provide increased capacity of a pile. However, all the parameters of the improved soil in compacted zone have to be specified manually that makes results of the calculation not plausible.

Another option is to apply volumetric strain in clusters. This is a good approximation of simulation of a pulse pile expansion in surrounding strata. As in previous method the result of the treatment has to be specified as input data manually. Displacements and stresses in soil are calculated in the model. However, there are limitations on the volumetric strain that can be specified in the model, and pressure from the pulse discharge treatment is the output of the model, not the input. A volumetric strain applied to the pile cluster is a result of a pulse treatment, that does not take into account a dynamic impact. To calculate the volumetric strain of the treated zone of pile cluster it is required to apply a loading on pile soil interface.

Attempts to simulate the source of treatment by applying the distributed load to the structure-soil surface is possible in Plaxis by means of static or dynamic load. Use of a static distributed load is a robust method to obtain expansion of the pile body. The equivalent static pressure can be applied to the walls of borehole as suggested in Annex D of BS EN 1991-1-7:2006 (2006) for the internal explosions case. However, to be able to calculate equivalent pressure, laboratory and field tests have to be performed to obtain reliable values for various soil and grout combinations. Also, it does not take into account the time of action, that in case of PDT treatment is critical. Modelling dynamics in Plaxis allows to specify not only the amplitude of the dynamic load but also the time and frequency of its action. The amplitude and time multiplier of the dynamic load can be calculated using published data (see Figure 4-9 from Park et al. (2011)).

Dynamic calculation in Plaxis 2D allows to model variable loading when it is required to consider stress waves or vibrations propagated in soil. Dynamic loading can be specified by means of dynamic load or dynamic prescribed displacement. Simulation of PDT treatment as horizontal distributed dynamic load have been applied in this study to obtain theoretical expansion values and analyse pulse pile performance. Values of the pressure on the walls have been applied based on available information, therefore dynamic prescribed displacement has not been considered.

3.3.4.2 Analysis in coarse grained soil

During this initial sensitivity analysis of the pulse pile using dynamic loading, up to 10 pulses were tested in coarse grained soil. 5 to 10 pulses is approximate number of pulses applied in industry. A single pile was specified as a soil cluster of 150mm radius 10m long, the geometry of the piles used in the field tests . Material properties

of the pile cluster for the dynamic load calculation were assumed as wet concrete/mortar (see Table 3-3). Sand properties were the same as the relevant CFA pile model (e.g. in Table 3-9, the calculation case “sand_E30000phi33d” has an angle of friction of 33° and Young’s modulus of 30,000 kN/m^2). Dynamic load was applied to the bottom 1m of a pile that simulated under-reaming from the pulse treatment at one level. A dynamic load amplitude of 5000kN/m/m was specified for a pulse 0.002s long with 0,001s time between pulses. Vertical load at the top of the pile for the load test simulation was specified as a prescribed displacement of 10% of pile diameter applied at the top of pile (see detail on Figure 3-18).

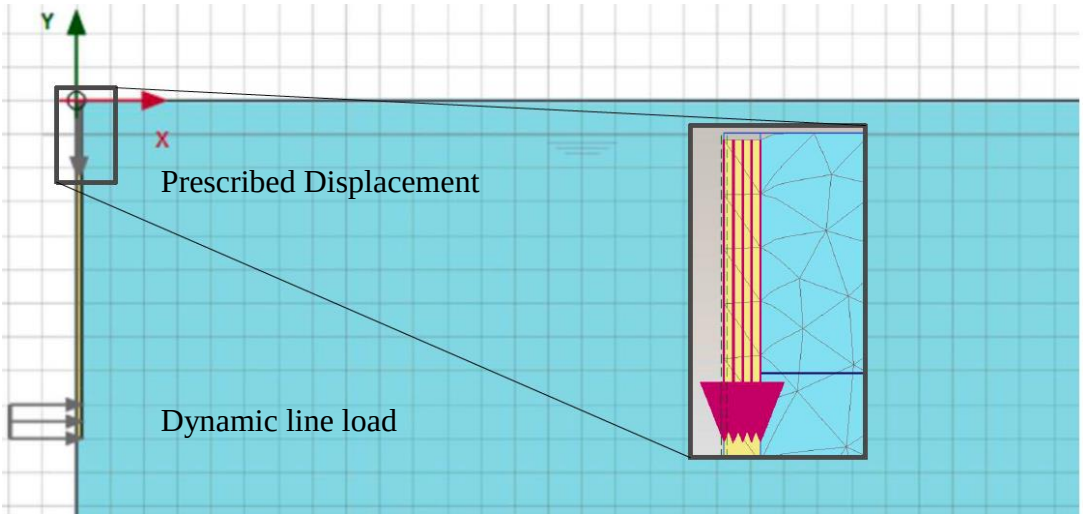

Figure 3-18 – Pulse pile model layout showing dynamic line load and detail on applied prescribed displacement

Table 3-11 – Pulse Pile model sensitivity to the number of pulses in coarse grained soil

Calculation case	Augered Diameter	Pile Length	Results		Comments
			Max Defl.	Vertical Load	
	m	m	m	kN	
Bored_sand_E30Kphi33	0.3	10	0	310.45	cfa pile
Pulse_sand_dyn1p	0.3	10	0.0347	406.30	1 pulse
Pulse_sand_dyn2p	0.3	10	0.0533	448.78	2 pulses
Pulse_sand_dyn3p	0.3	10	0.0764	545.34	3 pulses
Pulse_sand_dyn4p	0.3	10	0.0818	622.67	4 pulses
Pulse_sand_dyn5p	0.3	10	0.1278	814.30	5 pulses
Pulse_sand_dyn6p	0.3	10	0.1648	892.76	6 pulses
Pulse_sand_dyn7p	0.3	10	0.1800	1065.24	7 pulses
Pulse_sand_dyn8p	0.3	10	0.2155	1124.61	8 pulses
Pulse_sand_dyn9p	0.3	10	0.2571	1308.39	9 pulses
Pulse_sand_dyn10p	0.3	10	0.2717	1280.12	10 pulses

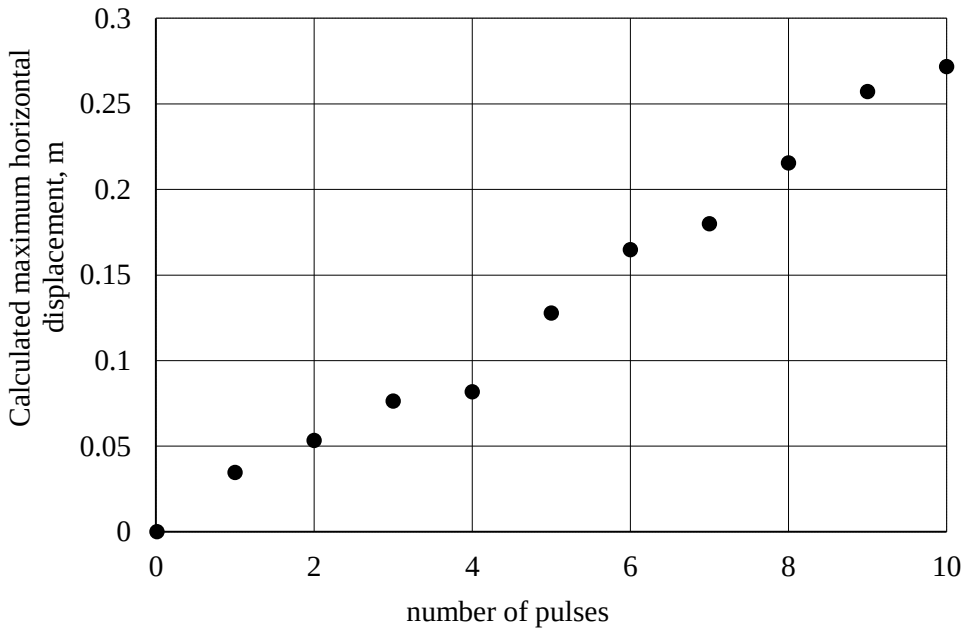

Figure 3-19 – Calculated expansion from dynamic load

Figure 3-19 shows the increase of horizontal displacement with the number of pulses. Mohr-Coulomb drained material model shows linear relation of horizontal displacement to the number of pulses of up to 10 pulses. Figure 3-20 shows the pile

capacity at settlement of 10% of pile diameter depending on the number of pulses of horizontal distributed dynamic loading.

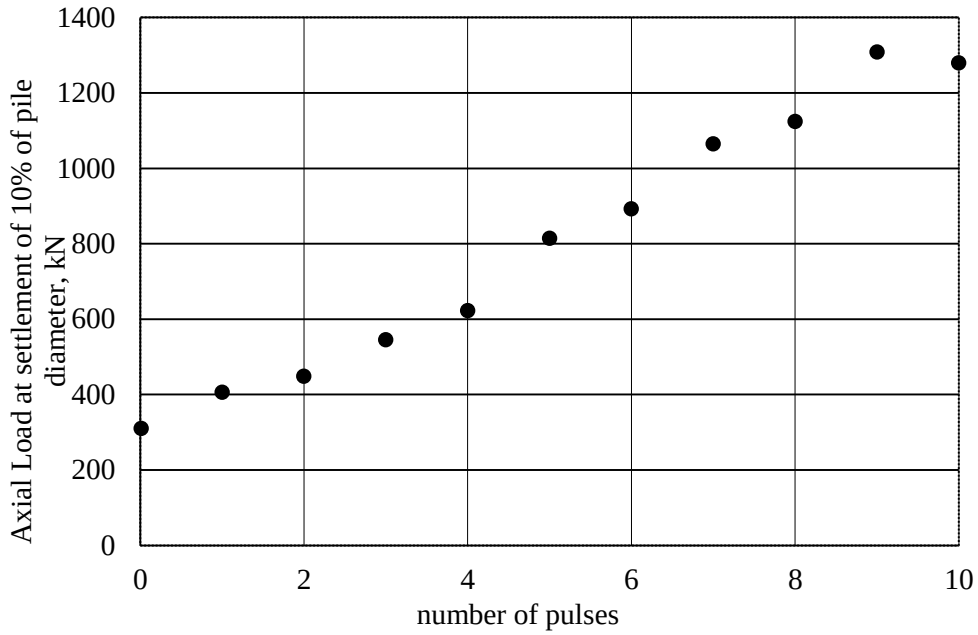

Figure 3-20 – Pile capacity depending on number of pulses

The results on Figure 3-20 show that an increase in the number of pulses improves the bearing capacity of a pile. This is consistent with available experimental data. The value of the capacity of the pulse pile after 10 pulses is excessive for 300mm diameter pile, it might not have enough structural rigidity for specified axial load. This can be explained by the increased diameter of the bottom 1m of a pile shaft (see Figure 3-21). Deformed mesh illustrates the expansion of the borehole after 10 pulses modelled as dynamic line load applied to drained Mohr-Coulomb material model. Dynamic load effectively under-reams the bottom of the pile.

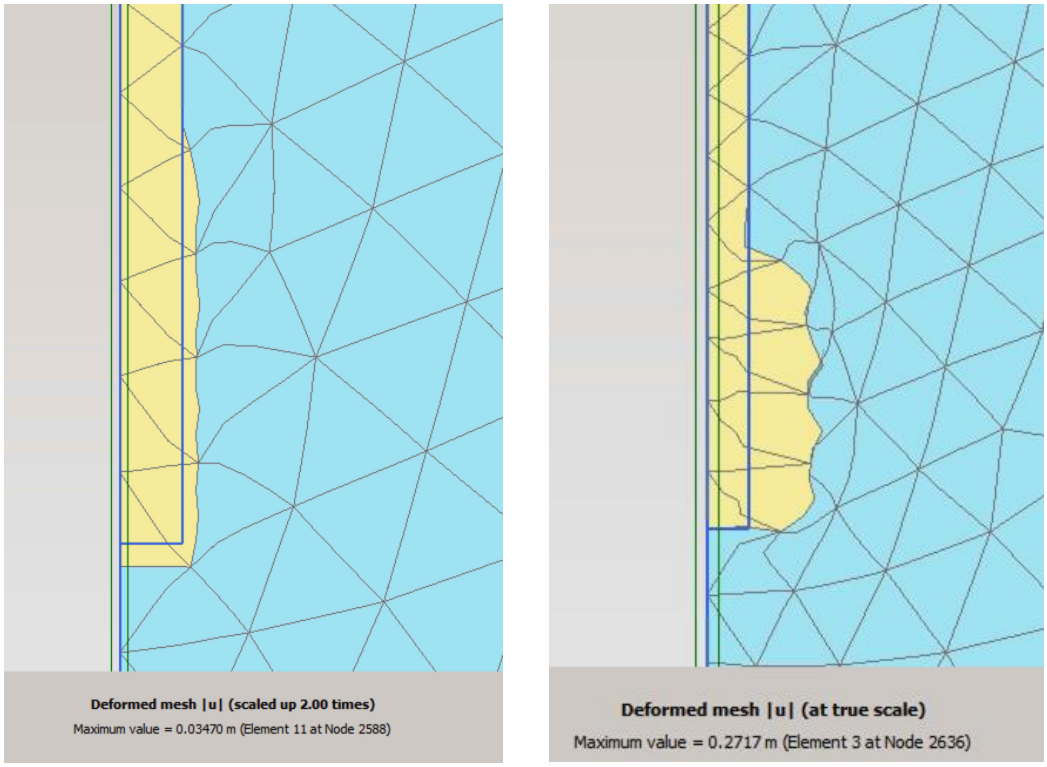

(a) (b)

Figure 3-21 – Deformation of the mesh after (a) 1 pulse and (b) 10 pulses of dynamic load in drained Mohr-Coulomb material model

Average number of pulses applied in the field by piling contractors is from 3 to 5 at each level due to equipment maintenance limitations. Therefore further calculations were made for 4 pulses treatment.

The amplitude of dynamic horizontal loading has been tested in sandy soil using the same soil and material parameters for the number of pulse calculations. Dynamic load was specified as 4 pulses 0.002s long at 0.003s between the peak values. The average amplitude considered in this chapter is 5000kN/m/m (Park et al. (2011)), therefore the amplitude range of values have been considered between 1000kN/m/m and 20000kN/m/m.

Table 3-12 – Pulse pile model sensitivity to the amplitude of pulses in coarse grained soil

Calculation case	Augered Diameter	Prescribed settlement at top of pile	Horizontal line load $q_{x,start,ref}$	Max. Expansion	Pile Capacity
	m	m	kN/m/m	m	kN
Simulation of a single pulse treatment					
Brd_snd_E30Kphi33d	0.3	0,03	0	0	310.45
Pulse_sand_d1p5amp	0.3	0,03	1000	0.003	339.08
Pulse_sand_d1p2amp	0.3	0,03	2500	0.009	367.00
Pulse_sand_d1p	0.3	0,03	5000	0.021	406.30
Pulse_sand_d1p1amp	0.3	0,03	10000	0.046	475.43
Pulse_sand_d1p3amp	0.3	0,03	15000	0.071	534.60
Pulse_sand_d1p4amp	0.3	0,03	20000	0.096	588.18
Simulation of a double pulses treatment					
Brd_snd_E30Kphi33d	0.3	0,03	0.1	0	310.45
Pulse_sand_d2p5amp	0.3	0,03	1000	0.007	348.27
Pulse_sand_d2p2amp	0.3	0,03	2500	0.020	391.18
Pulse_sand_d2p	0.3	0,03	5000	0.045	448.78
Pulse_sand_d2p1amp	0.3	0,03	10000	0.099	544.00
Pulse_sand_d2p3amp	0.3	0,03	15000	0.154	621.61
Pulse_sand_d2p4amp	0.3	0,03	20000	0.208	689.61
Simulation of 4 pulses treatment					
Brd_snd_E30Kphi33d	0.3	0,03	0.1	0	310.45
Pulse_sand_d4p5amp	0.3	0,03	1000	0.012	394.29
Pulse_sand_d4p2amp	0.3	0,03	2500	0.034	497.49
Pulse_sand_d4p	0.3	0,03	5000	0.077	622.67
Pulse_sand_d4p1amp	0.3	0,03	10000	0.164	761.29
Pulse_sand_d4p3amp	0.3	0,03	15000	0.252	815.71
Pulse_sand_d4p4amp	0.3	0,03	20000	0.340	858.83

Figure 3-22 shows the expansion of the pile increases with the number of pulses and the magnitude of the pulses.

Figure 3-23 shows the vertical load at the top of the pile for a prescribed displacement increases as the number of pulses increases and the magnitude of the pulses increases.

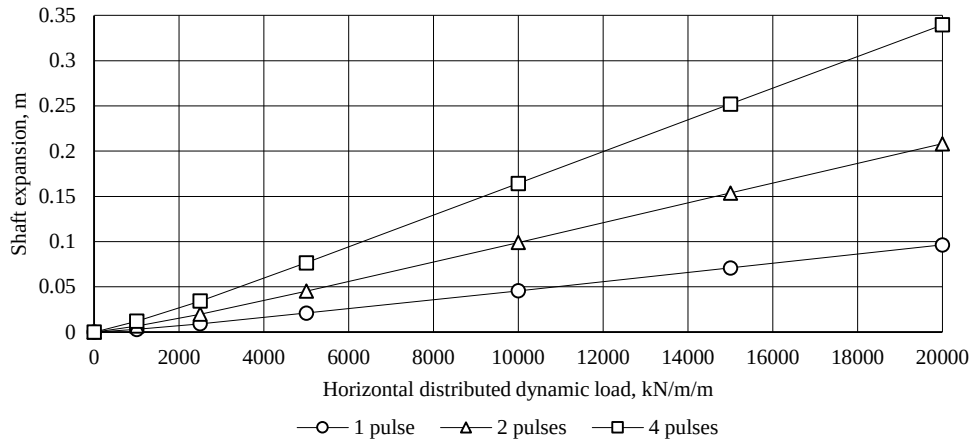

Figure 3-22 – Maximum value of expansion from horizontal distributed dynamic load

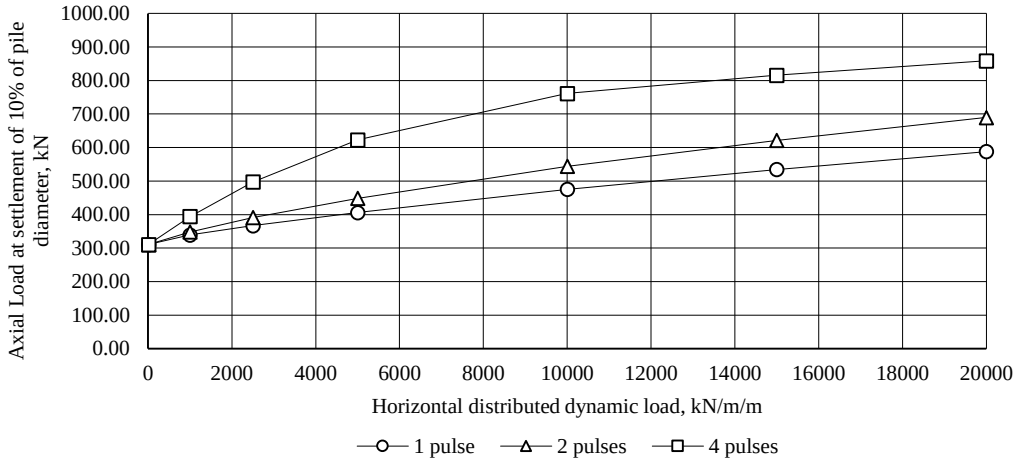

Figure 3-23 – Pile capacity at settlement of 10% of pile diameter from horizontal distributed dynamic load

A further set of amplitude sensitivity tests were performed for the option of pulse treatment of the bottom 5m of the pile in sandy soil. Amplitude values between 500kN/m/m and 10000kN/m/m have been considered based on average figure as for aforementioned 1m treatment calculation.

Table 3-13 – Pulse pile model sensitivity to the amplitude of the pulses with 5m length of treatment in coarse grained soil

Calculation case	Augered Diameter	Prescribed settlement at top of pile	Horizontal line load $q_{x,start,ref}$	Max. Expansion	Pile Capacity
	m	m	kN/m/m	m	kN
Brd_sand_E30Kphi33d	0.3	0.03	0	0	310.45
Pls_sand_d4p_5m+4a	0.3	0.03	500	0.005	588.88
Pls_sand_d4p_5m+1a	0.3	0.03	1000	0.013	781.08
Pls_sand_d4p_5m+5a	0.3	0.03	1750	0.024	1195.30
Pls_sand_d4p_5m+2a	0.3	0.03	2500	0.037	1414.42
Pls_sand_d4p_5m+	0.3	0.03	5000	0.080	1808.85
Pls_sand_d4p_5m+3a	0.3	0.03	10000	0.166	2119.16

The maximum deflection from the horizontal dynamic loading is shown on Figure 3-24. The graph shows that the expansion of the pile is independent of the length of expansion.

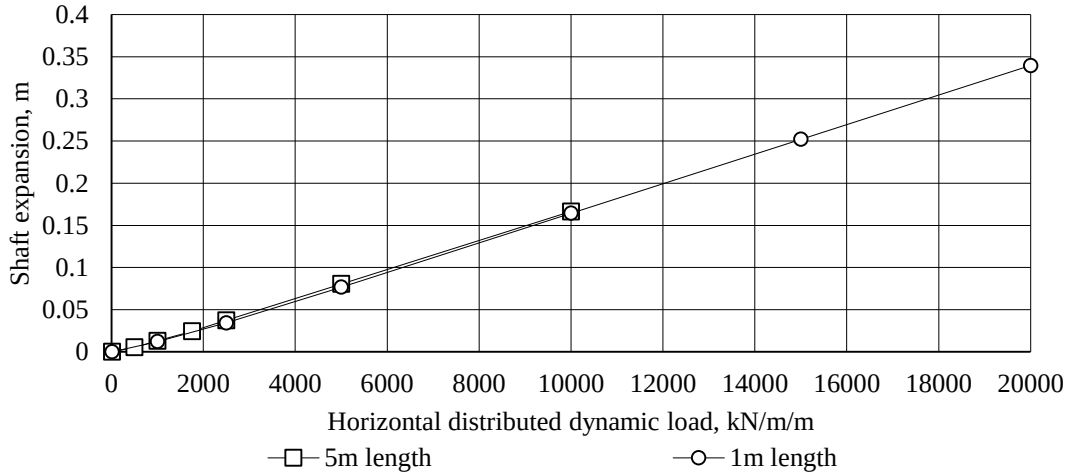

Figure 3-24 – Shaft expansion from horizontal distributed dynamic load

Figure 3-25 shows the pile capacity at a settlement of 10% of pile diameter for the 1m and 5m length of expansion. Increasing the length of the pile section treated by pulse discharges provides additional shaft friction resistance and improves the overall axial capacity.

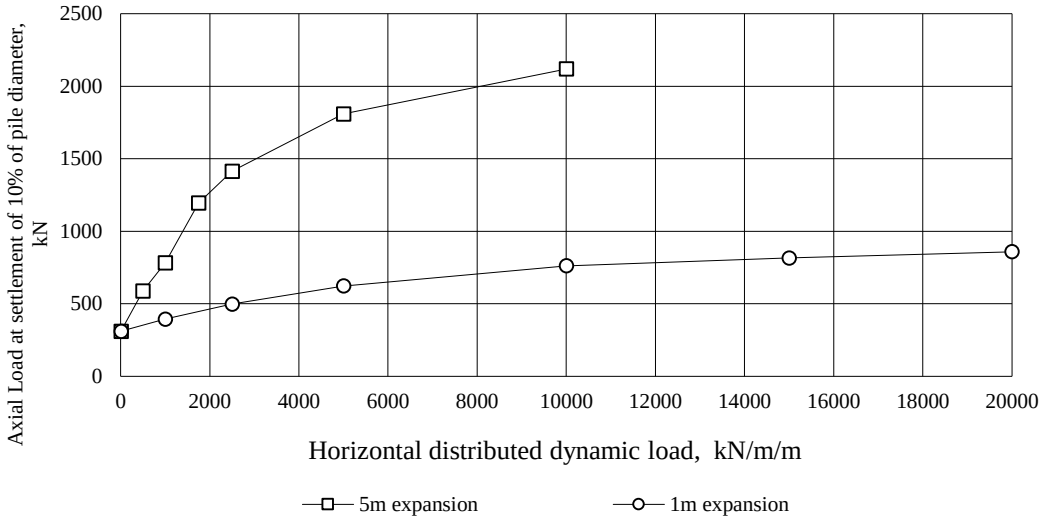

Figure 3-25 – Pulse pile capacity from horizontal distributed dynamic load

Sensitivity tests were performed in coarse grained soil as per Table 3-14 to investigate the length of the expanding section impact on pulse pile capacity.

Table 3-14 – Pulse pile model sensitivity analysis of the length of treatment from 1m to 9m in coarse grained soil

Calculation case	Prescribed settlement at top of pile	Horizontal line load $q_{x,start,ref}$	Length of treatment	Pile Capacity
	m	kN/m/m	m	kN
Brd_sand_E30Kphi33d	0.03	0	0	310.45
Pulse_sand_dyn4p	0.03	5000	1	622.67
Pulse_sand_d4p_2m+	0.03	5000	2	835.51
Pulse_sand_d4p_3m+	0.03	5000	3	1089.27
Pulse_sand_d4p_4m+	0.03	5000	4	1442.70
Pulse_sand_d4p_5m+	0.03	5000	5	1808.85
Pulse_sand_d4p_6m+	0.03	5000	6	1861.16
Pulse_sand_d4p_7m+	0.03	5000	7	1818.04
Pulse_sand_d4p_8m+	0.03	5000	8	1794.01

The required vertical load at the top of the pile for a vertical displacement of 0.03m is shown on Figure 3-26. The length of expansion of 1m to 8m at the bottom of the pile was considered. The graph shows an increase of the nominal working load of a pile with increase of the length of pulse treatment until the top 2 meters.

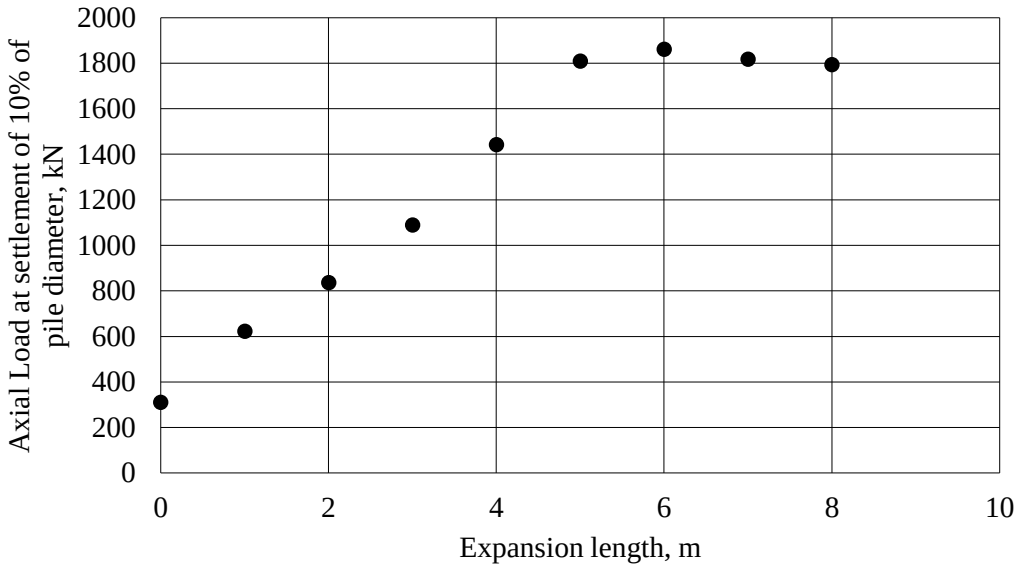

Figure 3-26 – Pulse pile capacity with the length of expansion

Additional runs have been performed to compare pulse pile performance with different time of 5 no. PDT pulses. Figure 3-27 shows the load-settlement curves for a bored piled compared to the cases with pulse duration of 1E-6, 1E-5, 1E-4, 1E-3 sec. The time of each pulse and interval between pulses are summarised in Table 3-15. The time interval between pulses of 1E-3 seconds has been assumed for each calculation case. There were attempts to run the Plaxis calculation with the time interval of 7-10 seconds as applied in industry, but the Plaxis Calculation Kernel failed after 6 days of calculation. Therefore specified time interval was used for dynamic analysis in Plaxis.

Table 3-15 - Dynamic multiplicator time parameters for additional calculation cases

Calculation case	Time of pulse, (seconds)	Interval between pulses (seconds)
Bored	-	-
1E-6	1E-6	1E-3
1E-5	1E-5	1E-3
1E-4	1E-4	1E-3
1E-3	1E-3	1E-3

As can be seen on Figure 3-27, the variation of time of pulses has a dramatic effect on pulse pile performance. A pulse specified in microseconds range gives almost no increase in capacity in comparison to the bored pile. Increasing the time of a pulse increases the calculated capacity. In this research to obtain the modelling results

comparable with the real PDT pile performance, the longer time of pulse will be applied with simplified dynamic load time multiplier. It is recommended that the pressure over time profile be taken from laboratory or field tests to use as a dynamic time multiplier in Plaxis.

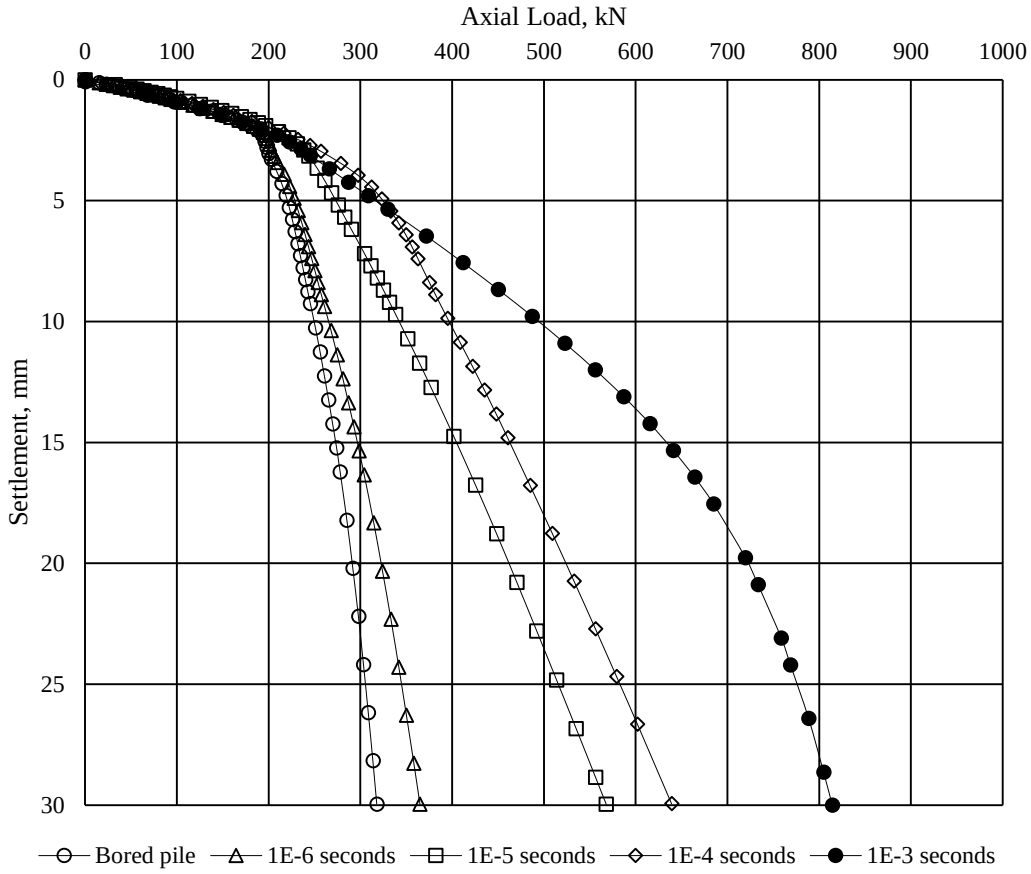

Figure 3-27 - Load-settlement curve for the dynamic analysis cases: (a) bored pile, (b) 1E-6 seconds pulse, (c) 1E-5 seconds pulse, (d) 1E-4 seconds pulse, (e) 1E-3 seconds pulse

3.3.4.3 Analysis in fine grained soil

The analysis of the pulse pile using dynamic calculation number of pulses from 1 to 10 have been tested in fine grained soil. The single pile was specified as a soil cluster of 150mm radius 10m long. The material properties of the pile cluster for the dynamic load calculation, assumed as wet concrete/mortar, are given in Table 3-3. Clay properties has been considered as per relevant bored pile model (Table 3-10, calculation case "CFA_clay_u_cu100") as Undrained (C), with undrained shear strength of 100kN/m^2 and Young's modulus of 24,000 kN/m^2. An additional consolidation phase has been considered in the calculation to simulate drained conditions of the ground after the pulses. The dynamic load was applied to the bottom

1m of a pile that simulated under-reaming from the pulse treatment at one level. A dynamic load amplitude of 5000kN/m/m was specified for a pulse 0.002s long with 0,001s time between pulses. The vertical load at the top of the pile for the load test simulation was specified as a prescribed displacement of 10% of pile diameter.

Table 3-16 – Pulse pile model sensitivity analysis of number of pulses in fine grained soil

Calculation case	Augered Diameter	Prescribed settlement at top of pile	Horizontal line load $q_{x,start,ref}$	Max. Expansion	Pile Capacity
	m	m	kN/m/m	M	kN
CFA_clay_u(A)_phi20	0.3	0.03	0	0	221.11
Pulse_clay_dyn1pC_u(A)	0.3	0.03	5000	0.017	264.01
Pulse_clay_dyn2pC_u(A)	0.3	0.03	5000	0.06334	295.33
Pulse_clay_dyn3pC_u(A)	0.3	0.03	5000	0.1348	321.90
Pulse_clay_dyn4pC_u(A)	0.3	0.03	5000	0.2222	391.81
Pulse_clay_dyn5pC_u(A)	0.3	0.03	5000	0.2863	566.48
Pulse_clay_dyn6pC_u(A)	0.3	0.03	5000	0.4037	863.78
Pulse_clay_dyn7pC_u(A)	0.3	0.03	5000	0.5308	1256.09
Pulse_clay_dyn8pC_u(A)	0.3	0.03	5000	0.6617	1479.45
Pulse_clay_dyn9pC_u(A)	0.3	0.03	5000	0.8082	2501.57
Pulse_clay_dyn10pC_u(A)	0.3	0.03	5000	0.9439	3158.95

Figure 3-28 shows the calculated displacement depending on the number of pulses of the dynamic horizontal loading applied to Mohr-Coulomb undrained (A) material model. The values of displacement are over-predicted for the undrained material model and not acceptable for reliable prediction of pile capacity. Deformed mesh is shown on Figure 3-29. Excessive distortion of the mesh effectively increase end bearing of the pile. One of the reasons for such distortion of the mesh can be approximated time interval of the dynamic load in Plaxis model. Thus the interval between pulses is normally 7 to 10 seconds, but in the model interval of 0.001 seconds has been applied. Microseconds range of shockwave and millisecond range of gas-vapor cavity expansion is transformed to millisecond range of dynamic loading in Plaxis. Undrained (A) Mohr-Coulomb material model is very sensitive to dynamic

time interval of the calculation phase. Additional research is required to explore the appropriate material models for fine grained soils for dynamic module of Plaxis.

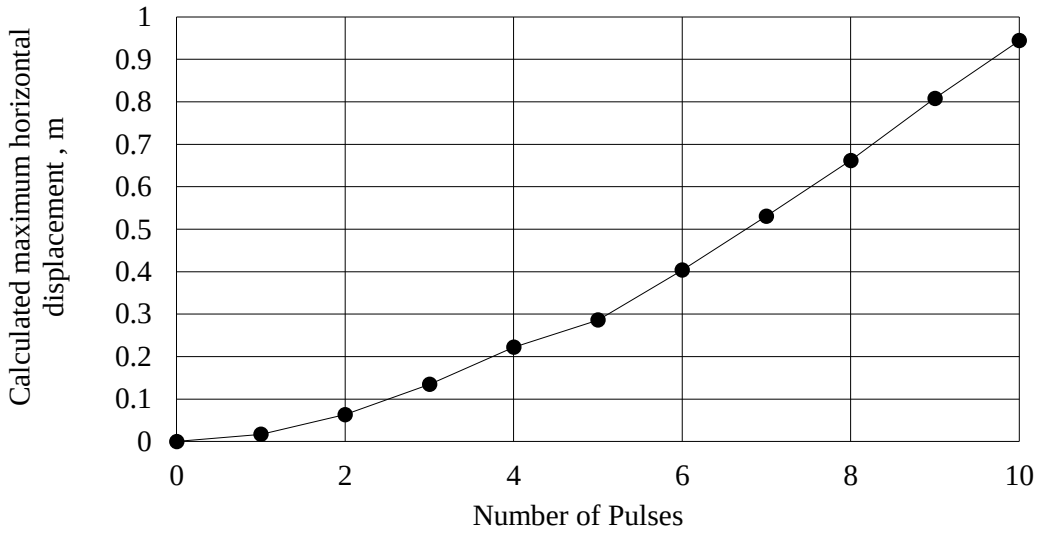

Figure 3-28 – Calculated expansion from dynamic load

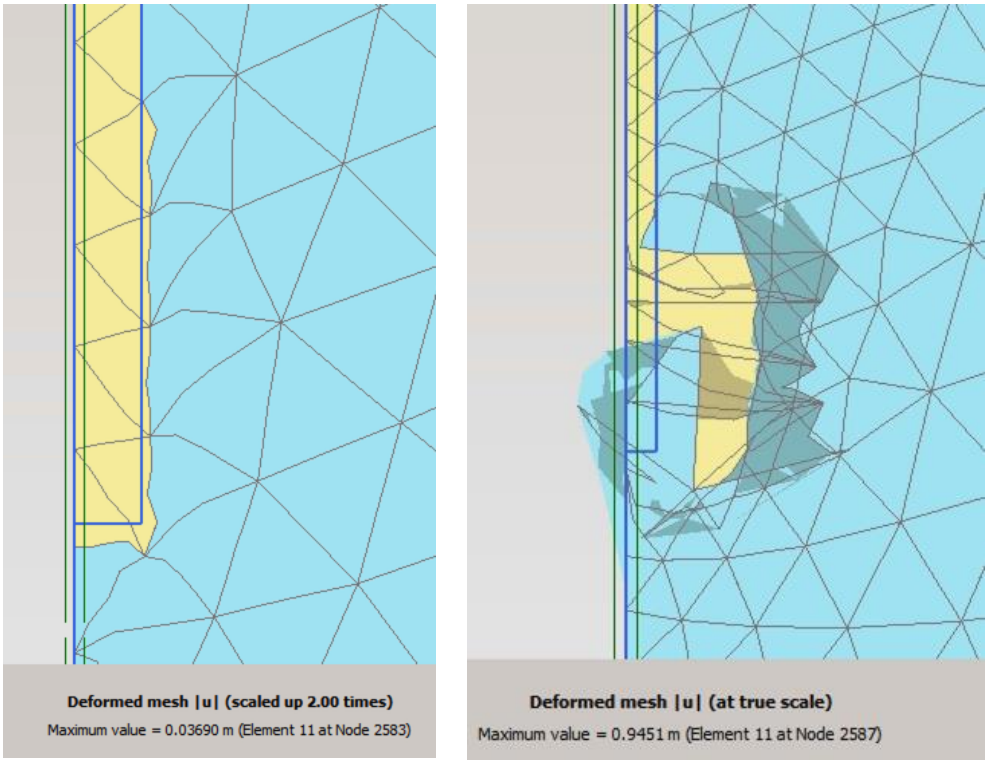

(a) (b)

Figure 3-29 – Deformation of mesh after (a) 1 pulse and (b) 10 pulses of dynamic load in undrained (A) Mohr-Coulomb material model

Figure 3-30 shows the pile capacity at settlement of 10% of pile diameter depending on the number of pulses of dynamic horizontal loading. Based on excessive horizontal deflection of the pile shaft the performance of pulse pile is over-predicted. The results

of pulse pile model of up to 10 pulses in undrained (A) Mohr-Coulomb material model using dynamic load are not satisfactory.

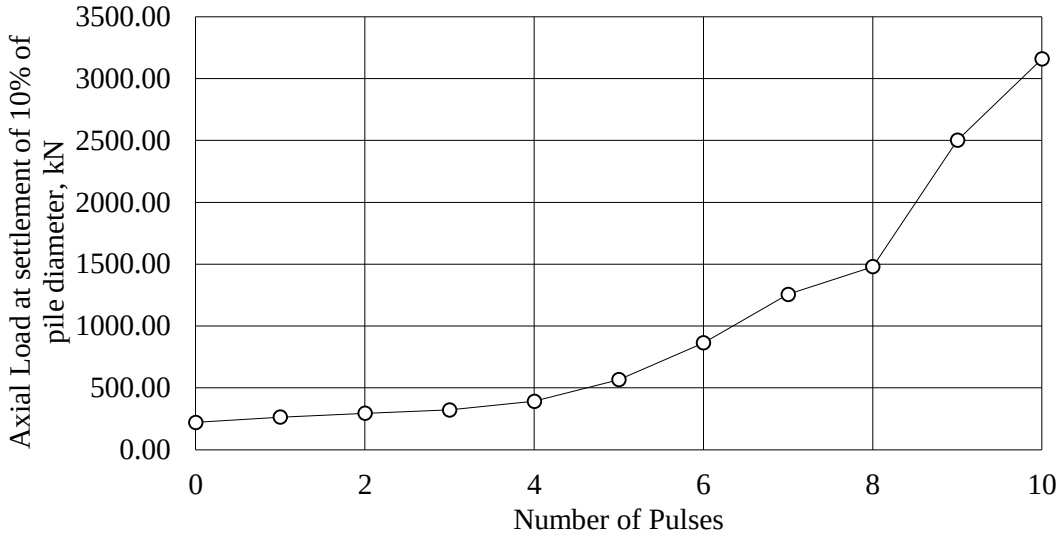

Figure 3-30 – Pile capacity with the number of pulses

The amplitude of dynamic horizontal loading has been tested in a fine grained soil. Soil and material parameters considered as per previous pulse pile calculation (Table 3-10, calculation case "CFA_clay_u_cu100"). The dynamic load was specified as 4 pulses 0.002s long at 0.003s between the peak values. Number of pulses was chosen based on average number of pulses applied in industry as it was done for coarse grained soil sensitivity analyses. Amplitude values have been considered between 1000kN/m/m and 20000kN/m/m. Considered values of amplitude were taken based on published data (Park et al. (2011)), however in the future work it is recommended to obtain new measurement in laboratory tests.

Table 3-17 – Pulse pile model sensitivity analysis of amplitude of pulses in fine grained soils

Calculation case	Prescribed settlement at top of pile	Horizontal line load $q_{x,start,ref}$	Max. Expansion	Pile Capacity
	m	kN/m/m	m	kN
CFA_clay_u(A)_phi20	0.03	0	0	221.11
Pulse_clay_dyn4pC1amp_u(A)	0.03	1000	0.009	252.63
Pulse_clay_dyn4pC2amp_u(A)	0.03	2500	0.068	302.18
Pulse_clay_dyn4pC_u(A)	0.03	5000	0.188	331.16
Pulse_clay_dyn4pC3amp_u(A)	0.03	10000	0.423	359.79
Pulse_clay_dyn4pC4amp_u(A)	0.03	15000	0.647	374.07
Pulse_clay_dyn4pC5amp_u(A)	0.03	20000	0.857	383.75

The maximum deflection from the horizontal dynamic load is plotted on Figure 3-31. The graph shows an increase of the expansion with higher horizontal stress at the wall of the borehole from the shock wave induced by a 5 no. pulse discharges.

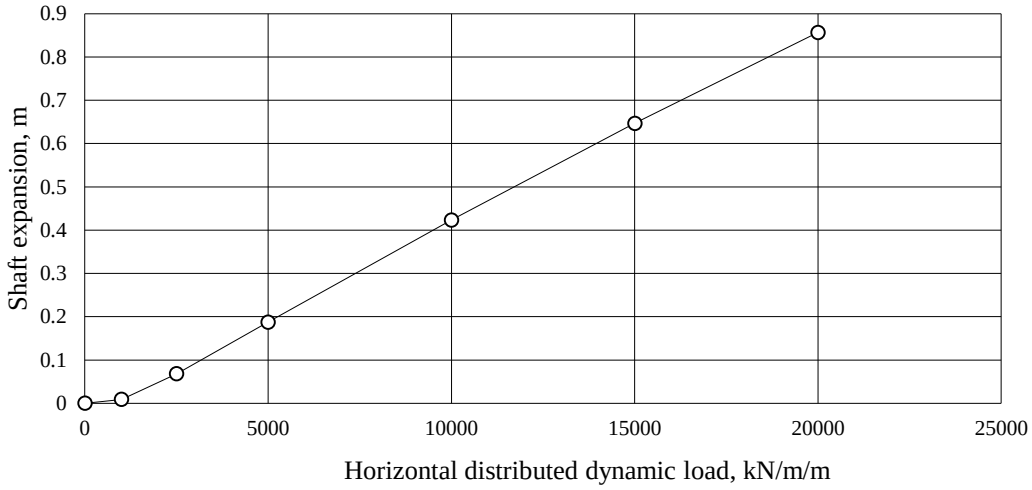

Figure 3-31 – Shaft expansion with horizontal distributed dynamic load

Figure 3-32 shows the vertical load at the top of the pile after vertical load is simulated by prescribed displacements for the pulse piles that have been treated by different value of dynamic horizontal load. As expected, an increase in the dynamic horizontal loading at the bottom 1m of the pile increases the bearing capacity of the pile.

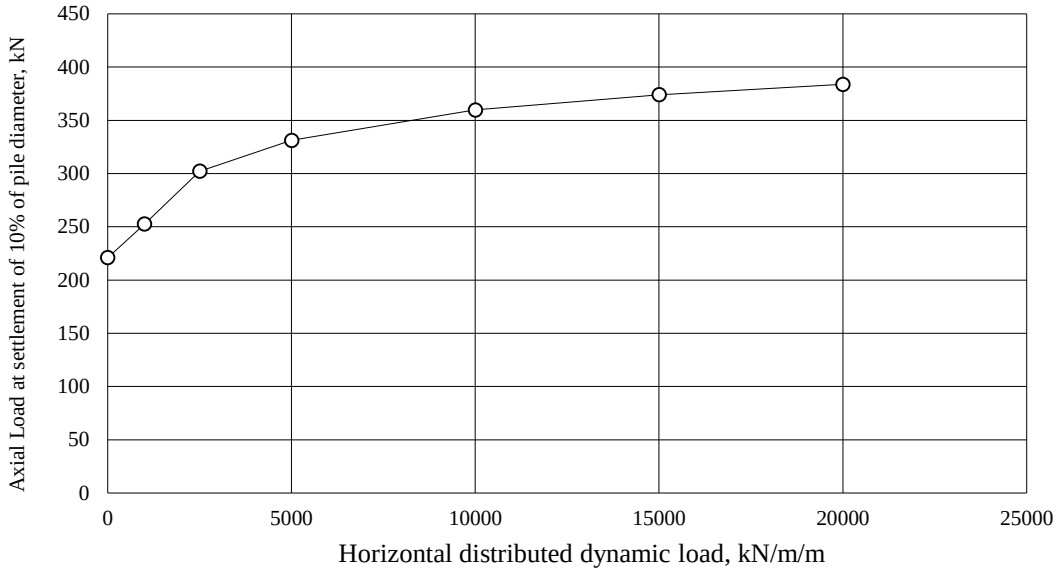

Figure 3-32 – Pulse pile capacity with horizontal distributed dynamic load

Further amplitude sensitivity tests were performed for the option of pulse treatment of the bottom 5m of the pile in clayey soil. Amplitude values between 500kN/m/m and 10000kN/m/m were considered. The maximum deflection from the horizontal dynamic loading is shown on Figure 3-33. The graph shows that the expansion of the pile is independent of the length of expansion for a range of dynamic loads.

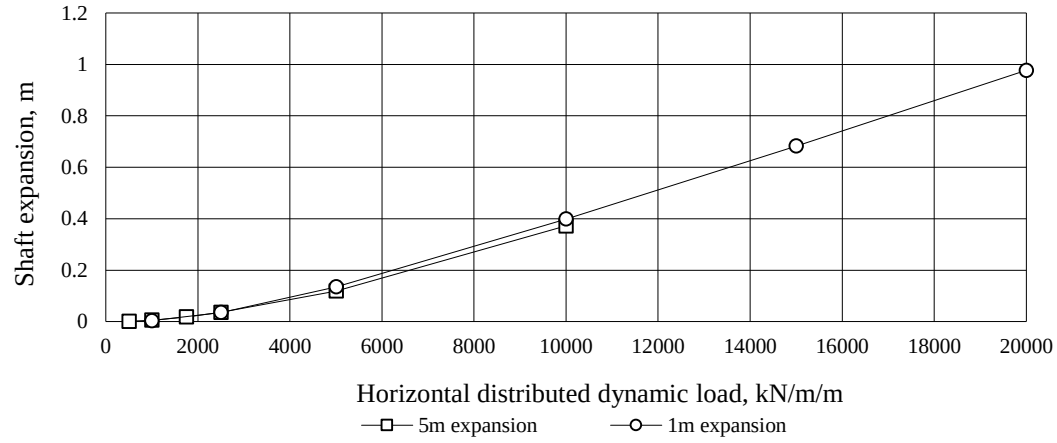

Figure 3-33 – Shaft expansion with horizontal distributed dynamic load

Figure 3-34 shows the load at the top of the pile to reach a vertical deflection of 0.03m for the 1m and 5m length of expansion. An increase of the length of the pile section treated by pulse discharges provides additional friction resistance and improves the axial capacity.

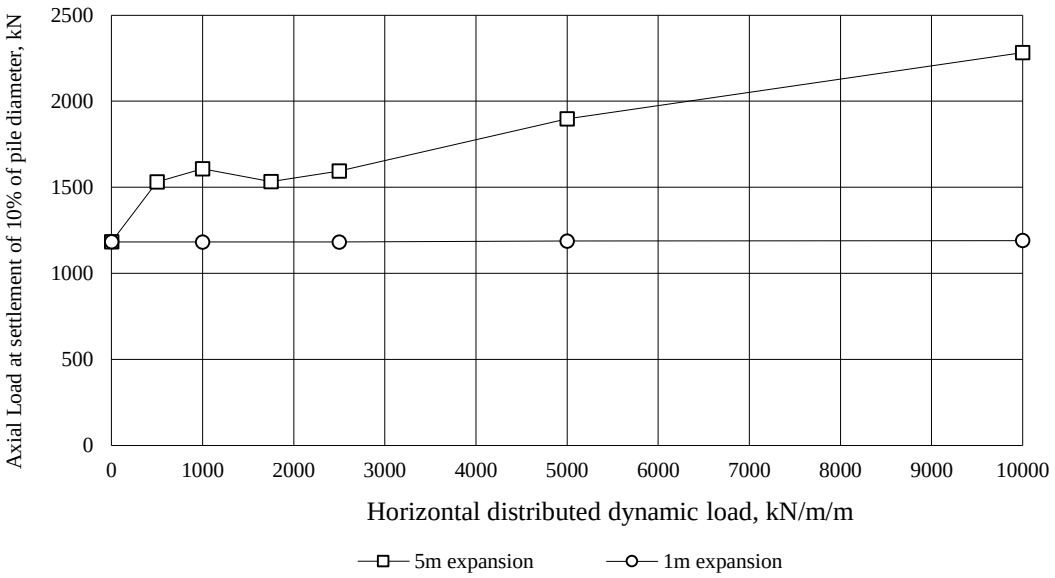

Figure 3-34 – Pile capacity with horizontal distributed dynamic load

Length of expansion sensitivity tests have been performed in clayey soil. Summary of the results of this analyses can be found in Table 3-18 and on Figure 3-35.

Table 3-18 – Pulse pile sensitivity analysis of length of expansion in fine grained soils

Calculation case	Prescribed settlement at top of pile	Horizontal line load $q_{x,start,ref}$	Length of treatment	Pile Capacity
	m	kN/m/m	m	Kn
CFA_clay_u(A)_phi20	0.03	0	0	221.11
Pulse_clay_d4pC_uA	0.03	5000	1	331.16
Pulse_clay_d4pC_2m_uA	0.03	5000	2	433.59
Pulse_clay_d4pC_3m_uA	0.03	5000	3	524.49
Pulse_clay_d4pC_4m_uA	0.03	5000	4	730.18
Pulse_clay_d4pC_5m_uA	0.03	5000	5	1213.68
Pulse_clay_d4pC_6m_uA	0.03	5000	5	1495.01

The required vertical load at the top of the pile for vertical displacement of 0.03m shown on Figure 3-35 depends on the length of expansion. Although the length of expansion from 1m to 9m at the bottom of the pile has been considered, after increasing the length of treatment above 4m below ground level Plaxis calculation failed due to possible soil collapse. The graph shows an increase of axial capacity of a pile with an increase of length of expansion from 1m to 6m.

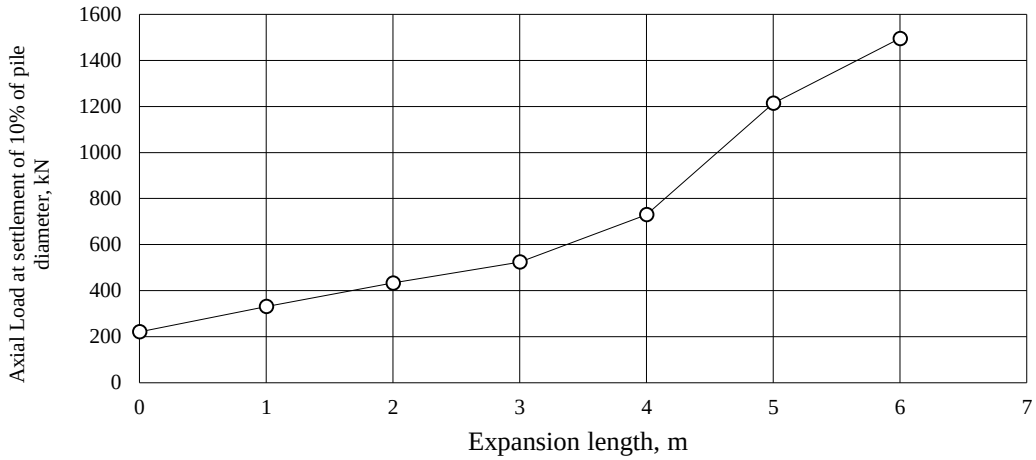

Figure 3-35 – Pile capacity with the length of expansion

3.3.4.4 Multi-layered soil analysis

A series of the multi-layered soil tests have been performed in Plaxis. 5m of sand overlying clay have been considered for sand-clay option. 5m of clay overlying sand were considered for the clay-sand option. Soil properties for each soil layer was taken as per previous pulse pile models (Table 3-9, calculation case "sand_E30000phi33d"; Table 3-10, calculation case "CFA_clay_u_cu100"). The length of expansion of 1m to 9m at the bottom of the pile were analysed for each sand-clay and clay-sand options (see Figure 3-36 which shows an indicative length).

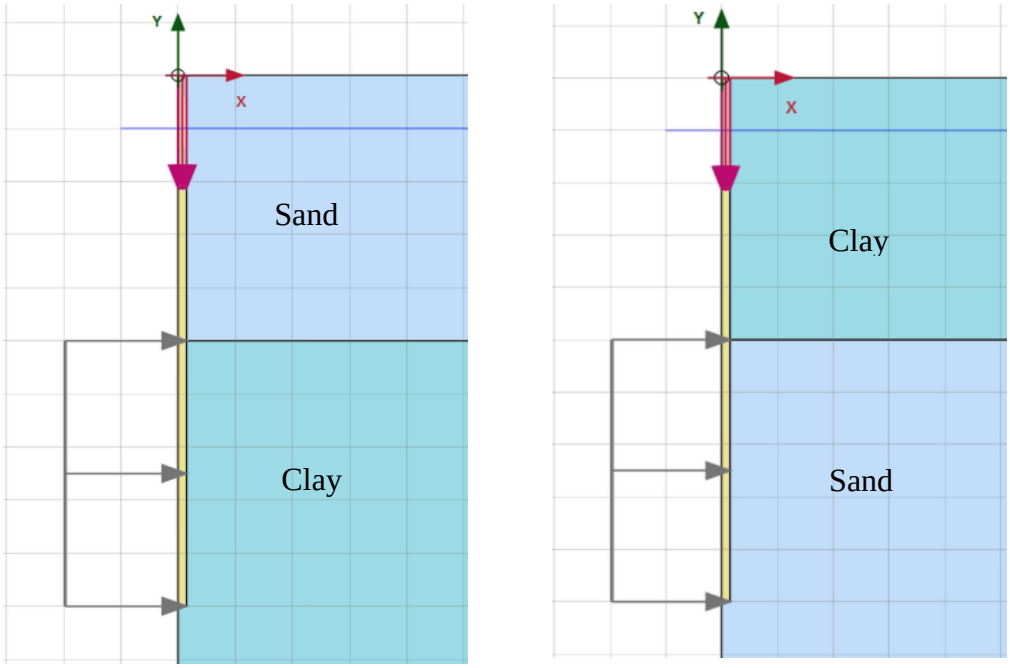

(a) (b)

Figure 3-36 – Multi-layered layouts of (a) sand-clay and (b) clay-sand models

Table 3-19 – Pulse pile sensitivity analysis of the length of treatment in multi-layered soil

Calculation case	Prescribed settlement at top of pile	Horizontal line load $q_{x,start,ref}$	Length of treatment	Pile Capacity
	M	kN/m/m	m	kN
Sand-clay multi-layered model				
Pulse_sand-clay_dyn5pC	0.03	5000	1	797.34
Pulse_sand-clay_dyn4pC_2m	0.03	5000	2	823.49
Pulse_sand-clay_dyn4pC_3m	0.03	5000	3	976.88
Pulse_sand-clay_dyn4pC_4m	0.03	5000	4	1121.08
Pulse_sand-clay_dyn4pC_5m	0.03	5000	5	1121.78
Pulse_sand-clay_dyn4pC_6m	0.03	5000	6	1465.32
Pulse_sand-clay_dyn4pC_7m	0.03	5000	7	1612.34
Pulse_sand-clay_dyn4pC_8m	0.03	5000	8	1803.20
Clay-sand multi-layered model				
Pulse_clay-sand_dyn5pC	0.03	5000	1	1075.13
Pulse_clay-sand_dyn5pC_2m	0.03	5000	2	1240.54
Pulse_clay-sand_dyn5pC_3m	0.03	5000	3	1402.41
Pulse_clay-sand_dyn5pC_4m	0.03	5000	4	1649.81
Pulse_clay-sand_dyn5pC_5m	0.03	5000	5	2231.55
Pulse_clay-sand_dyn5pC_6m	0.03	5000	6	2826.02
Pulse_clay-sand_dyn5pC_7m	0.03	5000	7	5690.92
Pulse_clay-sand_dyn5pC_8m	0.03	5000	8	7012.03

Figure 3-37 shows the vertical load at the top of the pile required for a vertical deflection of 0.03m for different lengths of the treated zone of pile in single and multi-layered soil conditions.

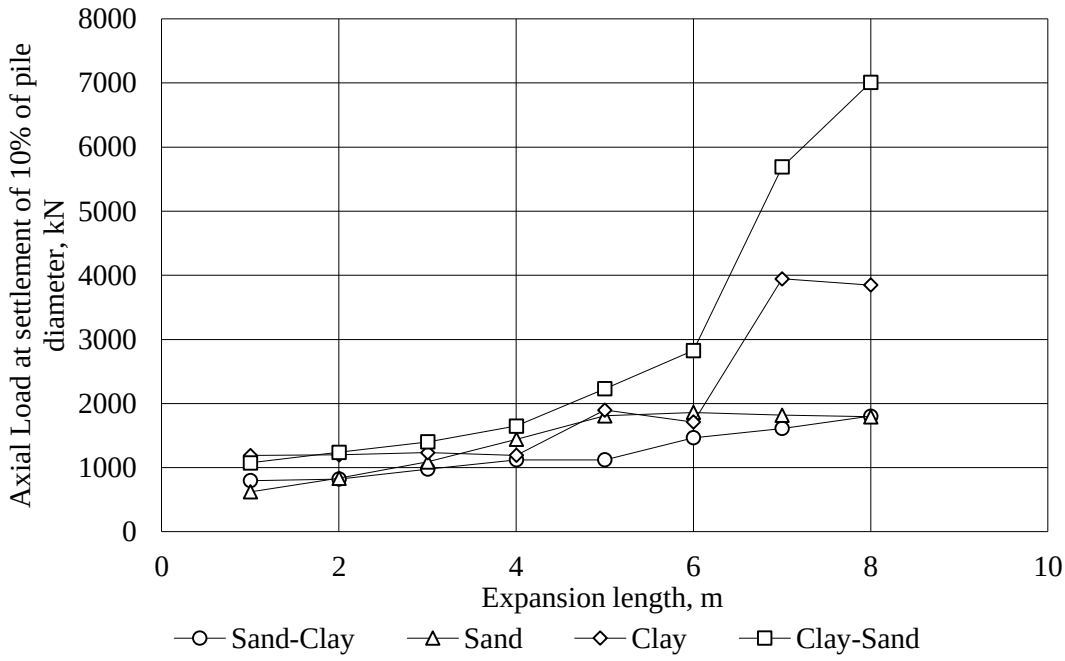

Figure 3-37 – Pile capacity with the length of expansion

Comparing results for the different soil strata cases it can be noted that the nominal working load at settlement of 10% of pile diameter increases with the length of expansion for all soil combinations up to a length of 8m. Cases of coarse grained material at the top layer of the model or single layer model show similar behaviour approaching the maximum length of expansion. Fine grained models show dramatic increase of pile capacity from 6m to 8m length of expansion.

Fine grained soil in multi-layered models have been specified as undrained (B) material. As mentioned in Chapter 5 Plaxis developers do not recommend (Plaxis-Standard (2017)) to use this model for undrained condition. Undrained (A) material model is used further in this study for fine grained soils.

3.4 Conclusions

Plaxis 2D is a convenient and common software package that is used for various geotechnical problems. To compare construction methods of CFA and pulse piles Plaxis 2D software can be utilised producing sensible results.

Dynamic calculation has been implemented to simulate PDT treatment of the borehole. Pulse pile models have been tested for number of pulses, amplitude of the PDT pressure on the walls of the borehole, intervals between pulses and length of the shaft treated by pulse discharges.

Bored and pulse piles models have been tested in single layer strata of sand or clay and two layers of strata for combinations of sand and clay.

Results of the modelling presented in this chapter show the initial development of a single bored and pulse pile models and require additional refinement of soil properties and detailed analysis of the modelling methodology.

Chapter 4
Modelling of the CFA and pulse piles in Plaxis 2D with refined soil parameters.

4.1 Introduction

From industrial experience, it is known that PDT increases pile capacity in fine and coarse grained soils. In current practice, for design purposes, empirical factors are used to calculate design capacity of pulse piles and CFA piles.

This chapter focuses on numerical investigation of pulse pile behaviour in a wide range of soils and comparison with the CFA pile load-settlement curves. One of the objectives of this study is to investigate methods of pulse pile design using Plaxis 2D. To achieve that, design curves have to be developed for pulse piles in various soil types to allow extrapolation of results for the design purposes by piling contractor companies as well as consultancies.

Plaxis 2D has been utilised to model single pile behaviour and dynamic analysis has been performed to simulate pulse discharge treatment of the borehole walls along the bottom 1, 3 and 5 meters of the pile length.

Refined soil parameters for sands based on empirical formulas and for clays extrapolated from the published soil data have been tested in this part of research. Mohr-Coulomb, Hardening Soil and Hardening Soil with small-strain stiffness constitutive models have been considered as they are the most common constitutive soil models for a range of soil types.

4.2 Refined Constitutive Models

Three materials are used in the analysis: soil, which can be fine or coarse grained, mortar to model the borehole installation and concrete to model a pile. There is no unified model for soil behaviour, a three-phase material, because of the complex nature of soil which is affected by the temporal and spatial variations of its properties, its composition, fabric and structure; and the temporal and spatial variations of external factors including load and infiltration. Therefore, a number of models were considered in this study.

Numerous models of soil behaviour exist ranging from the simple linear elastic soil model which is defined by one parameter to complex models such as Cam Clay which

requires five parameters. They tend to focus on the output requirement e.g. response to load, response to infiltration. In this case, a pulse pile model has to incorporate dynamic loading to model installation and static loading to model performance of the completed pile. The study of pulse pile installation and performance was carried out with an axisymmetric analysis using Plaxis 2D. The models available in Plaxis 2D are listed in Table 4-1.

Table 4-1 – Soil models available in Plaxis 2D (Brinkgreve & Broere (2015))

Model	Principle	Purpose	Input Parameters
Linear Elastic	Hooke's law of isotropic linear elasticity	Structural elements	Effective Young's modulus E', effective Poisson's ratio ν'
Mohr-Coulomb	Bi-linear elastic-perfectly plastic model	First approximation of soil behaviour	Effective Young's modulus E', effective Poisson's ratio ν', Effective cohesion c'_{ref}, Effective friction angle φ', Dilatancy angle ψ
Hardening Soil	Advanced elastoplastic hyperbolic model	Modelling of soil behaviour of coarse and fine grained soils	Secant stiffness in standard drained triaxial test E_{50}, Tangent stiffness for primary oedometer loading E_{oed}, Unloading/reloading stiffness E_{ur}, Power for stress-level dependency of stiffness m, Poisson's ratio for unloading-reloading ν_{ur}, Effective cohesion c', Effective angle of friction φ', Dilatancy angle ψ
Hardening Soil with small-strain stiffness	Advanced elastoplastic hyperbolic model with strain dependent stiffness moduli	Modelling of soil behaviour of coarse and fine grained soils	Secant stiffness in standard drained triaxial test E_{50}, Tangent stiffness for primary oedometer loading E_{oed}, Unloading/reloading stiffness E_{ur}, Power for stress-level dependency of stiffness m, Poisson's ratio for unloading-reloading ν_{ur}, Effective cohesion c', Effective angle of friction φ', Dilatancy angle ψ, Reference shear modulus at very small strains G_0^{ref}, shear strain at which $G_s = 0.722G_0$ $\gamma_{0.7}$
Soft Soil	Cam-Clay type visco-plastic model	Modelling of soil behaviour of soft soils: NC clays and peat	Modified compression index λ^*, Modified swelling index k^*, Effective cohesion c'_{ref}, Effective friction angle φ', Dilatancy angle ψ
Soft Soil Creep	Second order visco-plastic model	Time-dependent behaviour of soft soils	Modified compression index λ^*, Modified swelling index k^*, Modified creep index μ^*, Effective cohesion c'_{ref}, Effective friction angle φ', Dilatancy angle ψ

Model	**Principle**	**Purpose**	**Input Parameters**
Jointed Rock	Anisotropic elastic-perfectly plastic model	Anisotropic behaviour of stratified or jointed rock	Young's modulus of rock as a continuum E_1, Poisson's ratio of rock as a continuum ν_1, Young's modulus perpendicular on Plane 1 direction E_2, Shear modulus perpendicular on Plane 1 direction G_2, Poisson's ratio perpendicular on Plane 1 direction ν_2, Cohision c_i, Friction angle φ_i, Dilatancy angle ψ_i, Tensile strength $\sigma_{t,i}$
Modified Cam-Clay	Critical state model. Logarithmic relationship between void ratio and the mean effective stress	Behaviour of normally consolidated soft soils	Cam-Clay compression index λ, Cam-Clay swelling index k, Poisson's ratio ν, Initial void ratio for loading/unloading e_{init}, Tangent of the critical state line M
Hoek-Brown	Elastic perfectly-plastic model	Isotropic behaviour of rock	Young's modulus E, Poisson's ratio ν, Uniaxial compressive strength σ_{ci}, Material constant for the intact rock m_i, Geological Strength Index GSI, Disturbance factor D, Dilatancy at zero stress level ψ_{max}, Stress level at which dilatancy is fully suppressed σ_ψ
Sekiguchi-Ohta (Inviscid)	Cam-Clay type model for	Time-independent behaviour of fine-grained soils	Modified compression index λ^*, Modified swelling index k^*, Compression index C_c, Swelling index or reloading index C_s, Initial void ratio e_{init}, Tangent of the critical state line M
Sekiguchi-Ohta (Viscid)	Cam-Clay type model for	Time-dependent behaviour (creep) of fine-grained soils	Modified compression index λ^*, Modified swelling index k^*, Coefficient of secondary compression α^*, Initial volumetric strain rate $dotv_0$, Compression index C_c, Swelling index or reloading index C_s, Initial void ratio e_{init}, Tangent of the critical state line M

Material models in Plaxis have been developed to simulate specific soil and hydraulic conditions. Due to non-linearity of soil stress-strain behaviour under load, models of several levels of sophistication are available in Plaxis. A short introduction to the models used in this study is provided to explain why they were chosen.

PDT is usually applied in coarse and fine grained soils of low to medium strength. Therefore, in this study, models that only apply to those soils have been considered.

Applying pulse pile technology to normally consolidated clays results in an increased strength and stiffness of the surrounding soil. Therefore, soft soils models (e.g. Soft Soil, Cam-Clay, Sekiguchi-Ohta) are not appropriate. Further, bi-linear and hyperbolic models are the most common material models in Plaxis to simulate behaviour of coarse and fine grained soils of low to medium strength. Therefore, Mohr-Coulomb and Hardening Soil type models have been used to compute pulse pile loading.

4.2.1 Material Models for soil cluster

4.2.1.1 Mohr-Coulomb model (MC)

The Mohr Coulomb material model is a simple bi-linear elastic-perfectly plastic model that is suitable for a first-approximation of soil behaviour (Figure 4-1). Constant average stiffness is assumed for each soil layer, therefore computations can be relatively fast (Plaxis-Material (2017)). The model requires only five input parameters: Young's Modulus E and Poisson's ratio ν for stiffness, angle of friction φ and shear strength c for soil strength and angle of dilatancy ψ.

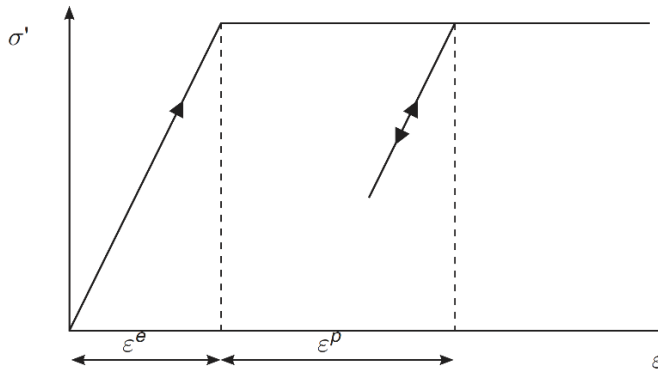

Figure 4-1 – Basic idea of an elastic perfectly plastic model (Plaxis-Material (2017))

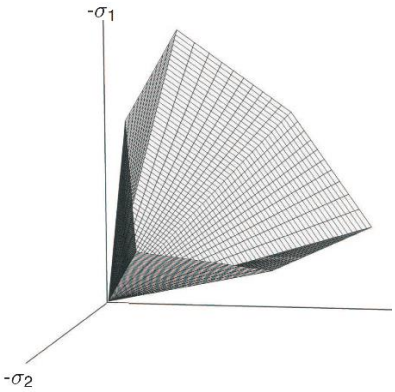

Figure 4-2 – The Mohr-Coulomb yield surface in principal stress space (Plaxis-Material (2017))

The drained condition at failure is represented by the Mohr-Coulomb failure criterion using effective strength parameters, φ' and c'. In the drained condition, excess pore pressures are not generated, hence this drainage type is only applicable for granular materials with high permeability or long-term behaviour of fine-grained soils.

There are three option for an undrained condition for Mohr-Coulomb material model in Plaxis: Undrained (A), Undrained (B) and Undrained (C). Method A is an undrained analysis in terms of effective stresses with both stiffness and strength being effective parameters. The advantage of Method A is that a realistic prediction of pore pressures can be made. There is no need to specify undrained cohesion, c_u, since it is an output of the model. Note that the Mohr Coulomb model can over predict c_u but the ability to use effective stress and allow for generation of pore pressures is an advantage of this model. Consolidation analysis can follow the undrained plastic calculation phase to model a realistic construction sequence.

Method B is an undrained analysis in terms of effective stresses but with inputs of total strength parameters, c_u, φ, and ψ. This method predicts pore water pressures but generally produces unrealistic results (Plaxis-Advanced (2017)). Therefore, with Method B, plastic calculation should not be followed by consolidation analysis. Generally, Method B is not recommended by experienced Plaxis users and developers (Plaxis-Standard (2017)), (Plaxis-Advanced (2017)).

Method C is an undrained analysis in terms of total stresses. Total strength parameters of undrained cohesion, c_u, as well as total stiffness parameters, E_u, ν_u = 0.495, should be specified in Method C. A disadvantage of Method C is that there is no prediction of pore pressures, since only total stresses are obtained. As with Method B, an undrained plastic phase cannot be followed by a consolidation calculation in Method C. Since pulse pile analysis involves both short term and long term load cases the only appropriate method to model fine grained soils is Method A.

The Mohr-Coulomb material model is linear elastic – perfectly plastic model. The linear elastic part is based on the Hooke's law.

$$\underline{\dot{\sigma}'} = \underline{\underline{D^e}}\,\underline{\dot{\varepsilon}^e} \tag{11}$$

where $\underline{\underline{D^e}}$ = elastic material stiffness matrix, $\underline{\dot{\varepsilon}^e}$ = elastic strain rate, $\underline{\dot{\sigma}'}$ = stress rate.

Perfectly plastic is based on the failure criterion:

$$|\tau| \leq |\sigma| \tan\varphi + c \tag{12}$$

where τ = shear strength, σ = normal stress, φ = angle of friction representing slope of the failure envelope, c = cohesion representing the value of shear strength at zero normal stress.

To find if plasticity occurs, a yield function is introduced:

$$f = \frac{1}{2}(\sigma_1 - \sigma_3) + \frac{1}{2}(\sigma_1 + \sigma_3)sin\varphi - ccos\varphi \tag{13}$$

where σ_1 and σ_3 are major and minor principle stresses, c is cohesion and φ is friction angle.

The yield function determines if plastic strain occurs, but does not describe the direction or magnitude of the plastic strain. For this purpose, another concept called a non-associated flow rule has been introduced

$$\dot{\varepsilon^p} = \lambda \frac{\partial g(\sigma)}{\partial \sigma} \tag{14}$$

where $\dot{\varepsilon^p}$= plastic strain, $g(\sigma)$ = plastic potential function of the normal stress representing direction of plastic strain, λ = scalar multiplier representing magnitude of plastic strain (Plaxis-Material (2017)).

The plastic potential function g is defined as follows:

$$g = \frac{1}{2}(\sigma_1 - \sigma_3) + \frac{1}{2}(\sigma_1 + \sigma_3)sin\psi + const \quad (15)$$

where σ_1 and σ_3 are major and minor principle stresses, ψ is dilatancy angle.

4.2.1.2 Hardening Soil model

The Hardening Soil model (HS) is one of the more advanced material models in Plaxis. HS is elastoplastic hyperbolic model with Mohr-Coulomb failure criterion (Equation 12) (Figure 4-3). As opposed to the Mohr-Coulomb bi-linear model in Hardening Soil model yield occurs before failure criterion is reached. Plastic volumetric strains are created by mean stresses as well as by shear stresses. Shear stresses generate plastic shear strains. Required input parameters of the Hardening Soil model are as follows:

- E_{50} = secant stiffness modulus depending on σ_3 (Equation 19);
- E_{oed} = tangent stiffness modulus depending on σ_1 (Equation 21);
- E_{ur} = unloading/reloading stiffness modulus depending on σ_3 (Equation 20);
- m = power for stress- level dependency of stiffness (value is relevant to certain soil: sands m ≈ 0.5, clays m ≈ 1.0).

It should be noted E_{50} and E_{oed} are plastic stiffness parameters whereas E_{ur} is an elastic stiffness parameter (Plaxis-Material (2017)).

The strength parameters of the HS model are the same as for MC model:

- c'_{ref} = effective cohesion
- φ' = effective angle of friction
- ψ = angle of dilatancy.

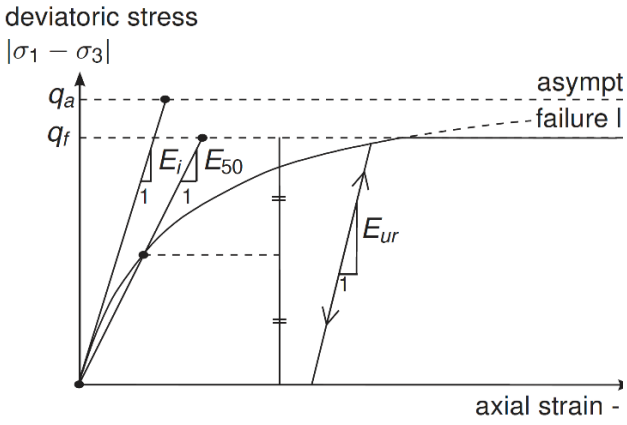

Figure 4-3 – Hyperbolic stress-strain relation in primary loading for a standard drained triaxial test (Plaxis-Material (2017))

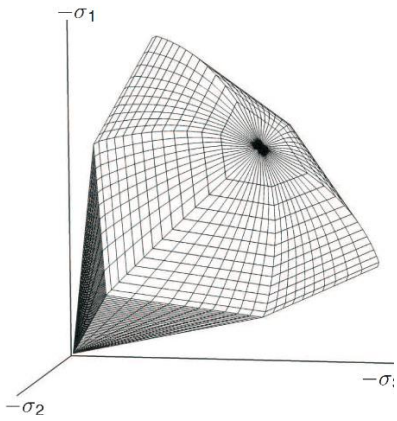

Figure 4-4 – Representation of total yield contour of the Hardening Soil model in principal stress space for granular soil (Plaxis-Material (2017))

The Hardening Soil model cannot be used for a total stress analysis since it is defined in terms of effective stresses. There is an option to specify undrained shear strength, c_u, but there will be limitations, such as no stress dependent stiffness and no compression hardening. The Hardening Soil model is also called Double-Hardening model because it includes shear hardening and compression hardening. Shear hardening is for the irreversible strains due to the primary deviatoric loading.

The yield function for the shear hardening (cone):

$$f^s = \frac{q_a}{E_{50}} \cdot \frac{q}{q_a - q} - \frac{2q}{E_{ur}} - \gamma^{ps} \tag{16}$$

where γ^{ps} is a state parameter that defines the opening of the cone (Plaxis-Advanced (2017)). In a triaxial test with no plastic volumetric deformation, $\gamma^{ps} = 2\varepsilon^{p}_{1}$, hence the yield function is:

$$f^s = \frac{q_a}{E_{50}} \cdot \frac{q}{q_a - q} - \frac{2q}{E_{ur}} - 2\varepsilon^{p_1} \tag{17}$$

Compression hardening is for modelling irreversible plastic strains due to primary compression in oedometer loading and isotropic loading.

Yield function for the density hardening:

$$f_c = \frac{\tilde{q}^2}{\alpha^2} - p'^2 - p_p^2 \tag{18}$$

where p_p is a state parameter that remembers the position of the cap (Plaxis-Material (2017)).

All stiffness moduli depend on the current stress level:

$$E_{50} = E_{50}^{ref}\left(\frac{ccos\varphi - \sigma'_3 sin\varphi}{ccos\varphi - p^{ref} sin\varphi}\right)^m \tag{19}$$

$$E_{ur} = E_{ur}^{ref}\left(\frac{ccos\varphi - \sigma'_3 sin\varphi}{ccos\varphi - p^{ref} sin\varphi}\right)^m \tag{20}$$

$$E_{oed} = E_{oed}^{ref}\left(\frac{ccos\varphi - \sigma'_1 sin\varphi}{ccos\varphi - p^{ref} sin\varphi}\right)^m \tag{21}$$

In the tangent stiffness modulus equation, vertical stress $-\sigma'_1 = \frac{-\sigma'_3}{K_0^{nc}} = p^{ref}$, where K_0^{nc} = lateral earth pressure coefficient, p^{ref} = reference stress (Plaxis-Material (2017)).

Due to the fact Hardening Soil model has the same failure criterion as Mohr-Coulomb, it gives the same failure. Therefore, in case of the drained failure analysis Hardening Soil model has little advantage over the Mohr-Coulomb material model.

4.2.1.3 Hardening Soil with small-strain stiffness model (HS-small).

The Hardening model assumes a hyperbolic stiffness, whereas the small strain stiffness model assumes a variation of stiffness with strain derived from real soil behaviour during loading. The Hardening Soil with small-strain stiffness (HS-small) model is an advanced elastoplastic hyperbolic model similar to the Hardening Soil model. This model can be used to simulate various reactions of soils from small strains (e.g. vibrations with strain below 10^{-5}) to large strains (engineering strain above 10^{-3}) by the means of the strain dependent stiffness moduli. The Hardening Soil model simplifies real soil behaviour assuming elastic material behaviour during unloading-reloading. In fact, there is a very small range in which soils can be assumed truly

elastic (Plaxis-Material (2017)). Soil stiffness reduces non-linearly with increase of strain as shown on Figure 4-5:

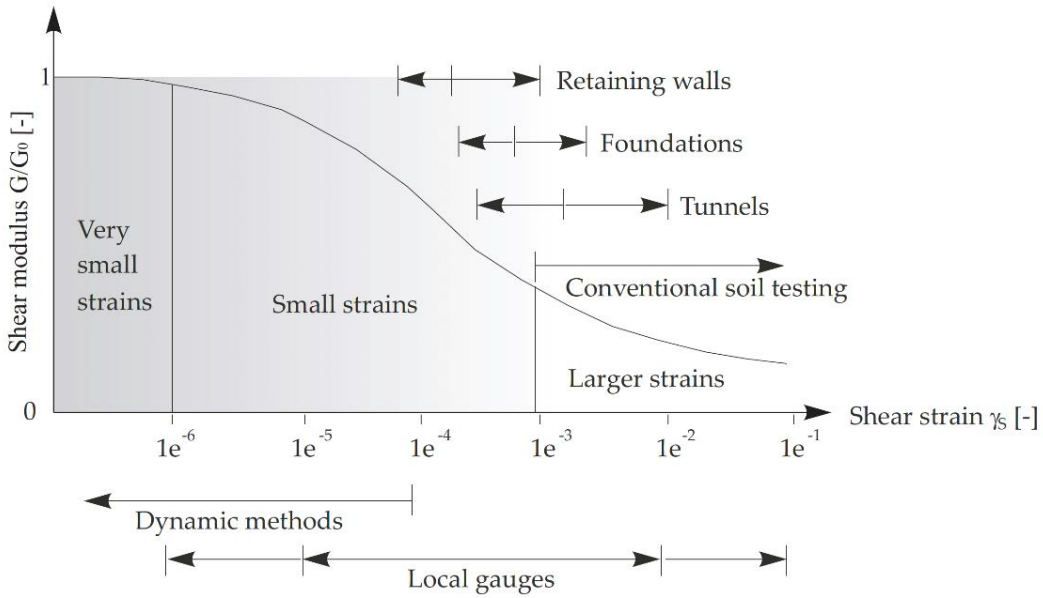

Figure 4-5 – Characteristic stiffness-strain behaviour of soil with typical strain ranges for laboratory tests and structures (Atkinson & Sallfors (1991))

The Hardening Soil with small-strain stiffness model as opposed to the Hardening Soil model applies strain dependent stiffness. Therefore, the Hardening Soil with small-strain stiffness model uses the same parameters as the Hardening Soil model with two additional parameters describing the variation of stiffness with strain:

- G_0 = initial shear modulus
- $\gamma_{0.7}$ = the shear strain level at which the secant shear modulus G_s is approximately 70% of G_0.

The details of the Hardening Soil with small-strain stiffness model (Figure 4-5) are described in Plaxis-Material (2017).

PDT treatment of a shaft of a borehole induces plastic deformations with the large strains in the mobilized zone. Allowing for reduced with larger strains stiffness using HS-small soil model will provide more accurate results of calculation.

4.2.2 Material models for pile cluster

The pile can exist in two states: - mortar during installation; concrete during operations. The mortar is necessary to simulate expansion due to the application of a

pulse. The concrete is necessary to simulate a rigid pile (relative to the soil) to assess the performance of a pulse pile.

4.2.2.1 Mohr-Coulomb model

Modelling of the pulse treatment involves a liquid phase to simulate fresh concrete pile material in the pre-augered borehole. Liquid phase of concrete during Pulse discharge treatment has been considered as submerged sand, gravel and cement particles, that is a composite soil. Sand, gravel and cement will behave as a fine granular material. Using a linear elastic model would be inappropriate for the liquid phase of the mortar due to plasticity of the material. Therefore, the Mohr-Coulomb material model has been chosen for this material as a first approximation solution. More sophisticated models can also be used for the mortar, however since it would require more input parameters based on laboratory tests results, advanced material models have not been used in this research. It is recommended to consider advanced models for the fresh concrete in the future studies.

4.2.2.2 Linear Elastic model

The linear elastic model is a simple model representing Hooke's law of isotropic linear elasticity (Brinkgreve & Broere (2015)). This type of material model has been used for a stiff phase of concrete for the long-term analysis of pile loading test. The linear elastic model involves following elastic stiffness parameters:

E' = Effective Young's modulus

ν' = Effective Poisson's ratio

4.3 Material characterization.

Comparison of the pile-soil behaviour of the bored and PDT treated piles in different soil conditions is one of the main objectives of this study. To allow the numerical analysis to be validated against test data and produce design curves. Mohr Coulomb as well as Hardening Soil and Hardening Soil with small-strain stiffness models have been applied, therefore, a corresponding set of materials had to be specified for each of the material models. Refined material properties in the model have been assigned based on recommended empirical formulas and published data.

4.3.1 Sand parameters

Brinkgreve et al (Brinkgreve et al. (2010)) has derived empirical formulas for computation of coarse grained soil parameters based on relative density (RD) of soil. The relative density is defined as follows:

$$RD = \frac{e_{max} - e}{e_{max} - e_{min}} \tag{22}$$

where e = current void ratio, e_{max} = maximum void ratio and e_{min} = minimum void ratio.

Following formulas have been used to calculate parameters of HS-small material model:

Table 4-2 – Empirical formulas for computation of coarse grained soils parameters (Brinkgreve et al. (2010))

Parameter	Name	Value	Unit
Unsaturated Unit Weight	γ_{unsat}	15 + 4RD/100	kN/m^3
Saturated Unit Weight	γ_{sat}	19 + 1.6RD/100	kN/m^3
Reference Stiffness	p_{ref}	100	kN/m^2
Secant stiffness in standard drained triaxial test	E_{50}^{ref}	60,000RD/100	kN/m^2
Tangent stiffness for primary oedometer loading	E_{oed}^{ref}	60,000RD/100	kN/m^2
Unloading/reloading stiffness	E_{ur}^{ref}	180,000RD/100	kN/m^2
Reference shear modulus at very small strains	G_0^{ref}	60,000 + 68,000RD/100	kN/m^2
Rate of Stress Dependency	m	0.7 – RD/320	-
Threshold shear strain at which $G_s = 0.722G_0$	$\gamma_{0.7}$	(2-RD/100)10-4	-
Angle of friction	φ'	28 + 12.5RD/100	°
Angle of dilatancy	ψ'	-2 +12.5RD/100	°
Failure Ratio between asymptotic and failure value of differential stress	R_f	1 - RD/100	

Poisson's ratio for unloading-reloading ν_{ur} = 0.2, the recommended default value has been assumed for HS and HS-small material models. A recommended value of 0.3 has been considered for the Poisson's ratio for the MC model (Plaxis-Material (2017)).

Sands in the range from very loose (5%RD) to medium dense (50%RD) have been considered using the reference model for loose sand (20%RD).

Table 4-3 gives parameters of loose to medium dense sand assumed in this study for HS-small model derived using empirical formulas given in Table 4-2 as well as relevant parameters for the Hardening Soil and Mohr-Coulomb models:

Table 4-3 – Parameters of coarse grained soils for the MC, HS and HS-small material models

MC	*RD*	γ_{unsat}	γ_{sat}	E'					φ'	ψ		
HS	*RD*	γ_{unsat}	γ_{sat}	E_{50}^{ref}	E_{oed}^{ref}	E_{ur}^{ref}			φ'	ψ		*m*
HSS	*RD*	γ_{unsat}	γ_{sat}	E_{50}^{ref}	E_{oed}^{ref}	E_{ur}^{ref}	G_0^{ref}	$\gamma_{0.7}$	φ'	ψ	R_f	*m*
		kN/m^3	kN/m^3	kN/m^2	kN/m^2	kN/m^2	kN/m^2		°	°		
	5%	15.2	19.08	3,000	3,000	9,000	63,400	0.000195	28.625	0	0.99375	0.684375
	10%	15.4	19.16	6,000	6,000	18,000	66,800	0.00019	29.25	0	0.9875	0.66875
	20%	15.8	19.32	12,000	12,000	36,000	73,600	0.00018	30.5	0.5	0.975	0.6375
	30%	16.2	19.48	18,000	18,000	54,000	80,400	0.00017	31.75	1.75	0.9625	0.60625
	40%	16.6	19.64	24,000	24,000	72,000	87,200	0.00016	33	3	0.95	0.575
	50%	17	19.8	30,000	30,000	90,000	94,000	0.00015	34.25	4.25	0.9375	0.54375

The range of coarse grained soils in this study is from very loose to medium dense~~.~~. Hence relative density is low and corresponding permeability is high. Specified range of coarse grained soils considered in the research allowed to investigate the pattern of the pile performance variation with increase of soil properties. Different parameters can be considered in the future studies. Dense sand was not considered because pulse piles are not used in soils of that type.

It will require laboratory testing to obtain the comprehensive understanding of the drainage condition during the pulse treatment. Since a pulse discharge blast is rapid and the loading rate is high, undrained conditions could be considered for the pulse treatment phase even for coarse grained soils. In some situations liquefaction is possible in practice. In this case, modelling of the pile performance would have to be preceded by consolidation phase. Pile performance would have to be modelled with undrained (A) option though ignoring undrained behaviour. Since the drained analysis of the coarse-grained soil is used for the model of the bored pile performance, it has

been also assumed in the pulse pile model to obtain comparable results so that the same constitutive model was used for the cfa and pulse piles allowing a direct comparison of the impact of the pulses.

4.3.2 Clay Parameters

Material model parameters for fine grained are usually more difficult to derive without laboratory test results (Plaxis-Advanced (2017)). Although it is possible to obtain an analytical expression for undrained cohesion, it is recommended to perform SoilTest numerical check in Plaxis to confirm applied values. Published data have been used to produce reference material models for fine grained soils. The drainage conditions for fine-grained soils have to be analysed according to the construction sequence. The undrained (A) option has been applied for all construction phases to obtain comparable results with the bored pile analyses so that the same constitutive model was used for the cfa and pulse piles allowing a direct comparison of the impact of the pulses. Consolidation phase precedes the pile performance analysis. FEM analysis of undrained conditions can be performed using effective stresses (method A). Thomas Benz (2007) has published material data for HS-small model, including parameters for clays. This data has been summarised and used for the material set of soft to firm fine grained soil parameters as per Table 4-4:

Table 4-4 – Parameters of fine grained soils for the MC, HS and HS-small material models

MC	p_{ref}	I_p	γ_{unsat}	γ_{sat}	E'					c'	φ'	ψ		
HS	p_{ref}	I_p	γ_{unsat}	γ_{sat}	E_{50}^{ref}	E_{oed}^{ref}	E_{ur}^{ref}			c'	φ'	ψ		m
HSS	p_{ref}	I_p	γ_{unsat}	γ_{sat}	E_{50}^{ref}	E_{oed}^{ref}	E_{ur}^{ref}	G_0^{ref}	$\gamma_{0.7}$	c'	φ'	ψ	R_f	m
			kN/m^3	kN/m^3	kN/m^2	kN/m^2	kN/m^2	kN/m^2		kN/m^2	°	°		
	100	25%	19	20	1,500	1,500	4,500	9,000	0.0003	0	21	0	0.9	0.9
	100	15%	19	20	2,500	2,500	7,500	15,000	0.0003	0	23	0	0.9	0.9
	100	7%	19	20	5,000	5,000	15,000	30,000	0.0003	0	25	0	0.9	0.9
	100	5%	19	20	7,500	7,500	22,500	45,000	0.0003	0	25	0	0.9	0.9
	100	4%	19	20	10,000	10,000	30,000	60,000	0.0003	0	25	0	0.9	0.9
	100	3%	19	20	12,500	12,500	37,500	75,000	0.0003	0	25	0	0.9	0.9

Clays considered in this study are soft to firm. Pulse piles are not used in stiff clays. In specified range of fine grained soils, it could be possible to obtain congruent shaped

curves of pile performance. Studies of firm to stiff clays could be considered for the future studies. Calculation involves modelling of the construction method that means both short term and long term conditions are of interest. The dynamic calculation phase is followed by consolidation to simulate what happens in practice before the vertical load is applied. Therefore, it is necessary to consider undrained condition during loading and to obtain a realistic prediction of pore pressures to be able to perform a consolidation analysis between installation and loading. Therefore, the only appropriate drainage type for clay material is undrained (A).

4.3.3 Pile material parameters

The main aim of the modelling is to study pile and soil behaviour during and after pulse discharge treatment. Therefore, a single pile had to be modelled as a cluster with specified parameters for each phase of construction – initial phase before installation, fresh concrete phase just after filling the borehole with mortar, pulse treatment phase before the concrete is cured and pile load phase with the body of pile made of stiff concrete. Fresh concrete material model has been assumed as Mohr-Coulomb, whereas stiff concrete phase has been modelled as linear elastic as recommended for structural elements (Table 4-1). Material properties for the pile cluster used as per Table 3-3.

4.4 Model formulation

The design procedure for a piled foundation involves calculation of the geotechnical capacity of a single pile. Safe working load as well as ultimate capacity of a pile determine the design parameters of the foundation structure. To develop a method of design for the new type of pile, the pulse pile, it is necessary to check the geotechnical behavior of the pulse treated pile with numerical modeling. Plaxis 2D was used to produce an accurate computation of a single pile behavior under axial loading.

In this study, a 2D model of a single pile is developed to simulate CFA and pulse piles. Bored piles and pulse piles have a number of important differences to be considered in modelling. In bored pile model, the installation effect can be ignored as the change in stresses around the pile are negligible. In a pulse pile, which is a displacement pile, the stresses increase around the pile during pulse discharge treatment, inducing an increase of strength and stiffness of surrounding soil.

Therefore, to model a pulse pile, the construction sequence has been simulated from initial phase with undisturbed soil to the load test phase to obtain load-settlement curve of the pre-formed pile settlement under loading.

4.4.1 Model Geometry

According to Plaxis Reference Manual (Brinkgreve & Broere (2015)), uniform circular structures with loading along the central axis or single-source vibration situations can be simulated using an axisymmetric 2D model. Therefore, a single bored pile being a circular structure has been modelled as an axisymmetric system.

The pile body is specified as a soil cluster with assigned material parameters for different calculation phases. The geometry of the pile is based on available field test data. A circular pile, 10m in length and 300mm diameter (150mm radius), has been modelled using 15-noded elements.

The reference model material has been assigned as a single layered isotropic soil cluster 20m wide and 30m deep. Specified boundaries of the model are sufficient to provide reliable computation. Default boundary conditions comprise of fixed displacements in both directions for the bottom soil contour and fixed horizontal displacements for the lateral soil contour (Brinkgreve & Broere (2015)).

By default, soil parameters have been specified by defining a borehole with a water table at 1m below ground level. In fact, groundwater level can vary from the ground level to below tip of the pile but, in practice, in the UK, a ground water level at 1m is a reasonable assumption for this sensitivity analysis. Impact of a variation in groundwater level was not in the scope of this research. Different groundwater properties can be analysed in the future studies.

The installation of a bored pile is modelled as a soil cluster to allow the borehole to expand when a pulse is applied. Thus, the borehole and cluster are connected; that is there is no need to have interface models. This also applies to the expansion phase which includes consolidation. The purpose of the interface elements is to model correctly soil-structure interaction. Interface elements usually applied to the structure elements in Plaxis. Since the pile structure is modelled as cluster application of the interface elements to the pile surface can lead to incorrect mesh. Main objective of

this research is to compare bored and pulse pile behaviour; therefore, interface elements have not been applied to avoid numerical inconsistencies.

Figure 4-6 shows the development of a bored pile in coarse grained soils.

1. The mesh is created for a cluster to represent the pile geometry and a cluster to represent the soil. Both clusters have the same properties as this represents the state of the ground before the pile is installed. Gravity is applied. This is referred to as the K_o procedure (Figure 4-6 a).
2. The pile cluster is converted to mortar (Figure 4-6 b) to model the pile installation. This imposes a pressure on the borehole wall, expanding the borehole thus compressing the surrounding soil.
3. The pile cluster is converted to concrete (Figure 4-6 c) thus completing the pile installation.
4. The performance of the pile is assessed by observing the axial load/settlement behavior (Figure 4-6 d). The load is applied as a distributed load across the top of the pile.

Since the pile has been modelled as axisymmetric system, loading had to be calculated per radian of the circular pile section. Hence, results of the modelling have to be post-processed in Excel to produce load-settlement curves in standard units.

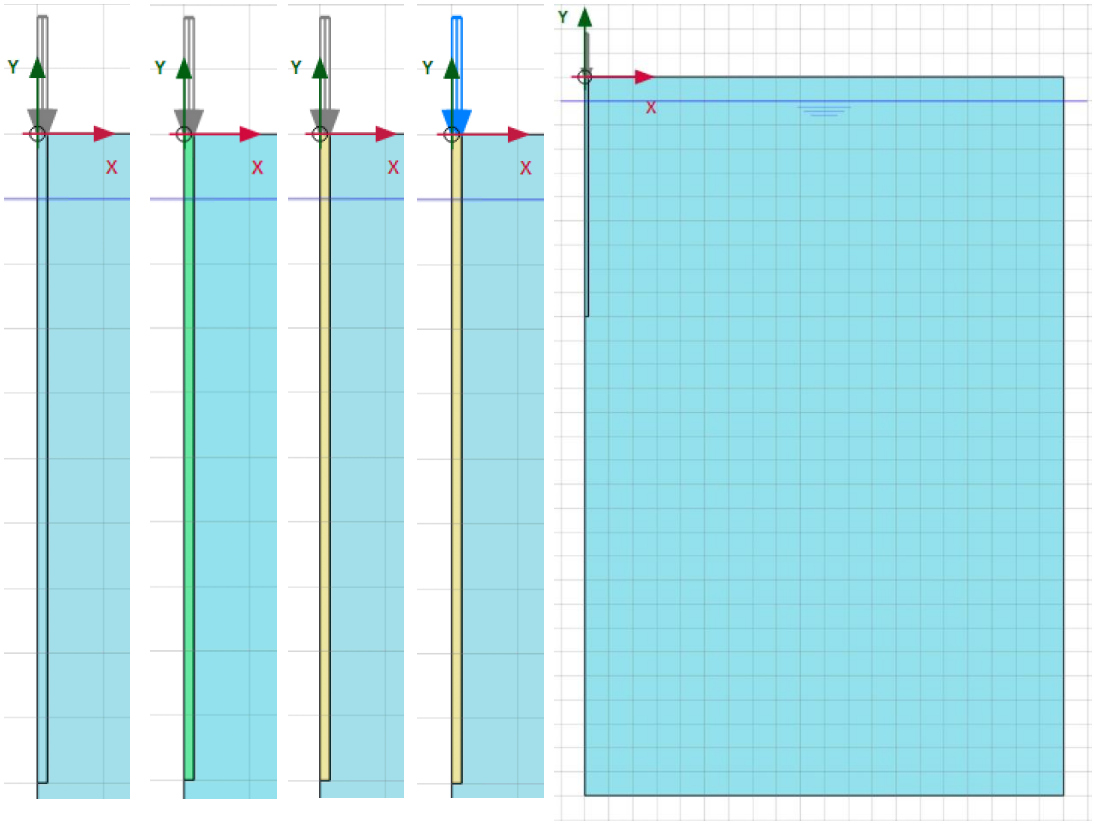

(a) (b) (c) (d) (e)

Figure 4-6 – Single CFA pile model in layout (e) and calculation phases for granular material: initial phase (a) - K0 procedure, phase 1 (b) - pile material set to mortar, phase 2 (c) - pile material set to concrete, phase 3 (d) - pile performance load applied

The installation of a pulse pile (Figure 4-7a and Figure 4-7 b) are the same as those for the cfa pile. In the pulse pile analyses, dynamic loading (Figure 4-7 c) was applied to the bottom part of the pile to simulate pulse discharge treatment. In practice, a shockwave from the point of pulse discharge is delivered to the walls of the borehole to create a spherical expansion. In practice, pulses are performed at multiple levels resulting in a cylindrical expansion of the shaft. To simplify modelling of this phenomenon, a cylindrical distributed loading has been considered. In this research, three lengths of expansion have been considered: 1m, 3m and 5m of the shaft length for a full length of a pile of 10m. Thus, a distributed load is applied to the vertical pile-soil surface over the specified length simulating cylindrical expansion of the pile.

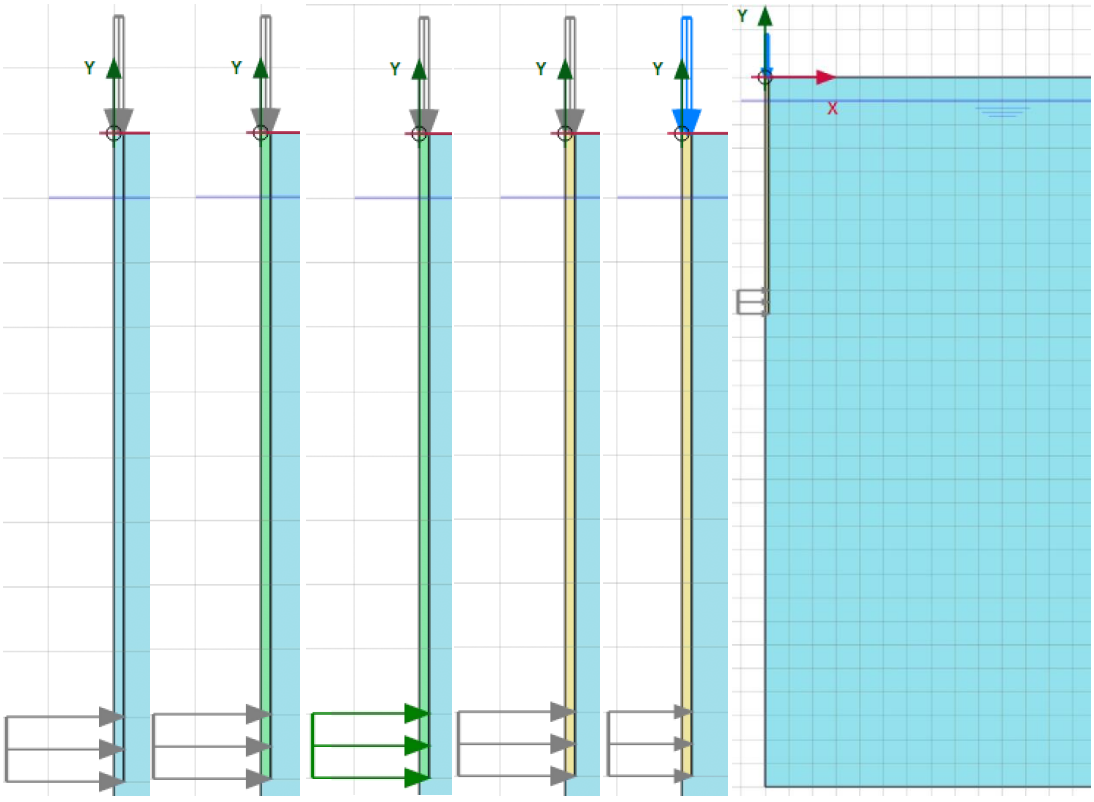

(a) (b) (c) (d) (e) (f)

Figure 4-7 – Single pulse pile model in layout (f) and calculation phases for granular material: initial phase (a) - k0 procedure, phase 1 (b) - pile material set to mortar, phase 2 (c) – PDT treatment, phase 3 (d) - pile material set to concrete, phase 4 (e) - pile performance load applied

4.4.2 Mesh

15-noded triangular elements mesh have been applied in the model. Mesh coarseness of medium element size (coarseness factor of 1.0) with enhanced mesh refinements has been generated. Coarseness factor of 0.1 has been assigned for the cluster of a pile to avoid calculation distortions.

In the pulse pile model, the bottom 1 to 5 meters of the pile cluster were subject to dynamic loading. In practice, the surface of the resulting pulse pile is uneven, hence, it has been assumed that there is no interface reduction; that is the interface strength is that of the soil and no slippage occurs. Therefore, no interface elements have been generated between the pile and soil clusters. To provide comparable results between bored and pulse piles no interface elements have been considered in the standard bored pile model as well.

Figure 4-8 depicts the generated coarse mesh for a single bored pile. In the axisymmetric cross-section with the axis in the centre of the pile, there is one element underneath the tip of the pile and 47 elements along the shaft of the pile. The same mesh was used for bored and pulse piles to allow a direct comparison to be made.

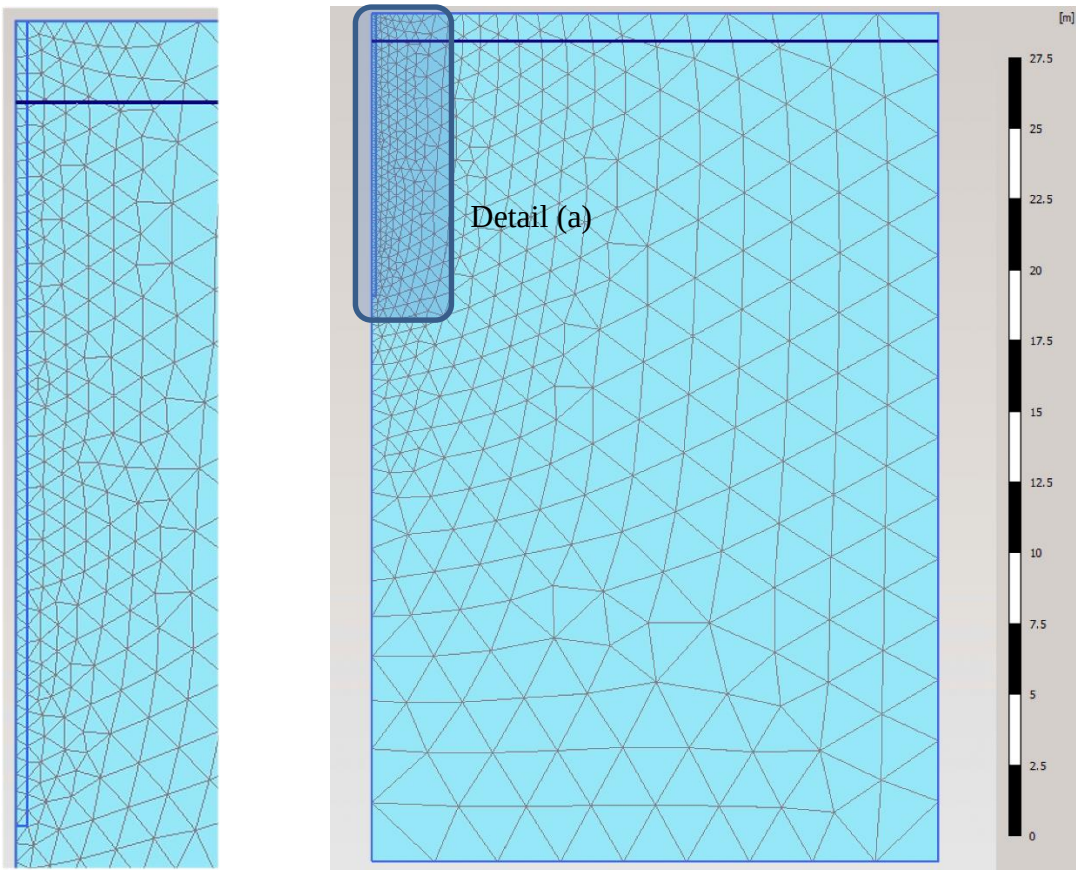

(a) (b)

Figure 4-8 – Mesh coarseness of the reference model layout (b) and detail (a)

4.4.3 Phases of calculation

To be able to simulate pulse treated piles, it is required to model the process of pile installation, including pulse discharges. It is impossible to model pre-augering of the ground in finite elements so far. Therefore, a certain level of simplification has to be allowed for in the modelling. The initial horizontal stresses in the soil (and pile initially modelled as a soil) cluster are generated using the Plaxis K_0-procedure as specified in 3.2.2. Initial conditions of undisturbed ground are considered by specifying surrounding soil properties to the pile cluster (Table 4-5 to Table 4-8). At calculation phase 1 following the initial phase, displacements are reset to zero, since initial displacements are not of interest. At phase 1, bored pile installation implies

replacing of soil in the pile cluster by the liquid phase of the fresh concrete. Considering the bored pile to be installed using cfa technique, walls of the pre-augered shaft will be retained by mortar. Next step is to substitute mortar with the stiff concrete parameters as the liquid material cures. Properties of the mortar and concrete for the pile cluster are specified in Table 3-3. Now the load test on the completed pile can be simulated.

Calculation phases have been adjusted for coarse and fine grained soil models of bored and pulse piles. To be able to obtain comparable results between bored and pules pile models, displacements at all phases except phase 1 have not been reset to zero. It is important to keep displacements calculated at dynamic loading phase so that during the pile load test calculation the updated stresses in soil and the uneven shape of the pile are remembered.

4.4.3.1 Bored piles in sand

Modelling of bored piles in sand follows the general procedure. Sand considered in this study is loose to medium dense granular drained material. Bored pile performance model in coarse grained soil does not require consideration of the undrained soil properties due to relatively quick dissipation of the pore water pressure in soils with high permeability. Therefore, short and long term conditions can be modelled without manual update of soil properties and drainage type.

In Table 4-5, construction phases for the bored pile load test in coarse grained soil are specified.

Table 4-5 – Construction phases for the bored pile model in coarse grained soil

Phase ID	Type of analysis	Comments
Initial phase	K_0 procedure	Generating initial stresses
Phase 1	Staged construction	Pile cluster set to mortar
Phase 2	Staged construction	Pile cluster set to concrete
Phase 3	Staged construction	Vertical distributed load applied

4.4.3.2 Bored piles in clay

Clay material has to be modelled with a different approach than the one has been used in a coarse-grained soil model. Very soft to soft clays considered in this study have to be modelled in both short and long term conditions. Undrained (A) drainage type has been applied for the short-term analysis. Although excess pore water pressure in fine

grained soils can take longer than the time period from pile installation to the load test, consolidation still has to be considered. Thus, additional consolidation phase has been added to the analysis after the pile cluster material has been replaced by the solid concrete before applying the vertical distributed load.

In Table 4-6 construction phases for the bored pile load test in clay are specified.

Table 4-6 – Construction phases for the bored pile model in clay

Phase ID	Type of analysis	Comments
Initial phase	K_0 procedure	Generating initial stresses
Phase 1	Staged construction	Pile cluster set to mortar
Phase 2	Staged construction	Pile cluster set to concrete
Phase 3	Consolidation	Time interval – 3* days
Phase 4	Staged construction	Vertical distributed load applied

* this is a notional figure, considered as a minimum allowable duration before testing the pile

4.4.3.3 Pulse piles in sand

A blast induced by a high voltage discharge in the mortar has a very rapid action on the walls of the shaft. To be able to model that, static loading would not be an accurate simplification since it is impossible to specify time interval of the static loading action. There is a dynamic analysis available in Plaxis, where dynamic loading can be specified with the time interval and dynamic multipliers.

Bored pile model described in section 4.4.3.1 has been used as a basis for modelling of the pulse piles. Dynamic analysis phase has been added to simulate pulse discharge treatment of the shaft walls over the specified length. The dynamic calculation phase follows Phase 2, the installation of the mortar filled borehole. The distributed dynamic loading induces volumetric strains in the pile cluster and surrounding soils.

Coarse grained material is considered as drained for all phases of the calculation. However, drainage type during the pulse discharge dynamic impact could have been analysed as undrained due to the rapid nature of the blast. In this case modelling of the pile performance would have to be preceded by consolidation phase. Pile performance would have to be modelled with undrained (A) option though ignoring undrained behaviour. Excess pore pressure from pulse loading would dissipate in coarse grained soils quicker than in fine grained soils.

In Table 4-7, construction phases for the pulse pile load test in coarse grained soil are specified.

Table 4-7 – Construction phases for the pulse pile model in coarse grained soil

Phase ID	Type of analysis	Comments
Initial phase	K_0 procedure	Generating initial stresses
Phase 1	Staged construction	Pile cluster set to mortar
Phase 2	Dynamic analysis	Time interval – 0.1s
Phase 3	Staged construction	Pile cluster set to concrete
Phase 4	Staged construction	Vertical distributed load applied

4.4.3.4 Pulse piles in clay

A pulse pile model in clay includes additional calculation phases in comparison with coarse grained soils. Construction sequence is summarised in Table 4-8 for the pulse pile load test in clay. Clay modelled as undrained (A) type of material in terms of effective stresses. Undrained phase of calculation for installation of the pile and dynamic loading from the pulses has to be followed by drained analysis of the load test phase after excess pore pressure is dissipated. Therefore Phase 4 - consolidation follows the dynamic analysis of the pulse treatment.

Table 4-8 – Construction phases for the pulse pile model in clay

Phase ID	Type of analysis	Comments
Initial phase	K_0 procedure	Generating initial stresses
Phase 1	Staged construction	Pile cluster set to mortar
Phase 2	Dynamic analysis	Time interval – 0.1s
Phase 3	Staged construction	Pile cluster set to concrete
Phase 4	Consolidation	Time interval - 3 days
Phase 5	Staged construction	Vertical distributed load applied

4.5 Dynamic analysis formulation

During the pulse discharge treatment, the volume of exposed pile section increases following the shockwave propagation from the impulse source to the walls of the pile shaft which results in an expanding cavity in soil. The resulting shape of a pulse pile

is uneven and hard to predict. The dynamics analysis in Plaxis have been used to simulate PDT treatment. It is described in detail in section 3.3.4. Dynamic analysis allows a specified time period for the applied loading and available data of the measured pressure from the shockwave can be used without pre-processing.

4.5.1 Dynamic load formulation

Dynamic loading in Plaxis can be formulated as a dynamic prescribed displacement or actual dynamic loading. The objective of the dynamic analysis in this study is to obtain a realistic prediction of the pile treated by PDT. This means that the displacements from the dynamic impact of the shockwave should be calculated in the model. Therefore, dynamic loading has been specified in terms of distributed dynamic loads instead of dynamic prescribed displacements.

Input value of the dynamic load is equal to amount of pressure that can be measured on the contact between pile and soil. In this study, published data has been processed to specify a value of the dynamic distributed loading over the exposed length.

Park et al. (2011) have produced number of laboratory tests of the PDT in chambers with diameters of 110mm and 250mm. Their experimental setup has been equipped with pressure sensors on the walls of the chamber. Fresh concrete parameters used in the tests were: cement-to-water ratio = 0.5, unit weight = 24kN/m^3. A capacitor bank of 1.6uF capacitance was used to charge electricity at 6kV voltage. An electric pulse was delivered to the point of treatment through the ∅28mm co-axial cable. Results of the laboratory tests including pressure on the wall of the test chamber have been published as shown on the Figure 4-9. Diagrams show the pressure measured in the 110mm and 250mm diameter chambers.

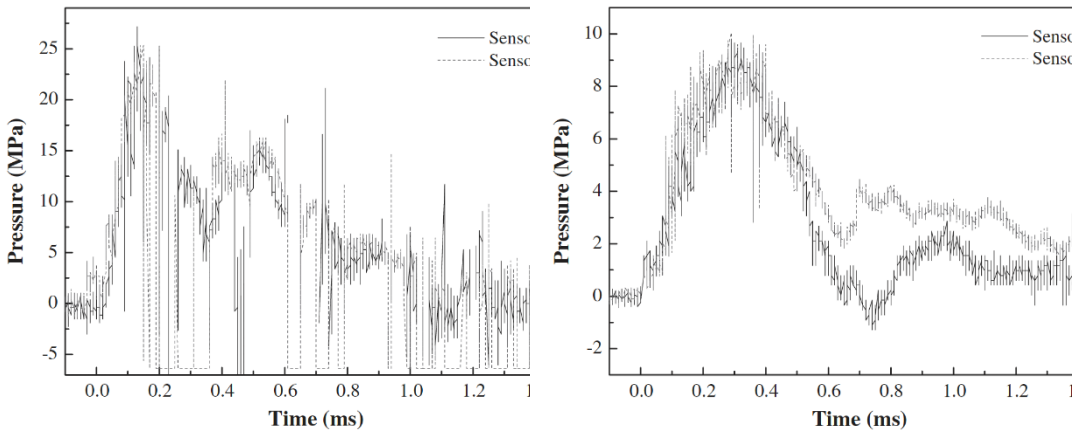

(a) (b)

Figure 4-9 – Measured pressure on the walls of (a) 110 mm diameter chamber and (b) a 250mm diameter chamber (Park et al. (2011))

Based on this data, reference pressure on the walls of the 300mm borehole has been assumed to be 5MPa. Note that a single pulse results in a significant increase in pressure but that only occurs once. This is the basis of the dynamic loading in this analysis. Dynamic distributed loading has been applied to 1m, 3m and 5m from the pile tip. Figure 4-10 shows the distributed dynamic load applied for a specified length. The time increment of the shockwave pressure acting in dynamic analysis can be specified by dynamic load multipliers.

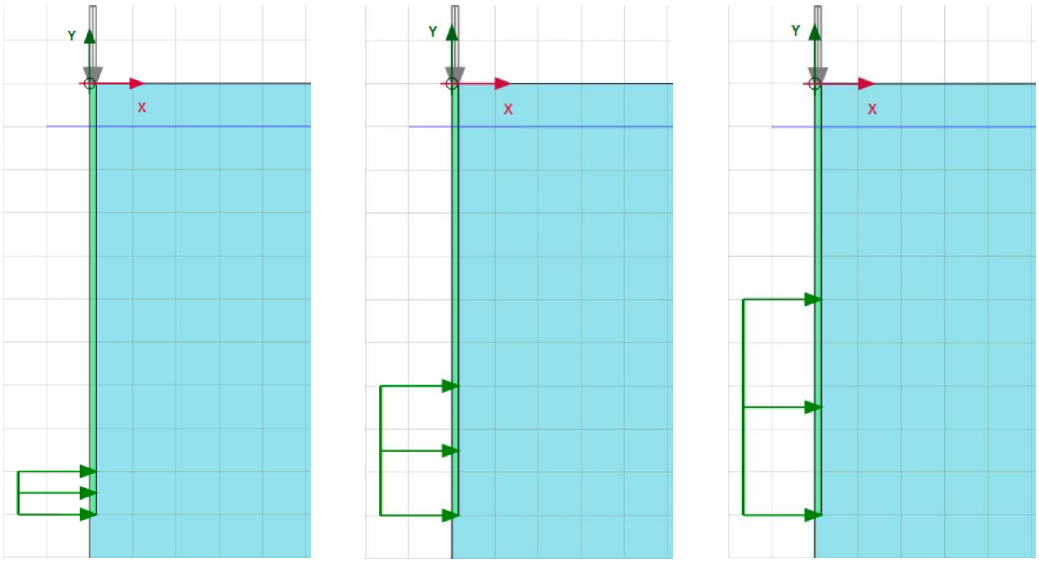

(a) (b) (c)

Figure 4-10 – Distribution of the dynamic load on the walls of the borehole for (a) 1m length of treatment, (b) 3m length of treatment and (c) 5m length of treatment

4.5.2 Dynamic load multipliers

Pulse discharge treatment of bored pile comprises of a number of pulses at the time interval of approximately 10 seconds between pulses to be performed at one level of the pile section. In practice, 5 to 10 pulses per level are performed before changing the level of treatment. In this study, only one pulse is applied in the model.

In the current model, dynamic loading is considered as a distributed load over the specified length. The cylindrical shape of the wave pressure propagation is considered instead of the spherical shape of the actual shock wave at each level.

The signal of a dynamic load can be specified with the input value and dynamic multiplier. A dynamic multiplier determines the dynamic value at certain time increment so that the dynamic load equals the input value multiplied by the dynamic multiplier. A dynamic multiplier can be applied to either the dynamic loading or prescribed displacement.

The signal of the dynamic load can be specified as harmonic or in table format. In this study, dynamic load multipliers have been specified in table format as per Table 4-9. Figure 4-11 is a diagram of the dynamic multiplier specified at each time increment. Shockwave pressure from the high voltage discharge acts as shown on Figure 4-9. Single pulse unity multiplier is applied at 1 millisecond as a simplified approximation of the oscillations. Each pulse can be modelled as individual phase with individual dynamic time interval. For the purposes of this study, single pulse has been considered at dynamic time interval of 0.1 second. Thus, each pulse consists of a dynamic load applied for 1ms (Figure 4-11) followed by a period to allow the effects of the dynamic load to take place.

Table 4-9 – Dynamic load multipliers

Time [s]	Multiplier
0	0
0.001	1
0.002	0
1	0

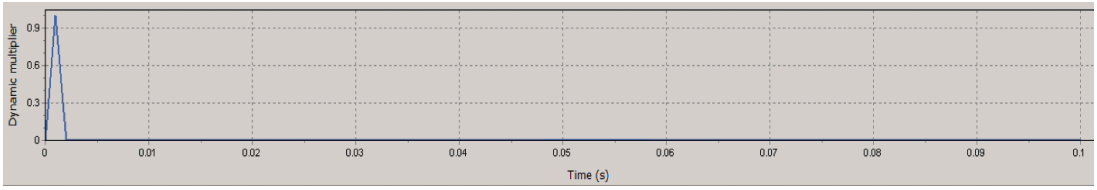

Figure 4-11 – Diagram of Dynamic Multiplier against time

In reality, pulse discharges generate a spherical shape shockwave that delivers pressure to the walls of the borehole. When the discharger is lowered to the deepest point of the borehole, pulse treatment compresses soil horizontally and vertically. While extracting the discharger and performing pulse treatment at higher levels most of the energy is applied to the walls of the borehole and soil compresses horizontally. Therefore, in this current study, only horizontal loading has been applied to simulate pulse treatment. No spherical shaped loading has been specified at each level, however this can be considered in the future studies.

Time parameters of the pulse treatment vary in different industrial applications as they depend on the type and properties of the equipment. Generic time between pulses is usually approximately 7-10 seconds. As shown on Figure 4-9 pressure is rapidly increases over 0.2ms to 0.4ms and then gradually decreases. This behaviour depends on voltage and capacitance parameters of the machine. In the model time, properties have been simplified for the first approximation analysis. On Figure 4-11, the dynamic multiplier in the model is conservatively considered to increase input value of distributed load to 100% at 1ms and set back to zero at 2ms. Compared to the time parameters obtained during testing by Park et al. (2011) this is a simplified dynamic multiplier, taking into account no oscillations shown on Figure 4-9. More rigorous dynamic multiplier table data can be recommended for future research.

4.6 Calculation outputs

Computation in Plaxis 2D of the pulse pile is based on the bored pile performance model with addition of simulation of pulse treatment by means of the dynamic analysis. To compare the performance of bored and pulse piles, a sensitivity analysis has been performed for a range of parameters of coarse and fine grained soils. Six soil cases have been considered for each bored and pulse pile case. Three soils models have been used for bored piles - Mohr-Coulomb, Hardening Soil and Hardening Soil with small-strain stiffness material models. Advanced material models together with

dynamic analysis were not considered due to the time constraints. Pulse piles in this research have been modelled only with the Mohr-Coulomb model. It is recommended to perform computation of pulse piles in advanced material models in the future studies. Pulse piles have been simulated for 1m, 3m and 5m of treated length of the shaft. Performed analyses are summarised in Table 4-10:

Table 4-10 – Summary of analysis in Plaxis 2D

Structure	Soil Type	Material Model	Dynamic analysis	Pile Performance Analysis	Comment
CFA pile	Coarse grained	MC	-	Pile load performance, soil sensitivity analysis	6 soil cases have been considered
		HS			
		HS-small			
	Fine grained	MC			
		HS			
		HS-small			
Pulse pile	Coarse grained	MC	1m	Pile load performance, soil sensitivity analysis	6 soil cases have been considered
			3m		
			5m		
	Fine grained	MC	1m	Pile load performance, soil sensitivity analysis	6 soil cases have been considered
			3m		
			5m		

Vertical stresses against vertical relative displacements (relative to the end of the consolidation phase) of the top of the pile have been generated in the output program in the curve manager to assess the performance of piles. Plaxis calculation outputs have been post-processed in Excel to obtain load-settlement curves in various combinations. Raw output data from the analyses in Plaxis can be found in the appendices.

4.6.1 Output mesh CFA vs pulse pile

Plaxis 2D output deformed mesh of the bored pile model after loading is shown on Figure 4-12 and that for a 5m long pulse pile after dynamic loading on Figure 4-13.

Comparing the insets from these two figures shows that the modelling of the pulse increases the diameter of the pile when compared to that for the bored pile.

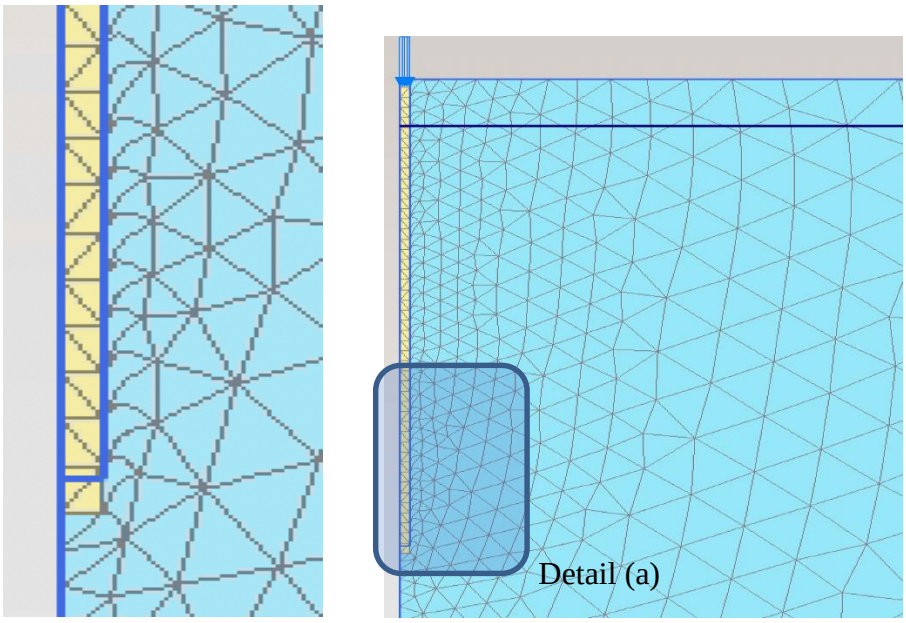

(a) (b) (scaled up 5.0 times)

Figure 4-12 – Deformed mesh for CFA pile analysis

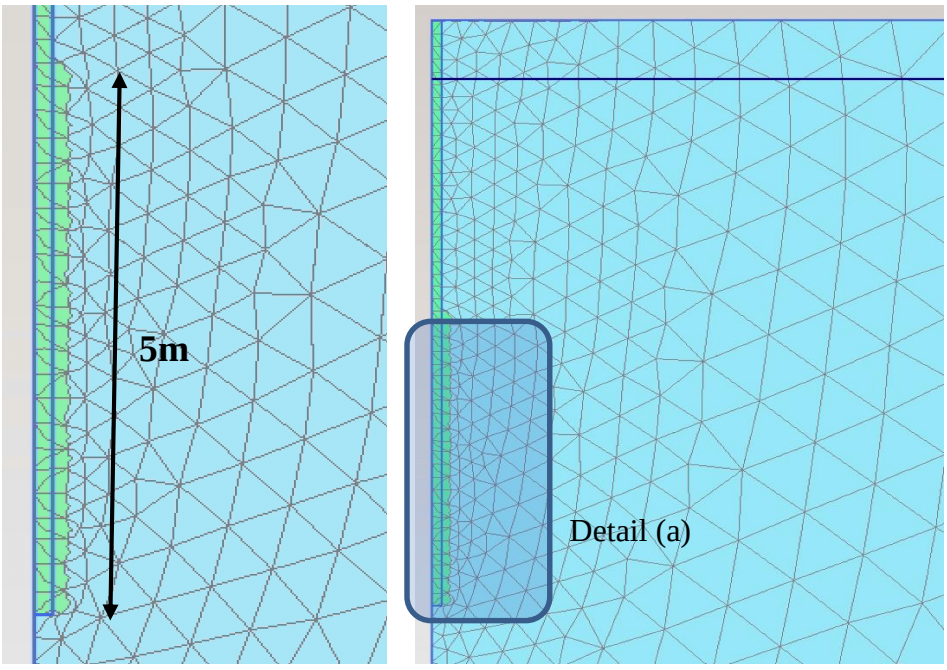

(a) (b) (scaled up 5.0 times)

Figure 4-13 – Deformed mesh for pulse piles analysis. Treated length: 5m

Pulse pile simulation stresses outputs have been obtained from Plaxis. Figure 4-14 shows the direction and scale of the effective principal stresses at each phase of the

calculation. The initial phase (a) for K_0 procedure and phase 1 (c), at which the pile cluster is set to mortar, show a similar distribution of principal stresses because the soil is at rest with the principle stresses vertical and horizontal. Changing the pile cluster from the initial soil state to mortar has little effect. The expansion of the bottom 1m of a pulse pile (Figure 4-14 e) shows that the dynamic loading increases the effective stress around the base of the pile and the zone of influence extends radially and vertically. Turning the pile cluster to concrete has little effect on the effective stress distribution (Figure 4-14 g). It was important to investigate pulse pile performance in comparable conditions with the bored pile, therefore displacements have not been reset to zero at any phase of calculation. Figure 4-14 i shows the expansion and scale of effective stress crosses at the end of the axial load test.

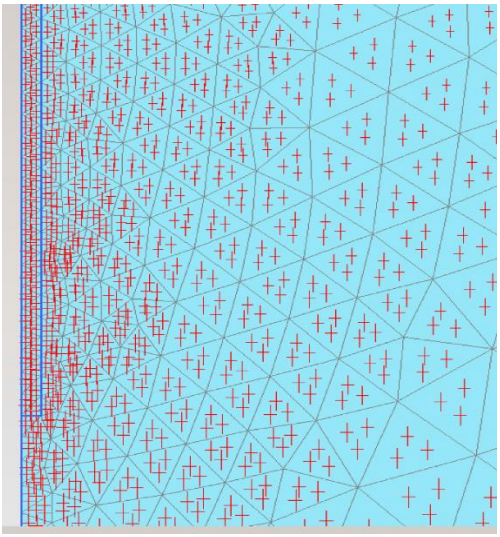

(a)

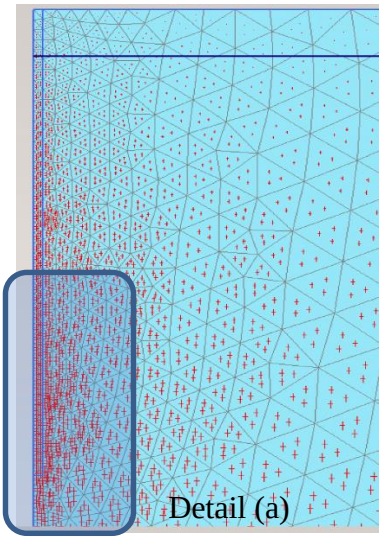

(b)

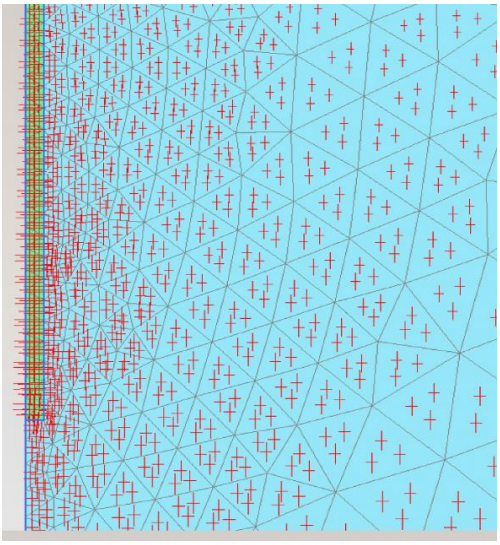

(c)

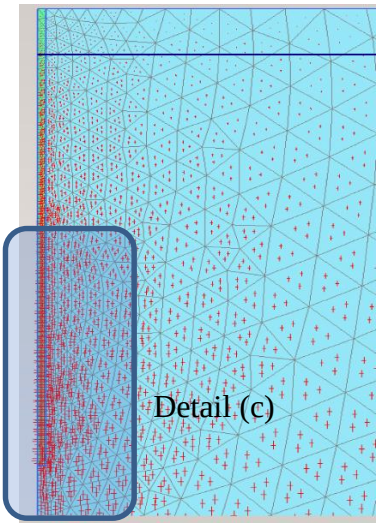

(d)

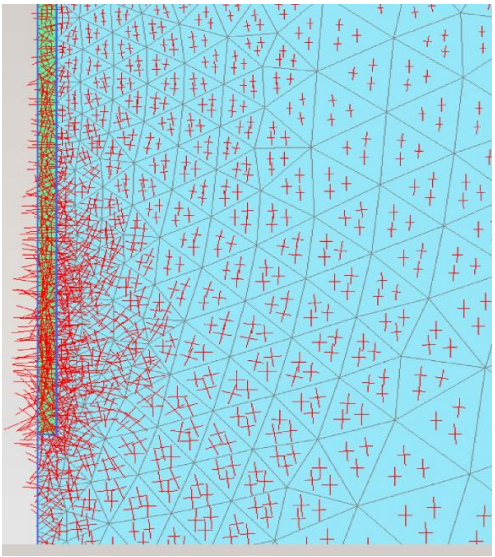

(e)

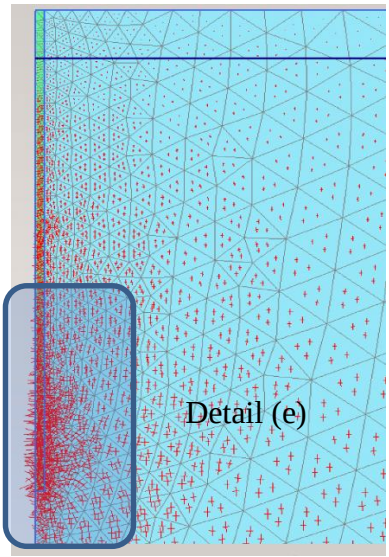

(f)

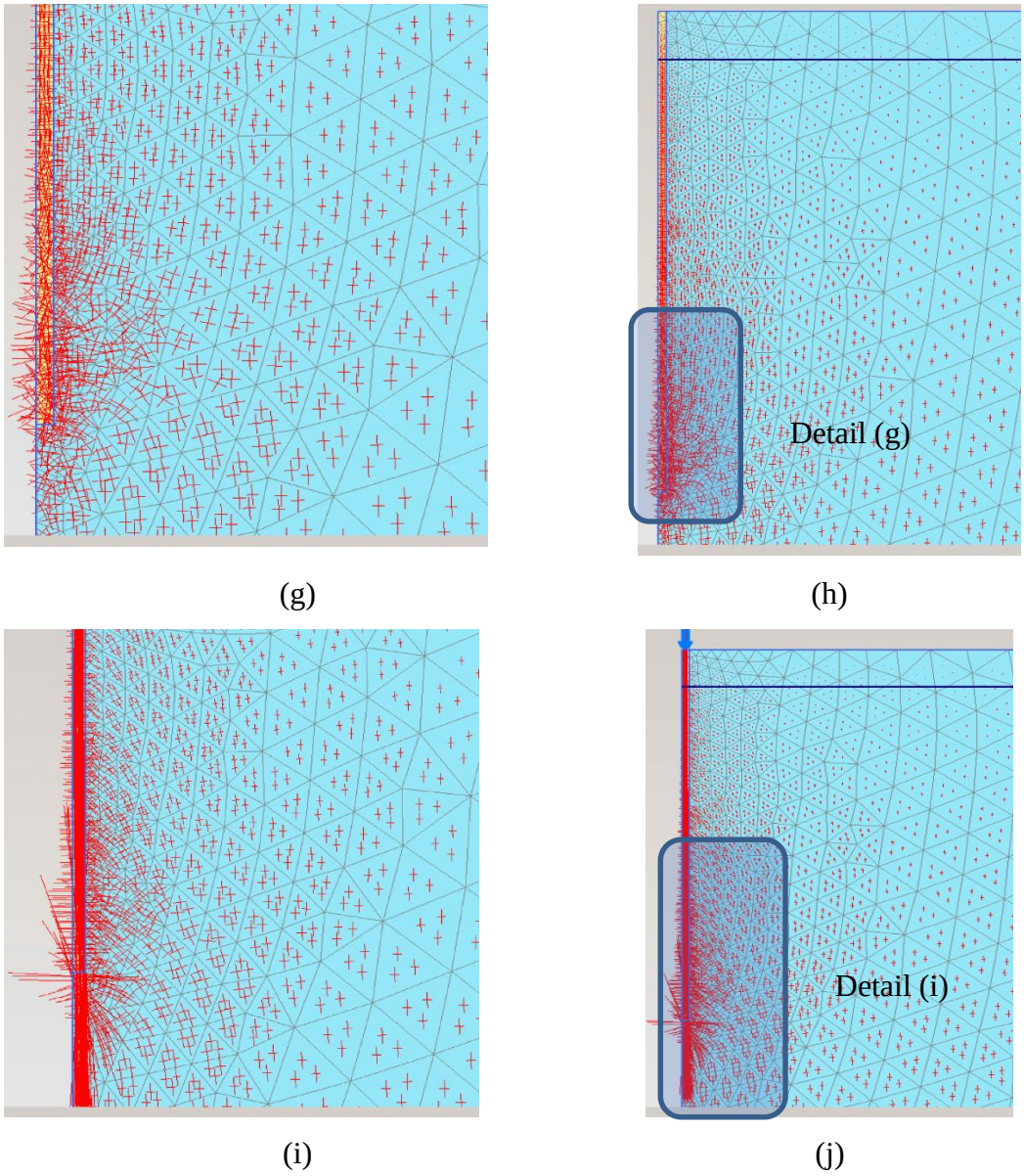

Figure 4-14 – Direction and scale of effective principal stresses (scaled up 2E-3 times). Initial phase - k0 procedure: (a)-(b); phase 1 - pile material set to mortar: (c)-(d); phase 2 – PDT treatment: (e)-(f); phase 3 – pile material set to concrete: (g)-(h); phase 4 - pile performance load applied: (i)-(j)

On Figure 4-15 contours of effective mean stress can be compared for calculation phases (a) – stress from application of dynamic PDT loading, (b) – residual stress after unloading, change of mortar to concrete, (c) – stress from vertical load application. Scale of the mean stress is the same for all phases to allow comparison.

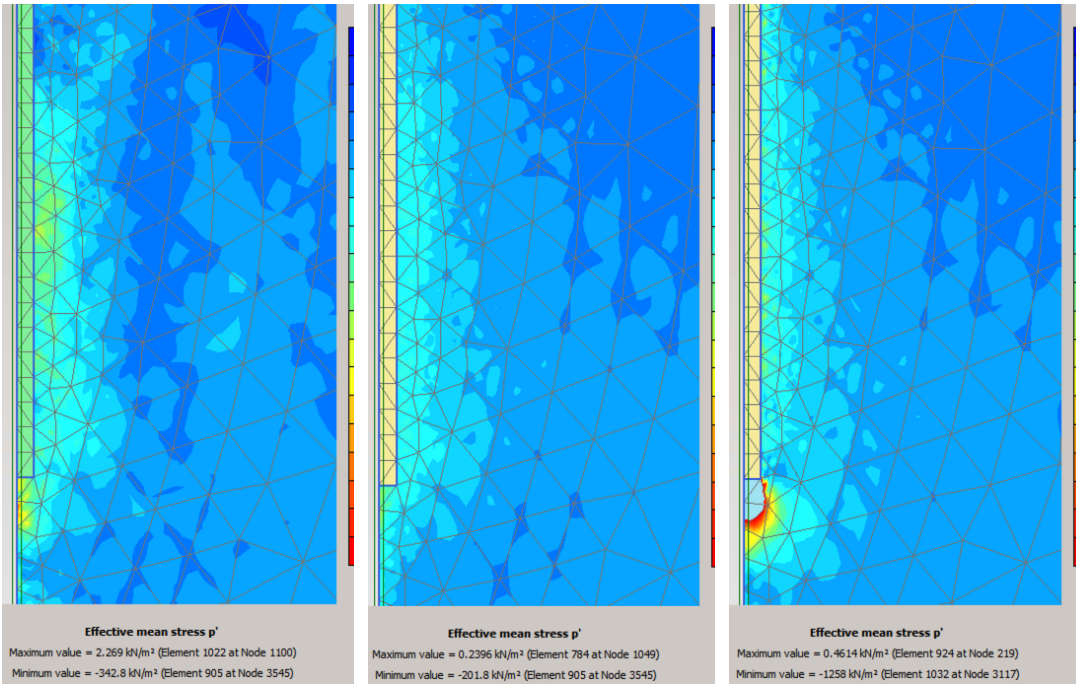

(a) (b) (c)

Figure 4-15 - Contours of effective mean stress can be compared for calculation phases (a) – stress from application of dynamic PDT loading, (b) – residual stress after unloading, change of mortar to concrete, (c) – stress from vertical load application

Figure 4-16 shows contours of effective mean stress *p'* under the tip of the pile. Stress concentration under the tip of the pile corresponds to the plastic bubble underneath the pile. Soil conditions shown on the drawing are at calculation phase of pile performance from the vertical load application.

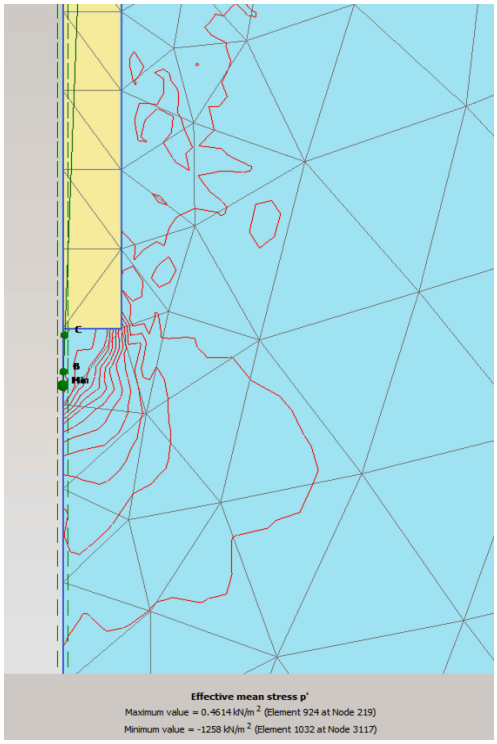

Figure 4-16 – Contours of effective mean stress p' on the model layout under the tip of the pile

Figure 4-17 shows diagrams of effective mean stresses *p'* at each phase of calculation. Phase 2 (c) is depicting increase of effective mean stresses magnitude adjacent to the dynamic loading application. Phase 4 (e) is showing the plastic bubble underneath the tip of volume pile. Note that this is plotted at a different scale.

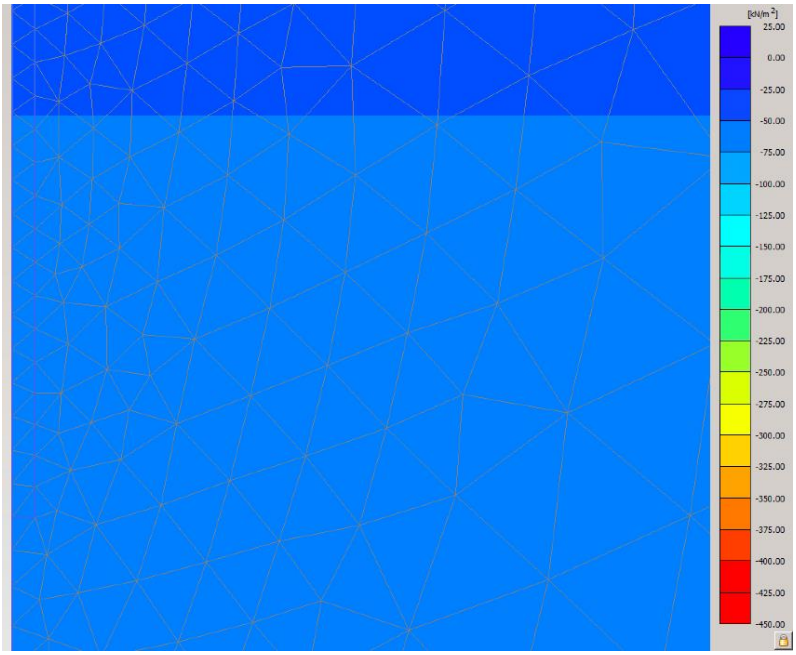

(a) Initial phase

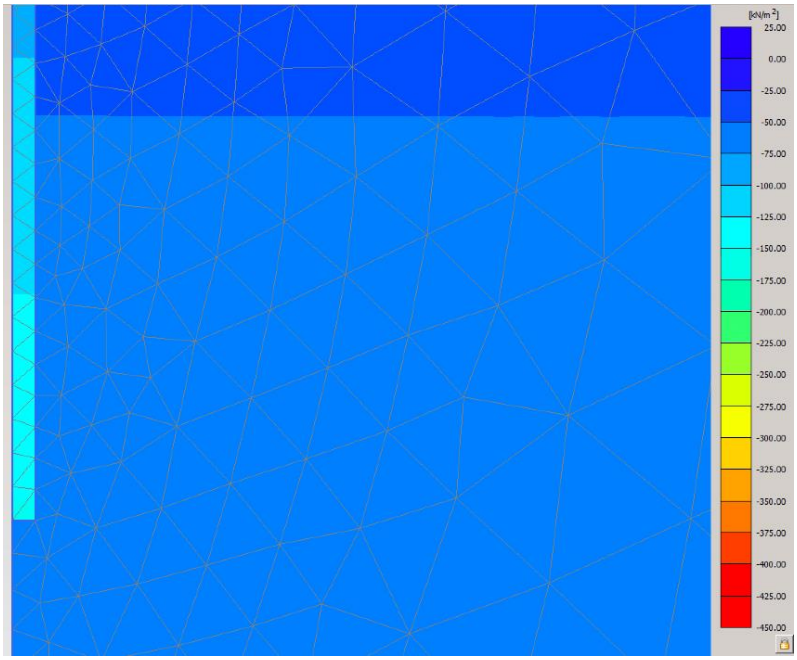

(b) Phase 1 – pile material set to mortar

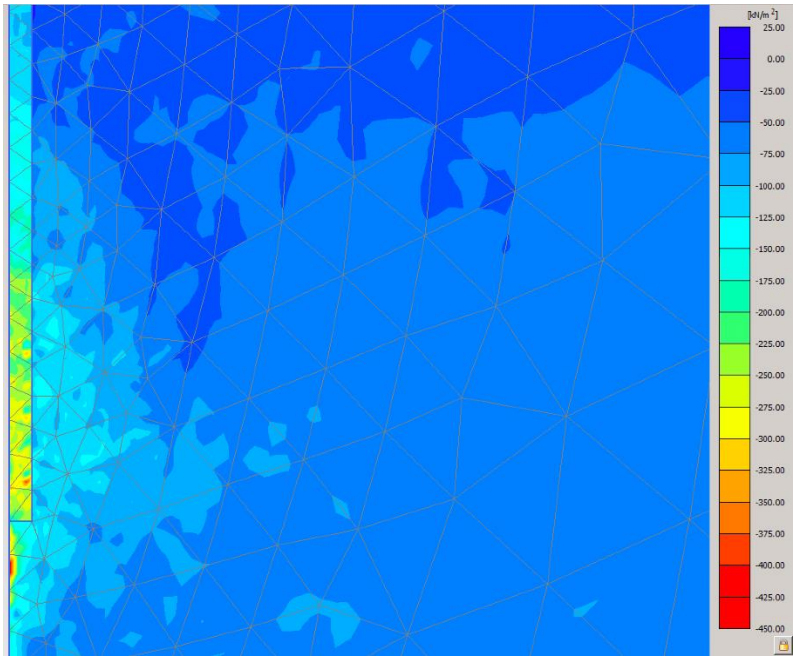

(c) Phase 2 – PDT treatment

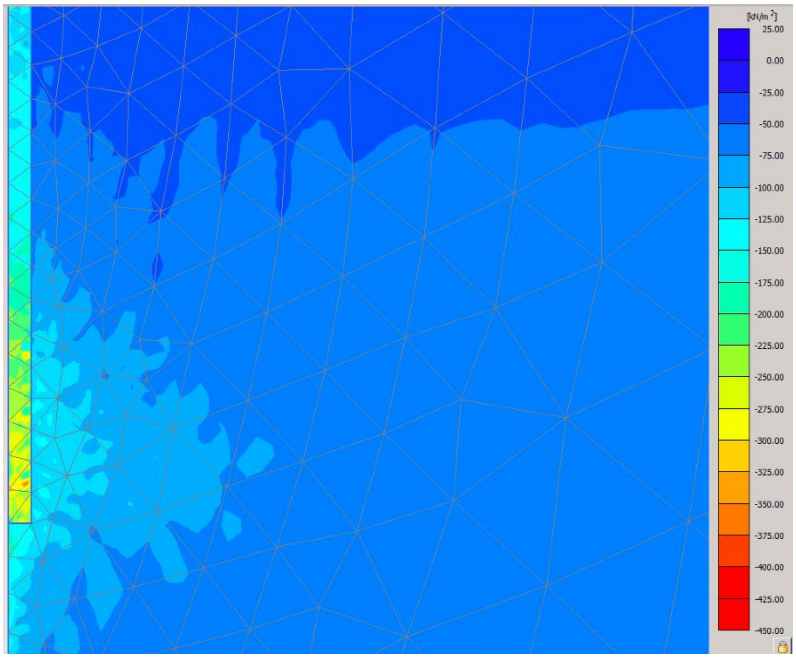

(d) Phase 3 – pile material set to concrete

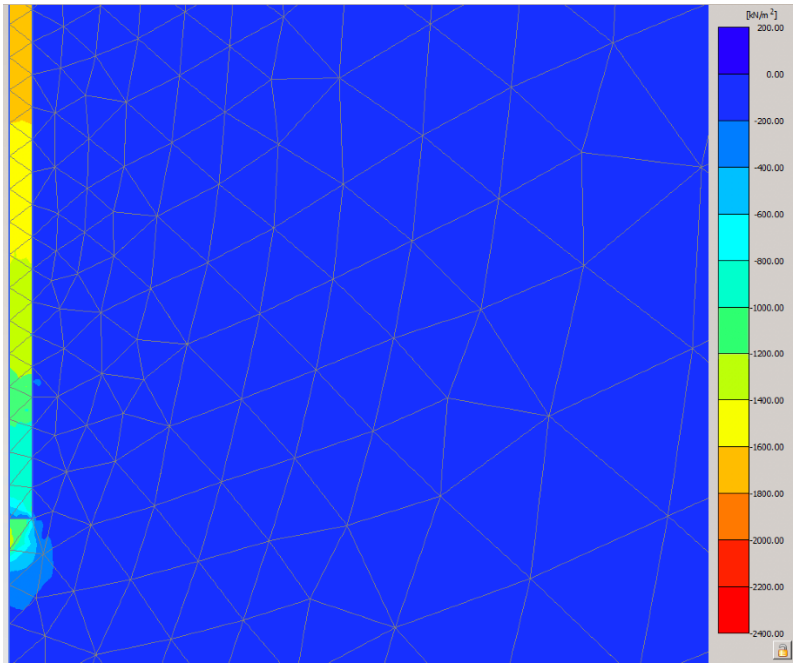

(e) Phase 4 – Pile performance test load applied

Figure 4-17 – Diagram of effective mean stresses p' at each phase of calculation

Plaxis 2D output total displacements contours of the pulse pile model after 5m long pulse treatment is shown on Figure 4-18 and that for the phase 4 after loading is shown on Figure 4-19. Displacements contours on Figure 4-19 are relevant to the working load at settlement of 10% of pile diameter. Comparing the contours from these two figures shows that displacement from pulse treatment is in the range of values for the displacement from vertical load on pile.

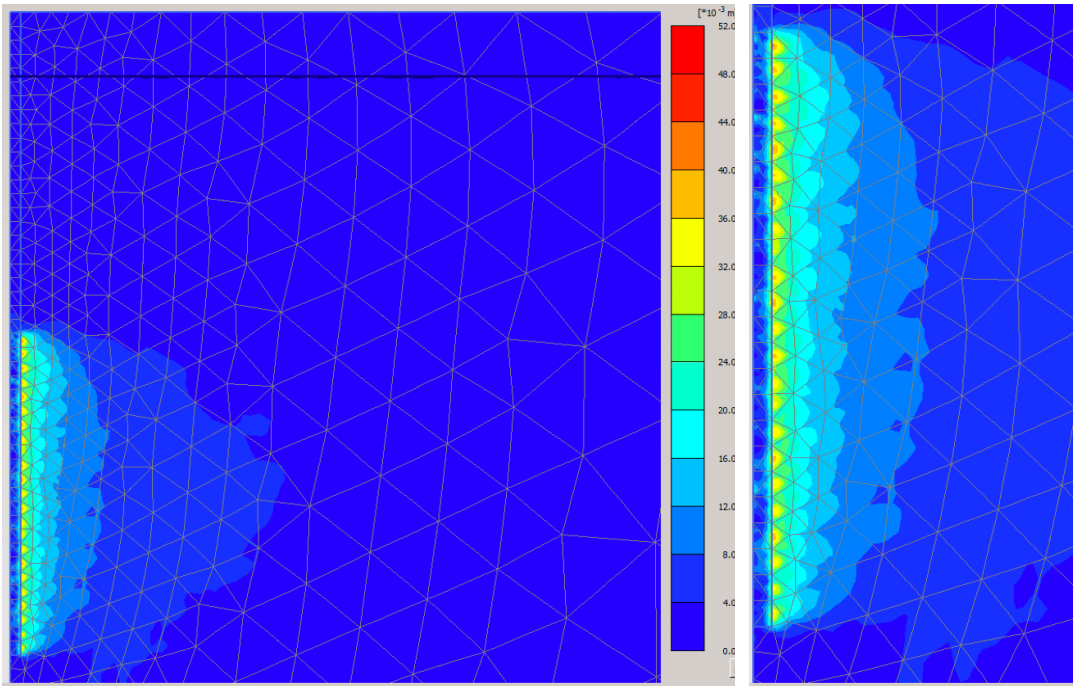

(a) (b)

Figure 4-18 – Total Displacements [u] contours at phase 2 - pulse treatment in mortar for the case of 5m long pulse treatment in coarse grained soils; (a) – full length of pile layout, (b) – pulse treatment zone layout

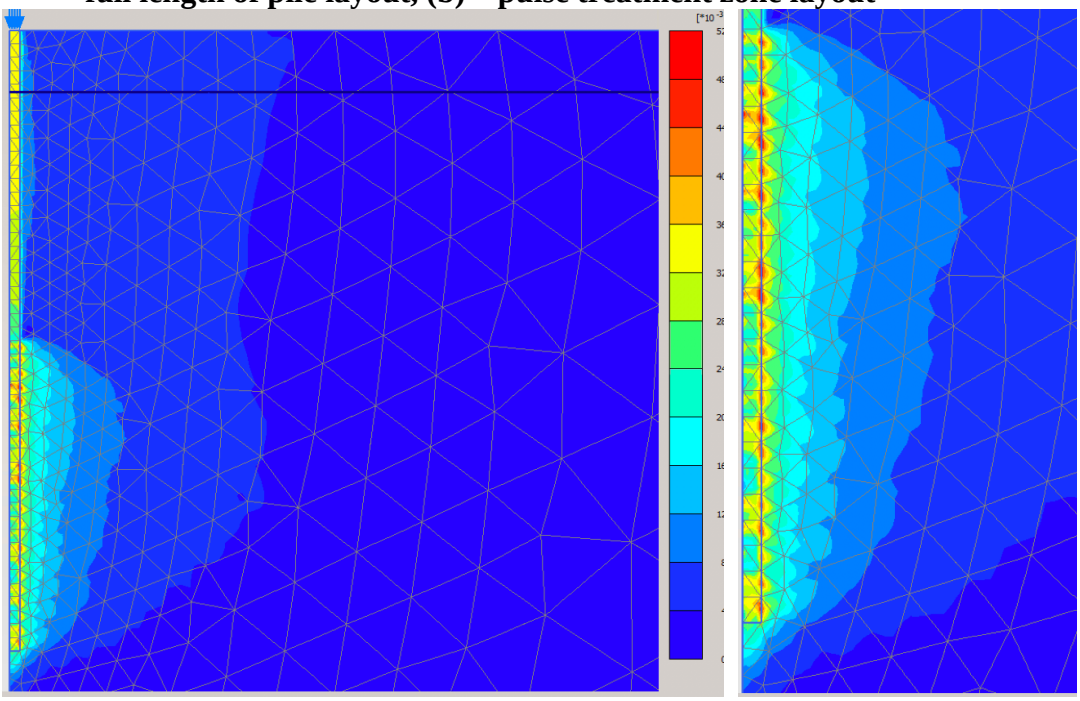

(a) (b)

Figure 4-19 – Total Displacements [u] contours at phase 4 - pile loading performance for the case of 5m length of treatment in coarse grained soils; (a) – full length of pile layout; (b) – pulse treatment zone layout

4.6.2 Bored pile modelling outputs

Single bored pile load test models have been compared with Mohr-Coulomb material parameters for six soil conditions of sand ranging from loose (RD 5%) to medium dense (RD 50%) sand to represent sand types in urban areas where pulse piles are feasible. Resulting Cartesian total vertical stress-total vertical displacement curves have been processed in Excel to obtain load settlement curves. To get results comparable with pulse pile modelling no displacements have been reset after Phase 1. Therefore, initial phase and phase one had to be disabled in curve manager before being copied to Excel. Data has been processed to ignore settlement not related to the axial loading.

Load-Settlement curves of loose to medium dense sands are shown on Figure 4-20. Settlement at the top of the pile has been calculated for the following soil cases:

Table 4-11 – Sand properties for the MC model of the bored pile

Soil case	**Relative Density**	**E'**	**φ'**	**ψ**
	%	kN/m^2	°	°
CFA sand MC d 0	5	3,000	28.625	0
CFA sand MC d 1	10	6,000	29.25	0
CFA sand MC d ref	20	12,000	30.5	0.5
CFA sand MC d 3	30	18,000	31.75	1.75
CFA sand MC d 4	40	24,000	33	3
CFA sand MC d 5	50	30,000	34.25	4.25

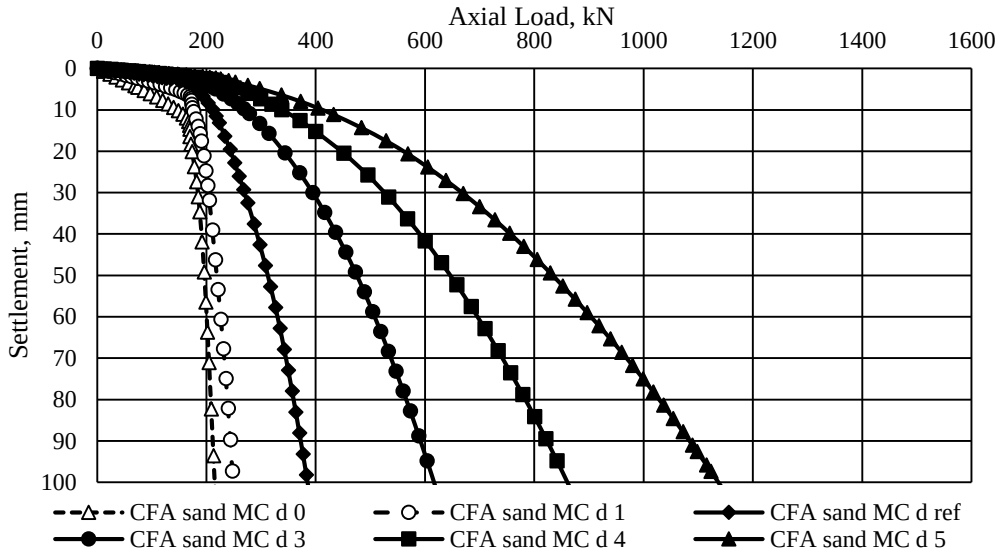

Figure 4-20 – Bored pile Load-Settlement curves for Mohr Coulomb material comparing coarse grained soil cases from loose to medium dense

The form of Figure 4-20 shows that the pile would have failed prior to the normal assumption that failure occurs at a settlement of 10% the pile diameter for relative density of 5% to 20%. This is acceptable since piles are used in these soils to transmit the structural load to a stiffer layer. The purpose of pulse piles is to enable shorter piles to be used in these type of soils.

Thus, an increase of friction angle of sand shows higher bearing capacity of pile. Soil cases 0 and 1 have dilatancy angle of 0 hence there is less distinction between resulting curves of the two. Adding even a minimum value of dilatancy angle gives an increase of bearing capacity.

Six different cases for fine grained soils have been compared for a single pile load test models with Mohr-Coulomb material properties. Resulting Cartesian total vertical stress - total vertical displacement curves have been post-processed in Excel to obtain load settlement curves. As in sand analyses no displacements have been reset after Phase 1. Data has been processed to ignore settlement not related to the axial loading. Load-Settlement curves for the case of Mohr- Coulomb constitutive model of soft to firm clays are shown on Figure 4-21. Clay have been assumed undrained (method A) in terms of effective stresses. Plasticity index I_p of 25% to 3% corresponds to very soft to firm clays. Fine grained soil case parameters compared in the analyses are summarised in Table 4-12.

Table 4-12 – Clay properties of the MC model of the bored pile

Soil case	I_p	E'	φ'	c'
	%	kN/m^2	°	°
CFA clay MC u(A) 0	25	1,500	21	0
CFA clay MC u(A) 1	15	2,500	23	0
CFA clay MC u(A) ref	7	5,000	25	0
CFA clay MC u(A) 3	5	7,500	25	0
CFA clay MC u(A) 4	4	10,000	25	0
CFA clay MC u(A) 5	3	12,500	25	0

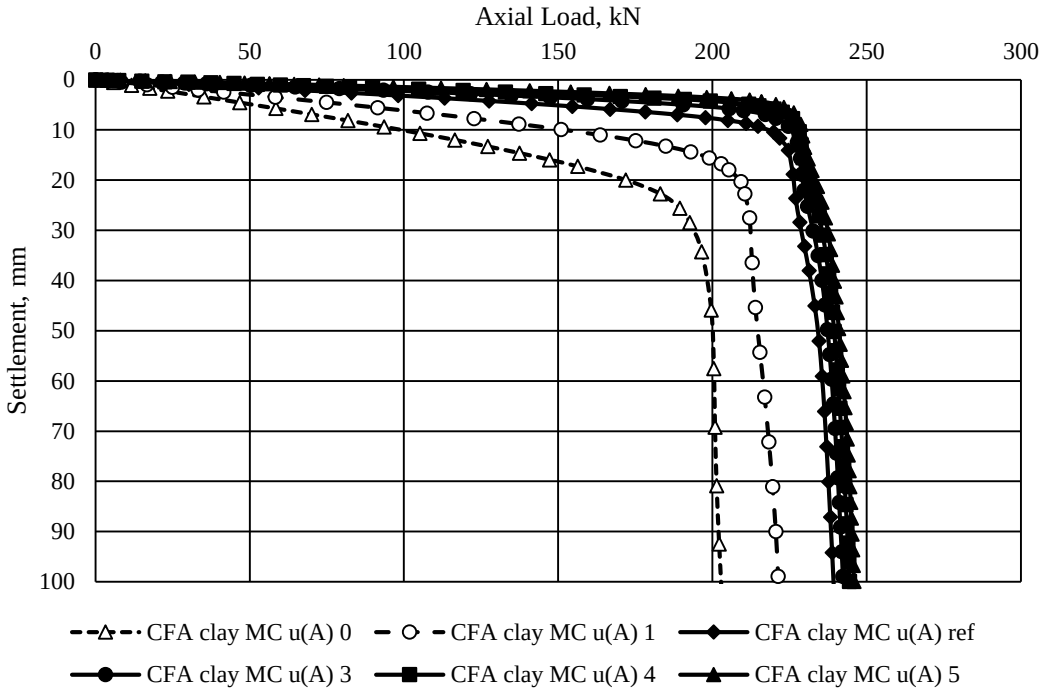

Figure 4-21 – Soil sensitivity (Clay) CFA – Load-Settlement curves – Mohr Coulomb

Effective parameters variation of reference models of clay used in the analyses has influenced the resulting load-settlement curves for the single bored pile. Whereas an increase of soil strength parameters between case 0 and ref ended up with distinctive increase of bearing capacity, variation of stiffness only had less impact on pile-soil behaviour (as can be seen on Figure 4-21).

4.6.3 Pulse piles modelling outputs – Sand

The Pulse pile modelling involved a dynamic calculation phase followed by an axial loading phase simulating a load test of the pile. Therefore, no reset of displacements could be applied after phase 1. Resulting Cartesian total vertical stress-total vertical displacement curves have been processed in Excel to obtain load settlement curves. Initial phase, phase 1 and phase 4 had to be disabled in curve manager before being copied to Excel. Vertical settlements not related to axial load have been ignored in post-processing. Pulse pile models in coarse grained soils are based on soil parameters as per Table 4-11.

The pulse piles treated over 1m, 3m and 5m from the pile tip have been modelled and results have been summarised. Load-settlement curves of bored, 1m, 3m and 5m pulse piles for each of 6 considered soil cases of coarse grained soil are shown on Figure 4-22 to Figure 4-27. Performance of pulse piles for each soil case (DYN sand MC d series) are compared with relevant curve obtained for the bored pile (CFA sand MC d series). The Mohr Coulomb constitutive model has been used in the sensitivity analysis.

A comparison is made between the length of pulse treatment and no treatment for each type of coarse grained soil (Figure 4-22 to Figure 4-27), and a comparison for each length of treatment of the effect on the type of soil (Figure 4-28 to Figure 4-30). They all show that increasing the length of treatment increases the capacity which is expected given that the pile diameter is increased. The simulation in the loose (RD5%) soil shows a significant increase in settlement (Figure 4-22) suggesting that the bored pile had reached its ultimate capacity before the nominal working load at a settlement of 10% of the pile diameter during loading but capacity and the amount of settlement increased as the length of the treated section increased. It is noted that the pulse treatment had little effect on the pile capacity up to the load that caused the bored pile to fail (170kN) for the very loose sand. However, the treatment was

insufficient in all cases for the very loose sand. In practice, more than one pulse would be generated, therefore, the treatment does improve the pile capacity sufficiently.

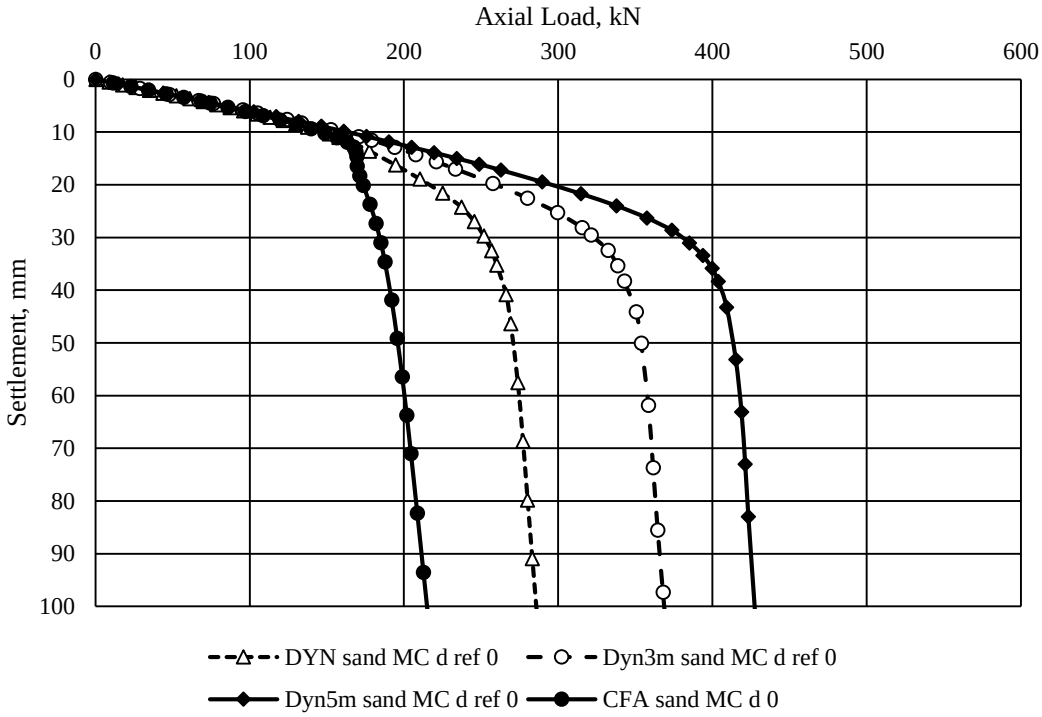

Figure 4-22 – Load-settlement curves of bored and pulse piles of 1m, 3m and 5m expansion length in very loose coarse grained soil (case 0), Mohr-Coulomb constitutive model

This conclusion also applied to the piles in all the very loose to loose sands though, in each case the treatment increased the capacity for a given settlement and the settlement for a given load decreased.

In the cases of the medium dense sand, the capacity also increased with the length of treatment but the ultimate capacity was not as clearly defined. This suggests failure in the loose sands was likely to be punching failure whereas shear failure occurred in the medium dense sands.

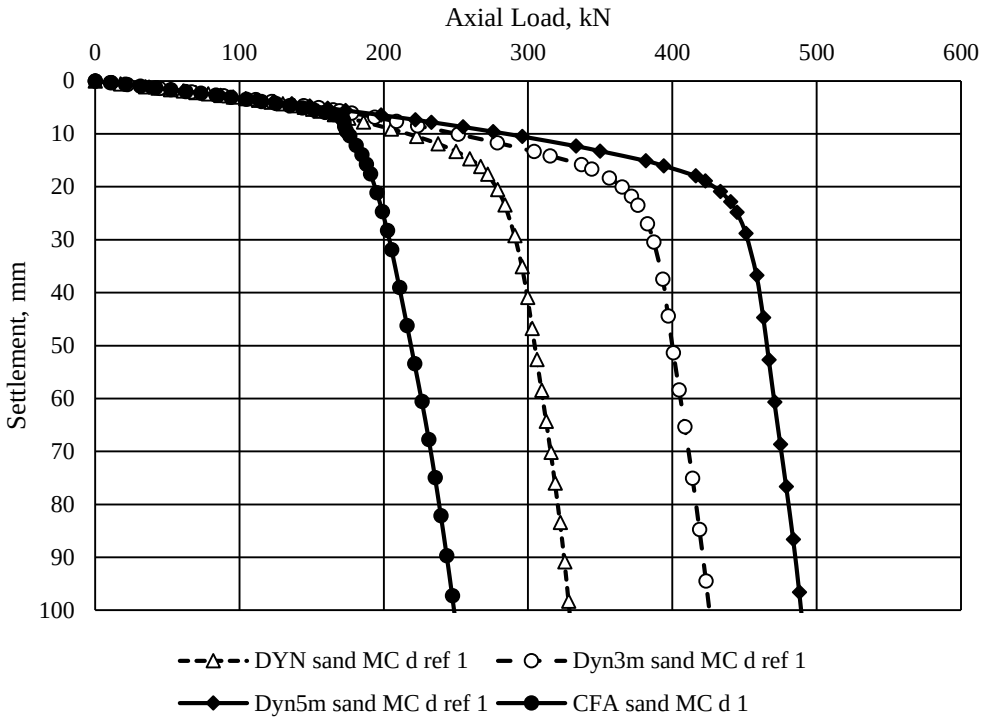

Figure 4-23 – Load-settlement curves of bored and pulse piles of 1m, 3m and 5m expansion length in very loose sand (case 1), Mohr-Coulomb constitutive model

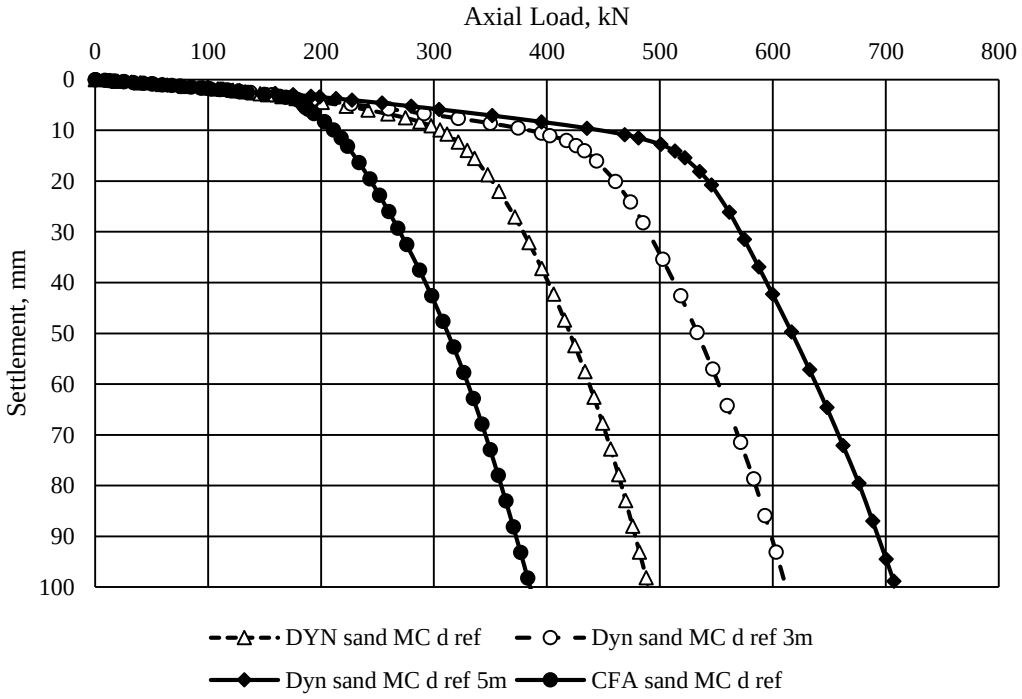

Figure 4-24 – Load-settlement curves of bored and pulse piles of 1m, 3m and 5m expansion length in loose sand (case ref), Mohr-Coulomb constitutive model

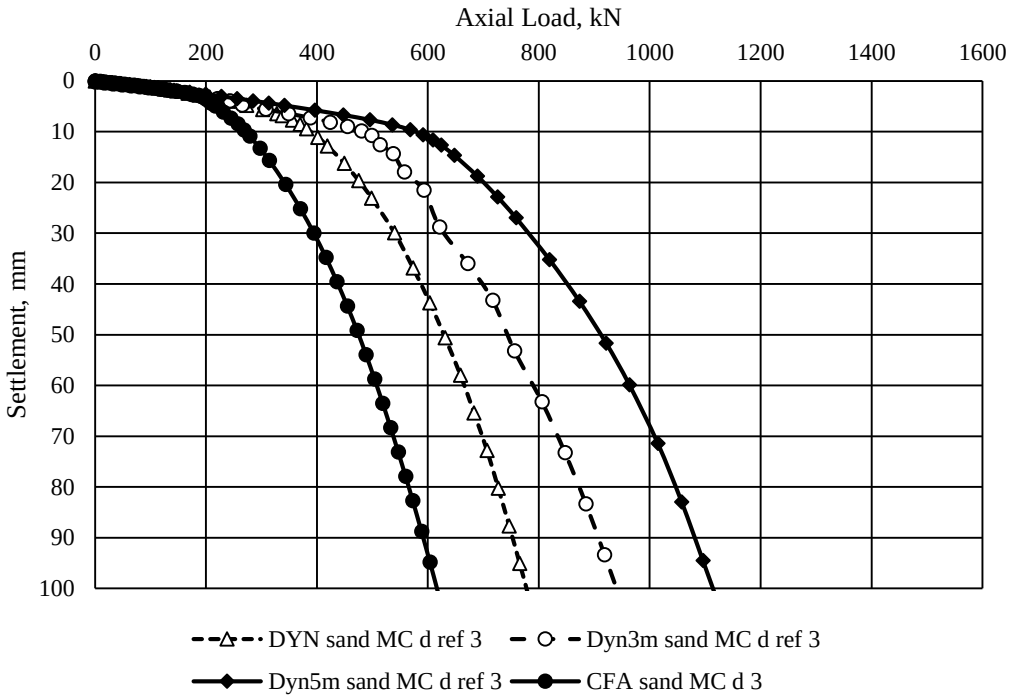

Figure 4-25 – Load-settlement curves of bored and pulse piles of 1m, 3m and 5m expansion length in loose sand (case 3), Mohr-Coulomb constitutive model

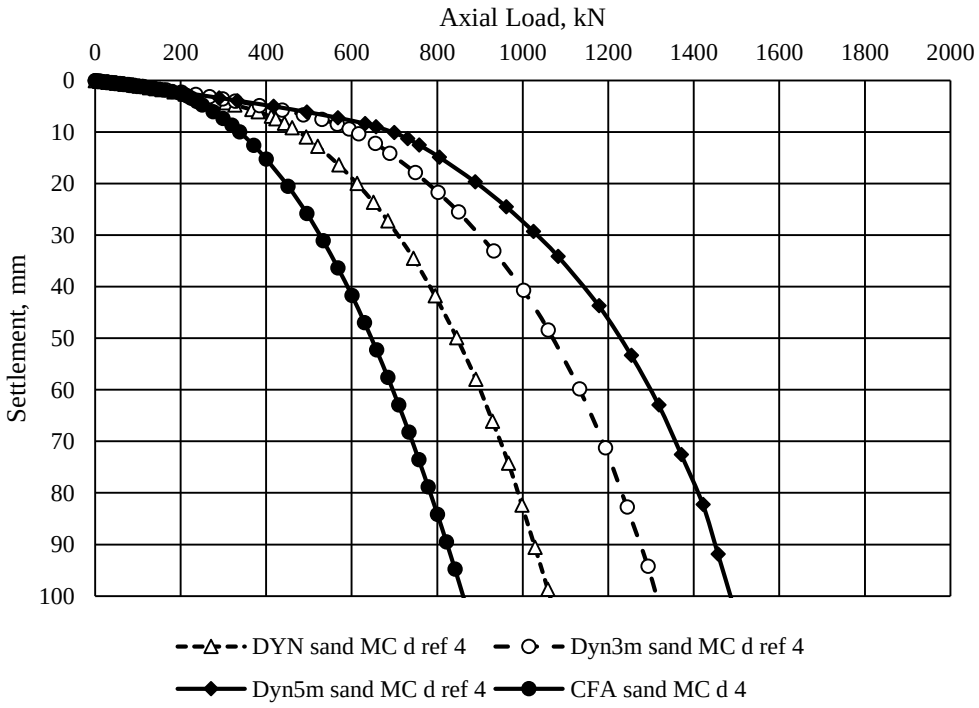

Figure 4-26 – Load-settlement curves of bored and pulse piles of 1m, 3m and 5m expansion length in medium dense sand (case 4), Mohr-Coulomb constitutive model

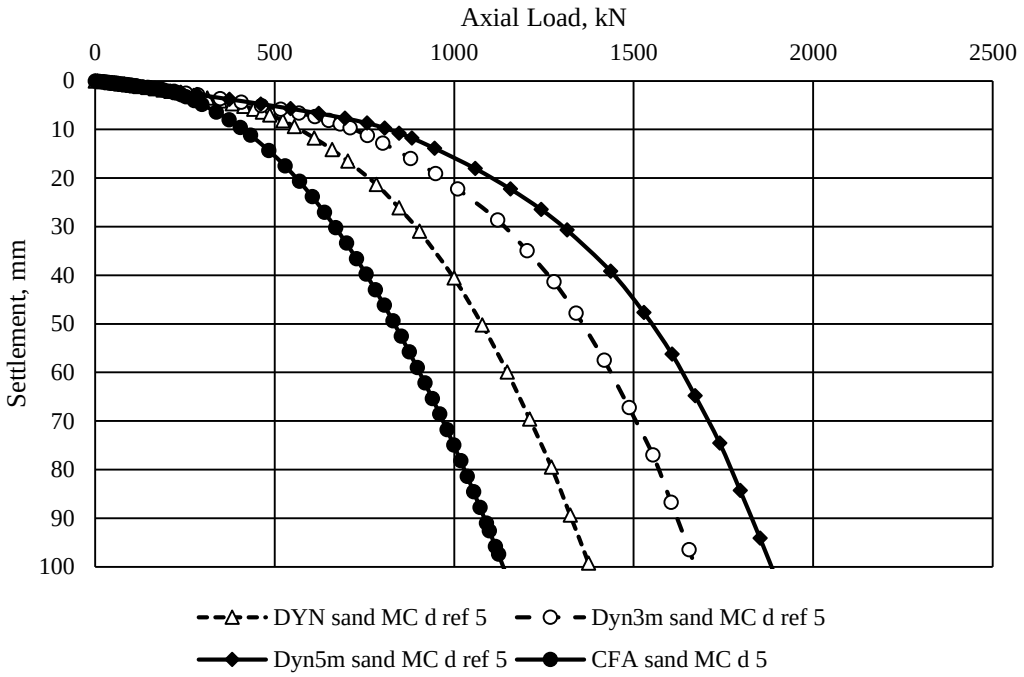

Figure 4-27 – Load-settlement curves of bored and pulse piles of 1m, 3m and 5m expansion length in medium dense sand (case 5), Mohr-Coulomb constitutive model

Comparison of model outputs shows congruence of the modelling results for coarse grained drained material. Increase of the length of pulse treatment leads to increase of ultimate load of pile. Comparing offset of curves of pile performance between the bored and pulse piles of variable exposed lengths for six specified soil cases is showing no substantial difference in capacity increments from loose to medium dense coarse grained soil.

Load-settlement behaviour has been compared for the six soil cases. Figure 4-28 depicts load-settlement curves for the pulse pile with expansion length of 1m in very loose to medium dense sands. Soil cases considered in this comparison specified in Table 4-11.

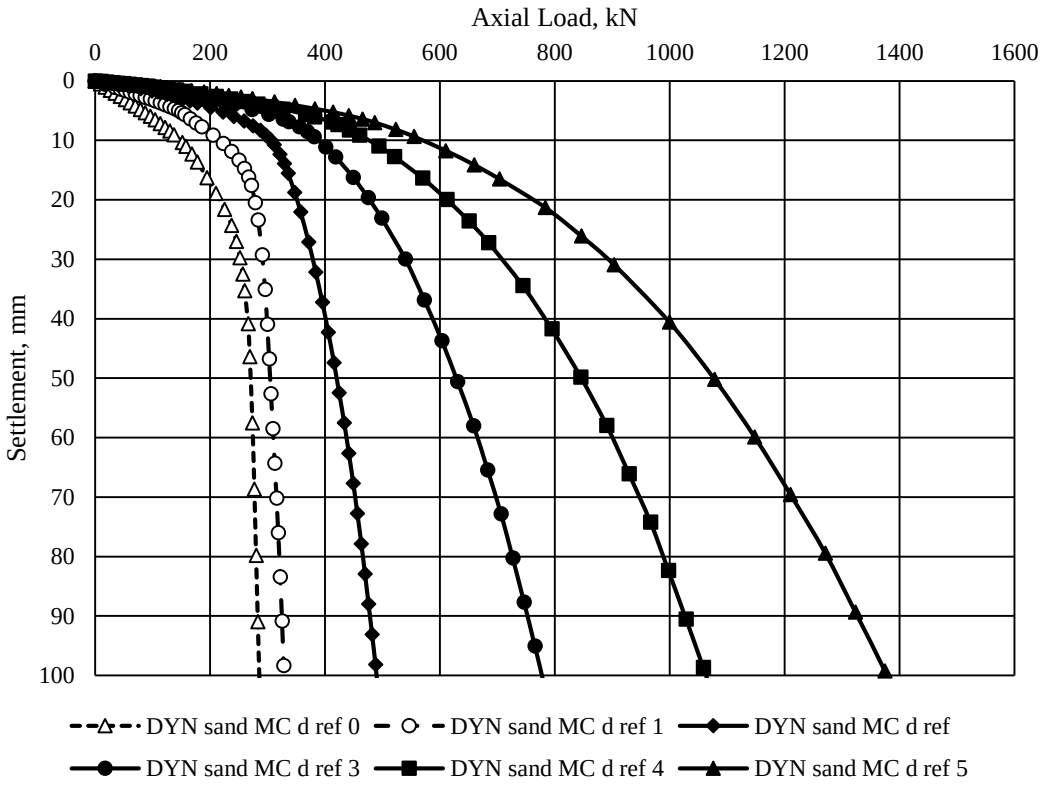

Figure 4-28 – Load-settlement curves of pulse piles expansion length of 1m in very loose (case 0) to medium dense (case 5) sands

Comparison of soil cases corresponds with the one for the bored pile shown on Figure 4-20.

Shape of the curves at equal scale does not change for bored and pulse piles of variable treated length. Load-settlement curves for the pulse pile with expansion length of 3m and 5m in very loose to medium dense sands are shown on Figure 4-29 and Figure 4-30 respectively.

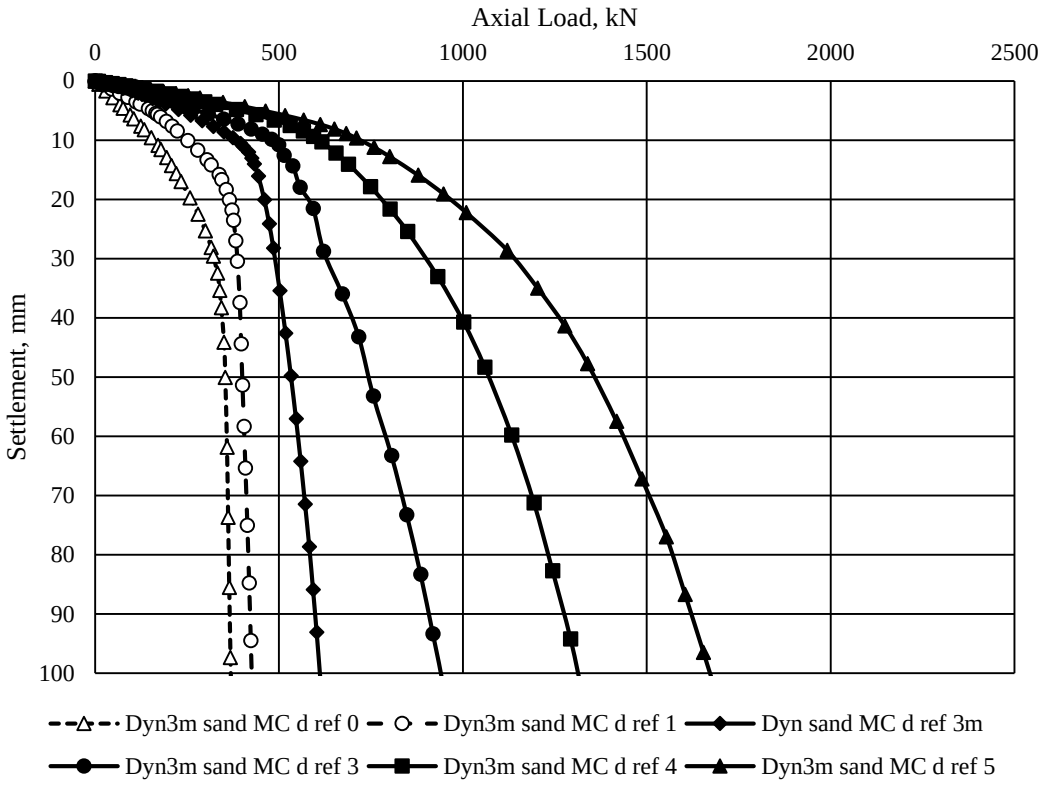

Figure 4-29 – Load-settlement curves of pulse piles expansion length of 3m in very loose (case 0) to medium dense (case 5) sands

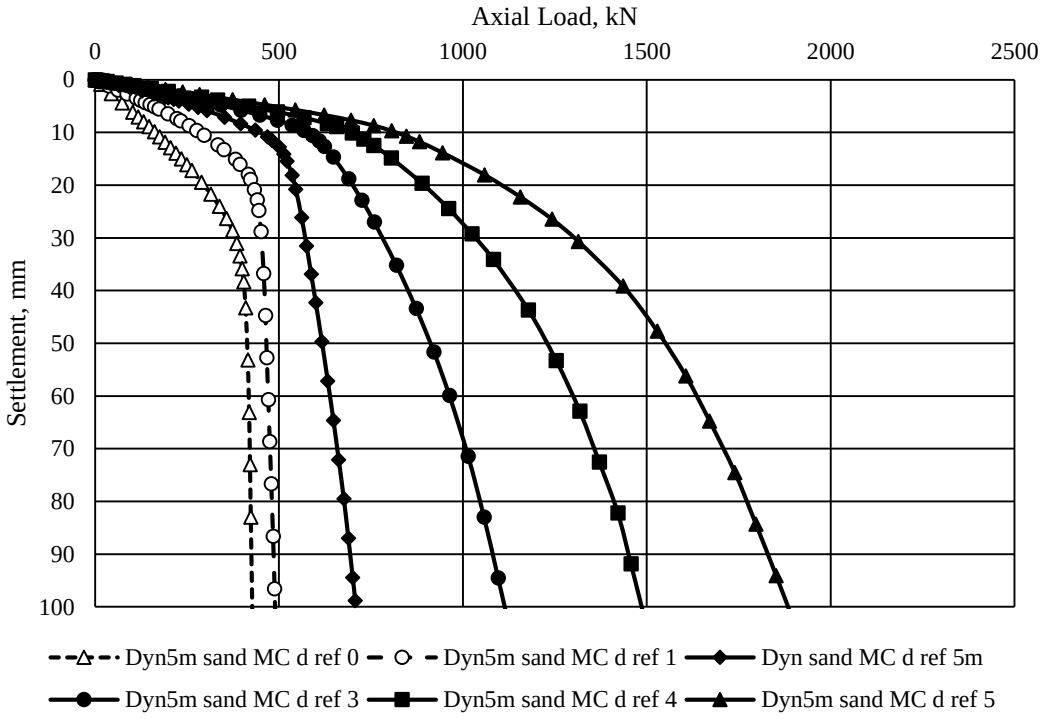

Figure 4-30 – Load-settlement curves of pulse piles expansion length of 5m in very loose (case 0) to medium dense (case 5) sands

4.6.4 Pulse piles modelling outputs – Clays

The pulse piles in clays have been modelled with Mohr-Coulomb material properties as specified in Table 4-12. Clay has been specified as undrained (method A) material in terms of effective stresses. Consolidation phase followed the dynamic loading calculation. Pulse pile modelling in clays involved dynamic calculation phase followed by axial loading phase simulating load test of pile. Therefore, no reset of displacements could be applied after phase 1. Resulting Cartesian total vertical stress-total vertical displacement curves have been processed in Excel to obtain load settlement curves. Initial phase, phase 1, phase 2 and phase 4 had to be disabled in curves manager before being copied to Excel. Vertical settlements not related to axial load have been ignored in post-processing.

The pulse piles treated over 1m, 3m and 5m from the pile tip have been modelled and results have been summarised. Load-settlement curves of bored, 1m, 3m and 5m pulse piles for each of six considered soil cases are shown on Figure 4-31 to Figure 4-36.

Mohr Coulomb constitutive model has been used in the sensitivity analysis.

A comparison is made between the length of pulse treatment for each type of fine grained soil (Figure 4-31 to Figure 4-36), and a comparison for each length of treatment of the effect on the type of soil (Figure 4-36 to Figure 4-38). They all show that increasing the length of treatment increases the capacity due to the increase in pile diameter. The simulation in the very soft clayey (case 0) soil shows a significant increase in settlement suggesting the bored pile had reached its ultimate capacity before the nominal working load at a settlement of 10% of the pile diameter during loading but capacity and the amount of settlement increased as the length of the treated section increased. The pulse treatment had little effect on the pile capacity up to the load that caused the bored pile to fail (185kN) for the very soft clay. However, the treatment was insufficient in all cases for the very soft clay. This is one reason why, in practice, more than one pulse is applied.

This conclusion also applied to the piles in all the very soft to firm clays, in each case the treatment increased the capacity for a given settlement and the settlement for a given load decreased. This suggests failure in the very soft to firm clays was likely to be punching failure.

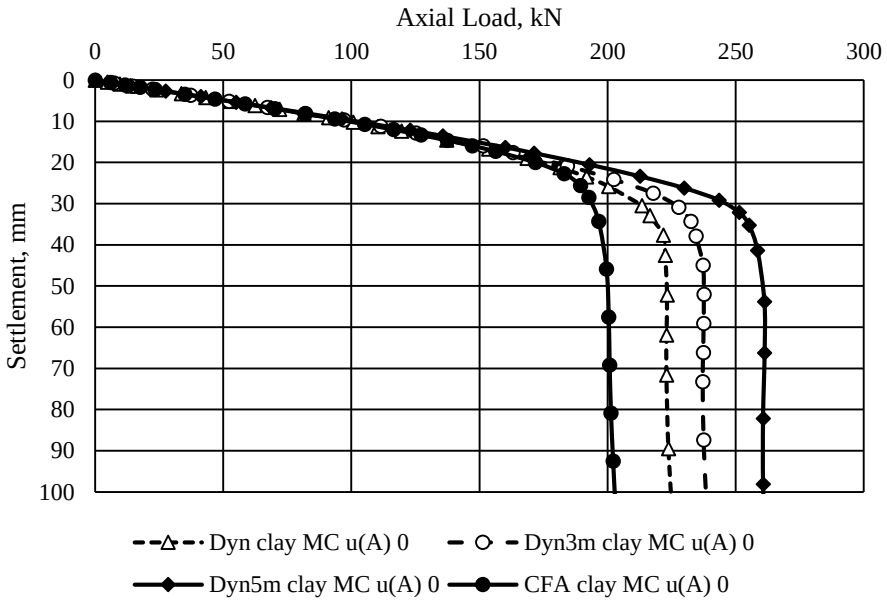

Figure 4-31 – Load-settlement curves of bored and pulse piles of 1m, 3m and 5m expansion length in very soft clay (case 0), Mohr-Coulomb constitutive model

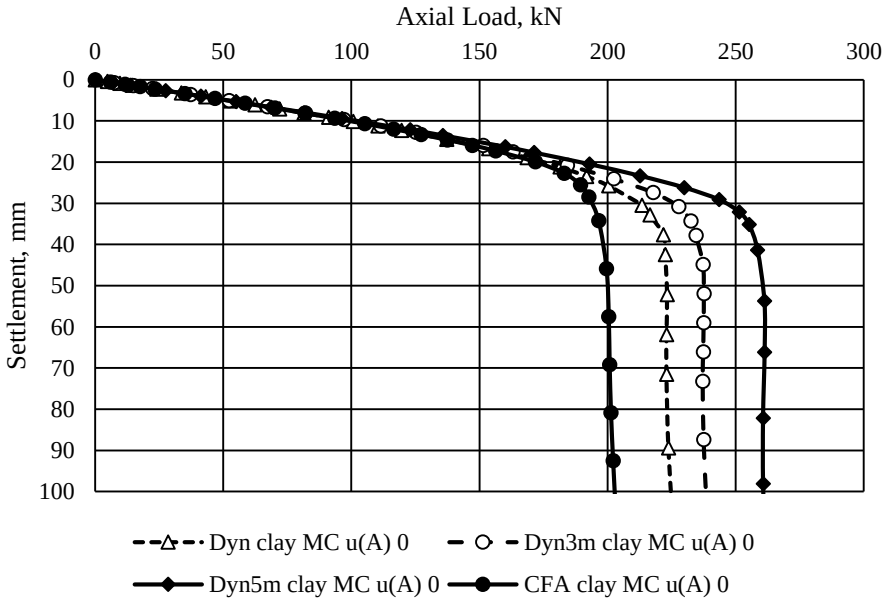

Figure 4-32 – Load-settlement curves of bored and pulse piles of 1m, 3m and 5m expansion length in very soft clay (case 1), Mohr-Coulomb constitutive model

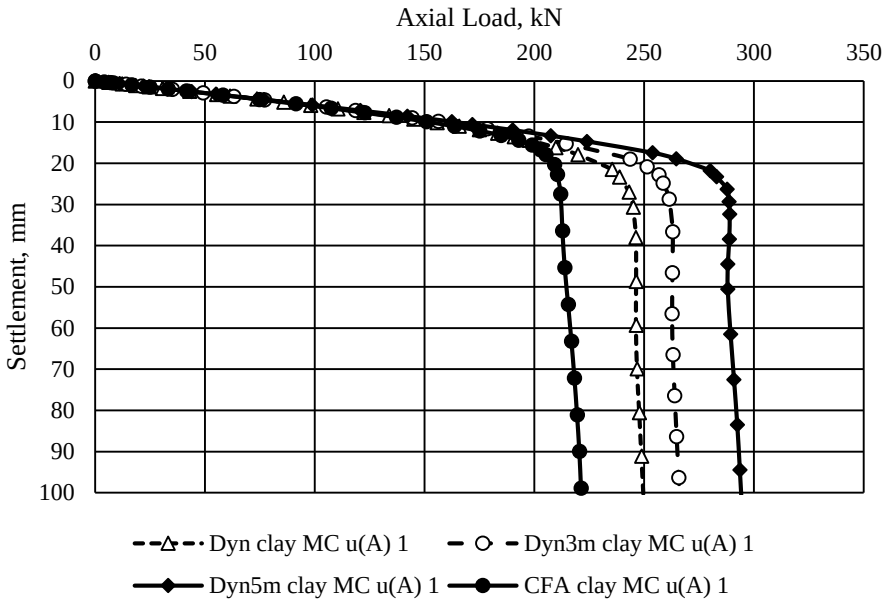

Figure 4-33 – Load-settlement curves of bored and pulse piles of 1m, 3m and 5m expansion length in soft clay (case ref), Mohr-Coulomb constitutive model

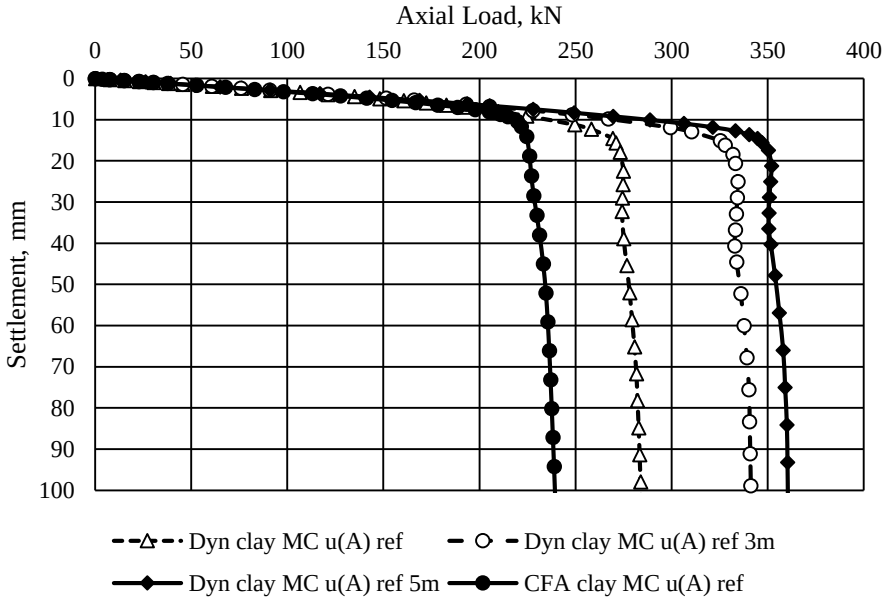

Figure 4-34 – Load-settlement curves of bored and pulse piles of 1m, 3m and 5m expansion length in soft to firm clay (case 3), Mohr-Coulomb constitutive model

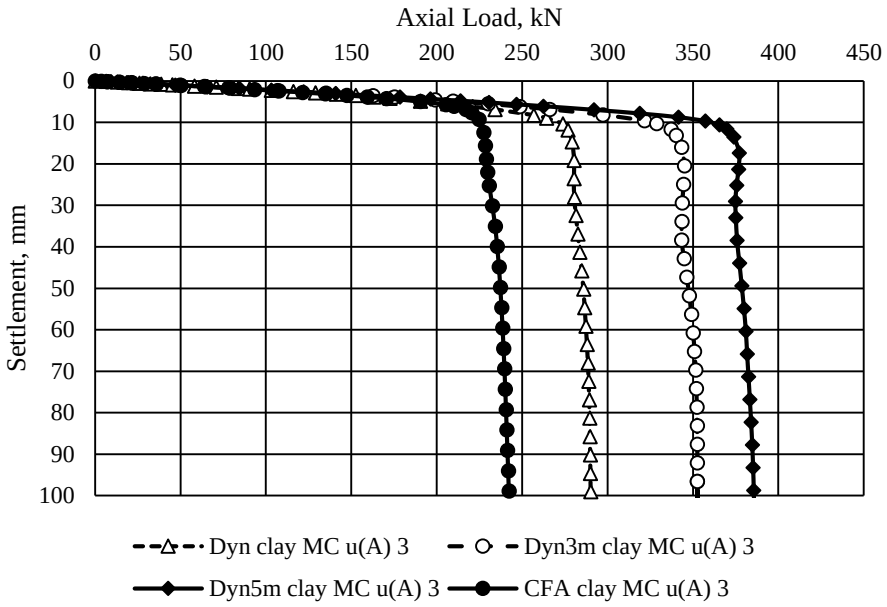

Figure 4-35 – Load-settlement curves of bored and pulse piles of 1m, 3m and 5m expansion length in firm clay (case 4), Mohr-Coulomb constitutive model

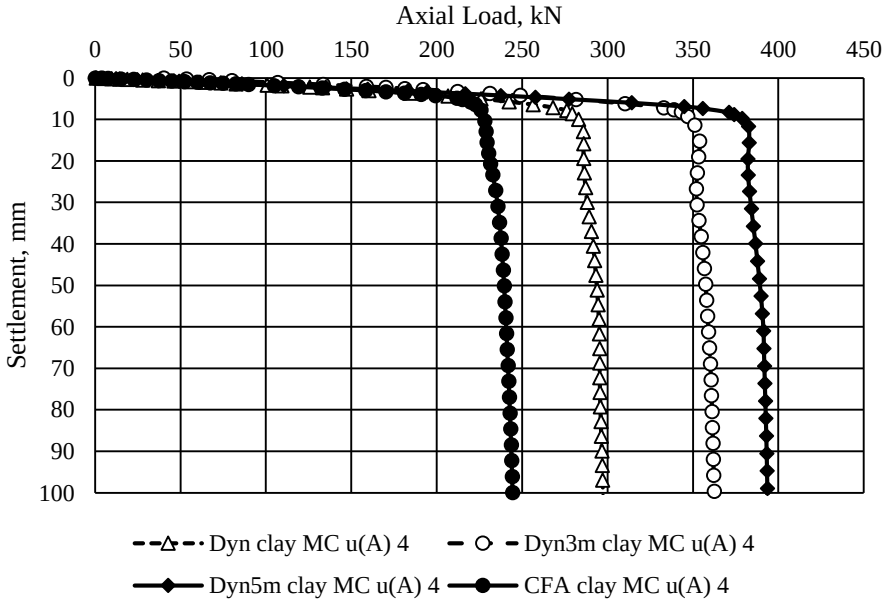

Figure 4-36 – Load-settlement curves of bored and pulse piles of 1m, 3m and 5m expansion length in firm clay (case 5), Mohr-Coulomb constitutive model

The load-settlement curves in clays are similar for bored and pulse piles; that is they both show punching failure. As expected increase of the length of applied dynamic loading increase pile capacity.

Load-settlement behaviour has been compared for the six soil cases in clays. Figure 4-37 depicts load-settlement curves for the pulse pile with expansion length of 1m in very soft to firm clays.

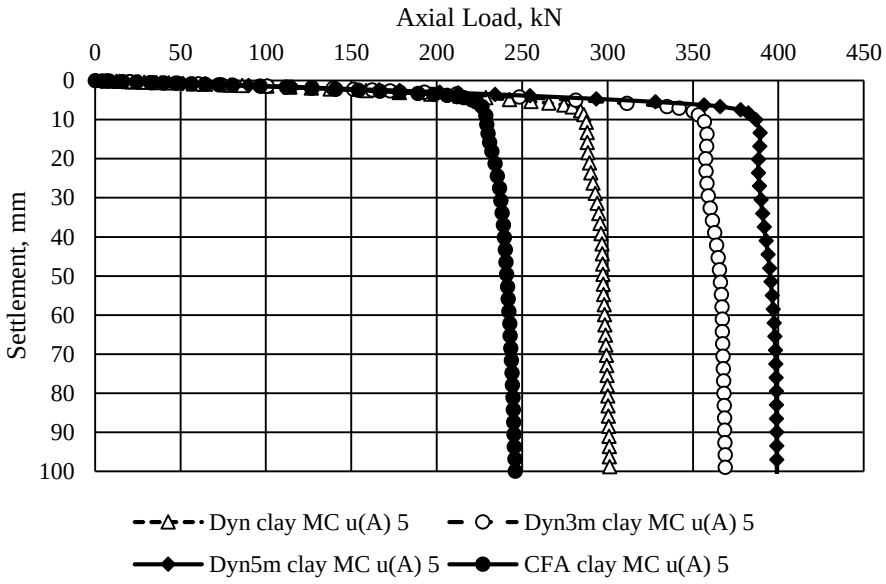

Figure 4-37 – Load-settlement curves of pulse piles expansion length of 1m in very soft (case 0) to firm (case 5) clays

Results for pulse piles are comparable with the bored pile curves. Load-settlement curves for the pulse pile with expansion length of 3m and 5m in very soft to firm clays shown on Figure 4-37 and Figure 4-38 respectively.

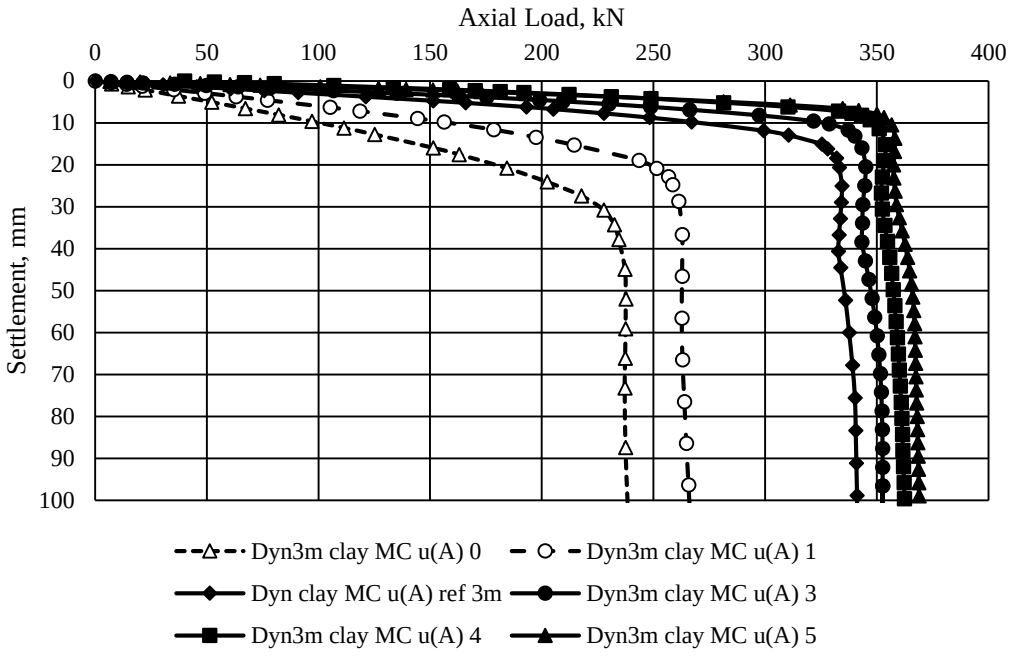

Figure 4-38 – Load-settlement curves of pulse piles expansion length of 3m in very soft (case 0) to firm (case 5) clays

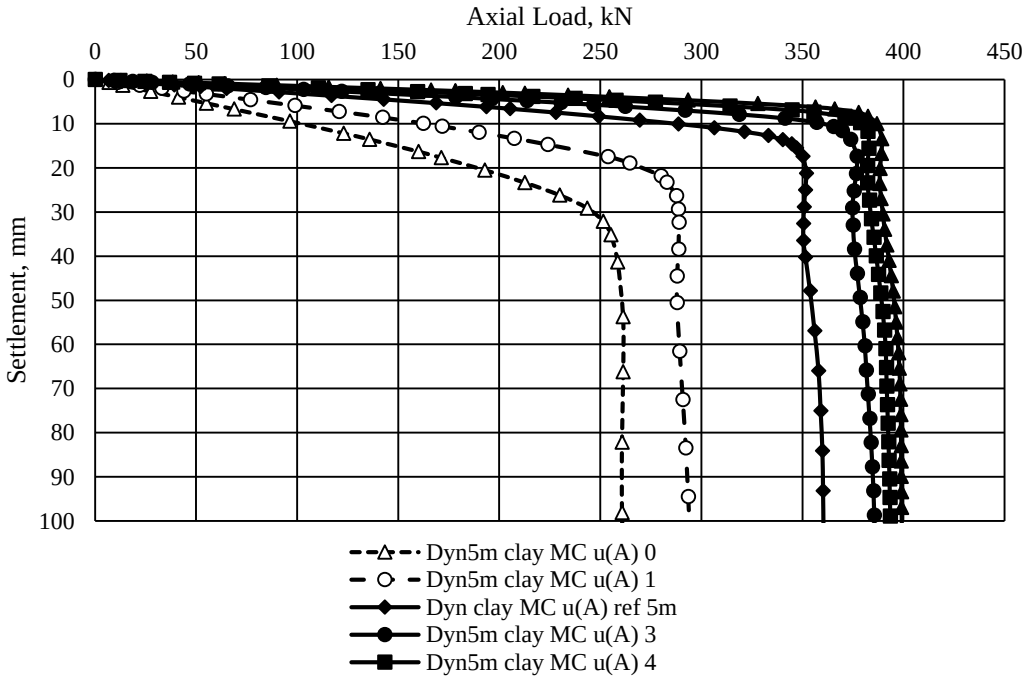

Figure 4-39 – Load-settlement curves of pulse piles expansion length of 5m in very soft (case 0) to firm (case 5) clays

4.6.5 Modelling outputs of bearing capacity of bored piles – MC, HS, HSS

Soil sensitivity analysis has been performed in coarse grained material using Mohr-Coulomb, Hardening Soil and HS-small models. Soil parameters have been from relationships with relative density. Loose to medium dense sands have been analysed. Analysis of a bored single pile behaviour is performed.

Axial capacity at settlement of 10% of pile diameter have been compared for six soil cases from very loose (case 0) to medium dense (case 5) sands showing (Figure 4-40) an increase of pile capacity with improvement of soil properties. The soil types are summarised in Table 4-13.

Table 4-13 – Constitutive models compared for calculation of bearing capacity of pile in sand

Case	Soil type	Constitutive model	Pile type
CFA Sand MC - drained	Sand (very loose to medium dense)	Mohr-Coulomb	Bored
CFA Sand HS - drained	Sand (very loose to medium dense)	Hardening Soil	Bored
CFA Sand HSS - drained	Sand (very loose to medium dense)	HS-small	Bored

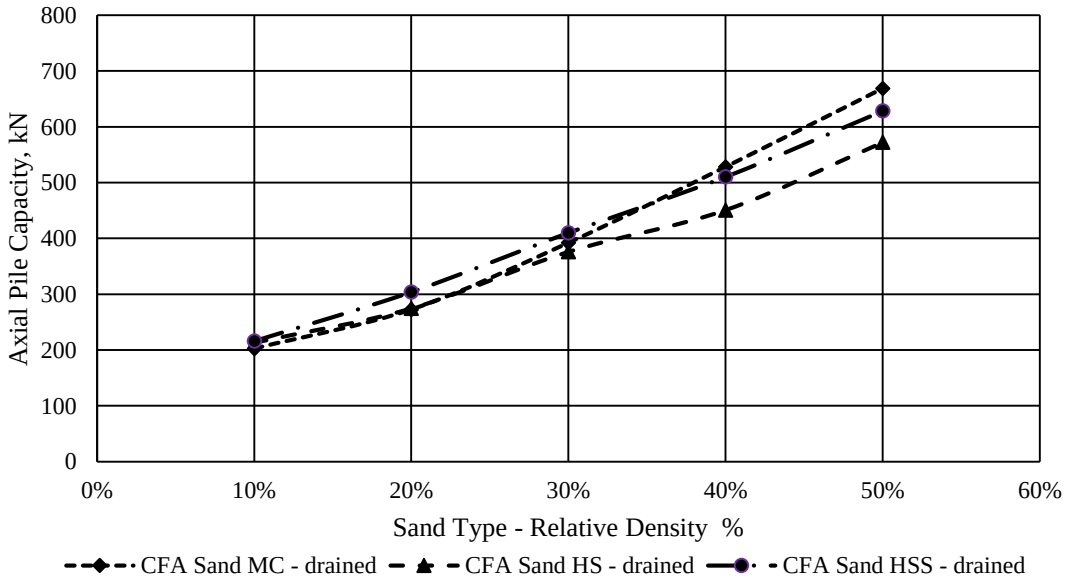

Figure 4-40 – Working load on bored piles in coarse grained soils calculated with Mohr Coulomb, Hardening Soil and Hardening Soil – small stiffness constitutive models

Soil sensitivity analysis has been performed for fine grained soils using Mohr-Coulomb, Hardening Soil and HS-small models. Soil parameters have been ranged in relation to the effective stiffness. Very soft to firm clays have been considered. Analysis of a CFA single pile behaviour is performed.

Axial capacity at settlement of 10% of pile diameter have been compared for six soil cases from very soft (case 0) to firm (case5) clays. Figure 4-41 depicts increase of pile capacity with improvement of soil properties. No increase of strength properties of clay is resulting in flattening of the curve. Considered material model cases summarised in Table 4-14

Table 4-14 – Constitutive models compared for calculation of bearing capacity of pile in clay

Case	Soil type	Constitutive model	Pile type
CFA Sand MC - drained	Clay (very soft to firm)	Mohr-Coulomb	Bored
CFA Sand HS - drained	Clay (very soft to firm)	Hardening Soil	Bored
CFA Sand HSS - drained	Clay (very soft to firm)	HS-small	Bored

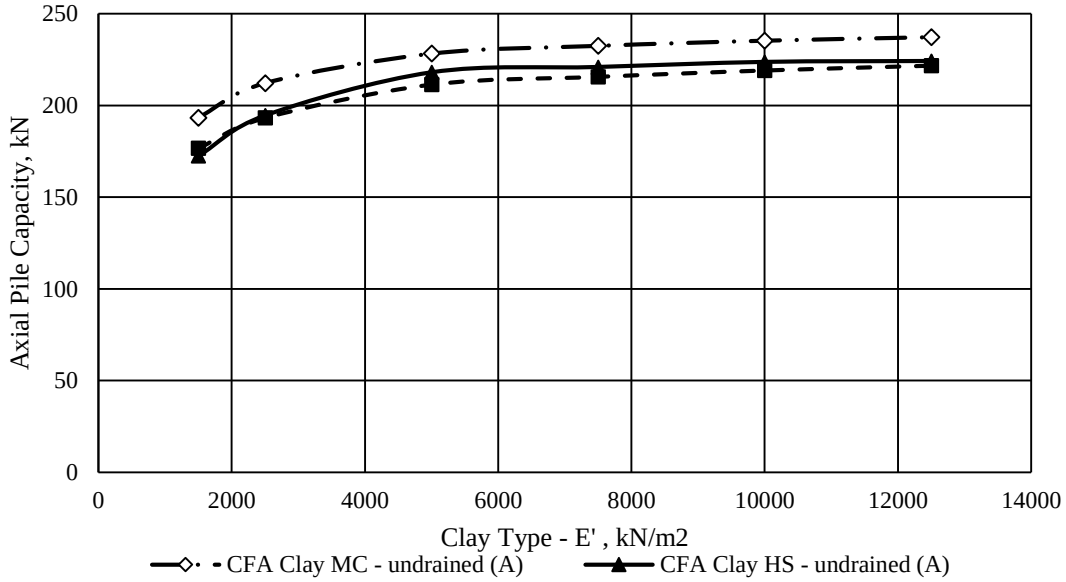

Figure 4-41 – Working load on bored piles in clays calculated with Mohr Coulomb, Hardening Soil and Hardening Soil – small stiffness constitutive models

However, the Hardening Soil and Hardening Soil with small-strain stiffness provide more representative results than the Mohr-Coulomb material model but the Mohr

Coulomb model has proved adequate for this pilot study to demonstrate that it is possible to model pulse piles and show an increase in capacity. Therefore, further analyses in this research were undertaken using the Mohr-Coulomb material model.

4.6.6 Modelling outputs of bearing capacity of CFA and pulse piles: Mohr Coulomb

Soil sensitivity analyses have been performed in coarse grained material using Mohr-Coulomb for bored and pulse piles behaviour. Axial capacity at pile settlement of 10% of pile diameter have been considered.

Figure 4-42 shows curves representing increase of pile capacity with improvement of coarse grained soil parameters and increase of pulse treated length of pile. The soil types and geometry to compare bearing capacity at displacement of 10% of pile diameter are specified in Table 4-15

Table 4-15 – Considered cases of bored and pulse piles to compare pile bearing capacity in coarse grained soil

Case	Pile type	Length of expansion
CFA Sand MC – drained	Bored	0m
DYN 1m Sand MC – drained	Pulse	1m
DYN 3m Sand MC – drained	Pulse	3m
DYN 5m Sand MC – drained	Pulse	5m

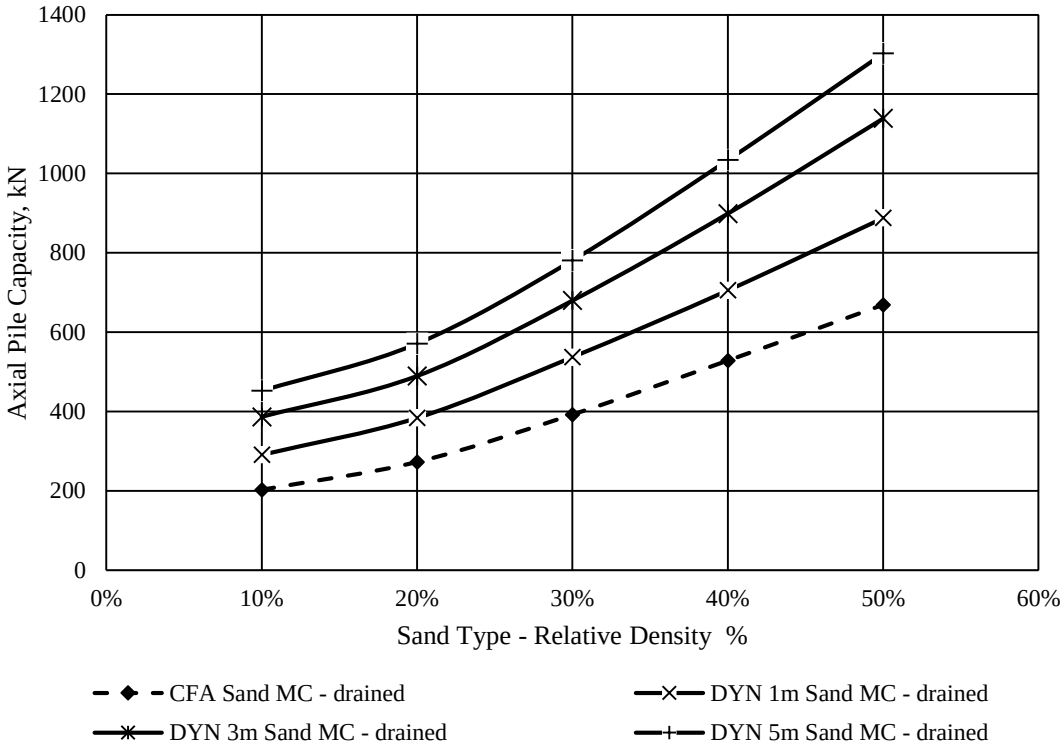

Figure 4-42 – Working load on bored and pulse piles in coarse grained soils calculated with Mohr Coulomb, constitutive model

Resulting curves show increase of bearing capacity of piles with improved density and relevant properties of coarse grained soil and increased length of pulse treatment.

Soil sensitivity analyses have been performed in fine grained soils using Mohr-Coulomb for CFA and pulse piles behaviour. Axial capacity at pile settlement of 10% of pile diameter have been considered.

Figure 4-43 shows curves representing increase of pile capacity with improvement of soil parameters and increase of pulse treated length of pile. The soil types and geometry used to compare bearing capacity at displacement of 10% of pile diameter are specified in Table 4-16

Table 4-16 – Considered cases of bored and pulse piles to compare bearing capacity in clay

Case	Pile type	Length of expansion
CFA Clay MC – undrained (A)	Bored	0m
DYN 1m Clay MC – undrained (A)	Pulse	1m
DYN 3m Clay MC – undrained (A)	Pulse	3m
DYN 5m Clay MC – undrained (A)	Pulse	5m

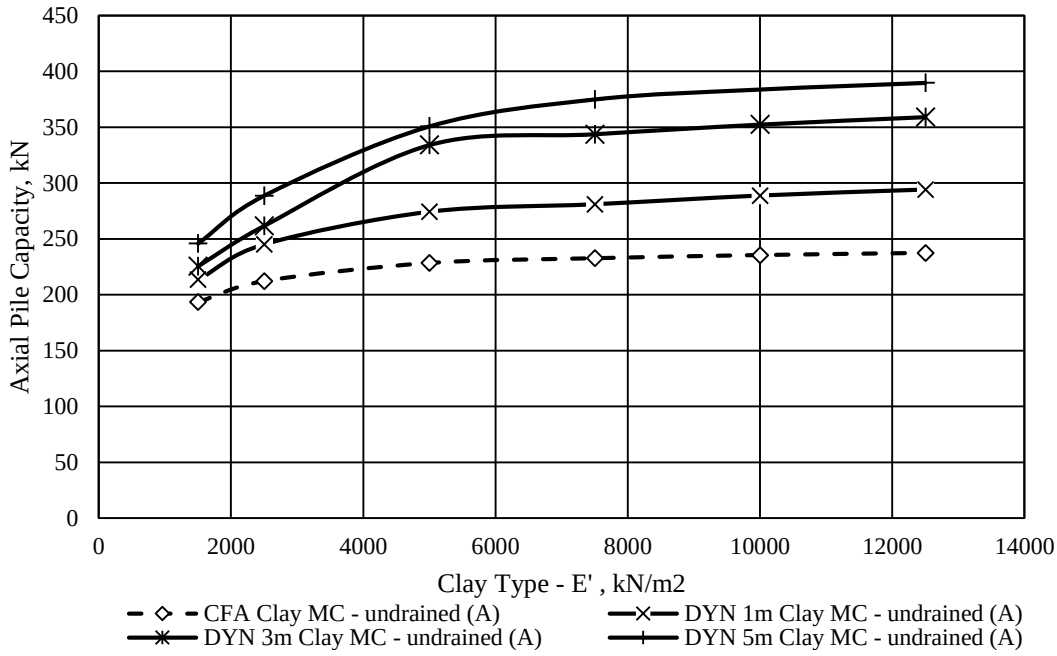

Figure 4-43 – Bearing capacity of CFA and pulse piles in clays calculated with Mohr Coulomb, constitutive model

In clays bearing capacity is increased with soil improvement and increase of treated length of pulse piles. However, stiffness parameters of clay have less impact on bearing capacity improvement than strength.

Chapter 5
Validation of numerical analysis with semi-empirical method

5.1 Introduction

BS EN 1997-1-2004 Eurocode 7 (2004) prescribes the commonly recognized calculation models to be used for the ultimate limit state design as analytical, semi-empirical or numerical. Analytical methods are not often applicable (section 6.5.2.2, BS EN 1997-1-2004 (2004)), therefore only semi-empirical and numerical methods have been considered in this paper.

In this chapter, the results of numerical modelling are compared with hand calculated pile performance obtained using semi-empirical methods.

5.2 Scope of works

The main objective of this chapter is to compare two methods of calculating the settlement of a pulse pile, the semi-empirical method by Fleming and finite element modelling in Plaxis. A sensitivity analysis has been performed for various input parameters to investigate the effect of parameter selection on the validation. Both bored and pulse piles have been considered as rigid piles hence no elastic shortening have been added to shaft and base pile performance.

5.3 Semi-empirical method for prediction of settlement of a single pile.

The problem of predicting pile performance is quite complex and requires sophisticated calculation methods including finite element modelling. However, there are simplified methods of calculating pile settlement that can be used to obtain reliable results. Poulos (1989) summarised available design procedures categorised by level of sophistication of calculation technique (Table 5-1). He categorised methods for evaluation of axial pile response from empirical to semi-analytical and advanced numerical techniques, including finite element modelling.

Table 5-1 – Categories of analysis/design procedures (Poulos (1989))

Category	Subdivision	Characteristics	Method of parameter determination	Axial pile capacity evaluation methods	Settlement evaluation method
1	-	Empirical – not based on soil mechanics principles	Simple in situ or laboratory tests, with correlations	Correlations with CPT/SPT; Total stress (α) method	Approximate correlations with pile diameter Column deflexion multiplied by a factor
2	2A	Based on simplified theory or charts – uses soil mechanics principles – amenable to hand calculation. Theory is linear elastic (deformation) or rigid plastic (stability)	Routine relevant in situ tests – may require some correlations	Effective stress (β) method	Elastic solutions
	2B	As for 2A, but theory is non-linear (deformation) or elasto-plastic (stability)		Effective stress method	Elastic solutions modified for slip
3	3A	Based on theory using site-specific analysis, uses soil mechanics principles. Theory is linear elastic (deformation) or rigid plastic (stability)	Careful laboratory and/or in situ tests which follow the appropriate stress paths	Plasticity solutions for end bearing capacity	Elastic finite element analysis
	3B	As for 3A, but non-linearity is allowed for in a relatively simple manner		Non-linear load transfer analysis Non-linear boundary element analysis Non-linear finite element analysis	
	3C	As for 3A, but non-linearity is allowed for by way of proper constitutive models of soil behaviour		Finite element analysis, including simulation of pile installation	

Chin (1970) suggested a load – settlement relationship as follows:

$$\frac{\Delta}{P} = m\Delta + C_1 \tag{23}$$

where P is applied load, C_1 is a constant and $1/m$ is the inverse slope that gives ultimate value of P. This is 2A type of method. Figure 5-1 shows a bilinear relationship between settlement and settlement/load ratio: shaft friction (A) and total load (B).

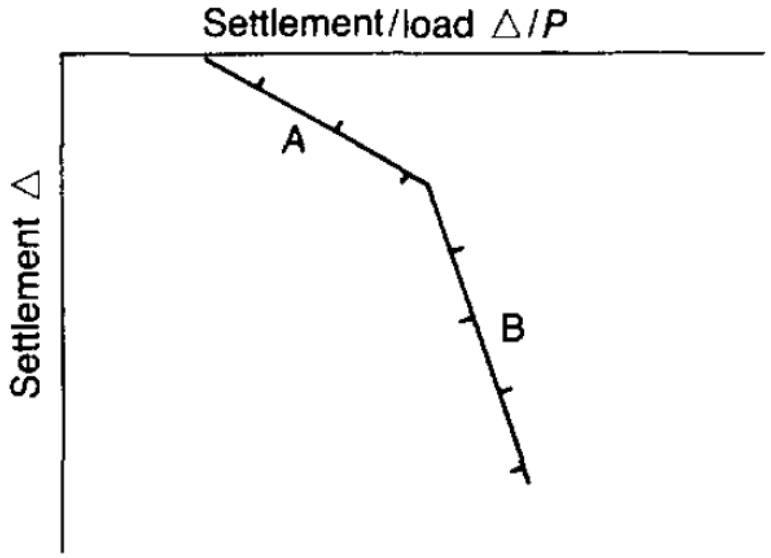

Figure 5-1 - Relationship of settlement and settlement/load

In his paper, Fleming (1992) developed the method specified by Chin and suggested to characterise skin friction and end bearing behaviour using two hyperbolic functions. According to Poulos's classification this is category 2B method. In this chapter, the results of this category 2B calculation will be compared with finite element modelling that is a category 3 method.

5.3.1 Introduction to Fleming's method

Fleming (1992) derived following relation for the ultimate shaft friction, U_s:

$$U_s = \frac{\Delta_s}{\left(\frac{\Delta_s}{P_s}\right) - K_s} \tag{24}$$

where Δ_s = settlement at the top of the pile under any load P_s, K_s = inverse function of ultimate shaft friction. Rearranging the equation (24) gives:

$$\Delta_s = \frac{K_s U_s P_s}{U_s - P_s} \tag{25}$$

A similar equation for base performance has been suggested as follows:

$$\Delta_B = \frac{K_B U_B P_B}{U_B - P_B} \tag{26}$$

Where U_B = ultimate base load, P_B = load, corresponding to Δ_B = settlement. $\Delta_B = \Delta_S$ for the case of a rigid pile. On Figure 5-2 (A) represents ultimate shaft friction slope and (B) is the ultimate end bearing slope (Fleming (1992)).

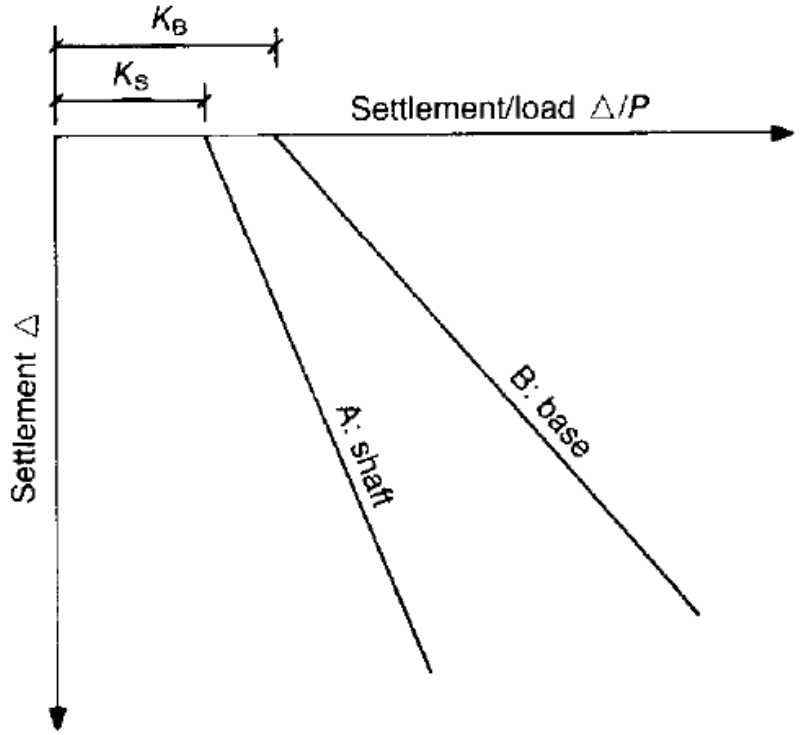

Figure 5-2 - Individual shaft and base performance (Fleming (1992))

5.3.1.1 Shaft Friction

In his paper, Fleming (1992) is referencing the finite element calculation results of Randolph & Wroth (1982), claiming that settlement of a pile shaft is a function of the diameter D_S. He has also suggested an equation for K_S as the inverse function of ultimate shaft friction:

$$K_S = \frac{M_S D_S}{U_S} \tag{27}$$

Where M_S = flexibility factor (dimensionless) representing the tangent slope at the origin of the shaft friction hyperbolic function. Combining equations (25) and (27), the settlement at the top of a shaft is:

$$\Delta_s = \frac{M_s D_s P_s}{U_s - P_s} \tag{28}$$

Further in this study, M_S is $\zeta\tau_S/2G$, as suggested by Randolph & Wroth (1978, 1982) where $\zeta = ln(r_m/r_c)$, with r_m = radius at which soil deflections become negligible, r_c = pile radius, τ_S = shear stress on pile/soil surface and G = soil shear modulus.

5.3.1.2 Base Load

For the base settlement, Δ_B, further equations have been suggested by Fleming (1992):

$$\Delta_B = \frac{\pi}{4}\frac{q}{E_B} D_B (1 - \nu^2) f_1 \tag{29}$$

Where E_B = modulus of the soil under the tip of the pile, q = applied base pressure, D_S = diameter, ν = Poisson's ratio, f_1 = standard settlement reduction factor depending on depth of foundation. Using empirical values for some parameters, Fleming obtained the following equation for K_B:

$$K_B = \frac{0.58}{D_B E_B} \approx \frac{0.6}{D_B E_B} \tag{30}$$

Combining equations (26) and (30), the base settlement can be determined:

$$\Delta_B = \frac{0.6 U_B P_B}{D_B E_B (U_B - P_B)} \tag{31}$$

5.3.1.3 Total settlement of a rigid pile

A load – settlement hyperbolic function has been suggested by Fleming (1992) by combination of expressions for shaft and base settlements. Thus, total load $P_T = P_B + P_S$ has been obtained by combining equations (28) and (31):

$$P_T = P_B + P_S = \frac{U_S \Delta_S}{M_S D_S + \Delta_S} + \frac{D_B E_B \Delta_B U_B}{0.6 U_B + D_B E_B \Delta_B} \tag{32}$$

This expression has been reformulated with a total settlement value Δ_T:

$$P_T = \frac{a\Delta_T}{c + \Delta_T} + \frac{b\Delta_T}{d + e\Delta_T} \tag{33}$$

where $a = U_S$, $b = D_B E_B U_B$, $c = M_S D_S$, $d = 0.6U_B$ and $e = D_B E_B$.

To derive total settlement from equation (33), a quadratic equation has to be solved:

$$(eP_T - ae - b)\Delta_T^2 + (dP_T + ecP_T - ad - bc)\Delta_T + cdP_T = 0 \tag{34}$$

The solution for this equation can be written as follows:

$$\Delta_T = \frac{-(dP_T + ecP_T - ad - bc) \pm \sqrt{(dP_T + ecP_T - ad - bc)^2 - 4(eP_T - ae - b)cdP_T}}{2(eP_T - ae - b)} \tag{35}$$

With only positive values to be considered for total settlement.

5.3.1.4 Elastic shortening

The elastic shortening of a pile was also suggested by Fleming (1992) in addition to the settlement of a rigid pile. It consists of three incremental values for initial shortening over the low friction zone, shortening along the total length of transferred friction and shortening when the ultimate shaft friction is exceeded. Thus, total elastic shortening can be computed using either for the loads, up to ultimate shaft friction:

$$\Delta_E = \frac{4}{\pi}\frac{P_T(L_0 + K_E L_F)}{D_S^2 E_C} \tag{36}$$

or for the loads exceeding ultimate shaft friction:

$$\Delta_E = \frac{4}{\pi}\frac{1}{D_S^2 E_C}[P_T(L_0 + L_F) - L_F U_S(1 - K_E)] \tag{37}$$

where L_0 = length of friction-free or low friction zone, L_F = length of frictional load transfer zone, K_E = coefficient applied to L_F to obtain effective column length, E_C – Young's modulus for the material of the pile.

The total settlement of a pile can be calculated combining equation (35) for settlement of a rigid pile and equation (36) or (37) for total elastic shortening.

In this chapter sensitivity analysis of range of parameters has been undertaken for geotechnical performance of a single pile. All of the calculations as in Chapter 4 have been performed for a single pile of the same diameter and length. Bored and pulse piles have been considered as rigid and elastic shortening as a constant structural

component of the pile settlement has not been considered for the purposes of comparison of geotechnical performance.

An Excel spreadsheet was developed to calculate the total settlement of a rigid pile based on described method. Input parameters used for the calculation are specified further in this chapter.

5.3.2 Ultimate load

One of the main input parameters for the semi-empirical method is the ultimate load as it is necessary to derive the ultimate load to be able to obtain a reliable prediction of pile settlement. As suggested by Terzaghi (1942), the ultimate load of a pile can be defined as a load at a settlement of 10% of the pile diameter. The method to calculate the ultimate load is described further in this section.

The bearing capacity of a single pile consists of base capacity and shaft capacity (Tomlinson & Woodward (2014)):

$$Q_p = Q_b + Q_s - W_p \tag{38}$$

where Q_p = ultimate resistance of a pile, Q_b = ultimate resistance of the base, Q_s = ultimate resistance of the shaft, W_p = weight of the pile. Weight of embedded length of a pile is comparable with the weight of relevant volume of displaced soil, therefore it is usually ignored.

The ultimate base and shaft resistances are calculated as follows (Clarke (2017)):

$$R_b = A_b q_b \tag{39}$$

$$R_s = \sum_{i}^{n} A_S q_s \tag{40}$$

where A_b = base area, A_s = shaft area of layer i, q_b = unit base resistance, q_s = unit shaft resistance.

There are different approaches to calculate unit resistances in coarse and fine grained soils.

In coarse grained soil, the unit shaft resistance is related to the interface angle of friction:

$$q_{s;ik} = K_{s;i}\sigma'_{v;i} \tan \delta_i \quad (41)$$

where δ_i = effective interface angle of friction, $K_{s;i}$ = earth pressure coefficient, $\sigma'_{v;i}$ = average vertical effective stress of soil layer i.

The ultimate base resistance in coarse grained soils is given by:

$$q'_b = N_q \sigma'_{vb} \quad (42)$$

where σ'_{vb} = vertical effective stress at pile base level, N_q = empirical bearing capacity factor, that can be obtained using relations developed by Berezantzev et al. (1961) as shown on Figure 5-3.

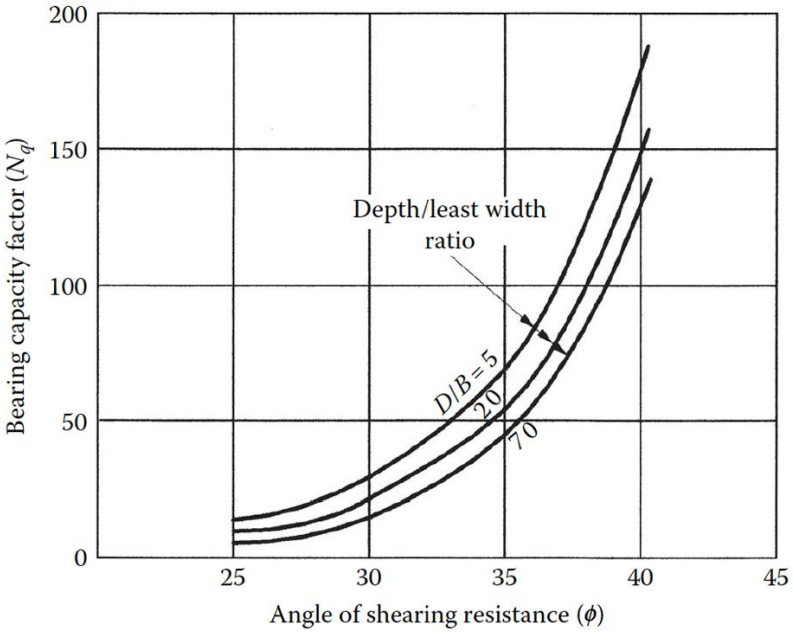

Figure 5-3 – Bearing capacity factors (Berezantzev et al. (1961)

In fine grained soils, the unit shaft friction is:

$$q_{s;ik} = \alpha_i c_{u;i} \quad (43)$$

where c_u = undrained shear strength of the layer i, α_i = empirical coefficient dependent on type of soils and pile installation method.

The ultimate base capacity of piles bearing on fine grained stratum can be calculated using the following equation:

$$q'_b = N_c c_{ub} \quad (44)$$

Where c_{ub} = undrained shear strength of the end-bearing stratum, N_c = bearing capacity factor. The recommended value of the bearing capacity factor is 9 (Tomlinson & Woodward (2014)).

5.4 Input parameters for the semi-empirical method

Input parameters that were considered for the range of calculations are specified in this section. Bored piles of the same length and diameter in same soil conditions as those considered in Chapter 4 have been specified for the semi-empirical calculation. A circular section bored pile 0.3m diameter 10m long was considered.

Coarse grained soil properties

The earth pressure coefficient $K_{s;i}$ of 0.8 was specified in accordance with BS 8004:2015 (2015) for the continuous flight auger piles in fine to coarse sand. Average vertical effective stress of each soil layer $\sigma'_{v;i}$ is proportionate to soil unit weight γ. Unit weight of 19kN/m^3 for coarse grained soil was considered as in Plaxis model.

An effective interface angle of friction δ_i has been assumed equal to the angle of friction of soil specified for the six soil cases considered in chapter 4 (Table 4-11). The angle of dilatancy has not been applied in the semi-empirical method.

An empirical bearing capacity factor N_q has been taken from Berezantzev et al. (1961) for relevant length to pile diameter ratio.

Fine grained soil properties

In the Plaxis model, shear strength parameters have been specified in terms of effective stresses. Therefore, for the semi-empirical method, values of undrained shear strength of each layer have been back-calculated using effective input parameters in Plaxis (Table 4-12). Fine grained soil properties are summarised in Table 5-2:

Table 5-2 – Clay properties for semi-empirical calculation

Soil case	E'	c_u
	kN/m^2	kN/m^2
CFA clay MC u(A) 0	1,500	12
CFA clay MC u(A) 1	2,500	20
CFA clay MC u(A) ref	5,000	40
CFA clay MC u(A) 3	7,500	60
CFA clay MC u(A) 4	10,000	80
CFA clay MC u(A) 5	12,500	100

The empirical coefficient α_I has been assumed equal to 0.5 as recommended by London District Surveyors Association (2009) for London clay. Adhesion factor has been assumed constant for all soil cases.

Tangent slope *Ms*

Fleming suggested that the tangent slope M_S is equal to w^*/d based on Randolph and Wroth (1982) where w^* = local displacement, d = pile diameter. Typical values of *Ms* recommended by Randolph (1981) for piles in over-consolidated clay range from 0.5% to 2%. A sensitivity analysis for *Ms* was performed to obtain the values for considered soil cases.

5.5 Settlement prediction of a single bored pile. Comparison of the results obtained in semi-empirical calculation with FEM in Plaxis 2D

To determine the optimal parameters for semi-empirical calculation of bored pile settlement, a sensitivity analysis was performed. Ranges of M_S values have been tested in coarse and fine grained soil cases specified as for Plaxis modelling in Chapter 4.

5.5.1 Settlement of a bored pile in coarse grained soil

Two methods to predict pile performance have been compared for a range of coarse grained soils. M_S values from 0.001 to 0.02 (Fleming (1992)) have been applied for each soil case listed in Table 5-3. Resulting curves plotted for semi-empirical and Plaxis calculations can be found in appendices. As seen on the figures, the semi-empirical calculation results are sensitive to the value of M_S. The value of M_S also

depends on sand density. The data summarised in appendices have been used to determine the values of M_S to be used for relevant soil cases.

Figure 5-4 shows two load-settlement curves obtained with the Fleming's method described in section 5.2.1 and computed in Plaxis 2D as described in Chapter 4. The graph shows reference coarse grained soil case "Sand2/ref" corresponding to the relative density of 20%. The curve for the Fleming's method was obtained by calculating settlement from load increments of 10kN and with M_S value of 0.01. To be able to compare two calculation methods Plaxis results have been processed in Excel to derive settlement from the same load increments. Working load has been assumed as a limiting value for comparison of two methods. Comparison of the results has been performed using root mean square error.

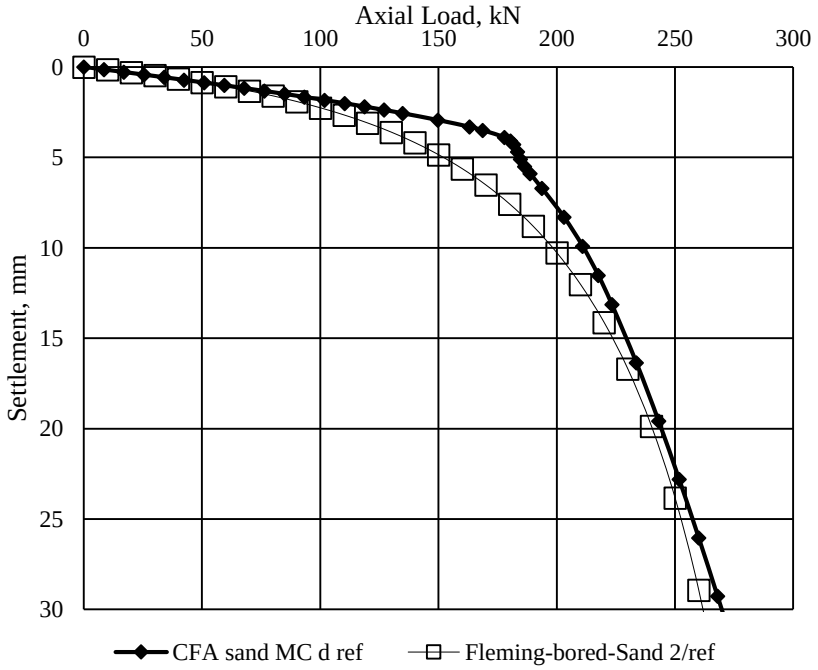

Figure 5-4 – Load-settlement curves: bored pile performance in coarse grained soil "Sand2/ref" calculated by Fleming's method with M_S=0.01 and computed in Plaxis

As can be seen from the Figure 5-4, two methods show acceptable convergence, which is relevant to the minimum value of calculated root mean square error (see Figure 5-5 (c)).

The root mean square error has been calculated for each coarse grained soil case for the working load of 1/3 of ultimate load. The value of root mean square error has been calculated as follows:

$$RMSE = \sqrt{\frac{\sum_{i=1}^{j}(\Delta_{T,Fleming,i} - \Delta_{T,Plaxis,i})^2}{j}} \quad (45)$$

Where $\Delta_{T,Fleming,i}$ is settlement from *i*-th applied load calculated by Fleming't method, $\Delta_{T,Plaxis,i}$ is settlement from *i*-th applied load calculated using Plaxis. One *i*-th load has been assumed of 10kN, hence *j* is a number of *i* loads on working load range for each soil case. Calculated working loads of 1/3 of ultimate load for each coarse grained soil case are summarised in the table below:

Table 5-3 – Calculated working load for coarse grained soil cases: Bored pile

Soil case	Working load
	kN
Sand 0	70
Sand 1	80
Sand 2/ref	90
Sand 3	100
Sand 4	120
Sand 5	130

On Figure 5-5 all calculated values of root mean square error are shown as graphs for each coarse grained soil case. Soil cases 0 and 1 for loose sand do not show the pick minimum value of the error on the considered range of M_S values. Soil cases 2 to 5 have pick minimum values of M_S that can be recommended for calculations of the coarse grained soils of specified density.

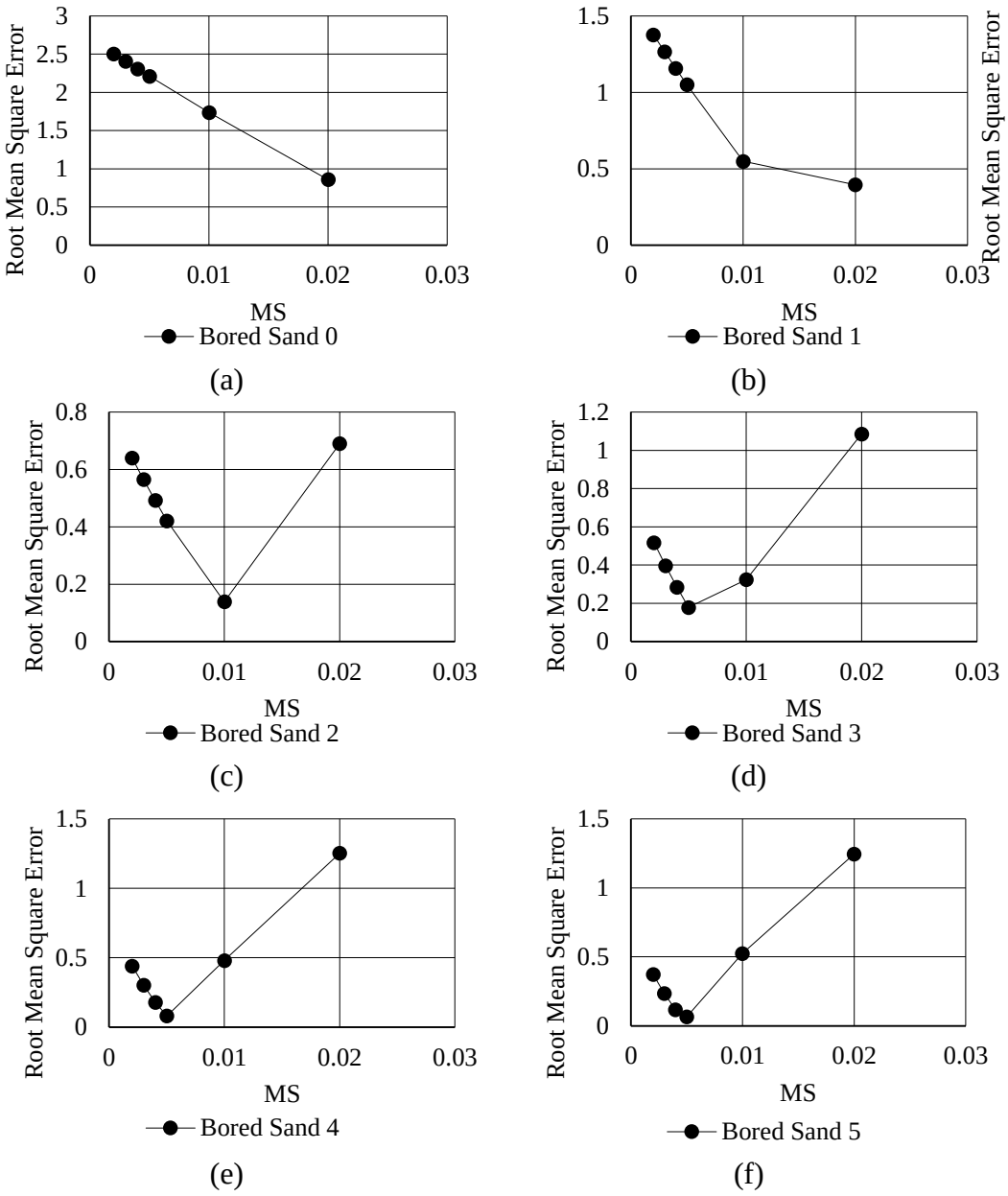

Figure 5-5 – Root Mean Square Error of M_S value for bored pile: (a) coarse grained soil case 0, (b) coarse grained soil case 1, (c) coarse grained soil case 2/ref, (d) coarse grained soil case 3, (e) coarse grained soil case 4, (f) coarse grained soil case 5

Comparable load-settlement curves for loose sands for the case 0 are relevant to M_S value of 0.02. An increase of sand density reduces the value of M_S to 0.005 for sand case 5. A summary with the optimum values of M_S are listed in Table 5-4.

Table 5-4 – Coarse grained soil cases and relevant values of M_S

Soil case	RD, %	M_S
Sand 0	5	0.02
Sand 1	10	0.02
Sand 2/ref	20	0.01
Sand 3	30	0.005
Sand 4	40	0.005
Sand 5	50	0.005

Figure 5-6 shows the plot of optimal M_S values relative to each coarse grained soil case for the bored pile model.

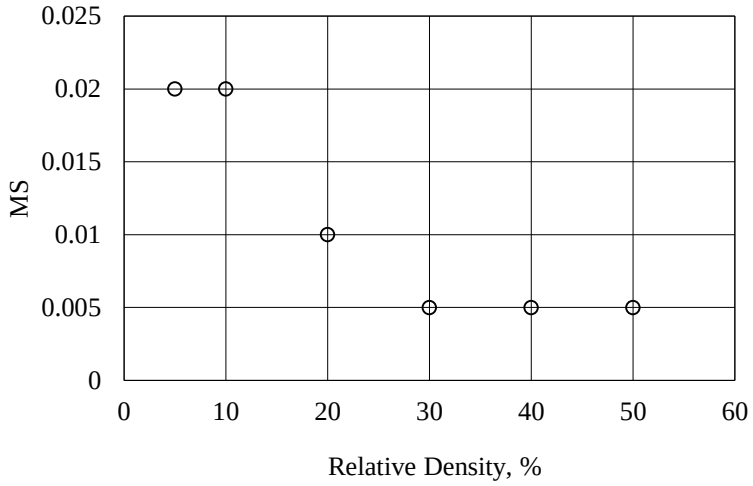

Figure 5-6 – M_S vs. Relative density of coarse grained soil: bored pile

The minimum value of root mean square error was obtained for the soil case Sand 5 with M_S value of 0.005. Figure 5-7 shows two curves with the minimum error within the working load range. Although the error is minimal, the ultimate load calculated by two methods are not congruent.

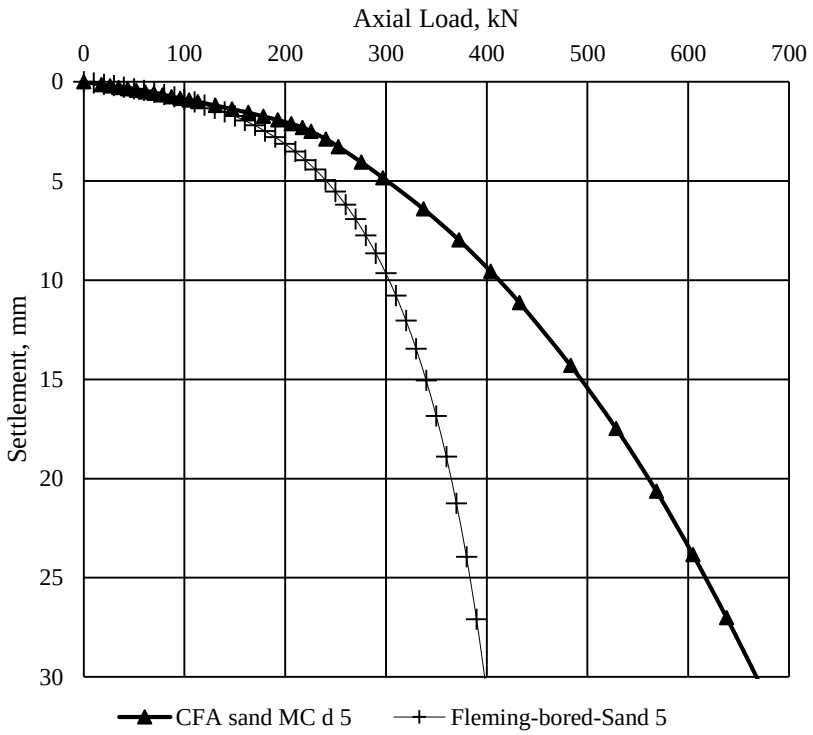

Figure 5-7 – Load-settlement curves: bored pile performance in coarse grained soil "Sand5" calculated by Fleming's method with M_S=0.005 and computed in Plaxis

Increase of density of sand without considering dilatancy of coarse grained soil resulted in different shape of curves beyond ultimate capacity. Whilst curves for two methods are almost identical for soil case of Sand 2/ref and M_S value of 0.005, Sand 5 shows closer to punching failure for semi-empirical method which has not allowed for dilatancy.

5.5.2 Settlement of a bored pile in fine grained soil

The two predictions have been compared for a range of fine grained soils. M_S values from 0.005 to 0.02 were applied for each soil case. Resulting curves can be compared on figures in appendices. Load-settlement curves showing the performance of bored pile in fine grained soil up to ultimate load at settlement of 10% of pile diameter. Each soil case from very soft Clay 0 to soft to firm Clay 5 have been considered. M_S values from 0.005 (Figure 9-8) to 0.02 (Figure 9-11) have been considered as recommended by Randolph (1981). Results for very soft clays show low convergence for two methods. Finite element modelling results show punching failure that differs from the prediction by the Fleming's method. Although the initial slopes for semi-empirical

and finite element methods are identical, the shape of the curves for each value of M_S varies between the two methods.

Figure 5-8 shows two curves, one for Plaxis calculation as per Chapter 4, second is for semi-empirical calculation method. The graph shows reference fine grained soil case "Clay2/ref" corresponding to the drained stiffness of 5,000kN/m^2. The curve for the Fleming's method was obtained by calculating settlement from load increments of 10kN and with M_S value of 0.015. Plaxis results have been processed in Excel to derive settlement from the same load increments. Working load has been assumed as a limiting value for comparison of two methods. Comparison of the results has been performed using root mean square error.

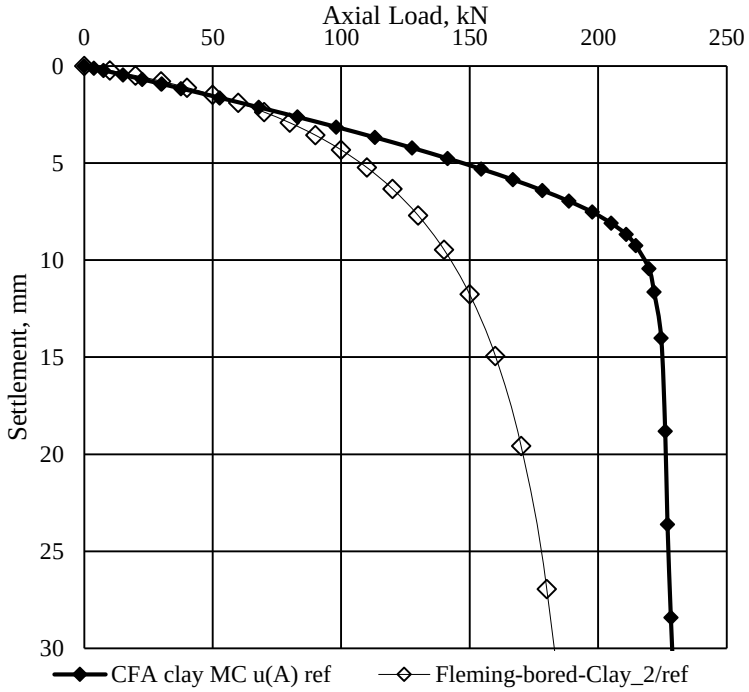

Figure 5-8 – Load-settlement curves: bored pile performance in fine grained soil "Clay2/ref" calculated by Fleming's method with M_S=0.015 and computed in Plaxis

Comparable results can be obtained within working load range. Convergence of two methods is relevant to calculated root mean square error as can be seen on Figure 5-9 (c).

Six fine grained soil cases have been considered to determine optimal M_S value. Root mean square error has been calculated for the following working load range using formula (46):

Table 5-5 – Calculated working load for fine grained soil cases: Bored pile

Soil case	Working load
	kN
Clay 0	20
Clay 1	30
Clay 2/ref	60
Clay 3	100
Clay 4	130
Clay 5	160

On Figure 5-9 all calculated values of root mean square error are shown as graphs for each fine grained soil case. Soil cases 0 to 3 (Figure 5-9 a to d) for very soft to soft clay show the pick minimum value of the error on the considered range of M_S values. These values of M_S can be recommended for soft fine grained soils of specified properties. Soil cases 4 and 5 (Figure 5-9 e and f) do not have pick minimum values of error on the considered range of M_S.

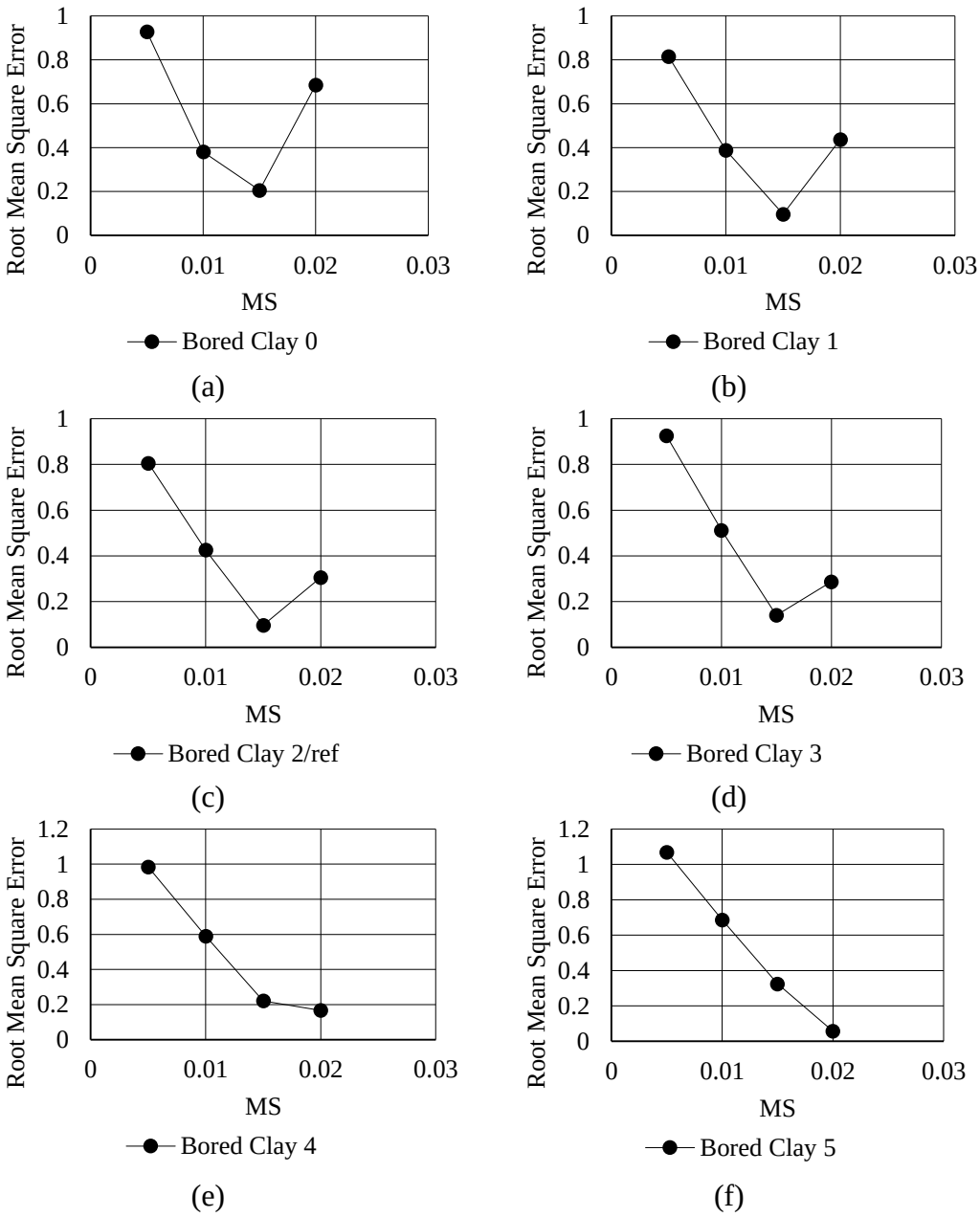

Figure 5-9 – Root Mean Square Error of M_S value for bored pile: (a) fine grained soil case 0, (b) fine grained soil case 1, (c) fine grained soil case 2/ref, (d) fine grained soil case 3, (e) fine grained soil case 4, (f) fine grained soil case 5

Figure 5-9 shows mean squared error for each case of fine grained soil for each value of M_S. Summary of M_S values relevant to the soil cases specified in Table 5-6. Figure 5-10 shows the optimal M_S values relative to each fine grained soil case for the bored pile model. Data from the Table 5-6 was plotted in Excel showing clay soil cases corresponding to M_S values.

Table 5-6 – Fine grained soil cases and relevant values of M_S

Soil case	E', kN/m^2	M_S
Clay 0	1,500	0.015
Clay 1	2,500	0.015
Clay 2/ref	5,000	0.015
Clay 3	7,500	0.015
Clay 4	10,000	0.02
Clay 5	12,500	0.02

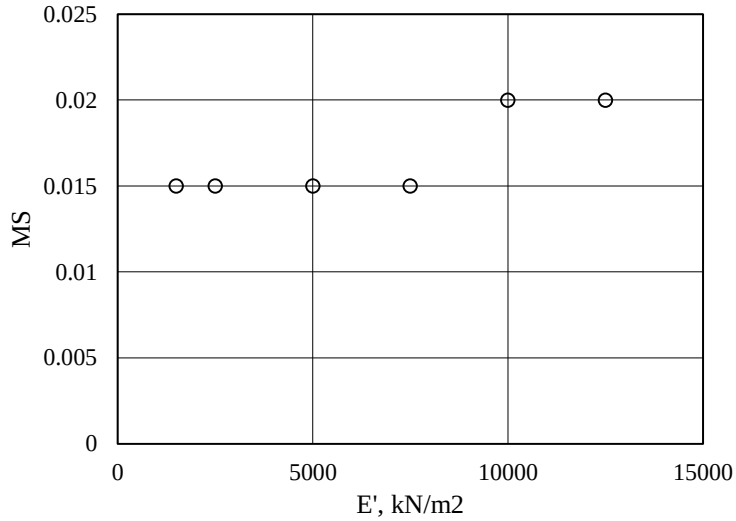

Figure 5-10 – M_S vs. Drained stiffness of fine grained soil: bored pile

The minimum value of root mean square error was obtained for the soil case Clay 5 with M_S value of 0.02. Figure 5-11 shows two curves with the minimum error within the working load range. Although the error is minimal the ultimate load calculated by two methods are not congruent.

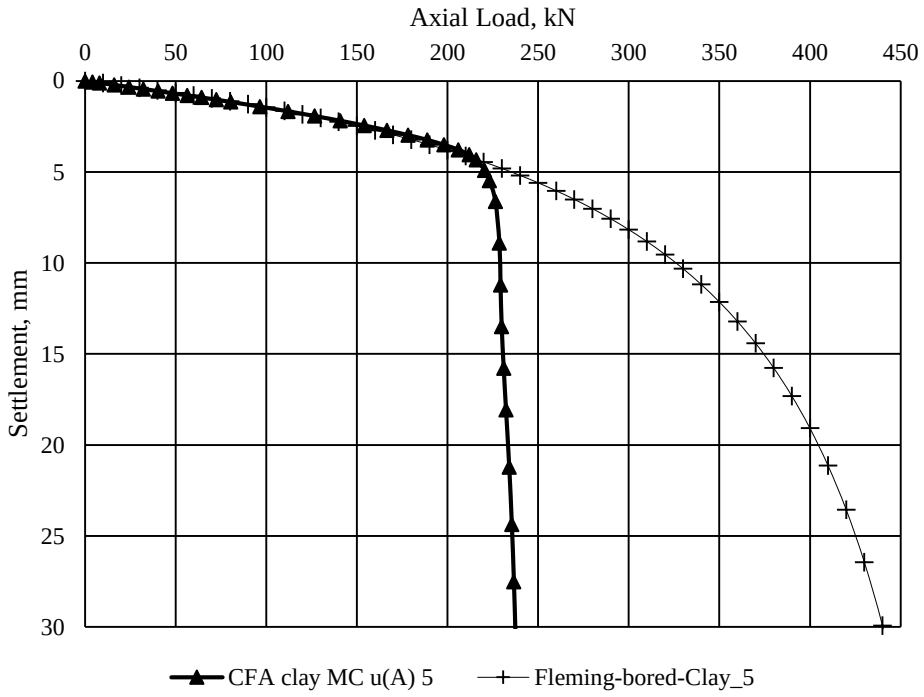

Figure 5-11 – Load-settlement curves: bored pile performance in fine grained soil "Clay5" calculated by Fleming's method with M_S=0.02 and computed in Plaxis

This graph shows that Fleming's method of prediction of pile capacity does not take into account punching failure in clayey soils. Considering the convergence of calculation results by finite element modelling and semi-empirical method, Plaxis provides better interpretation of behaviour of cohesive soils.

5.6 Settlement prediction of a single pulse pile. Comparison of the results obtained in semi-empirical calculation with FEM in Plaxis 2D

Reference values of M_S obtained for the bored pile were checked for the pulse pile performance. To calculate the settlement of a pulse pile using the semi-empirical method, the ultimate capacity calculation procedure had to be altered. Pulse piles were considered with an expansion zone 5m long from the bottom of the pile.

To obtain results comparable with the finite element modelling it was decided to apply empirical factors to shaft and base capacity only to the treated 5m long zone; that is the upper 5m did not contribute to the capacity. The values of empirical factors for enlarged length of pulse piles have been taken from NIIOSP (Table 5-7 and Table

5-8) for Electric Discharge Piling Technology "ЭРСТ" piles (Recommendations on application of bored piles, 2001).

Table 5-7 – End bearing capacity factor - Coefficient of working conditions γ_{cR} (NIIOSP (2001))

Pile Type	Soil Type			
	Sand	Clayey Sand	Silt	Clay
Electric Discharge Piling Technology (ЭРГТ)	2.4	2.4	1.8	1.8

Table 5-8 – Shaft capacity factor - Coefficient of working conditions γ_{cF} (NIIOSP (2001))

Pile Type	Soil Type			
	Sand	Clayey Sand	Silt	Clay
Electric Discharge Piling Technology (ЭРГТ)	2.4	2.4	1.9	1.9

Calculation of pulse pile capacity, Q_P, according to NIIOSP can be performed using following formula:

$$Q_P = \gamma_{cR} R_B + \sum_{1}^{n} \gamma_{cF,i} R_{S,i} \quad (46)$$

Where γ_{cR} = end bearing capacity factor, γ_{cF} = shaft capacity factor.

5.6.1 Settlement of a pulse pile in coarse grained soil

Two methods of calculation of pulse pile settlement in coarse grained soil have been compared, the semi-empirical method by Fleming and the finite element model in Plaxis. M_S values from 0.005 to 0.03 have been tested for each soil case. Recommended empirical factor γ_{cF} of 2.4 have been applied to calculate shaft capacity of the treated zone and γ_{cR} of 2.4 for the end bearing of the pile. Resulting curves plotted for semi-empirical and Plaxis calculations can be found in appendices. The data summarised in appendices have been used to determine the values of M_S to be used for relevant soil cases.

Figure 5-12 shows two load-settlement curves obtained with the Fleming's method and computed in Plaxis 2D as described in Chapter 4. The graph shows reference coarse grained soil case "Sand2/ref" corresponding to the relative density of 20%. The

curve for the Fleming's method was obtained by calculating settlement from load increments of 10kN and with M_S value of 0.02. Plaxis results have been processed in Excel to derive settlement from the same load increments. Working load has been assumed as a limiting value for comparison of two methods. Comparison of the results has been performed using root mean square error.

The graph shows acceptable convergence on the working load range relevant to minimum calculated root mean square error (see Figure 5-13 (c)).

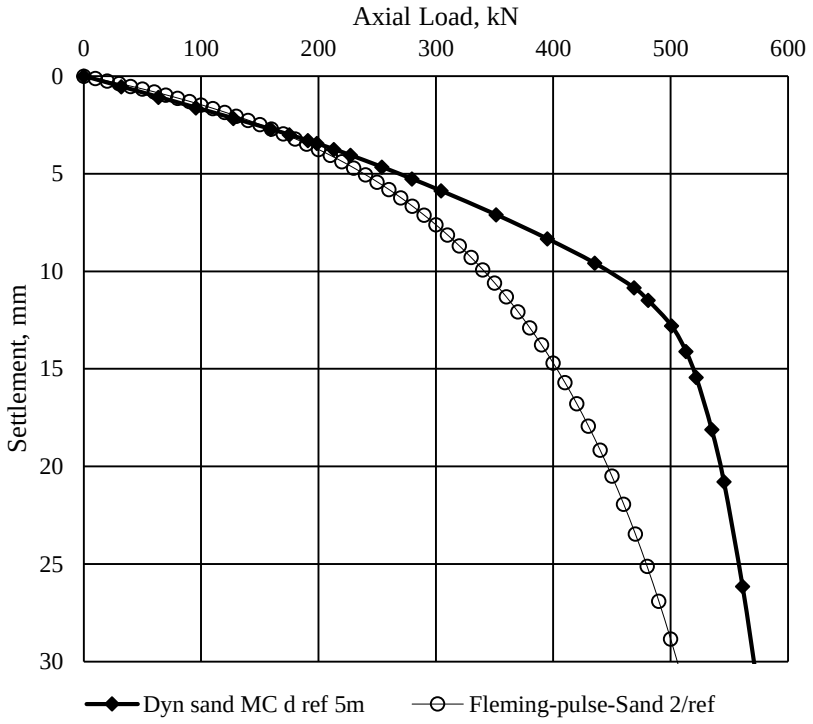

Figure 5-12 – Load-settlement curves: pulse pile performance in coarse grained soil "Sand2/ref" calculated by Fleming's method with M_S=0.02 and computed in Plaxis

Calculated working loads of 1/3 of ultimate load for each coarse grained soil case are summarised in the table below:

Table 5-9 – Calculated working load for coarse grained soil cases: pulse pile

Soil case	Working load
	kN
Sand 0	140
Sand 1	150
Sand 2/ref	180
Sand 3	200
Sand 4	230
Sand 5	260

On Figure 5-13 all calculated values of root mean square error are shown as graphs for each coarse grained soil case. As for bored piles, Pulse pile calculation soil cases 0 and 1 for loose sand do not show the pick minimum value of the error on the considered range of M_S values. Soil cases 2 to 5 have pick minimum values of error relevant to M_S values which can be recommended for calculations of the coarse grained soils of specified density.

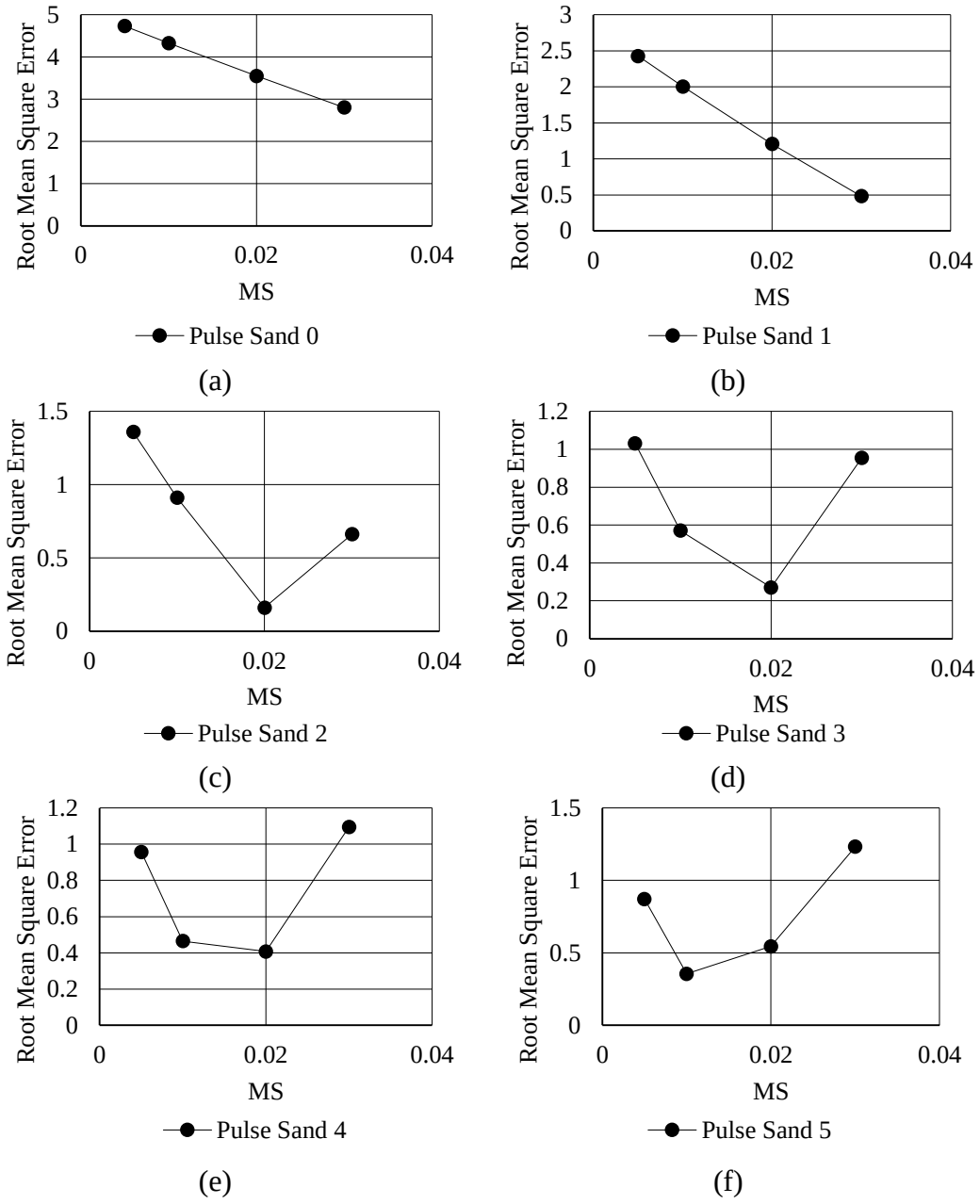

Figure 5-13 – Root Mean Square Error of M_S value for pulse pile: (a) coarse grained soil case 0, (b) coarse grained soil case 1, (c) coarse grained soil case 2/ref, (d) coarse grained soil case 3, (e) coarse grained soil case 4, (f) coarse grained soil case 5

Summary of the optimal M_S values specified in following table:

Table 5-10 – Pulse pile coarse grained soil cases with relevant values of M_S

Soil case	*RD*, %	M_S
Sand 0	5	0.03
Sand 1	10	0.03
Sand 2/ref	20	0.02
Sand 3	30	0.02
Sand 4	40	0.02
Sand 5	50	0.01

Figure 5-14 shows the plot of optimal M_S values relative to each coarse grained soil case for the pulse pile model.

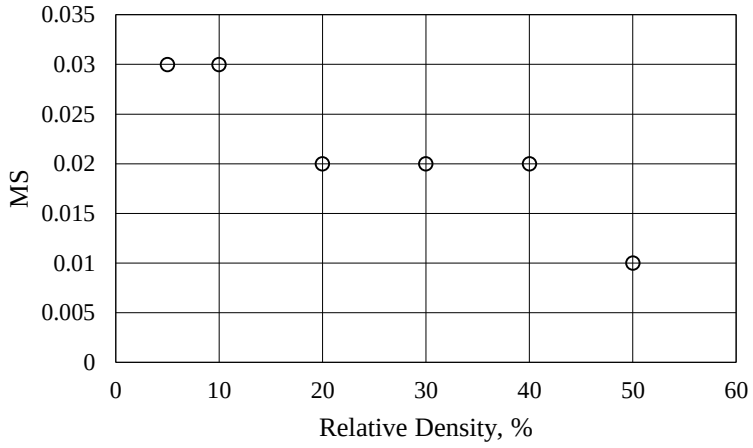

Figure 5-14 – M_S vs. Relative density of coarse grained soil: pulse pile

5.6.2 Settlement of a pulse pile in fine grained soil

Two methods of calculation of pulse pile settlement in the fine grained soil have been compared. M_S values from 0.01 to 0.025 have been tested for each soil case. Recommended empirical factor γ_{cF} of 1.9 have been applied to calculate shaft capacity of the treated zone and γ_{cR} of 1.8 to calculate end bearing of the pile. Resulting curves can be found in appendices.

Figure 5-15 shows two curves, one for Plaxis calculation as per Chapter 4, second is for semi-empirical calculation method. The graph shows fine grained soil case "Clay3" corresponding to the drained stiffness of 7,500kN/m^2. The curve for the Fleming's method was obtained by calculating settlement from load increments of 10kN and with M_S value of 0.025. Plaxis results have been processed in Excel to derive settlement from the same load increments. Working load has been assumed as

a limiting value for comparison of two methods. Comparison of the results has been performed using root mean square error.

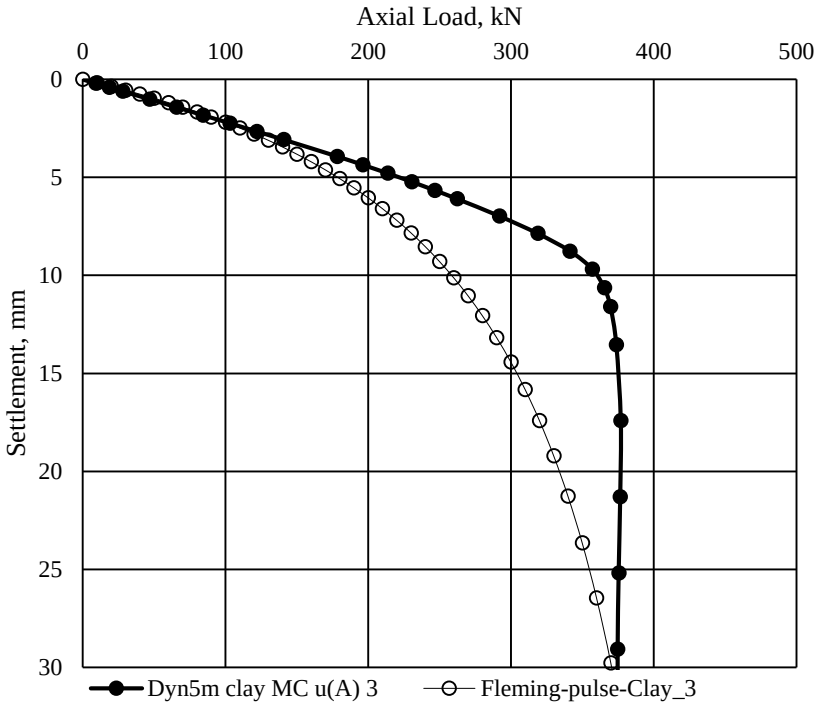

Figure 5-15 – Load-settlement curves: pulse pile performance in fine grained soil "Clay 3" calculated by Fleming's method with M_S=0.025 and computed in Plaxis

The graph shows acceptable convergence on the working load range relevant to minimum calculated root mean square error (see Figure 5-16 (d)). Root mean square error has been calculated for the following working load range using formula (46):

Table 5-11 – Calculated working load for fine grained soil cases: pulse pile

Soil case	Working load
	kN
Clay 0	30
Clay 1	40
Clay 2/ref	90
Clay 3	130
Clay 4	180
Clay 5	230

On Figure 5-16 all calculated values of root mean square error are shown as graphs for each fine grained soil case. Soil cases 0 and 1 (Figure 5-16 a and b) for very soft clay show the pick minimum value of the error on the considered range of M_S values.

These values of M_S can be recommended for pulse pile calculations in very soft fine grained soils of specified properties. Soil cases 2 to 5 (Figure 5-16 c to f) do not have pick minimum values of error on the considered range of M_S

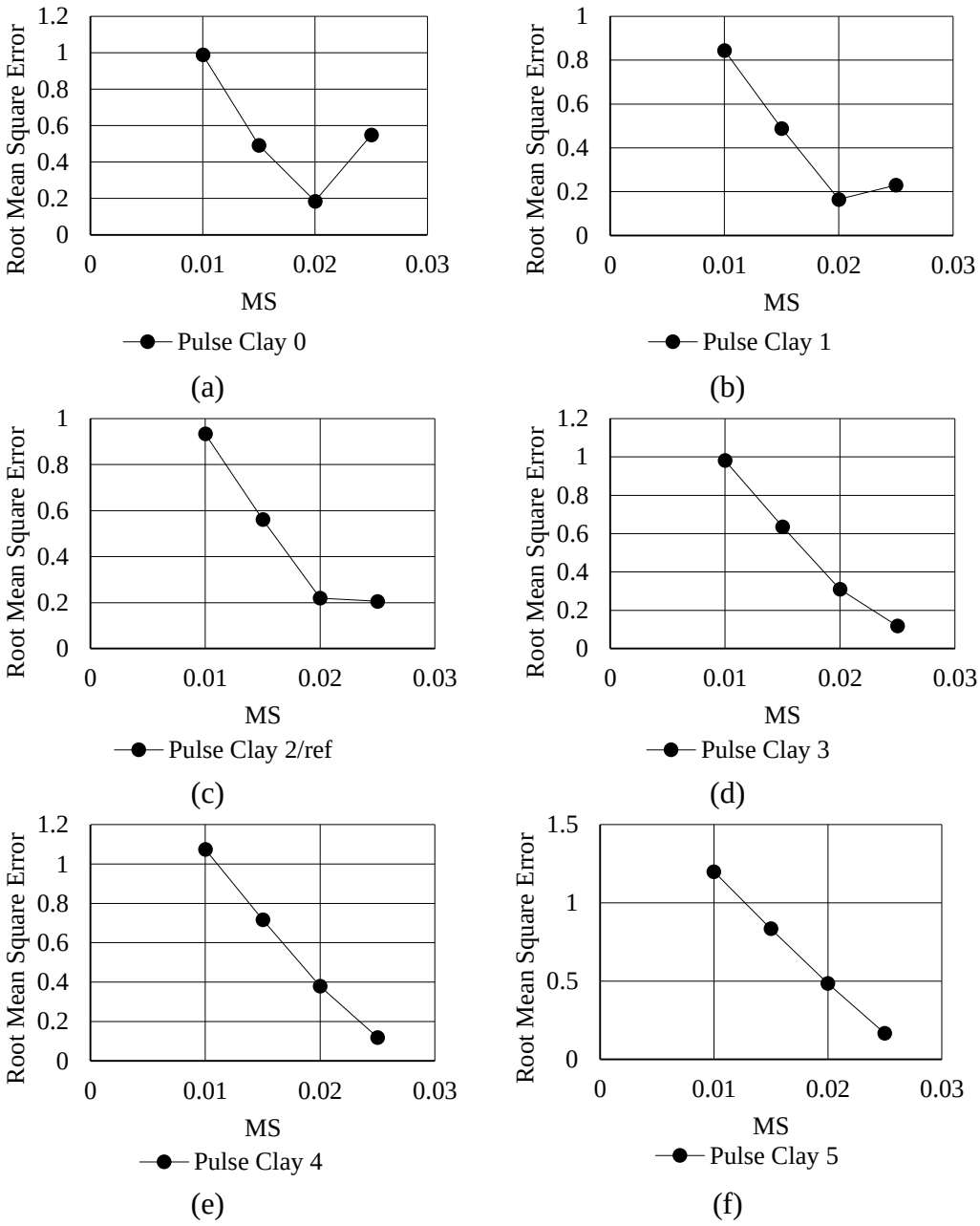

Figure 5-16 – Root Mean Square Error of M_S value for pulse pile: (a) fine grained soil case 0, (b) fine grained soil case 1, (c) fine grained soil case 2/ref, (d) fine grained soil case 3, (e) fine grained soil case 4, (f) fine grained soil case 5

Figure 5-16 shows mean squared error for each case of fine grained soil for each value of M_S. Summary of M_S values relevant to the soil cases specified in Table 5-12. Figure 5-17 shows the optimal M_S values relative to each fine grained soil case for the bored

pile model. Data from the Table 5-12 was plotted in Excel showing clay soil cases corresponding to M_S values.

Summary of the relevant soil cases and M_S values specified in following table:

Table 5-12 – pulse pile fine grained soil cases with relevant values of M_S

Soil case	E', kN/m^2	M_S
Clay 0	1,500	0.02
Clay 1	2,500	0.02
Clay 2/ref	5,000	0.025
Clay 3	7,500	0.025
Clay 4	10,000	0.025
Clay 5	12,500	0.025

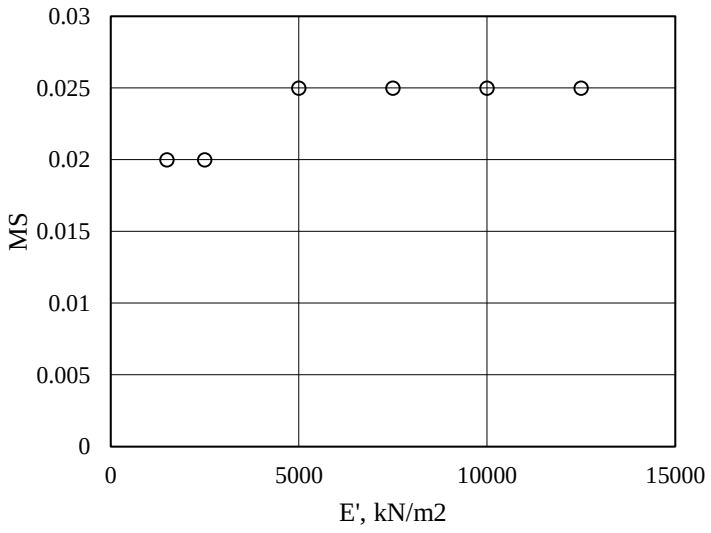

Figure 5-17 – M_S vs. Drained stiffness of fine grained soil: pulse pile

Chapter 6
Validation of predicted pile capacity with field test results

6.1 Introduction

To validate the theoretical and numerical approaches to predict pulse pile capacity, a number of field tests results have been compared with load settlement curves obtained by Fleming's method and by FE modelling in Plaxis 2D.

6.2 Field Tests: single pile tests: pulse piles vs. bored pile

Several bored and pulse pile load tests performed in Moscow have been obtained for this research. All the tests were carried out as for working piles. No preliminary pile tests to failure have been performed.

The ground investigation provided limited information for interpretation of soil parameters. Typical soil cases developed for this thesis in Chapter 4 have been used to characterise the relevant soil strata.

Bored and pulse piles were tested on the site for the Polytech Museum in Moscow in 2013. Both piles were Ø250mm in diameter and 15m and 12.65m long respectively. Ground stratigraphy on site is inconsistent and varies for two tested piles.

Two piles were tested on a site in Odintsovo in Moscow in 2018. Both were pulse piles, 13.75m long and 9m long.

6.2.1 Bored pile test

The Ø250mm 15m long pile on the site for the Polytech Museum in Moscow was bored through the soil stratigraphy summarised in Table 6-1. Groundwater level for this borehole is at 6.93m below existing ground level.

Table 6-1 – Soil properties next to bored pile on site Polytech Museum, Moscow

Stratum	Level (m BGL)
Made Ground	0.00 - 0.70
Sandy CLAY	0.70 – 6.00
Medium dense fine SAND	6.00 – 8.25
CLAY	8.25 – 12.10
Sandy CLAY	Below 12.10

The soil properties chosen for each prediction method are summarised in relevant section of this chapter.

6.2.2 Pulse pile tests

250mm diameter pulse piles were tested on the same site in Moscow. Soil composition relevant to the pile location on site is summarised in Table 6-2. Groundwater level was at 7.53m below existing ground level.

Table 6-2 – Soil properties next to pulse pile on site Polytech Museum, Moscow

Stratum	Level (m BGL)
Made Ground	0.00 - 1.65
Firm to stiff sandy CLAY	1.65 – 8.65
Medium dense fine SAND	Below 8.65

Two pulse piles were also tested on a site in Odintsovo in Moscow. The soil stratigraphy is summarised in Table 6-3.

Table 6-3 – Soil properties on site Odintsovo, Moscow

Stratum	Level (m BGL)
Made Ground	0.00 – 2.10
Firm SILT	2.10 – 4.50
Soft to firm SILT	4.50 – 5.50
Medium dense medium coarse SAND	Below 5.50

The characteristics of the soils for each prediction method are summarised in relevant section of this chapter.

6.3 Fleming's method prediction of pile settlement for specified field tests

The Fleming's method was used to calculate the load settlement of bored and pulse piles tested in Moscow. The total settlement was calculated using equation (35). The soil strata of all considered cases were comprised of three layers of soil. The shaft friction was calculated for each layer using equation (40). The end bearing was calculated using equation (39) for the soil stratum under the toe of the pile.

The capacity of the pulse piles was calculated using empirical factors suggested by NIIOSP (ref.) summarised in the Table 5-7 and Table 5-8 of Chapter 5.

6.3.1 Bored pile – Polytech

The semi-empirical method of pile settlement prediction was applied to simulate behaviour of load tested bored pile on site Polytech. Ultimate shaft and end bearing capacity were calculated using the procedure explained in Chapter 5 for a single bored pile Ø250mm diameter 15m long.

The soil investigation provided for the construction site is not satisfactory. There is no soil parameters given in the ground investigation report, therefore a generic soil model was developed for the semi-empirical calculation. The soil properties of each stratum were specified using soil cases developed in Chapter 4. Interpretation of soil investigation based on soil cases are summarised in Table 6-4.

Table 6-4 – Soil properties applied for Fleming's method calculation of tested bored pile on Polytech, Moscow

Stratum	Level (m BGL)	Soil case	Engineering parameters
MG – firm CLAY	0.00 - 6.00	Clay 2	γ = 20 kN/m^3; c_u = 40kN/m^2; E' = 5,000 kN/m^2
Medium dense fine SAND	6.00 – 8.25	Sand 3	γ = 19 kN/m^3; φ' = 31.75°; E' = 18,000 kN/m^2
Firm to stiff CLAY	Below 8.25	Clay 4	γ = 20 kN/m^3; c_u = 80kN/m^2; E' = 10,000 kN/m^2

Since most of the soil layers comprised of fine grained material, an M_S value of 0.02 has been applied to calculate settlement at the top of the bored pile. The resulting load settlement curve for Fleming's method is shown on Figure 6-2.

6.3.2 Pulse pile – Polytech

A 250mm diameter, 12.65m long pulse pile was tested on the same site as the bored pile - Polytech. The ground investigation showed that the soil profile was different from that at the location of the bored pile. Therefore, a different set of soil parameters were developed. Using the soil cases developed in Chapter 4, the interpretation of ground properties is summarised in Table 6-5.

Table 6-5 – Soil properties applied for Fleming's method calculation of tested pulse pile on Polytech, Moscow

Stratum	Level (m BGL)	Soil case	Engineering parameters
MG – firm CLAY	0.00 – 7.50	Clay 4	γ = 20 kN/m^3; c_u = 80kN/m^2; E' = 10,000 kN/m^2
Firm CLAY	7.50 – 8.50	Clay 4	γ = 20 kN/m^3; c_u = 80kN/m^2; E' = 10,000 kN/m^2
Medium dense fine SAND	Below 8.50	Sand 3	γ = 19 kN/m^3; φ' = 31.75°; E' = 18,000 kN/m^2

The load settlement curves of the pulse pile was compared to the load-settlement curve calculated by Fleming's method. An M_S value of 0.02 was applied as determined in Chapter 5.

6.3.3 Pulse pile – 13.75m long

A 300mm diameter, 13.75m long pulse pile was tested on the site in Odintsovo in Moscow. The ground is comprised of both granular and cohesive soils. The soil investigation provided for the site is very limited, therefore soil cases developed in Chapter 4 have been applied to calculate pile shaft and end bearing capacity. The soil properties used for the semi-empirical prediction of the pulse pile performance are summarised in Table 6-6. The layer of silt was considered as a fine grained soil, case Clay 3. While it is not satisfactory that a soil investigation was carried out without any tests to characterise the soil, the fact that the pile test results were being to compare the methods of prediction with the observed settlement is reasonable provided the assumed parameters are typical for those soils. The analyses in Chapters 3, 4 and 5 provide some confidence in this assumption..

Table 6-6 – Soil properties applied for Fleming's method calculation of tested piles on Odintsovo, Moscow

Stratum	Level (m BGL)	Soil case	Engineering parameters
Made Ground	0.00 - 2.00	Sand 5	γ = 19 kN/m^3; φ' = 34.25°; E' = 30,000 kN/m^2
Firm locally soft SILT	2.00 – 5.50	Clay 4	γ = 20 kN/m^3; φ' = 25°; E' = 10,000 kN/m^2
Medium dense medium coarse SAND	Below 5.50	Sand 5	γ = 19 kN/m^3; φ' = 34.25°; E' = 30,000 kN/m^2

The pulse pile were installed in layers of coarse and fine grained soil, therefore an M_S value of 0.004 was used. The load settlement curve for the semi-empirical prediction of pulse pile performance is shown on Figure 6-6.

6.3.4 Pulse pile – 9m long

A 300mm diameter, 9m long pulse pile was tested on the same construction site in Odintsovo in Moscow. The chosen soil parameters used to calculate pile settlement by semi-empirical method were the same as those for the 13.75m long pile shown in Table 6-6. An M_S value of 0.004 was applied for multi-layered soil case. The resulting load-settlement curve is shown on Figure 6-8.

6.4 Plaxis prediction of pile settlement for specified field tests

Plaxis 2D was used to create an axisymmetric model for the bored and pulse piles performance of the load tested examples considered in this chapter.

6.4.1 Bored pile – Polytech

A bored pile was modelled in Plaxis 2D using the axisymmetric type 15-noded layout. A body of the pile is a cluster of 15m depth and 0.125m radius. The material properties of the pile cluster were assigned as fresh concrete for pile installation Phase 1 and as solid concrete for remaining loading and unloading phases. The loading was specified as prescribed displacement (see Figure 6-1). Mesh coarseness was specified as medium with enhanced mesh refinements.

The soil properties for the Plaxis model summarised in Table 6-7. Groundwater level was at 1m below ground level.

Table 6-7 – Soil properties used in Plaxis 2D to model bored pile tested on site Polytech, Moscow

Stratum	Level (m BGL)	Material model	Drainage type	Engineering parameters
Clay 1	0.00 – 6.00	Mohr-Coulomb	Undrained (A)	γ_{unsat} = 19kN/m^3; γ_{unsat} = 20kN/m^3; φ' = 23°; c' = 0kN/m^2; E' = 2,500kN/m^2; ν' = 0.2
Sand 3	6.00 – 8.25	Mohr-Coulomb	Drained	γ_{unsat} = 16.20 kN/m^3; γ_{unsat} = 19.48 kN/m^3; φ' = 31.75°; E' = 18,000 kN/m^2; ν' = 0.3
Clay 2	Below 8.25	Mohr-Coulomb	Undrained (A)	γ_{unsat} = 19kN/m^3; γ_{unsat} = 20kN/m^3; φ' = 25°; c' = 1kN/m^2; E' = 5,000kN/m^2; ν' = 0.2

The loading was applied to the pile head in two phases. The first loading phase was specified as prescribed displacement. A universally distributed load at maximum observed settlement of the bored pile has been derived followed by unloading phase. A second loading phase specified as prescribed displacement to a settlement of 10% of pile diameter corresponding to the ultimate load.

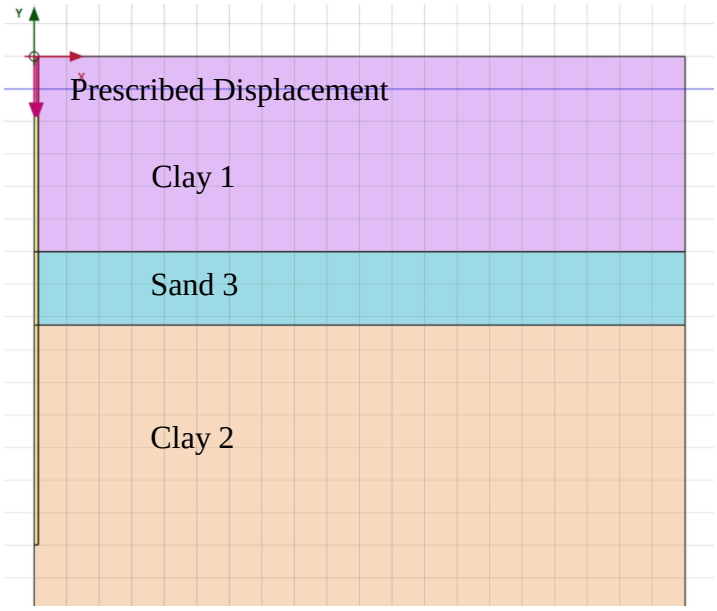

Figure 6-1 – Plaxis layout for analysis of the bored pile CFA Polytech

Load-settlement curves for the pile (Polytech-bored-250-15), predicted by Fleming's method (Fleming-bored) and predicted in Plaxis 2D (Plaxis-bored-back calc) are shown on Figure 6-2. Soil parameters of the Plaxis 2D model were specified to fit the curves for tested pile and Fleming's method. Groundwater level in Plaxis 2D was assumed at 1m bgl.

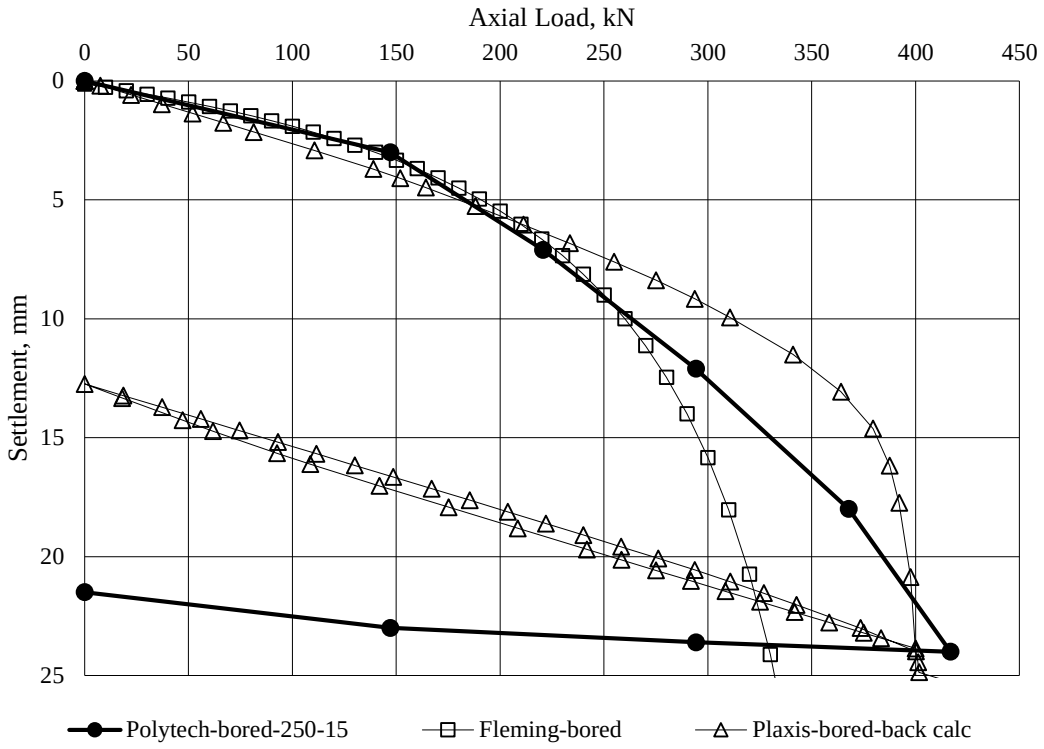

Figure 6-2 – Load-settlement curve of tested bored pile Polytech compared to pile performance predicted by Fleming's method and Plaxis 2D FE model

As can be seen from Figure 6-2, the semi-empirical prediction of bored pile performance is coinciding with the Plaxis FE modelled curve at the initial phase of loading. The root mean square calculated for Fleming-Tested pile on the range of loads from 0 to 120kN (design load of 1/3 of ultimate load) is 0.298; for Pulse-Tested pile, it is 0.44. Thus, the results of the Fleming method show better convergence with the results of the test pile for the working load range than those for the Plaxis model. However, the ultimate load was better predicted by Plaxis, whereas Fleming's method underestimated the ultimate capacity at a settlement of 10% of pile diameter.

6.4.2 Pulse pile – Polytech

The 250mm diameter, 12.65m long pulse pile was modelled in Plaxis 2D and compared to the test pulse pile at the site Polytech Moscow. Pulse discharge treatment has been applied along the pile shaft from 1.65m below ground level. A dynamic loading of 5000kN/m2 was used to simulate the pulse discharge treatment (see Figure 6-3). The dynamic loading was modelled as a single pulse with a pick value on 0.001 second over 0.002 seconds with the dynamic time interval of 0.1 seconds.

The soil model developed for pulse pile FE model used the reference models summarised in Table 6-8.

Table 6-8 – Soil properties used in Plaxis 2D to model pulse pile tested on site Polytech, Moscow (Pulse-ref)

Stratum	Level (m BGL)	Material model	Drainage type	Engineering parameters
Clay 2	0.00 – 1.65	Mohr-Coulomb	Undrained (A)	γ_{unsat} = 19kN/m^3; γ_{unsat} = 20kN/m^3; φ' = 25°; c' = 0kN/m^2; E' = 5,000kN/m^2; ν' = 0.2
Clay 4	1.65 – 8.50	Mohr-Coulomb	Undrained (A)	γ_{unsat} = 19kN/m^3; γ_{unsat} = 20kN/m^3; φ' = 25°; c' = 0kN/m^2; E' = 10,000kN/m^2; ν' = 0.2
Sand 4	Below 8.50	Mohr-Coulomb	Drained	γ_{unsat} = 16.60 kN/m^3; γ_{unsat} = 19.64 kN/m^3; φ' = 33°; E' = 24,000 kN/m^2; ν' = 0.3

The loading applied to the pulse pile was modelled in two phases as universally distributed load at the top of the pile (see Figure 6-3). Primary loading was specified as the maximum value applied to the test pulse pile and was followed by an unloading phase. A secondary loading provided pile performance to the ultimate load at a settlement of 10% of pile diameter.

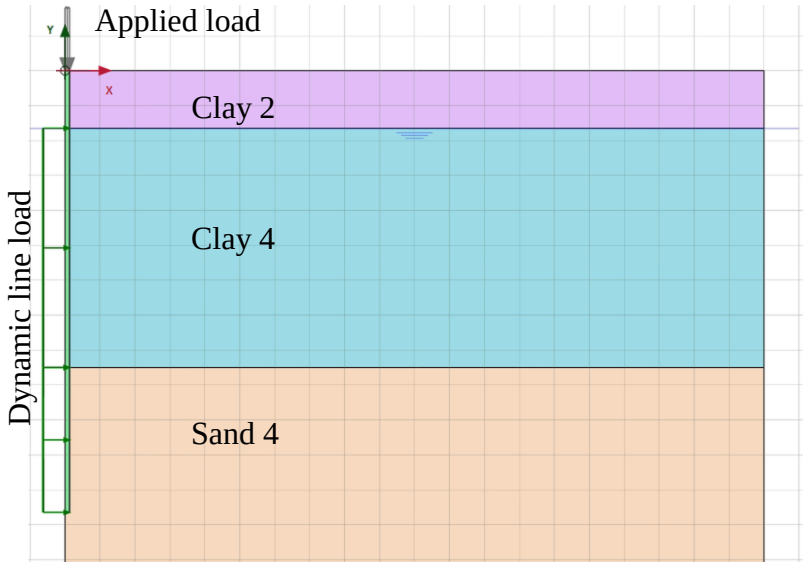

Figure 6-3 – Plaxis layout for analysis of the pulse pile Polytech.

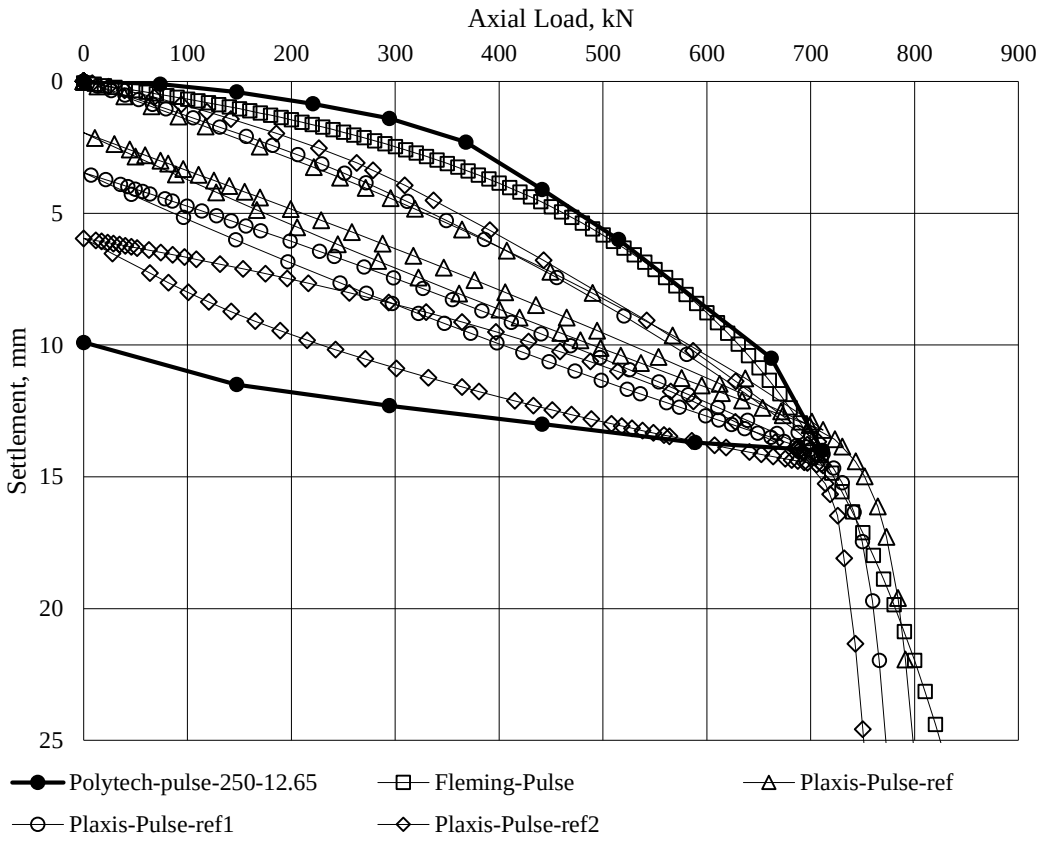

Figure 6-4 – Load-settlement curve of tested pulse pile Polytech compared to pile performance predicted by Fleming's method and Plaxis 2D FE model

A number of soil cases were used in Plaxis 2D to obtain better convergence with the test pile curve and Fleming's method of prediction. Reference 1 (Plaxis-Pulse-ref1) and reference 2 (Plaxis-Pulse-ref2) soil models are summarised in Tables 6-9 and 6-10. For ref 2 model firm to stiff clay parameters have been applied.

Table 6-9 – Soil properties used in Plaxis 2D to model pulse pile tested on site Polytech, Moscow (Pulse-ref1)

Stratum	Level (m BGL)	Material model	Drainage type	Engineering parameters
Clay 5	0.00 – 1.65	Mohr-Coulomb	Undrained (A)	γ_{unsat} = 19kN/m^3; γ_{unsat} = 20kN/m^3; φ' = 25°; c' = 0kN/m^2; E' = 5,000kN/m^2; ν' = 0.2
Clay 5	1.65 – 8.50	Mohr-Coulomb	Undrained (A)	γ_{unsat} = 19kN/m^3; γ_{unsat} = 20kN/m^3; φ' = 25°; c' = 0kN/m^2; E' = 10,000kN/m^2; ν' = 0.2
Sand 3	Below 8.50	Mohr-Coulomb	Drained	γ_{unsat} = 16.60 kN/m^3; γ_{unsat} = 19.64 kN/m^3; φ' = 33°; E' = 24,000 kN/m^2; ν' = 0.3

Table 6-10 – Soil properties used in Plaxis 2D to model pulse pile tested on site Polytech, Moscow (Pulse-ref2)

Stratum	Level (m BGL)	Material model	Drainage type	Engineering parameters
Clay 5+	0.00 – 1.65	Mohr-Coulomb	Undrained (A)	γ_{unsat} = 19kN/m^3; γ_{unsat} = 20kN/m^3; φ' = 25°; c' = 0kN/m^2; E' = 5,000kN/m^2; ν' = 0.2
Clay 5+	1.65 – 8.50	Mohr-Coulomb	Undrained (A)	γ_{unsat} = 19kN/m^3; γ_{unsat} = 20kN/m^3; φ' = 25°; c' = 0kN/m^2; E' = 10,000kN/m^2; ν' = 0.2
Sand 4	Below 8.50	Mohr-Coulomb	Drained	γ_{unsat} = 16.60 kN/m^3; γ_{unsat} = 19.64 kN/m^3; φ' = 33°; E' = 24,000 kN/m^2; ν' = 0.3

Figure 6-4 shows the Plaxis curves for the three reference soil cases, compared to the semi-empirical predictions and test pile performance. The root mean square error between the Fleming prediction and the results of the test pile curve for the load range from 0 to 270kN (design load at 1/3 of ultimate load) is 0.527, for Plaxis ref it is 1.77, Plaxis ref 1 – 1.598, and Plaxis ref 2 – 1.175. Fleming's method shows better convergence than Plaxis for the range of working load. Ultimate load prediction cannot be assessed due to lack of information from the field load test.

6.4.3 Pulse pile – 13.75m long

300mm diameter, 13.75m long pulse pile at the site in Odintsovo in Moscow was modelled in Plaxis 2D and compared with the semi-empirical prediction and field measured performance (see Figure 6-5). Soil properties of the FE model are summarised in Table 6-11. Groundwater level was assumed at -8.3m below ground level. Pulse discharge treatment has been applied along the pile shaft from 2m below ground level. A dynamic loading of 5000kN/m2 was used to simulate the pulse discharge treatment. The dynamic loading was modelled as a single pulse with a pick value on 0.001 second over 0.002 seconds with the dynamic time interval of 0.1 seconds.

Table 6-11 – Soil properties used in Plaxis 2D to model pulse piles tested on site Odintsovo, Moscow (Plaxis-Pulse-13.75-ref)

Stratum	Level (m BGL)	Material model	Drainage type	Engineering parameters
Sand 5	0.00 - 2.00	Mohr-Coulomb	Drained	γ_{unsat} = 17.00 kN/m^3; γ_{unsat} = 19.80 kN/m^3; φ' = 34.25°; E' = 30,000 kN/m^2; ν' = 0.3
Clay 4	2.00 – 5.50	Mohr-Coulomb	Undrained (A)	γ_{unsat} = 19kN/m^3; γ_{unsat} = 20kN/m^3; φ' = 25°; c' = 1kN/m^2; E' = 10,000kN/m^2; ν' = 0.2
Sand 5	Below 5.50	Mohr-Coulomb	Drained	γ_{unsat} = 17.00 kN/m^3; γ_{unsat} = 19.80 kN/m^3; φ' = 34.25°; E' = 30,000 kN/m^2; ν' = 0.3

The loading was applied in two phases. The first phase was for the primary loading to the maximum value applied on the test piles. An unloading phase is followed by the secondary loading phase to the ultimate load at settlement of 10% of pile diameter.

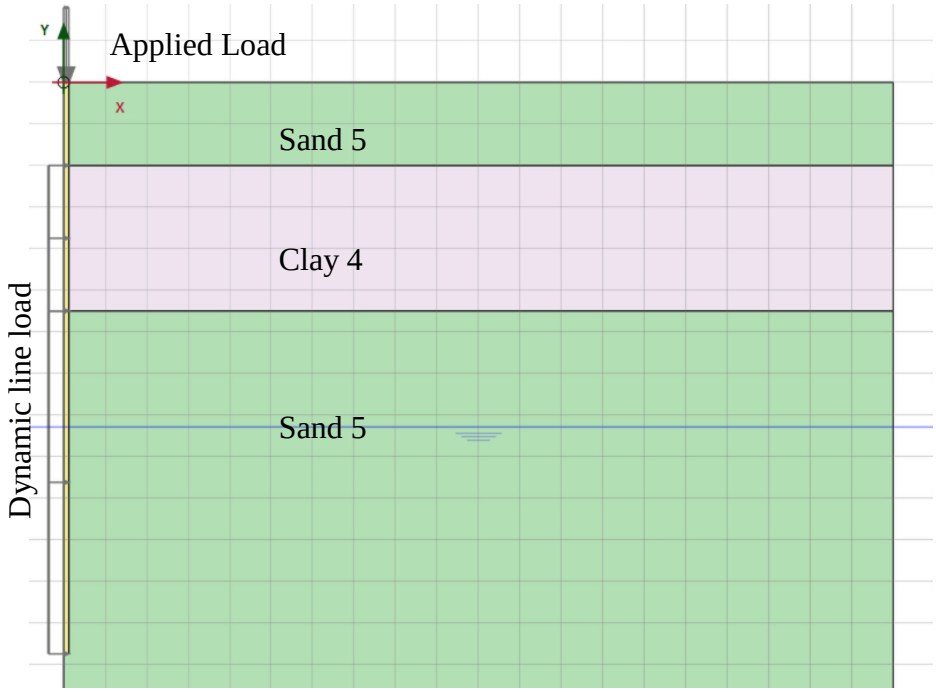

Figure 6-5 – Plaxis layout for analysis of the pulse pile Odintsovo 13.75

Resulting curves for Plaxis runs are shown on Figure 6-6.

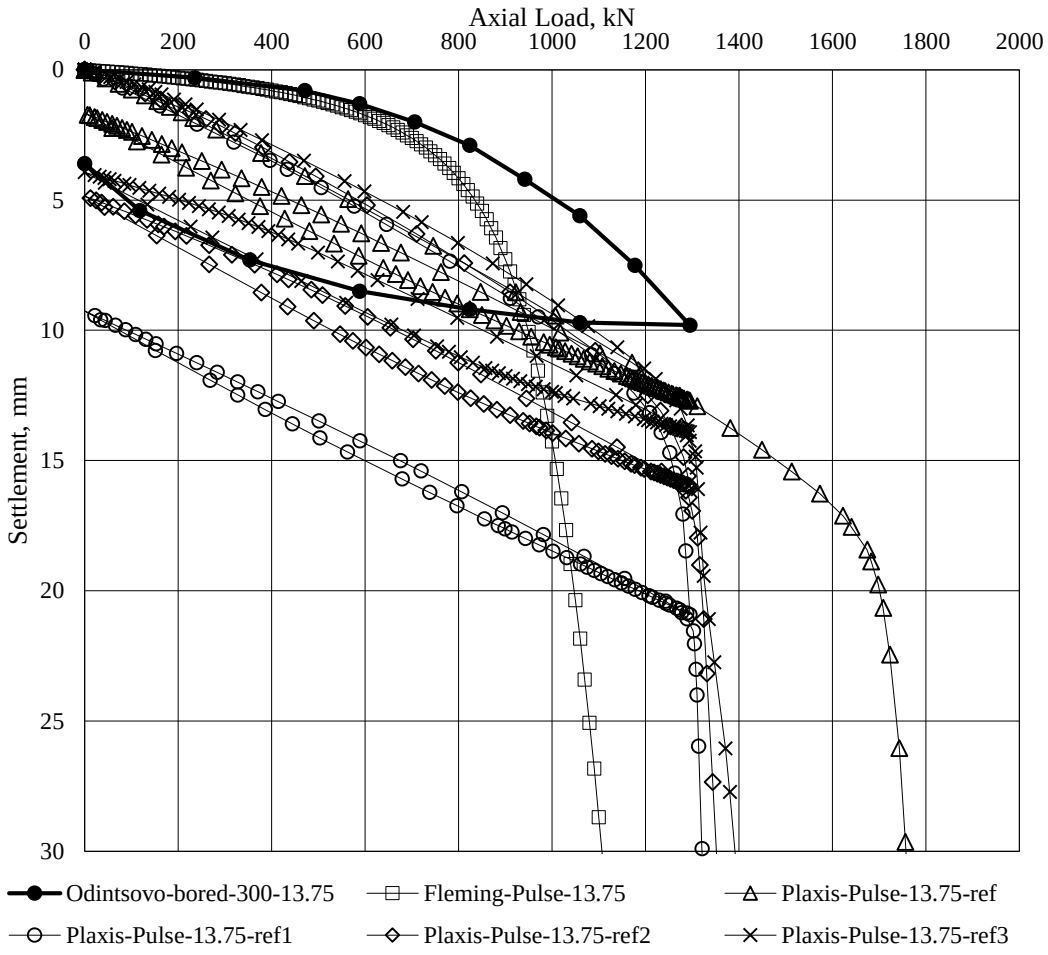

Figure 6-6 – Load-settlement curve of tested pulse pile 13.75m long (Odintsovo) compared to pile performance predicted by Fleming's method and Plaxis 2D FE model

Three more soil cases were used in Plaxis to obtain better convergence with the test pile curve and Fleming's method prediction. Reference 1 (Plaxis-Pulse-13.75-ref1), reference 2 (Plaxis-Pulse-13.75-ref 2) and reference 3 (Plaxis-Pulse-13.75-ref 3) soil models are summarised in Tables 6-12 to 6-14. Additional soil models with higher parameters have been developed for the ref 3 model. Groundwater level was assumed at 2m below existing ground level.

Table 6-12 – Soil properties used in Plaxis 2D to model pulse piles tested on site Odintsovo, Moscow (Plaxis-Pulse-13.75-ref1)

Stratum	Level (m BGL)	Material model	Drainage type	Engineering parameters
Fill	0.00 - 2.00	Mohr-Coulomb	Drained	γ_{unsat} = 15.60 kN/m^3; γ_{unsat} = 19.24 kN/m^3; φ' = 30°; E' = 9,000 kN/m^2; ν' = 0.3
Clay 4	2.00 – 5.50	Mohr-Coulomb	Undrained (A)	γ_{unsat} = 19kN/m^3; γ_{unsat} = 20kN/m^3; φ' = 25°; c' = 1kN/m^2; E' = 7,500kN/m^2; ν' = 0.2
Sand 5	Below 5.50	Mohr-Coulomb	Drained	γ_{unsat} = 17.00 kN/m^3; γ_{unsat} = 19.80 kN/m^3; φ' = 34.25°; E' = 30,000 kN/m^2; ν' = 0.3

Table 6-13 – Soil properties used in Plaxis 2D to model pulse piles tested on site Odintsovo, Moscow (Plaxis-Pulse-13.75-ref2)

Stratum	Level (m BGL)	Material model	Drainage type	Engineering parameters
Sand 5	0.00 - 2.00	Mohr-Coulomb	Drained	γ_{unsat} = 17.00 kN/m^3; γ_{unsat} = 19.80 kN/m^3; φ' = 34.25°; E' = 30,000 kN/m^2; ν' = 0.3
Clay 5	2.00 – 5.50	Mohr-Coulomb	Undrained (A)	γ_{unsat} = 19kN/m^3; γ_{unsat} = 20kN/m^3; φ' = 25°; c' = 1kN/m^2; E' = 12,500kN/m^2; ν' = 0.2
Sand 5	Below 5.50	Mohr-Coulomb	Drained	γ_{unsat} = 17.00 kN/m^3; γ_{unsat} = 19.80 kN/m^3; φ' = 34.25°; E' = 30,000 kN/m^2; ν' = 0.3

Table 6-14 – Soil properties used in Plaxis 2D to model pulse piles tested on site Odintsovo, Moscow (Plaxis-Pulse-13.75-ref3)

Stratum	Level (m BGL)	Material model	Drainage type	Engineering parameters
Sand 6	0.00 - 2.00	Mohr-Coulomb	Drained	γ_{unsat} = 17.40 kN/m^3; γ_{unsat} = 19.69 kN/m^3; φ' = 35.50°; E' = 36,000 kN/m^2; ν' = 0.3
Clay 5+	2.00 – 5.50	Mohr-Coulomb	Undrained (A)	γ_{unsat} = 19kN/m^3; γ_{unsat} = 20kN/m^3; φ' = 25°; c' = 1kN/m^2; E' = 45,000kN/m^2; ν' = 0.2
Sand 6	Below 5.50	Mohr-Coulomb	Drained	γ_{unsat} = 17.40 kN/m^3; γ_{unsat} = 19.96 kN/m^3; φ' = 35.50°; E' = 36,000 kN/m^2; ν' = 0.3

Figure 6-6 shows a comparison between the two methods of predicting pile performance and the pulse pile load test result. As in previous tests, Fleming's prediction shows good fit to measured performance on initial slope. However, the

ultimate capacity is lower than the projection of the test pile curve. Plaxis models show comparable performance for the working load range. The ultimate capacity of the Plaxis model is very sensitive to the groundwater level. Thus Reference model (Plaxis-Pulse-13.75-ref) with groundwater level at 8.3m below ground level shows a much better prediction of ultimate capacity than the predictions using ref 1 to ref 3 models with groundwater level at 2m b.g.l.

The root mean square error between the Fleming prediction and the results of the test pile range from 0 to 450kN (design load at 1/3 of ultimate load) is 0.0877; for Plaxis 13.75 ref it is 1.81, Plaxis 13.75 ref 1 – 1.91, Plaxis 13.75 ref 2 – 1.62, and Plaxis 13.75 ref 3 – 1.416. Fleming's method shows better convergence than Plaxis for the range of working load. Ultimate load prediction cannot be assessed due to lack of information from the pile load tests.

6.4.4 Pulse pile – 9m long

A 300mm diameter, 9m long pulse pile at the same site was modelled in Plaxis 2D. The same soil properties were used to model the shorter pile as in previous example (reference 1 in Table 6-12). An additional soil case has been considered for the 9m long pile model (see Figure 6-7) with the soil properties shown in Table 6-14. Groundwater level for the both reference (Plaxis-Pulse-9-ref) and reference 1 (Plaxis-Pulse-Ref1) has been assumed at 8.3m bgl. Pulse discharge treatment has been applied along the pile shaft from 2m below ground level. A dynamic loading of 5000kN/m2 was used to simulate the pulse discharge treatment. The dynamic loading was modelled as a single pulse with a pick value on 0.001 second over 0.002 seconds with the dynamic time interval of 0.1 seconds.

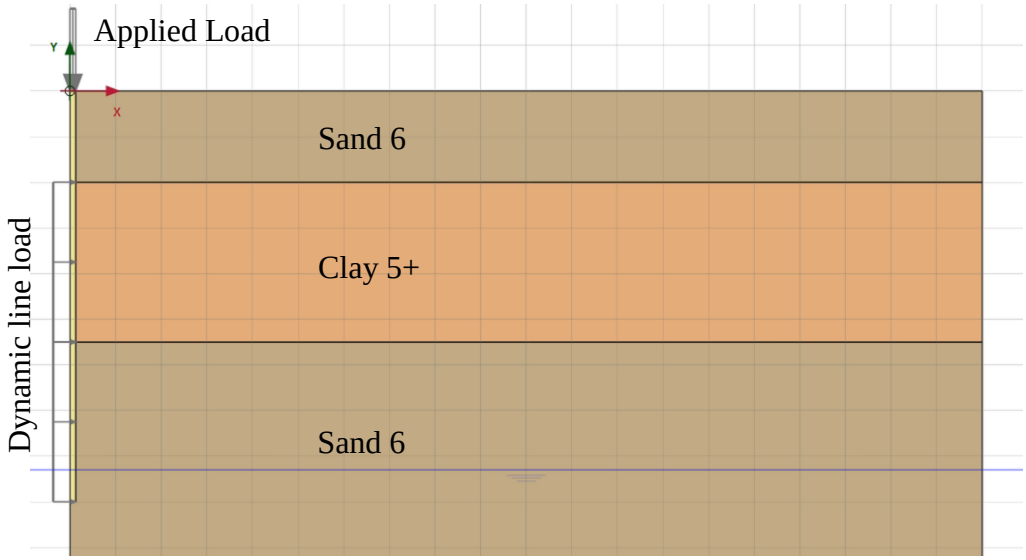

Figure 6-7 – Plaxis layout for analysis of the pulse pile Odintsovo 9

Resulting curves can be seen on Figure 6-8.

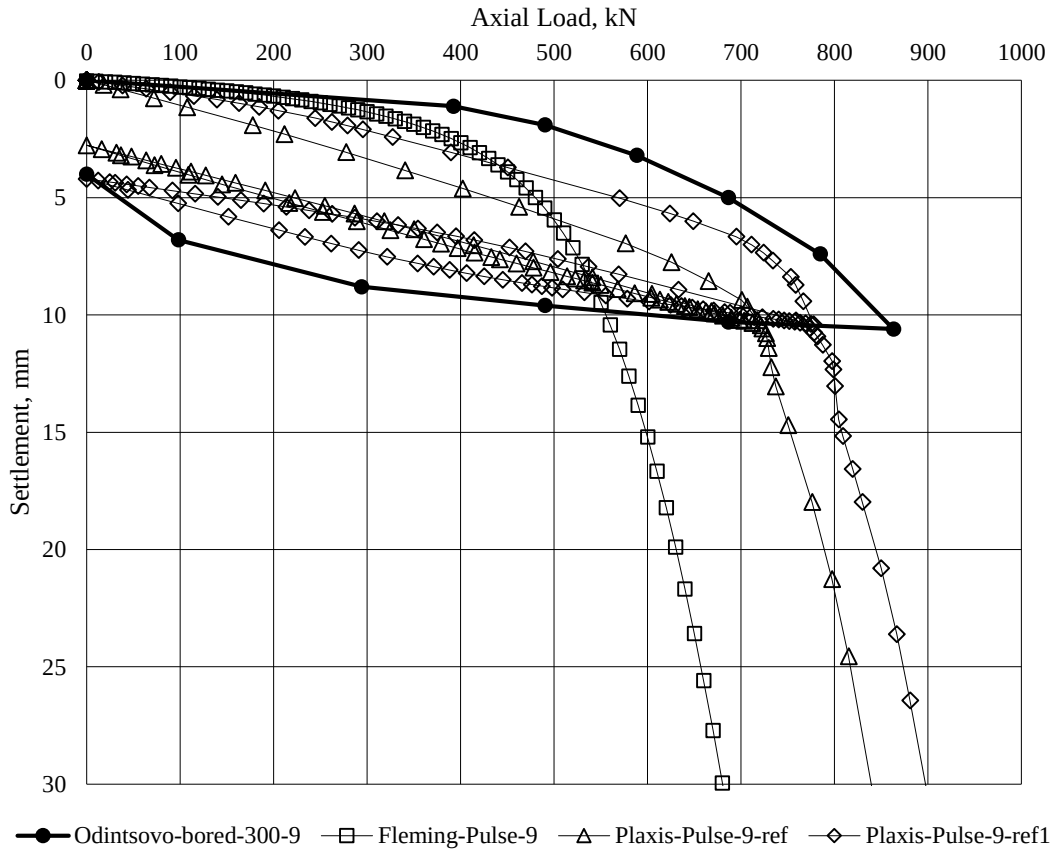

Figure 6-8 – Load-settlement curve of tested pulse pile 9m long (Odintsovo) compared to pile performance predicted by Fleming's method and Plaxis 2D FE model

The shorter pile in same soil conditions shows a different comparison between the predicted and measured results. Again Fleming's method shows better convergence with the results of the test pile compared to those from Plaxis for the design load, and underestimate the ultimate capacity at settlement of 10% of pile diameter. The root mean square error between the Fleming prediction and the results of the test pile for the load range from 0 to 300kN (design load at 1/3 of ultimate load) is 0.146, for Plaxis 9 ref it is 1.46, and Plaxis 9 ref 1 – 0.66. The ultimate load prediction cannot be assessed due to lack of information from the load tests. However, the Plaxis 2D predicts an ultimate capacity closer to the projection of the test curve than Fleming's prediction.

6.5 Discussion

In this chapter, a number of field test results have been compared with load settlement curves obtained by Fleming's method and by FE modelling in Plaxis 2D. The field tests were performed for commercial purposes and not specifically for this research. Therefore, there was no original scope of works submitted to the testing organisation beforehand, including requirements for a ground investigation, maximum value of the tested load/settlement, location of the tested pile in relation to the adjacent piles and structures, number of pulses at certain level or control of the pulse treatment. A ground investigation was carried out without any tests to characterise the soil, which is not satisfactory for the purposes of the research.

The predicting of capacity of piles by Fleming's method and by FE modelling in Plaxis required manual adjustment of soil properties based on load settlement curves. Both methods required selection of the soil properties of each considered soil layer to fit the load settlement curves to the tested results (Figures 6-2, 6-4, 6-6 and 6-8). Plaxis models were sensitive to the groundwater level, therefore lack of certainty on observed data on groundwater level during the field tests prevented to obtain reliable calculation outputs.

The bored pile load settlement curves for semi-empirical method and FE modelling showed good convergence with the field test result. However, the results for the pulse

piles modelled in Plaxis were less reliable. A root mean square error on the range of working load for pulse piles is not acceptable.

Although on the working load range the Fleming's method shows better fit of the load settlement curve to the tested curve, Plaxis allows to predict the ultimate load more accurately for the coarse and fine grained soils for both bored and pulse types of piles. The material models developed for Plaxis can be used to model a wide range of soils but require a detailed ground investigation. The results of the finite element modelling are as accurate as the input data.

In future work, it is recommended that the load tests should be carried out on pulse piles in accordance with the scope of works accompanied by a detailed ground investigation including the groundwater report. The soil propertied required for certain material models in Plaxis should be specified for laboratory tests to characterise the soil. The pulse treatment process should be controlled and recorded for detailed report on the number of pulses, the level of each point of electric discharges, a proximity to adjacent piles/structures. Additional testing of the pressure measured on the borehole wall of various diameters and in various types of soil will be useful for the accurate modelling of a dynamic impact.

Chapter 7
Conclusions and Recommendations for Further Work

7.1 Introduction

This research focused on predicting the capacity of a single pulse pile in coarse and fine grained soils. A finite element 2D axisymmetric model was developed to simulate construction sequence of a bored pile in Plaxis software. A dynamic tool was used to model the distributed load from the pulse discharge treatment along the shaft of the borehole filled with wet grout. The calculated settlement from a vertical load applied at the top of pile has been compared to the results of semi-empirical calculations of pile performance. Full-scale field test results were used to validate methodology of both calculation methods.

The finite element model in Plaxis 2D was developed and sensitivity analyses were performed to investigate the effect of soil properties, geometry, mesh coarseness, loading application and dynamic multipliers on the load settlement response. Values of soil properties recommended by Plaxis software developers were obtained for coarse and fine grained material models and results of the calculations are summarised in Chapter 4.

The semi-empirical method of pile settlement prediction developed by Fleming (1992) was studied to compare to the output from the finite element model of a pulse pile. Shaft friction and end bearing of the pile were calculated in the Fleming model using coefficients recommended by Russian institution NIIOSP (2001) for pulse piles. A sensitivity analysis of the variables was performed to investigate their influence on accuracy of pile performance prediction.

Full-scale field tests were obtained from a piling contractor from Moscow, Russia. The results of the load tests were analysed and compared with pile load-settlement curves predicted using the semi-empirical method and finite element models in Plaxis 2D. The root mean square error was calculated to confirm the accuracy of prediction techniques.

7.2 Effects of dynamic treatment of soil

In this study the effects of dynamic loading from pulse discharge treatment of soil was investigated. The shockwave created by an electric arc discharge in wet grout reaching the walls of a borehole provides enough pressure to create local failure of the ground surrounding the point of discharge. The mechanism can be likened to a cavity expansion. Cavity expansion theory developed for pressuremeters, for example, was not used because the rate of expansion in the pulse pile has to take into account dynamic effects. Repeated pulses increased the deflection from the initial cavity expansion. This process increased the volume of the borehole by redistribution of surrounding soil particles by means of voids space reduction. The shape of an expanded pile is impossible to predict due to irregularity and random shape of soil fines, but it can be assumed to be spherical due to the spherical nature of the shockwave propagation. Pulses performed at several levels along the pile make the shape of a pile very rough and increasing the friction on the soil-structure surface. It was assumed that this could be modelled as a cylindrical pile.

The equipment used in practice allowed a frequency of 1 pulse every 7 to 10 seconds. Electric discharge takes place in microseconds (see Figure 2-10) and the pressure on the borehole walls can reach a value of 25MPa (see Figure 2-17). This is assumed to be sufficient to produce a cavity expansion surrounding the point of electric discharge. The zone of influence of the pulse discharge treatment is unknown, but it is assumed to be within 3 pile diameters.

Pulse treatment normally commences from the bottom of the borehole, so that the increase in soil density is focused on the base of the pile. This has positive contribution to shaft friction as well as end bearing.

In coarse grained soils, pore pressures are likely to be developed during the dynamic loading but they will dissipate rapidly between pulses. Thus the pulse discharge process can be considered as drained behaviour. In fine grained soils, the excess pore pressures do not dissipate as quickly as in coarse grained soils because the permeability is significantly smaller. Therefore, undrained behaviour can be considered. However, due to the excess pore water pressure in fine grained soils in undrained condition, water from surrounding soil can migrate back to the grouted volume of the borehole because of the void space created in the grout due to

vaporisation of the water surrounding the electrodes during electric discharge. Thus, the magnitude of excess pore pressures in the fine grained soil can be less than expected. Consolidation will occur after the pulse treatment.

Redistribution of the soil particles in coarse grained soils increases the relative density of the soil. It means all the properties of a coarse grained soil increase according to the relations to relative density shown in Table 4-2. In fine grained soils, consolidation leads to an improvement in the relevant properties. Relationships between strength and stiffness properties proved difficult to derive but certain assumptions were made based on additional laboratory and field tests.

7.3 Calculation approach

There are number of ways to allow in the design for increased capacity of a pulse pile in comparison to the bored pile of the same augered diameter. Conventional design procedures to predict the capacity of a pulse pile including shaft friction and end bearing can be modified for the pulse pile by means of additional coefficients (see Table 5-7 and Table 5-8). To investigate the effect of the dynamic treatment due to the pulse, a finite element model of a single pile can be considered. Methods of simulation of change of geometry and parameters include:

- Assignment of soil clusters in the model with manual adjustment of soil properties and geometry
- Equivalent static pressure from the shockwave on the walls of a borehole
- Volumetric strain of the pile cluster
- Dynamic distributed load applied on pile-soil interface

In this research an axisymmetric finite element model in two dimensions has been studied using Plaxis software. The construction sequence, including the borehole creation, the filling of the borehole with wet concrete, the pulse discharge and the setting of the concrete was specified. A decision had to be made in regard to the way of modelling the treatment of walls of a borehole with the pulses. Although the shape of the shockwave propagation is assumed to be spherical, it was decided to model the dynamic load as a horizontal line load applied along the pile shaft. Treatment

underneath the toe of a pile was not considered in this study to reduce the time of calculation of each run. The increase in base area of the pile was considered.

Material models in Plaxis (see Table 4-1) considered in this research include Mohr-Coulomb, Hardening Soil and Hardening Soil with Small-Strain Stiffness. For the range of soils studied in this analysis, the difference in results for these material models was not significant, therefore the Mohr-Coulomb material model has been used in majority of the calculations.

Coarse grained soils have been modelled as drained material. For fine grained soils, undrained (A) properties were used for the analysis in terms of effective stresses. A consolidation phase followed the pulse treatment of a pile to model construction sequence.

Based on Plaxis outputs, the soil properties were not changed after the pulse treatment. The dynamic load applied to the wall of a borehole increased the pore water pressure and stresses in soils but the strength and stiffness properties were not affected in this analysis.

7.4 Plaxis 2D performance assessment

Modelling of the pulse treatment in Plaxis 2D using the dynamic load tool showed that this was feasible for a first approximation of a single pile capacity prediction. A dynamic load applied as a line load on the pile-soil interface showed plastic deformation similar to those of cavity expansion in the soil surrounding the pile. The mesh was deformed and the stresses in the soil in close proximity to the line load increased. Since the final shape of an actual pile is random and cannot be predicted, there is no certain way to assess whether the dynamic load sequence predicted the deformed shape. This is the load settlement prediction was used to assess the performance of a pile.

The dynamic tool used to simulate the pulse discharge treatment allowed the time and frequency of the pulses to be specified. It was not possible to model the current field practice exactly. The main disadvantage of the dynamic tool for PDT simulation is the calculation time. For the purposes of this research, to produce the data base of computational results, it was decided to model a single pulse of 1microsecond over

1/10 of a second multiplier. Even with this approximation, each run takes 45 to 60 minutes for a single pile in Plaxis 2D. This approximation can partially explain relatively poor convergence of predicted results with the field tests.

Another approximation used in this research is the line dynamic load for pulse treatment instead of spherical load at each point and no allowance for vertical loading at the bottom of the borehole. This means the end bearing of the pulse pile in the model could have been underestimated. Comparison of the predicted pile performance with the measured results of the field tests shows the error between the load-settlement curves and the FE prediction could be partially explained by the lack of modelled end bearing gain from the treatment of the pile toe.

The drainage properties of the soil specified in Plaxis allowed the pulse treatment to be modelled as a dynamic load in coarse and fine grained soils. Drained analysis due to the pulse showed more expansion than that in undrained soils. The undrained (A) material model was specified in terms of effective stresses to allow a realistic prediction of pore pressures. The consolidation phase followed the pulse treatment before the pile loading phase. Thus the described construction sequence replicated the field load testing process in fine and coarse grained soils. The value of pressure applied to the walls of the borehole in the model with dynamic multiplier was enough to create a deformed mesh in both undrained and drained analyses. While the dynamic analysis changed the geometry of the pile, it was assumed that the strength and stiffness of the soil did not change. In practice, a change in soil properties is expected.

7.5 Conclusions

PDT is a method to increase the capacity of a bored pile. A high voltage discharges in fresh grout causes the pile to expand. This method has been successfully used in Russia and South Korea for last 25 years. In the UK and Europe it was not widely recognised due to lack of equipment and theoretical basis for the design. This research focused on the development of a design approach to predict pulse pile capacity in accordance with European standards.

Plaxis 2D was used to simulate the construction sequence of the pulse pile followed by a load test to assess the pile performance. The FE analysis showed that the pulse pile had significantly more axial capacity than the bore pile. A semi-empirical method,

the Fleming method, was used to validate the results of finite element analyses. Field tests results obtained from private contractor have been compared with the analytical methods. These showed that the FE analysis predicted the ultimate capacity while the semi empirical method predicted the load settlement curve up to the working load.

The methods of prediction were very dependent on the chosen parameters. The ultimate load is the main input parameter for the semi-empirical method. It is important to have the confirmed values of shaft friction and end bearing for reliable prediction of load settlement. The Fleming's method is sensitive to the M_S value that is dependent on a type of soil. The FE modelling is very dependent on a detailed soil investigation. Certain material models in Plaxis should only be applied if the specific soil tests were carried out to characterise the soil.

The following aims have been addressed for this research:

- To review existing information in regard to the PDT to increase pile capacity

A critical review of literature relating to PDT was summarised in chapter 2, including the methodology, the design process and the application. The gaps in the knowledge were identified as follows: dynamic loading has not been used to simulate PDT treatment before; although numerical modelling of a PDT pile was performed by Park et al. (2011), the performance of the pile under vertical load was not considered.

- Development of the finite element model of a single Pulse pile

A 2D axisymmetric model has been developed in Plaxis and a sensitivity analysis has been produced. Effects of mesh coarseness, model boundaries, soil properties of fine and coarse grained soils were studied for bored and PDT pile models in Plaxis 2D. A dynamic load was applied to pile soil interface to simulate PDT and the sensitivity of the model to amplitude, frequency, number of pulses, length of line load were compared in fine and coarse grained soils. Refined soil parameters of basic and advanced material models were summarised and used for modelling of bored and pulse piles in Plaxis 2D. Plaxis 2D axisymmetric models were developed for validation of the field tests using the data from industrial application of PDT in Moscow.

- Validation of the results of finite element modelling

A semi-empirical method has been used to validate FEM analysis. Sensitivity analysis of a tangent slope M_S value used in Fleming method was performed to obtain optimal

parameters for a semi-empirical prediction of the pulse pile capacity. The root mean square error method was used to confirm the results of comparison. Field load test results were used to compare with theoretical calculation of bored and PDT pile capacity. Multi-layered soil models have been developed to simulate ground conditions specified for the field tested PDT piles in Moscow. Results of validation show it is appropriate to use semi-empirical method on the working load range and Plaxis 2D calculation for ultimate load prediction.

The limitations of the modelling have been acknowledged as follows:

- The shock front and gas-vapour pressures from a PDT discharge propagate spherically. Currently it is not possible to apply the dynamic load in Plaxis in a spherical manner, therefore the dynamic load has been applied as a line load. However, in practice, successive discharges at various depths produce, in effect, a nearly cylindrical pile which means the dynamic loading model is acceptable.

- Plaxis dynamics analysis running time increase exponentially with increase of time of dynamic phase. Calculation of 30 and 40 seconds PDT treatment was terminated due to Plaxis 2D Calculation Kernel failure. It is possible to split the dynamic simulation by individual pulses, however Plaxis developers recommend to model the gap between the pulses as a dynamic phase as well. Reduction of interval between pulses was an approximation to simulate the time parameters of PDT treatment used in industry.

- Updated mesh after dynamic calculation was not available until 2018 version of Plaxis 2D. It means the load test calculation phase did not take into account expanded geometry of the borehole.

7.6 Further work

Further work is recommended to improve the prediction. Advanced material models including the Hardening Soil, Hardening Soil with small-strain stiffness or user defined soil models should lead to a better prediction of the load settlement curve. The increase in strength and stiffness of the surrounding soil could be taken into account by using a user defined soil model.

The quality of the field tests results used in this research was limited by poor ground investigation data. In future work, it is recommended that full scale load tests should be carried out on pulse piles accompanied by a detailed ground investigation.

In this study only single pile performance has been considered. However groups of pulse piles can be installed creating compacted ground surrounding the foundation (cf stone columns). The effect of group pulse pile installation has to be investigated.

Loose to medium dense coarse grained soils and soft to firm fine grained soils have been considered in this research. However PDT has also successfully been used for soil treatment of very weak soils. Further work is recommended to explore feasibility of pulse treatment in different types of soils, particularly those that contain more than category of soil (e.g. sandy clay, clayey sand).

Recommended future work can be summarised as follows:

- The laboratory tests. The ground investigation data for the field tests were limited in quality and quantity. Further, the data may not be appropriate to provide data for dynamic modelling. Therefore, a study on the relevant parameters to model PDT technology is required. This means a specification for appropriate ground investigation is required.

- The field tests. Considering the field tests of the working or preliminary piles can be expensive and time consuming, it is important to plan and control future field tests. The field tests can provide very valuable information regarding the real PDT pile performance in various soil conditions and treatment at specified levels. It is also very important to arrange detailed ground investigation in close proximity to tested PDT piles.

- The modelling. It was proven that Plaxis 2D can be used to model single PDT piles. Pulse treatment can be simulated using dynamic analysis. Dynamic calculation considered in this research used a number of approximations. Time and frequency of pulses were simplified and approximated in this research. It is recommended that the pressure data from laboratory or field tests in the format that can be read by Plaxis should be used to determine the load multiplier. Dynamic line load was used to simulate PDT treatment – future versions of software may allow a spherical propagating of the PDT load.

Axysimmetric 2D model was used – 3D Plaxis can be used in the future to check the 3D effects of PDT pile installation. Only a single PDT pile has been considered – effect of a group of piles, adjacent structures, soil treatment or application of PDT for ground anchors should be considered. Certain features have been introduced in Plaxis only recently, that were not available for this research, like using updated mesh for the phases following dynamic calculation. Using latest version of Plaxis will be very useful to explore better methods of predicting the capacity of pulse piles.

Chapter 8
References

An, J., Tuan, C.Y., Cheeseman, B.A., and Gazonas, G.A., 2011. Simulation of Soil Behavior under Blast Loading. *International Journal of Geomechanics ASCE* 11(4):323-334

Aptikaev, S.F., 2001. Characteristic Features of Ground-Surface Oscillations near Technogenic Seismic Sources. *Soil Mechanics and Foundation Engineering*, 38 (1), 8–13.

Atkinson, J.H. and Sallfors, G., 1991. Experimental determination of soil properties (stress-stiain-time). *In*: *Proc. 10th Eur. Conf: Soil Mech., Florence*. 915.

Bakholdin, B. V and Dzhantimirov, K.A., 1998. New electric-discharge technologies in geotechnical construction. *Soil Mechanics and Foundation Engineering*, 35 (4–5), 154–159.

Benz, T., 2007. *Small-strain stiffness of soils and its numerical consequences*. Univ. Stuttgart, Inst. f. Geotechnik Stuttgart.

Berezantzev, V.G., Khristoforov, V., and Golubkov, V., 1961. Load bearing capacity and deformation of piled foundations. *In*: *Proceedings of the 5th International Conference on Soil Mechanics and Foundation Engineering*. 11–12.

Brinkgreve, R.B.J. and Broere, W., 2015. PLAXIS 2D Reference Manual 2015. *Delft, Netherlands2010*.

Brinkgreve, R.B.J., Engin, E., and Engin, H.K., 2010. Validation of empirical formulas to derive model parameters for sands. *Numerical methods in geotechnical engineering*, 137–142.

Brovin, S., 1994. *Performance characteristics of piles injected into predrilled holes to strengthen a weak soil mass [in Russian], dissertation of a Doctor Tech.,* Saint Petersburg: s.n.

BS EN 1991-1-7, 2006 Eurocode 1: Actions on structures. Part 1–7: General actions—Accidental actions.

BS EN 1997-1, 2004. Eurocode 7. Geotechnical Design. General Rules.

BSI, 2015. *Code of parctice for foundations.* s.l.:s.n.

Chin, F.K., 1970. Estimation of the ultimate load of piles from tests not carried to failure. *In*: *Proc. 2nd Southeast Asian Conference on Soil Engineering, Singapore, 1970*.

Gaba, A, Hardy, S, Doughty, L, Powrie, W, Selemetas, D, 2017. CIRIA C760 Guidance on embedded retaining wall design. CIRIA

Grigoryan, A.A. and Yushube, V.S., 1986. *Interaction of cast-in-place piles with soil under type II collapsibility conditions*. Soil Mechanics and Foundation

Engineering - SOIL MECH FOUND ENG.

Clarke, B.G., 2017. *Engineering of Glacial Deposits*. CRC Press, Taylor & Francis Group.

Dzhantimirov, K.A., Krastelev, E.G., Kryuchkov, S.A., Nistratov, V.M., and Smirnov, P. V, 2005. Geotechnical technology based on electrochemical explosion and equipment for its implementation. *Soil mechanics and foundation engineering*, 42 (5), 172–177.

Dzhantimirov, K., Kryuchkov, S. & Smirnov, P., 2003. Reconstruction of historical city and geotechnical construction, *Proceedings of international conference for Geotechnics part 2.* Saint Peterburg, s.n.

Dzhantimirov, K.A., Rytov, S.A., and Kryuchkov, S.A., 2010. Application of High-Power Electrical Sparks for Dynamic Compaction of Soil.

Evdokimov, V., Egorov, A. & Borisenkov, V., 1991. Grouted piles installed with application of electric impulse technology. *Design and engineering surveys*, pp. 17-19.

Fleming, W.G.K., 1992. A new method for single pile settlement prediction and analysis. *Geotechnique*, 42 (3), 411–425.

Frungel, F., 1948. * ZUM MECHANISCHEN WIRKUNGSGRAD VON FLUSSIGKEITSFUNKEN. *Optik*, 3 (1–2), 124–127.

Gavrilov, G., Egorov, A. & Korovin, S., 1991. *Electrohydraulic impulse technology in mining and construction [in Russian]*. Moscow: Nedra.

Gilman, Y., 1963. *Stabilizing of water saturated soils with the help of electric discharges [in Russian] dissertation of a Doctor tech,* Moscow: MISI.

Gilman, Y. & Lomize, G., 1962. *Electrospark method of soils compaction.* s.l.:Gidrotechnicheskoe Stroitelstvo, 5.

Golovchenko, V., 1977. *Research of comprehensive reinforcement of exploded foundation cavities [in Russian], dissertation of a Doctor tech.,* Moscow: s.n.

Jaky, J., 1948. On the bearing capacity of piles. *In*: *Proceedings of 2nd International Conference in Soil Mechanics and Foundation Engineering. Éditions AA Balkema, Rotterdam*. 100–103.

Kim, T.-H. and Cha, K.-S., 2008. A study on characteristics of an in-situ pile using pulse discharge technology I: Expansion characteristics of ground. *KSCE Journal of Civil Engineering*, 12 (5), 289–295.

Khlyupina, L., 1967. *Physical processes in sandy water saturated soils by high voltage* discharges *[in Russian] dissertation of a Doctor tech,* Moscow: MISI.

L. D. S., 2009. *Guidance notes for the design of straight shafted bored piles in London Clay*. No. 1 ed. London: LDSA Publications Bromley.

Lawrence, L.G., 1969. Electrohydraulic effect. *Electronics World, NY*, 81 (5), 44.

Lee, S.-R., Park, H., Kim, T.-H., and Cha, K.-S., 2011. Numerical Analysis of Uplift Behavior of Ground Anchor Underreamed by Pulse Discharge Technology. *In*: *The Twenty-first International Offshore and Polar Engineering Conference*. International Society of Offshore and Polar Engineers.

Lomize, G. & Khlyupina, L., 1965. Physical processes under electrospark sandy soil compaction [in Russian]. *Gidrotechnicheskoe stroitelstvo,* pp. 15-21.

Lomize, G., Meshcheryakov, A., Gilman, Y. & Fedorov, B., 1963. Compaction of sandy soils by electric discharger [in Russian]. *Gidrotekhnicheskoe stroitelstvo,* pp. 9-13.

Lyakhov, G.M., 1964. Principles of Explosion Dynamics in Soils and in Liquid Media. *Nedra, Moscow*, 61–66.

Lyakhov, G.M., 1982. Waves in soils and porous multicomponent media.

Mayne, P.W. and Kulhawy, F.H., 1982. Ko- OCR Relationships in Soil. *Journal of the Soil Mechanics and Foundations Division*, 108 (6), 851–872.

Naugolnykh, K.A. and Roii, N.A., 1974. *Electrical discharges in water. A hydrodynamic description*. FOREIGN TECHNOLOGY DIV WRIGHT-PATTERSONAFB OH.

NIIOSP, G., 2001. *Recommendations on application of bored piles.* Moscow: s.n.

Park, H., Lee, S.-R., Kim, T.-H., and Kim, N.-K., 2011. Numerical modeling of ground borehole expansion induced by application of pulse discharge technology. *Computers and Geotechnics*, 38 (4), 532–545.

Peck, R.B., Hanson, W.E., and Thornburn, T.H., 1974. *Foundation engineering*. Wiley New York.

Plaxis-Material, B. V, 2017. Plaxis material models manual. *Rotterdam: AA Balkema, 226p*.

Plaxis-Advanced, 2017. *Course on Computational Geotechnics.* Schiphol: s.n.

Plaxis-Standard, 2017. *Course on Computational Geotechnics.* Schiphol: s.n.

Poulos, H.G., 1989. Pile behaviour—theory and application. *Geotechnique*, 39 (3), 365–415.

Randolph, M.F., 1981. The response of flexible piles to lateral loading. *Geotechnique*, 31 (2), 247–259.

Randolph, M.F. and Wroth, C.P., 1978. Analysis of deformation of vertically loaded piles. *Journal of Geotechnical and Geoenvironmental Engineering*, 104 (ASCE 14262).

Randolph, M.F. and Wroth, C.P., 1982. *Recent developments in understanding the axial capacity of piles in clay*. University of Oxford Department of Engineering Science.

Rytov, S., 2009. Installation of boring piles using pulse discharge technology in different soil environments [in Russian] *dissertation of a Doctor tech.* , Moscow: NIIOSP.

Samarin, D., 2005. Improving of method of pile installation in partially saturated soils using pulse discharges [in Russian], *dissertation of a Doctor tech.*, Tomsk: s.n.

Semkin, B. V, Usov, A.F., and Kurets, V.I., 1995. Fundamentals of Electroimpulsive Fracture of Materials.

Semushkina, L., 1968. Experimental justification of the main technological process parameter during impulse achieved stabilization of water saturated soils by construction [in Russian], *dissertation of a Doctor tech.*, Moscow: MISI.

Shelyapin, R., Golovchenko, V. & Matveev, V., 1976. Spherical compaction of soil by underwater explosion treatment [in Russian]. *Issues of soil mechanics and geotechnical engineering, MISI*, pp. 64-80.

Terzaghi, K., 1942. Pile Driving Formulas. *In*: *Proceedings of ASCE*.

Tomlinson, M. and Woodward, J., 2014. *Pile design and construction practice*. CRC Press.

Tong, X., and Tuan, C.Y., 2007. Viscoplastic cap model for soils under high strain rate loading. *J. Geotech. Geoenviron. Eng.*, 133(2) 206-214

Ulitskii, V.M. and Shashkin, A.G., 1999. Geotechnical Accompaniment of Urban Reconstruction. *Assotsiatsiya Spetsial'nykh Bibliotek, Moscow*.

Yassievich, G.N., 1977. Research of bored piles installation method via electrohydraulic effect and its' work under vertical load [in Russian] *dissertation of a Doctor tech.. Leningrad, LISI [Leningrad Institute of Civil Engineering]*.

Yuschube, S., 1988. About interaction between single pile and soil environment. *Tomsk University*, p. 233.

Yutkin, L.A., 1986. Electro-hydraulic effect and its application in industry. *Leningrad: Engineering*.

Chapter 9
Appendices

9.1 Load-settlement curves: pile performance by Fleming's method compared to computed prediction in Plaxis 2D

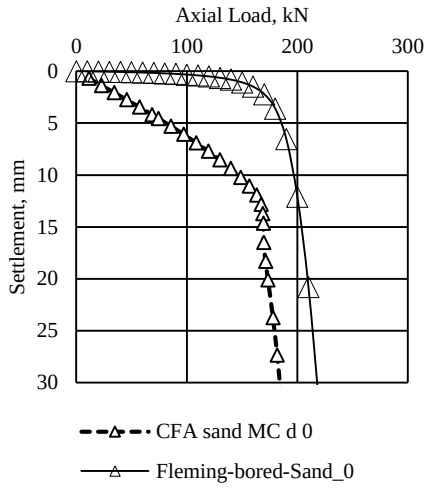

(a)

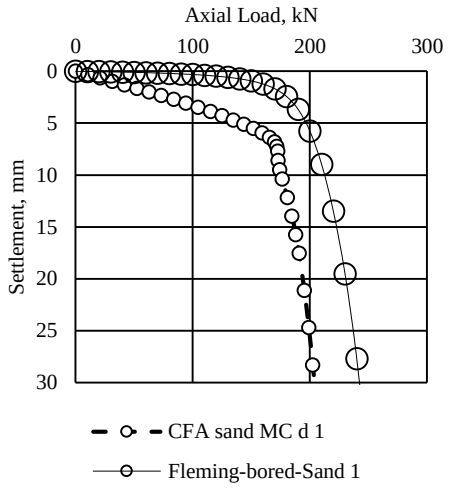

(b)

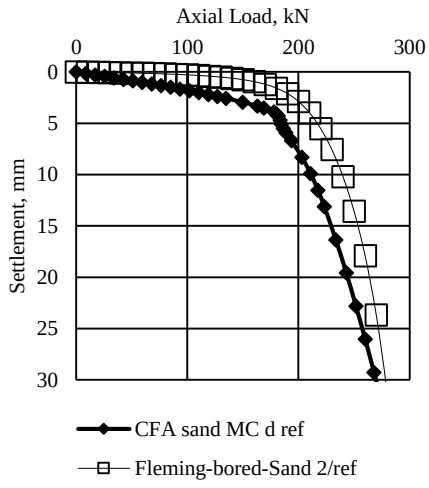

(c)

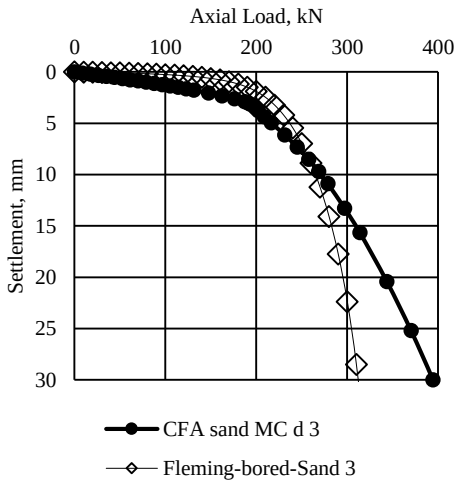

(d)

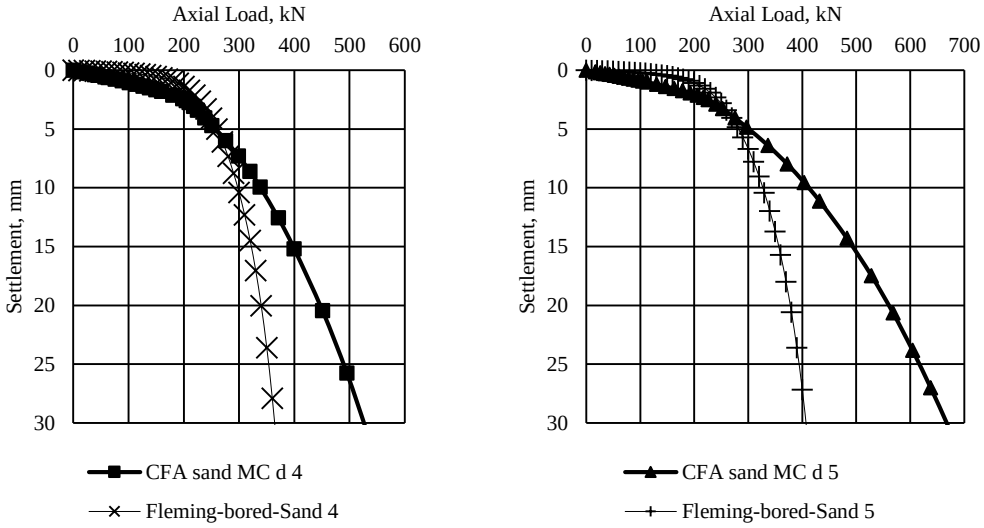

(e) **(f)**

Figure 9-1 – Load settlement curves: pile performance in coarse grained soils by Fleming method (*Ms*=0.001) and calculated in Plaxis: (a) soil case 0, (b) soil case 1, (c) soil case 2/ref, (d) soil case 3, (e) soil case 4, (f) soil case 5

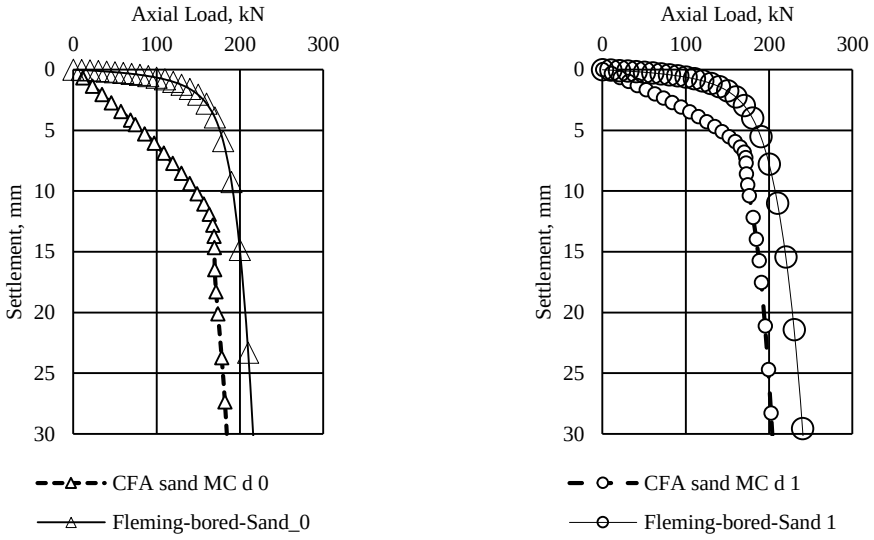

(a) **(b)**

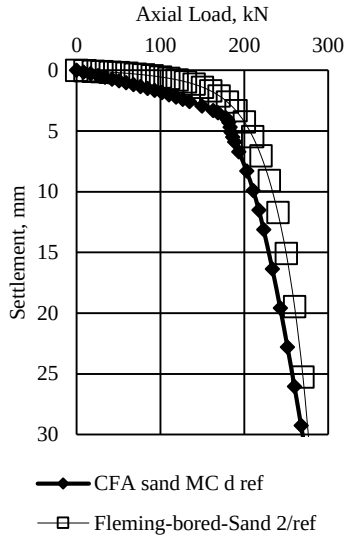

(c)

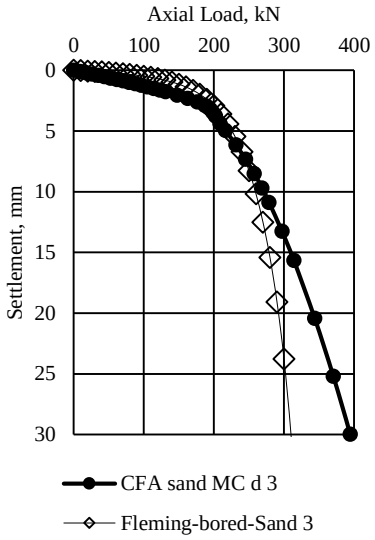

(d)

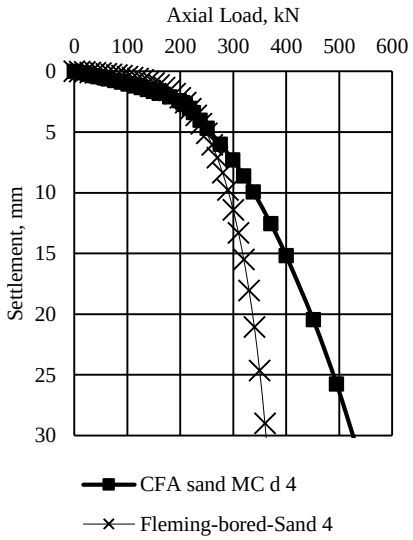

(e)

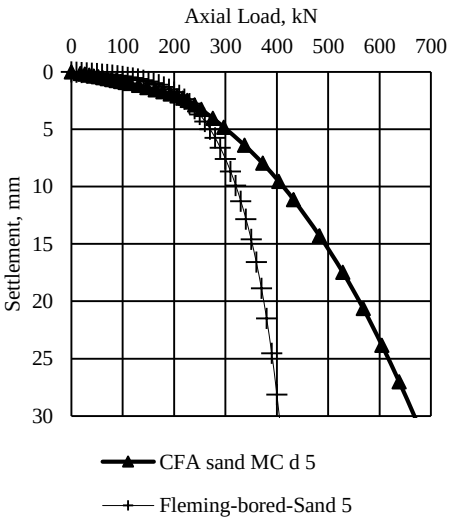

(f)

Figure 9-2 – Load settlement curves: pile performance in coarse grained soils by Fleming method (*Ms*=0.002) and calculated in Plaxis: (a) soil case 0, (b) soil case 1, (c) soil case 2/ref, (d) soil case 3, (e) soil case 4, (f) soil case 5

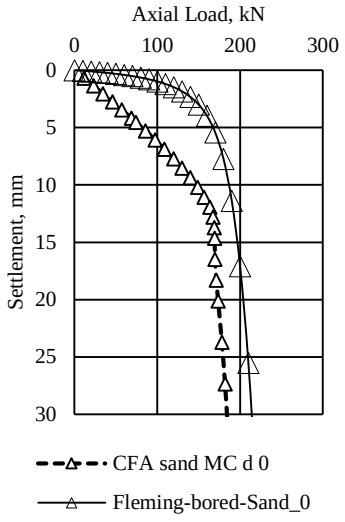
Axial Load, kN
0
100
200
300
Settlement, mm
0
5
10
15
20
25
30
CFA sand MC d 0
Fleming-bored-Sand_0

(a)

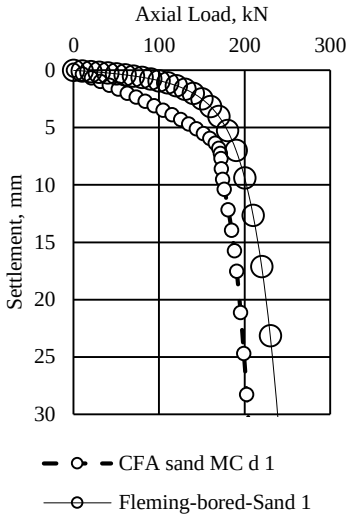
Axial Load, kN
0
100
200
300
Settlement, mm
0
5
10
15
20
25
30
CFA sand MC d 1
Fleming-bored-Sand 1

(b)

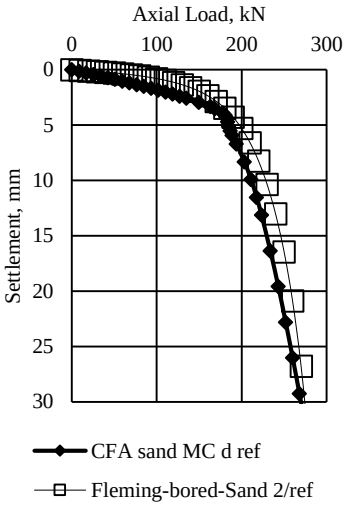
Axial Load, kN
0
100
200
300
Settlement, mm
0
5
10
15
20
25
30
CFA sand MC d ref
Fleming-bored-Sand 2/ref

(c)

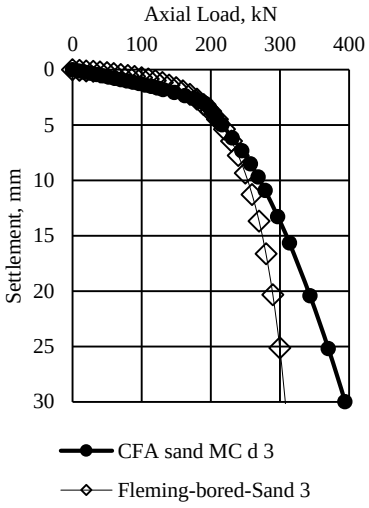
Axial Load, kN
0
100
200
300
400
Settlement, mm
0
5
10
15
20
25
30
CFA sand MC d 3
Fleming-bored-Sand 3

(d)

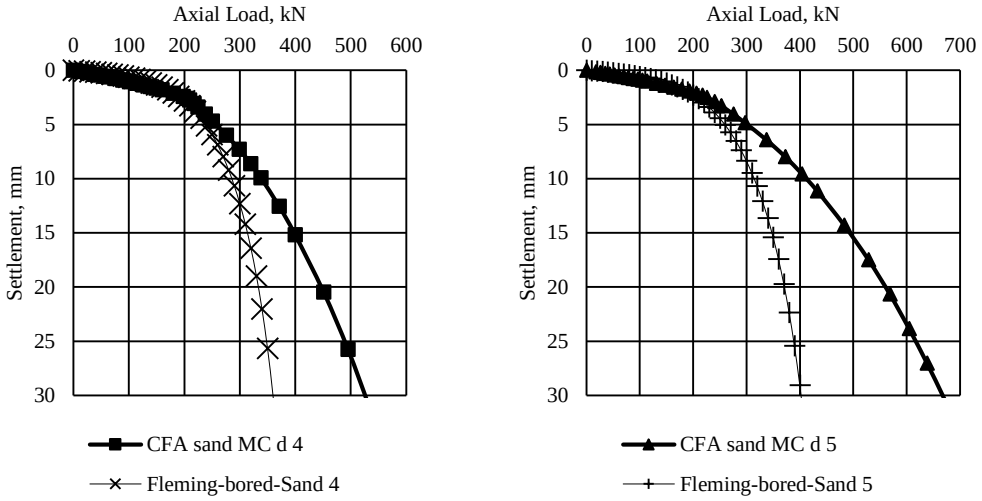

(e) **(f)**

Figure 9-3 – Load settlement curves: pile performance in coarse grained soils by Fleming method (*Ms*=0.003) and calculated in Plaxis: (a) soil case 0, (b) soil case 1, (c) soil case 2/ref, (d) soil case 3, (e) soil case 4, (f) soil case 5

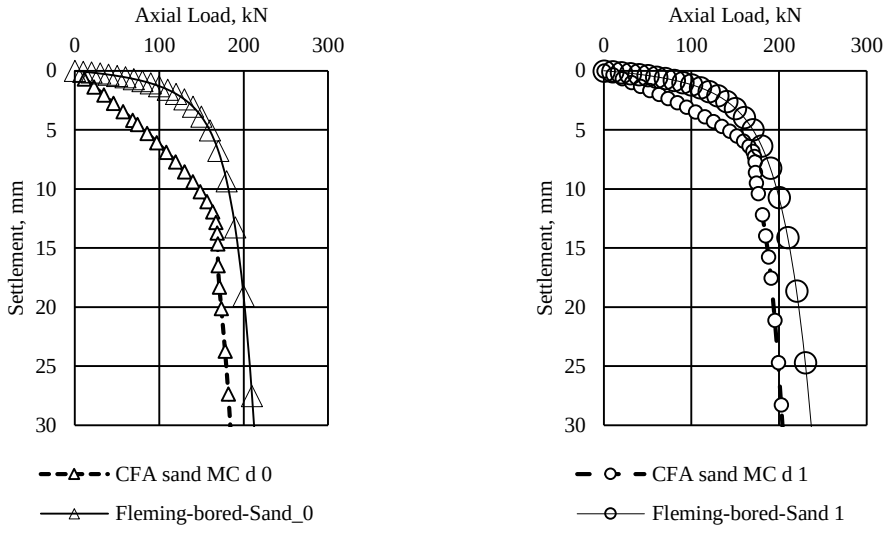

(a) **(b)**

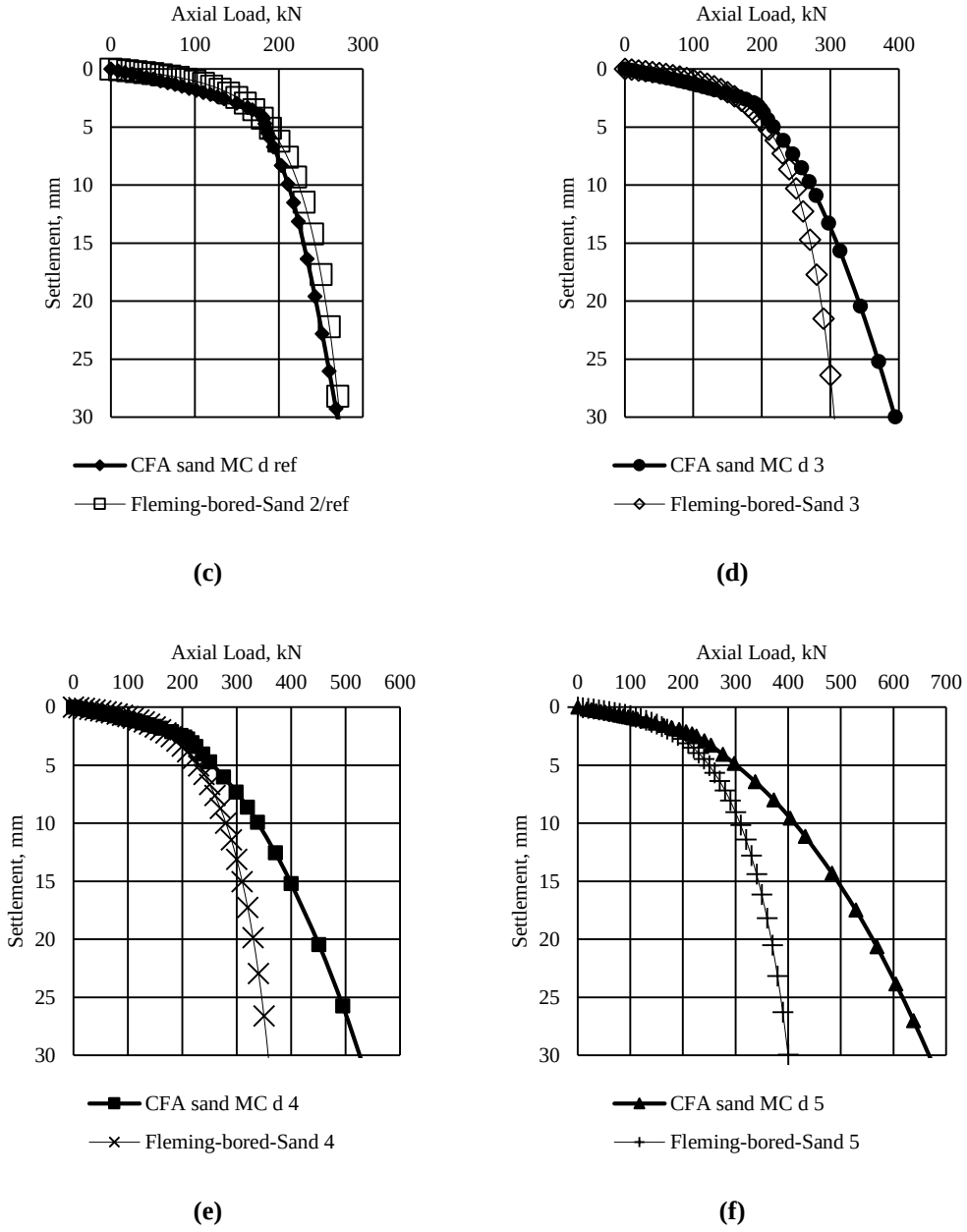

Figure 9-4 – Load settlement curves: pile performance in coarse grained soils by Fleming method (*Ms*=0.004) and calculated in Plaxis: (a) soil case 0, (b) soil case 1, (c) soil case 2/ref, (d) soil case 3, (e) soil case 4, (f) soil case 5

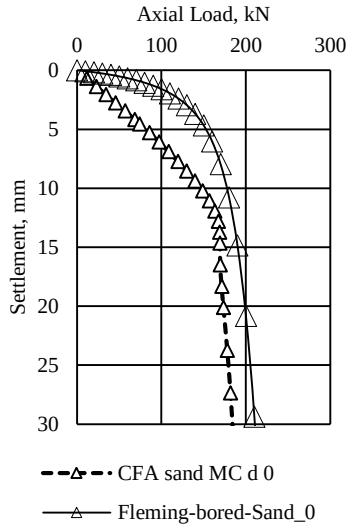
Axial Load, kN
0
100
200
300
Settlement, mm
0
5
10
15
20
25
30
CFA sand MC d 0
Fleming-bored-Sand_0

(a)

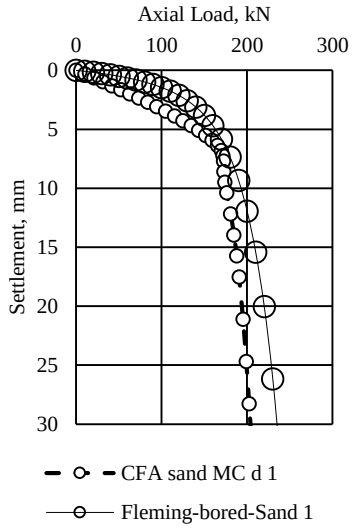
Axial Load, kN
0
100
200
300
Settlement, mm
0
5
10
15
20
25
30
CFA sand MC d 1
Fleming-bored-Sand 1

(b)

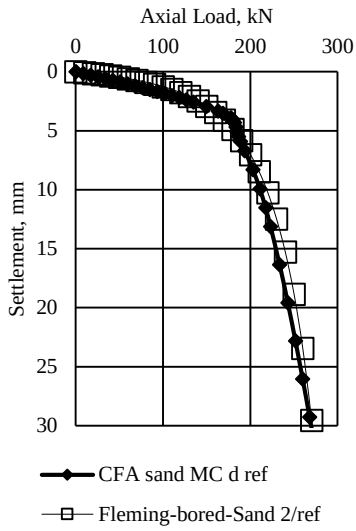
Axial Load, kN
0
100
200
300
Settlement, mm
0
5
10
15
20
25
30
CFA sand MC d ref
Fleming-bored-Sand 2/ref

(c)

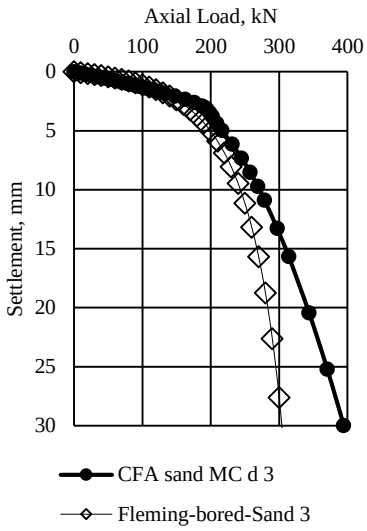
Axial Load, kN
0
100
200
300
400
Settlement, mm
0
5
10
15
20
25
30
CFA sand MC d 3
Fleming-bored-Sand 3

(d)

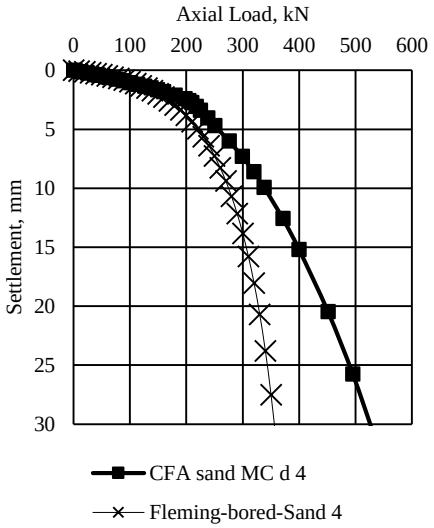

(e)

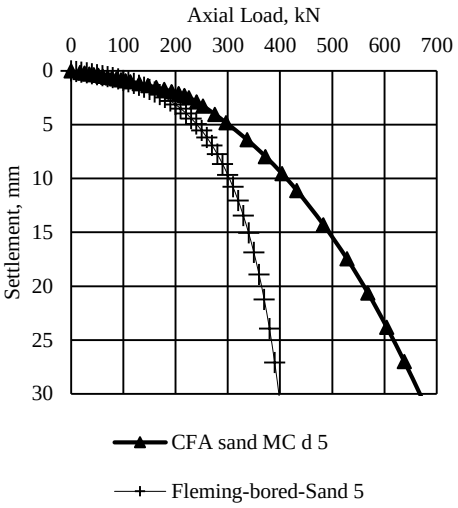

(f)

Figure 9-5 – Load settlement curves: pile performance in coarse grained soils by Fleming method (*Ms*=0.005) and calculated in Plaxis: (a) soil case 0, (b) soil case 1, (c) soil case 2/ref, (d) soil case 3, (e) soil case 4, (f) soil case 5

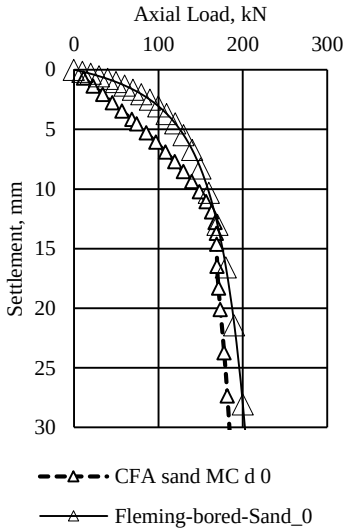

(a)

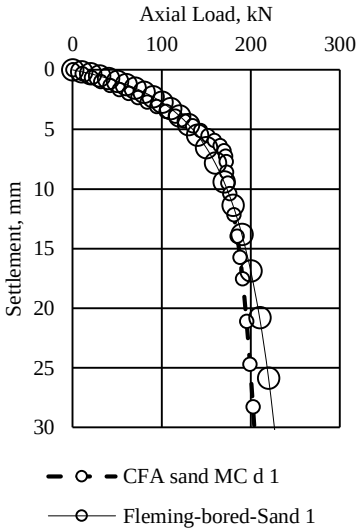

(b)

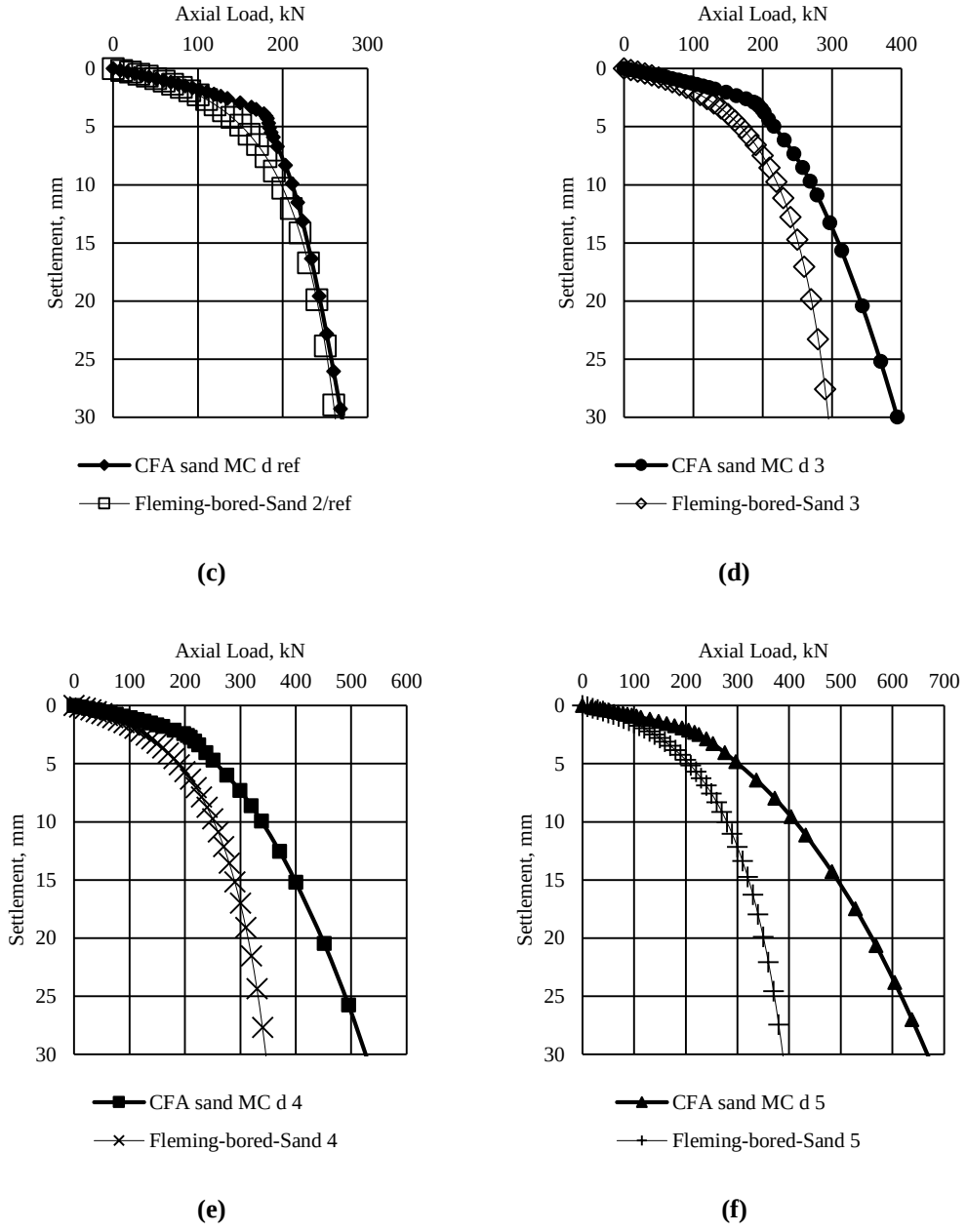

Figure 9-6 – Load settlement curves: pile performance in coarse grained soils by Fleming method (*Ms*=0.01) and calculated in Plaxis: (a) soil case 0, (b) soil case 1, (c) soil case 2/ref, (d) soil case 3, (e) soil case 4, (f) soil case 5

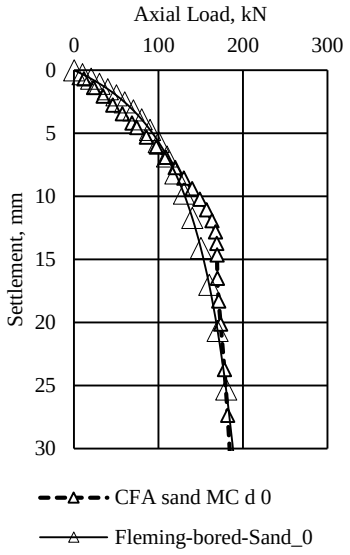
Axial Load, kN
0
100
200
300
Settlement, mm
0
5
10
15
20
25
30
CFA sand MC d 0
Fleming-bored-Sand_0

(a)

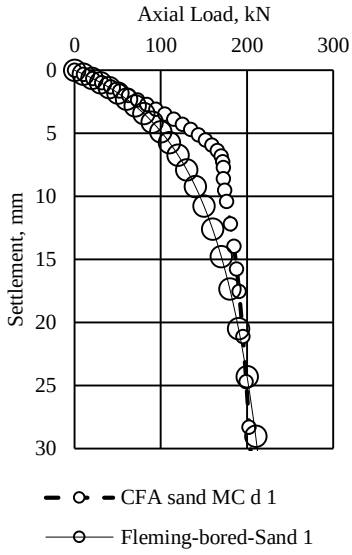
Axial Load, kN
0
100
200
300
Settlement, mm
0
5
10
15
20
25
30
CFA sand MC d 1
Fleming-bored-Sand 1

(b)

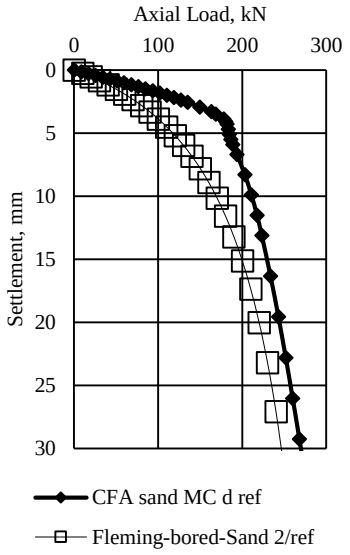
Axial Load, kN
0
100
200
300
Settlement, mm
0
5
10
15
20
25
30
CFA sand MC d ref
Fleming-bored-Sand 2/ref

(c)

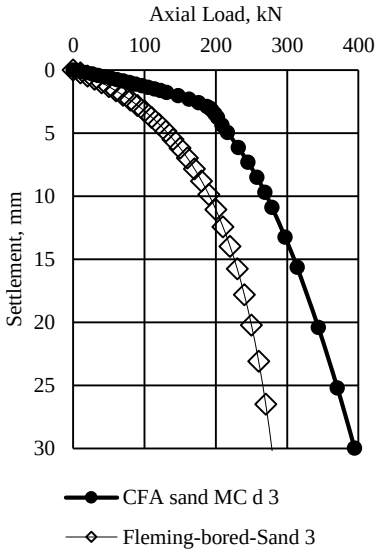
Axial Load, kN
0
100
200
300
400
Settlement, mm
0
5
10
15
20
25
30
CFA sand MC d 3
Fleming-bored-Sand 3

(d)

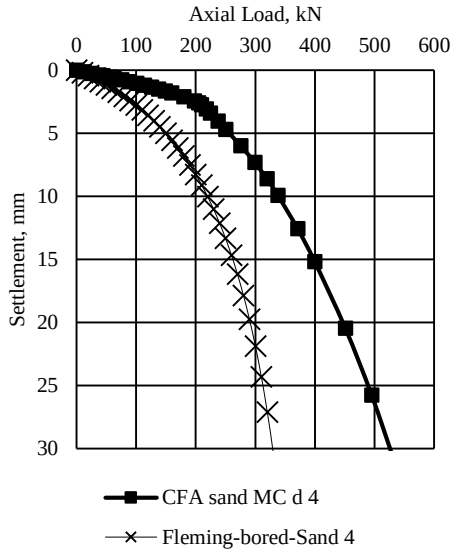

(e)

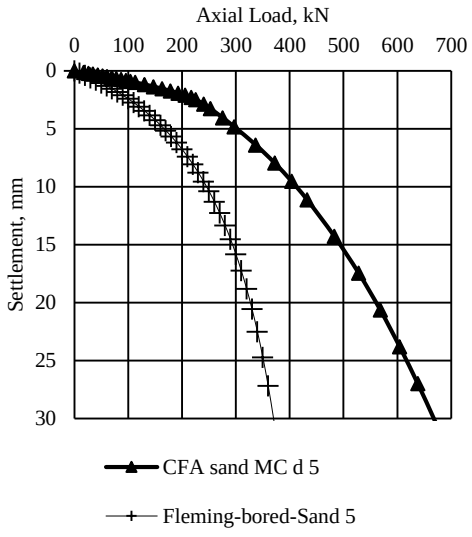

(f)

Figure 9-7 – Load settlement curves: pile performance in coarse grained soils by Fleming method (*Ms*=0.02) and calculated in Plaxis: (a) soil case 0, (b) soil case 1, (c) soil case 2/ref, (d) soil case 3, (e) soil case 4, (f) soil case 5

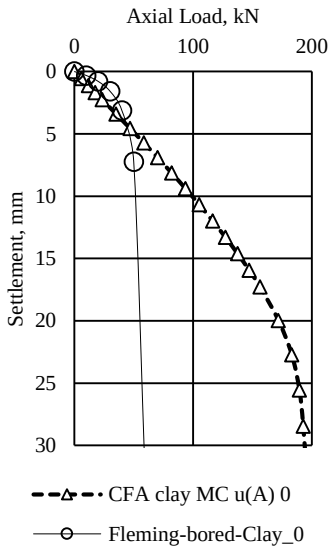

(a)

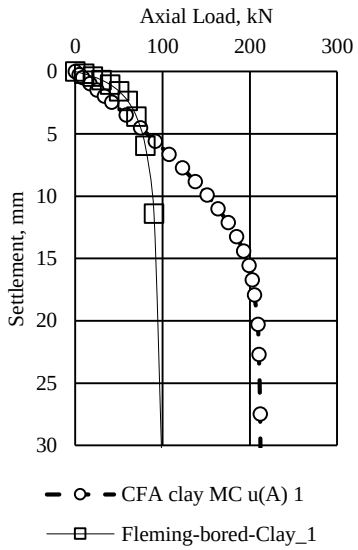

(b)

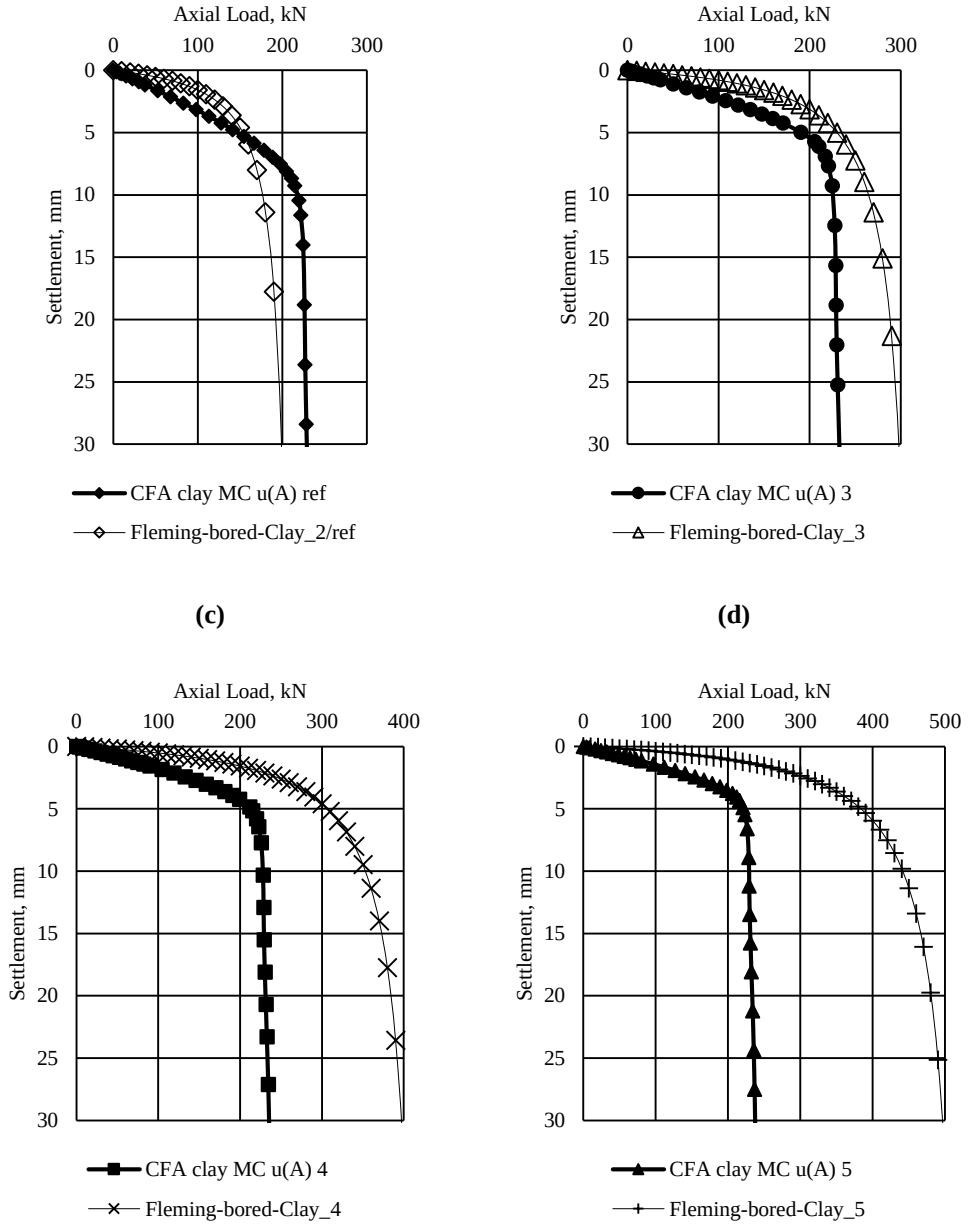

Figure 9-8 – Load settlement curves: pile performance in fine grained soils by Fleming method (*Ms*=0.005) and calculated in Plaxis: (a) soil case 0, (b) soil case 1, (c) soil case 2/ref, (d) soil case 3, (e) soil case 4, (f) soil case 5

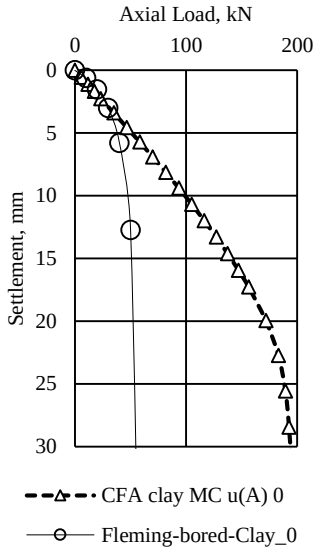
Axial Load, kN
0
100
200
Settlement, mm
0
5
10
15
20
25
30
CFA clay MC u(A) 0
Fleming-bored-Clay_0

(a)

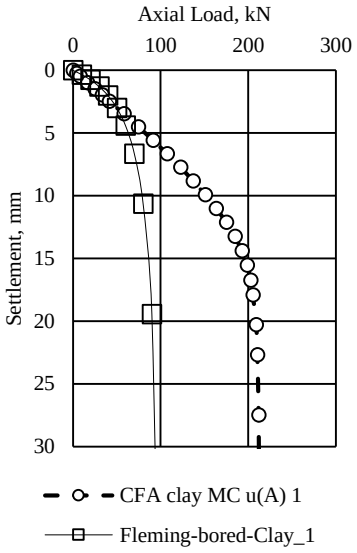
Axial Load, kN
0
100
200
300
Settlement, mm
0
5
10
15
20
25
30
CFA clay MC u(A) 1
Fleming-bored-Clay_1

(b)

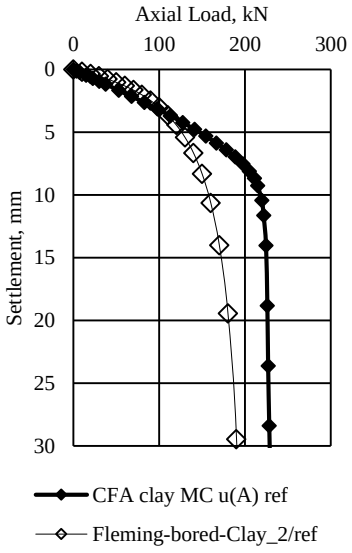
Axial Load, kN
0
100
200
300
Settlement, mm
0
5
10
15
20
25
30
CFA clay MC u(A) ref
Fleming-bored-Clay_2/ref

(c)

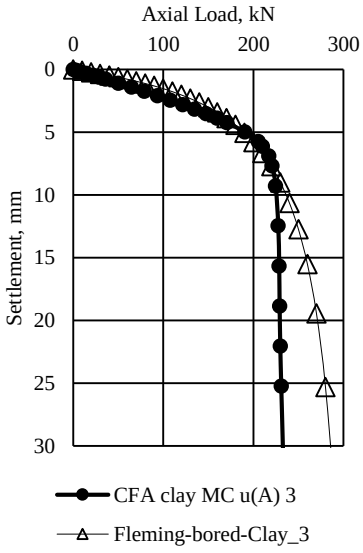
Axial Load, kN
0
100
200
300
Settlement, mm
0
5
10
15
20
25
30
CFA clay MC u(A) 3
Fleming-bored-Clay_3

(d)

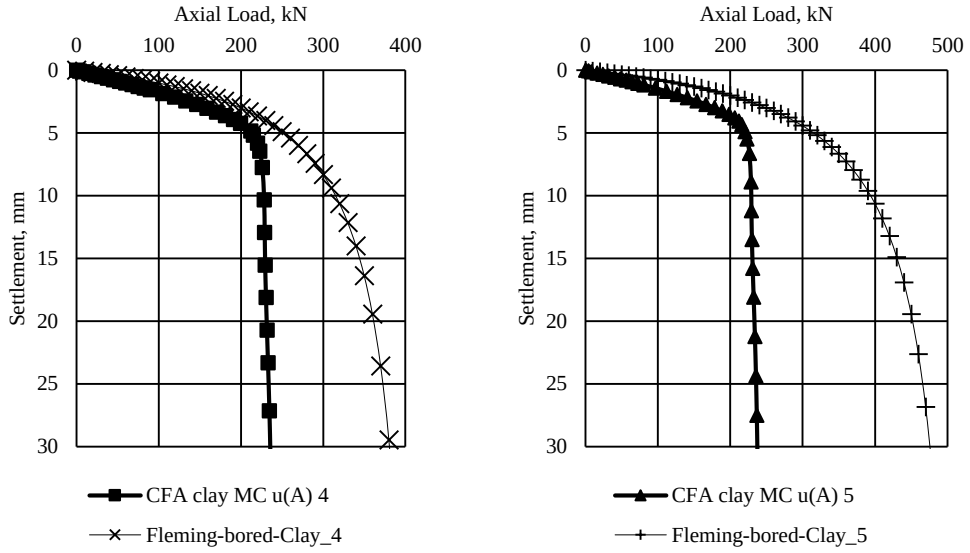

(e) **(f)**

Figure 9-9 – Load settlement curves: pile performance in fine grained soils by Fleming method (*Ms*=0.01) and calculated in Plaxis: (a) soil case 0, (b) soil case 1, (c) soil case 2/ref, (d) soil case 3, (e) soil case 4, (f) soil case 5

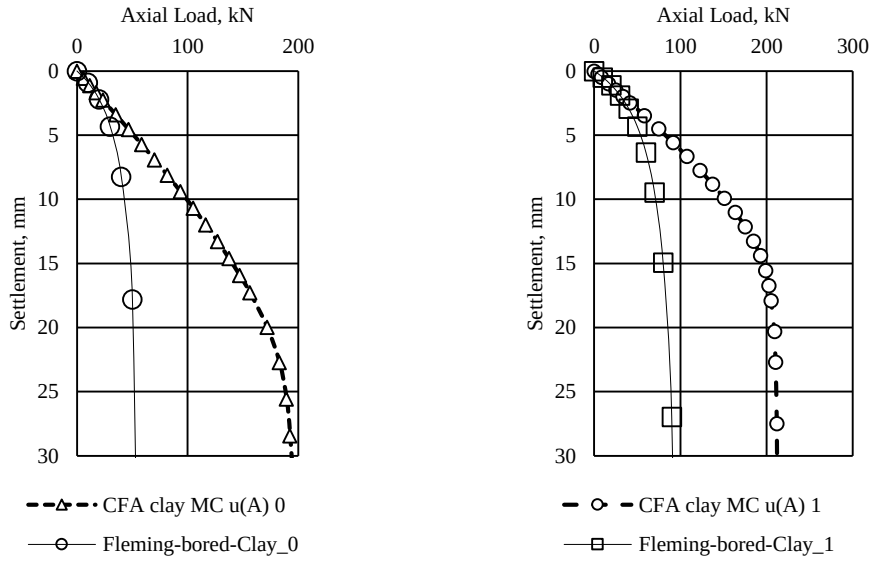

(a) **(b)**

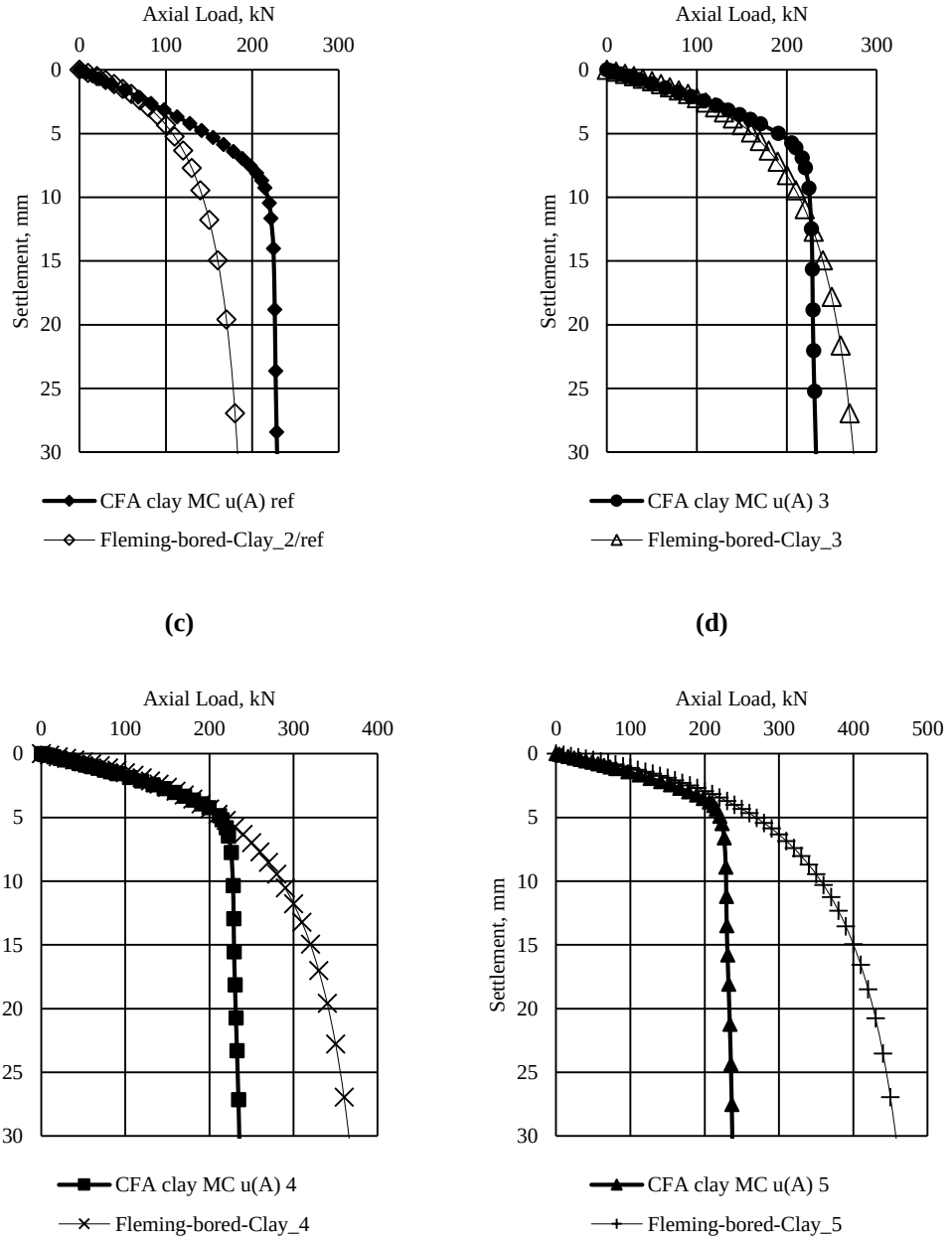

Figure 9-10 – Load settlement curves: pile performance in fine grained soils by Fleming method (*Ms*=0.015) and calculated in Plaxis: (a) soil case 0, (b) soil case 1, (c) soil case 2/ref, (d) soil case 3, (e) soil case 4, (f) soil case 5

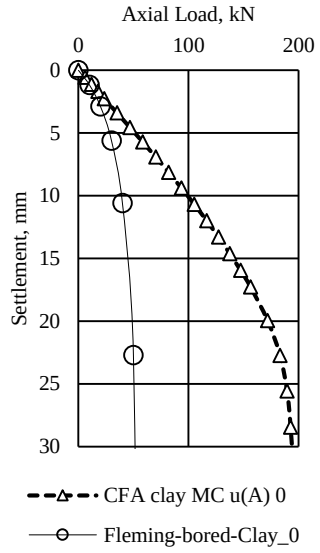
Axial Load, kN
0
100
200
Settlement, mm
0
5
10
15
20
25
30
CFA clay MC u(A) 0
Fleming-bored-Clay_0

(a)

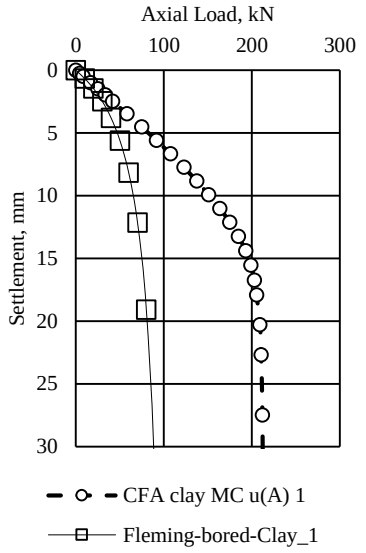
Axial Load, kN
0
100
200
300
Settlement, mm
0
5
10
15
20
25
30
CFA clay MC u(A) 1
Fleming-bored-Clay_1

(b)

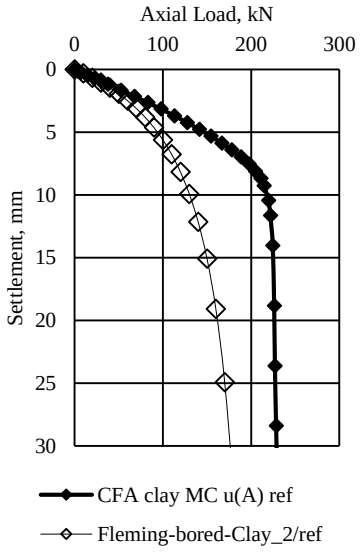
Axial Load, kN
0
100
200
300
Settlement, mm
0
5
10
15
20
25
30
CFA clay MC u(A) ref
Fleming-bored-Clay_2/ref

(c)

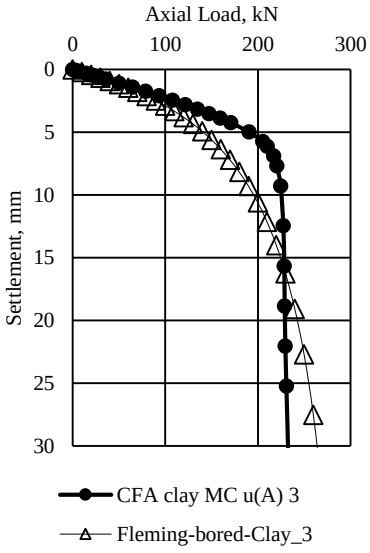
Axial Load, kN
0
100
200
300
Settlement, mm
0
5
10
15
20
25
30
CFA clay MC u(A) 3
Fleming-bored-Clay_3

(d)

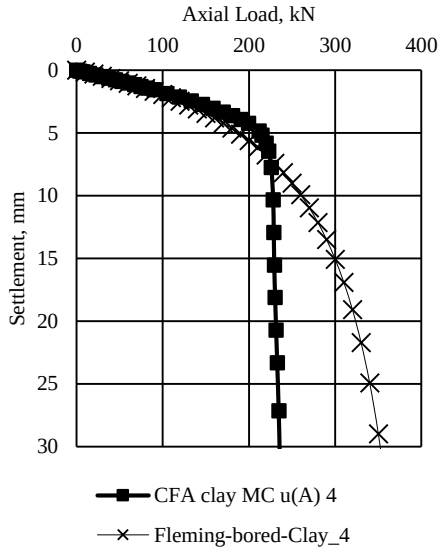

(e)

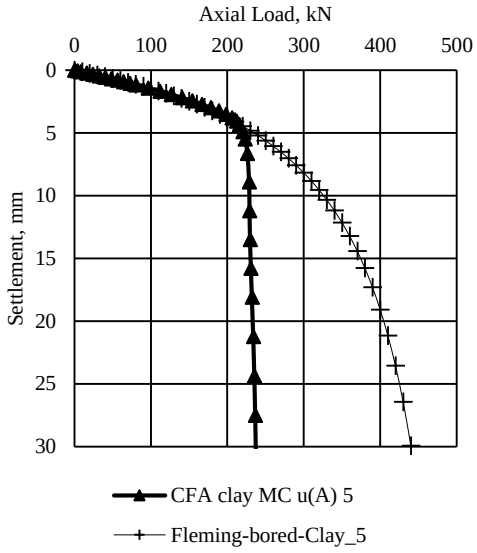

(f)

Figure 9-11 – Load settlement curves: pile performance in fine grained soils by Fleming's method (*Ms*=0.02) and calculated in Plaxis: (a) soil case 0, (b) soil case 1, (c) soil case 2/ref, (d) soil case 3, (e) soil case 4, (f) soil case 5

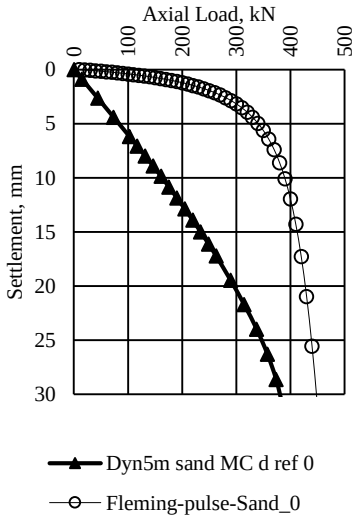

(a)

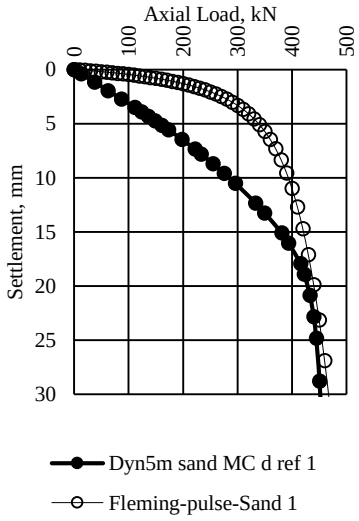

(b)

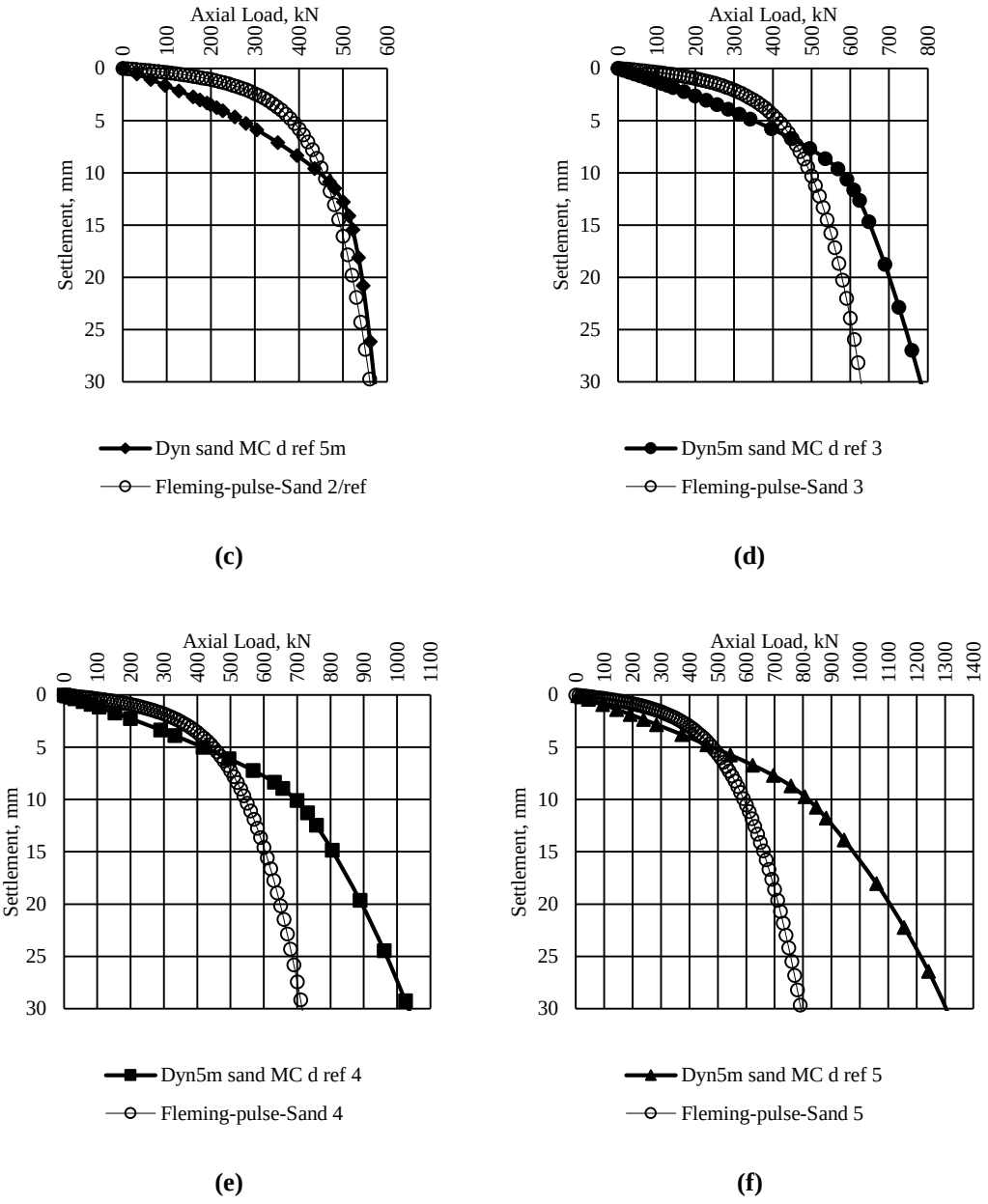

Figure 9-12 – Load settlement curves: Pulse pile performance in coarse grained soils by Fleming method (*Ms*=0.005) and calculated in Plaxis: (a) soil case 0, (b) soil case 1, (c) soil case 2/ref, (d) soil case 3, (e) soil case 4, (f) soil case 5

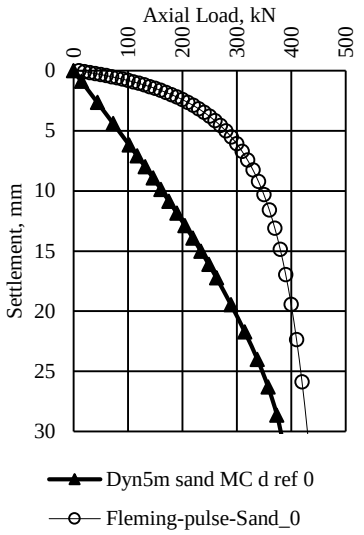
Axial Load, kN
0
100
200
300
400
500
Settlement, mm
0
5
10
15
20
25
30
Dyn5m sand MC d ref 0
Fleming-pulse-Sand_0

(a)

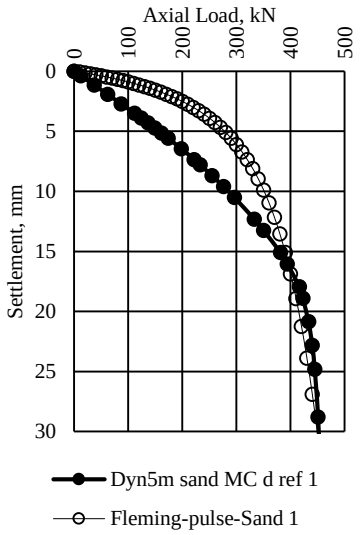
Axial Load, kN
0
100
200
300
400
500
Settlement, mm
0
5
10
15
20
25
30
Dyn5m sand MC d ref 1
Fleming-pulse-Sand 1

(b)

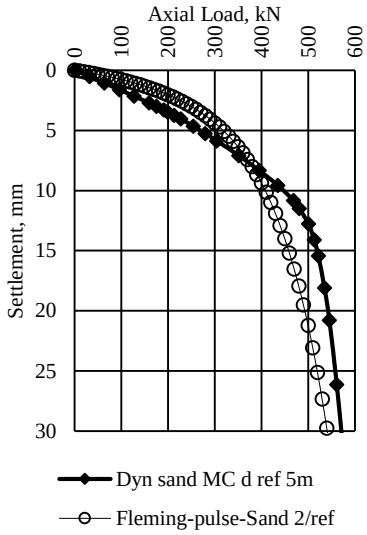
Axial Load, kN
0
100
200
300
400
500
600
Settlement, mm
0
5
10
15
20
25
30
Dyn sand MC d ref 5m
Fleming-pulse-Sand 2/ref

(c)

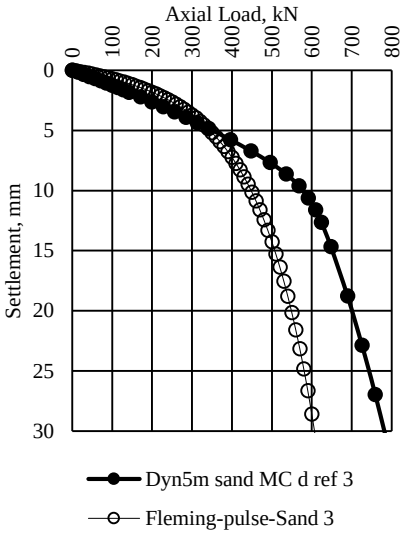
Axial Load, kN
0
100
200
300
400
500
600
700
800
Settlement, mm
0
5
10
15
20
25
30
Dyn5m sand MC d ref 3
Fleming-pulse-Sand 3

(d)

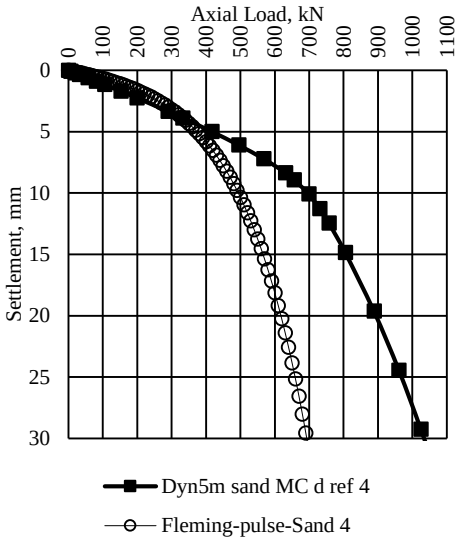

(e)

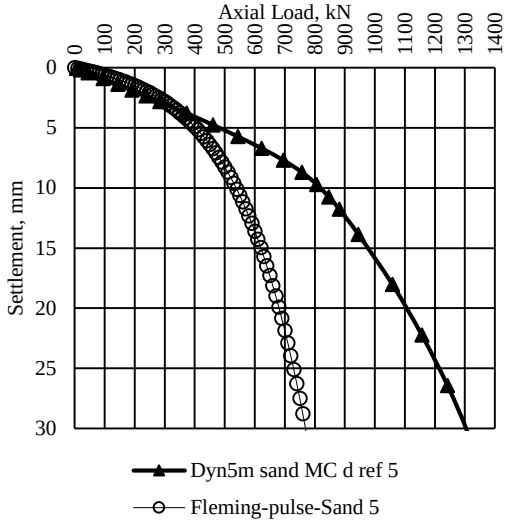

(f)

Figure 9-13 – Load settlement curves: Pulse pile performance in coarse grained soils by Fleming method (*Ms*=0.01) and calculated in Plaxis: (a) soil case 0, (b) soil case 1, (c) soil case 2/ref, (d) soil case 3, (e) soil case 4, (f) soil case 5

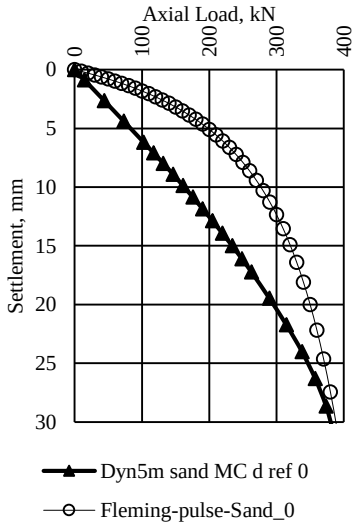

(a)

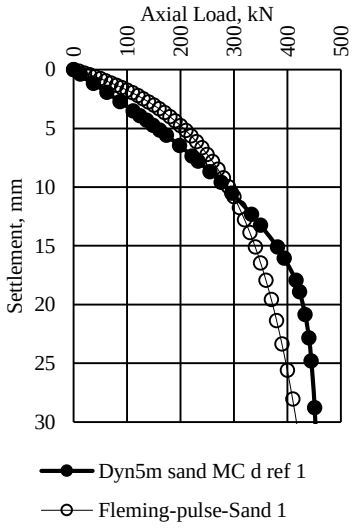

(b)

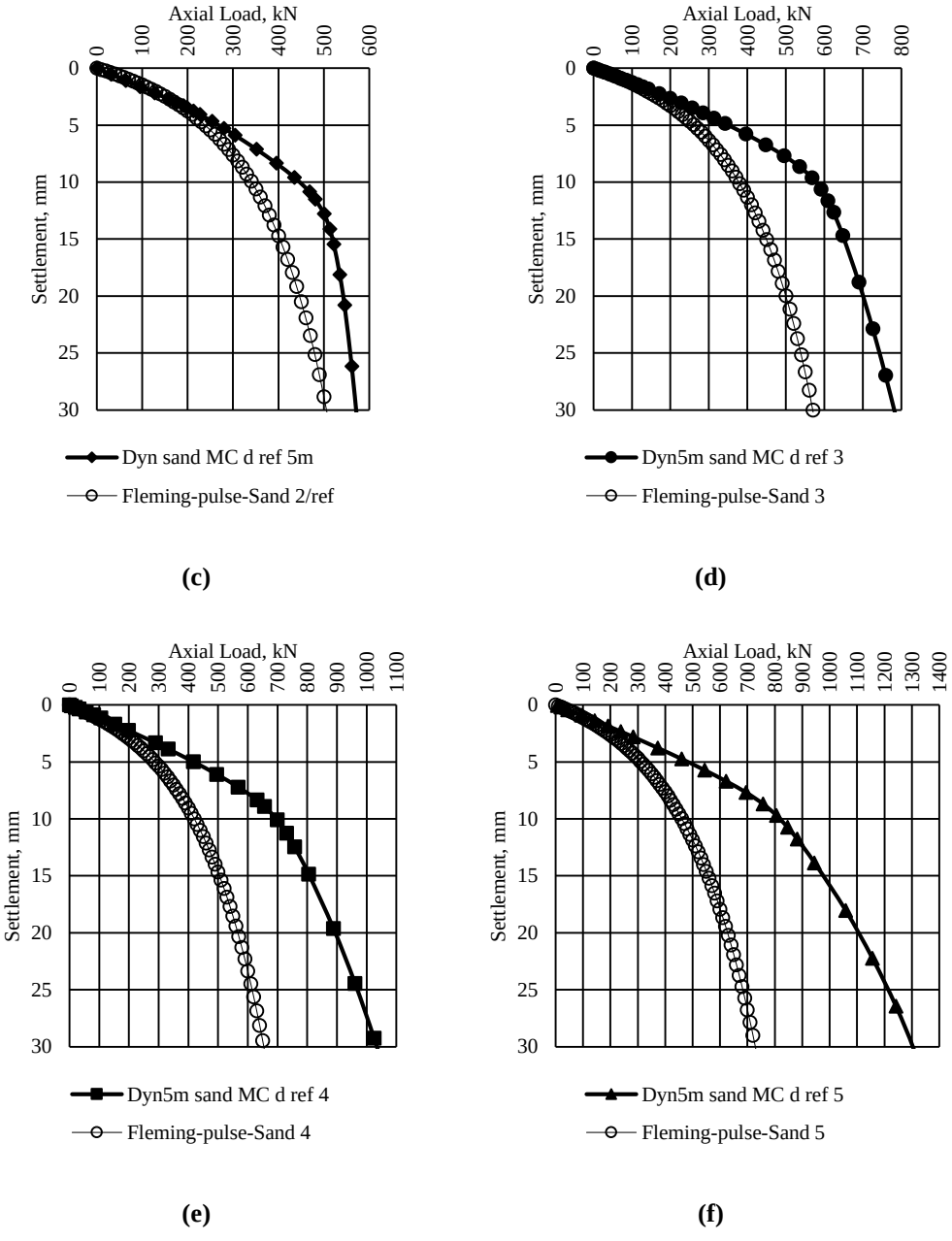

Figure 9-14 – Load settlement curves: Pulse pile performance in coarse grained soils by Fleming method (*Ms*=0.01) and calculated in Plaxis: (a) soil case 0, (b) soil case 1, (c) soil case 2/ref, (d) soil case 3, (e) soil case 4, (f) soil case 5

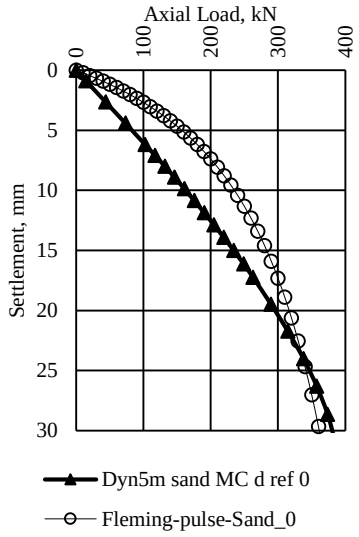
Axial Load, kN
0
100
200
300
400
Settlement, mm
0
5
10
15
20
25
30
Dyn5m sand MC d ref 0
Fleming-pulse-Sand_0

(a)

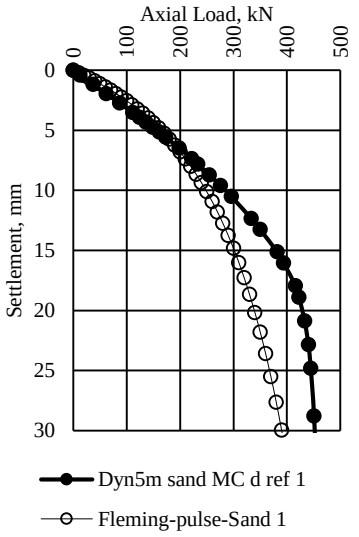
Axial Load, kN
0
100
200
300
400
500
Settlement, mm
0
5
10
15
20
25
30
Dyn5m sand MC d ref 1
Fleming-pulse-Sand 1

(b)

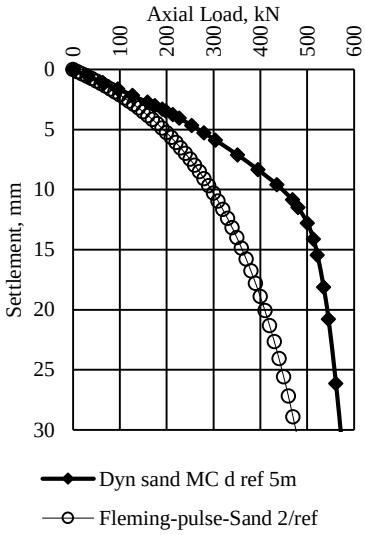
Axial Load, kN
0
100
200
300
400
500
600
Settlement, mm
0
5
10
15
20
25
30
Dyn sand MC d ref 5m
Fleming-pulse-Sand 2/ref

(c)

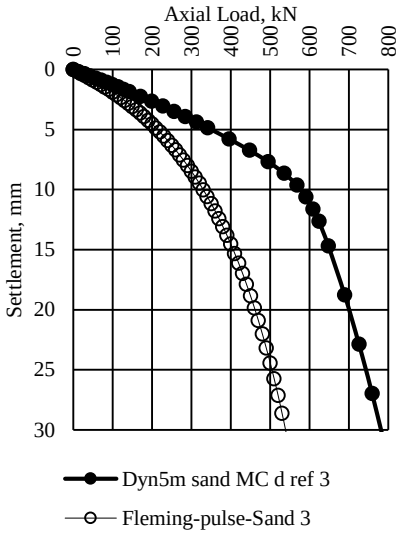
Axial Load, kN
0
100
200
300
400
500
600
700
800
Settlement, mm
0
5
10
15
20
25
30
Dyn5m sand MC d ref 3
Fleming-pulse-Sand 3

(d)

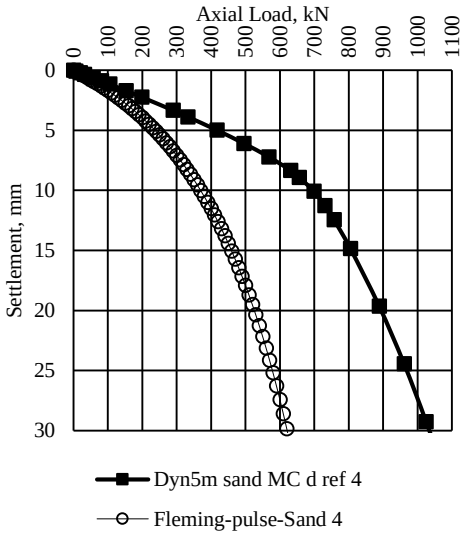

(e)

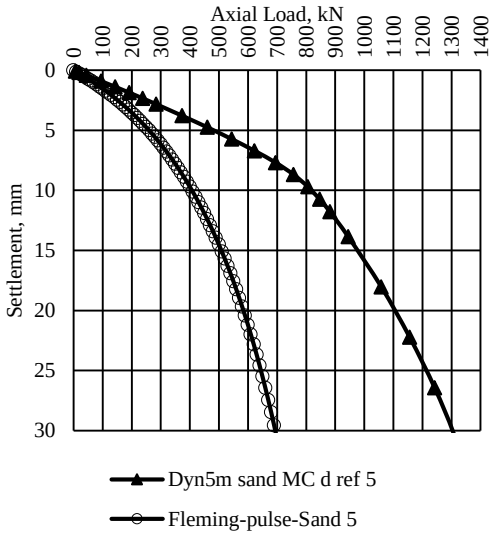

(f)

Figure 9-15 – Load settlement curves: Pulse pile performance in coarse grained soils by Fleming method (*Ms*=0.03) and calculated in Plaxis: (a) soil case 0, (b) soil case 1, (c) soil case 2/ref, (d) soil case 3, (e) soil case 4, (f) soil case 5

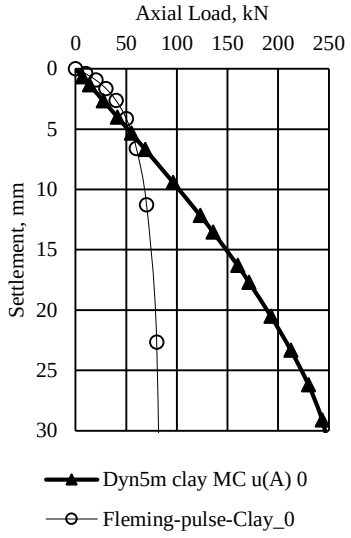

(a)

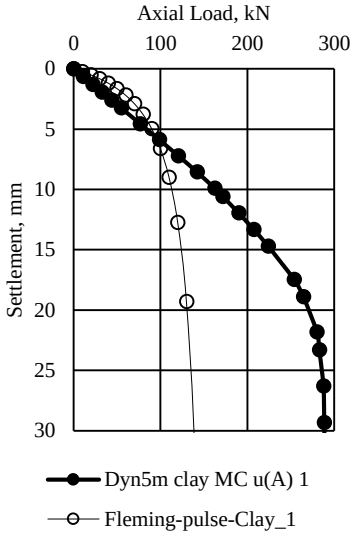

(b)

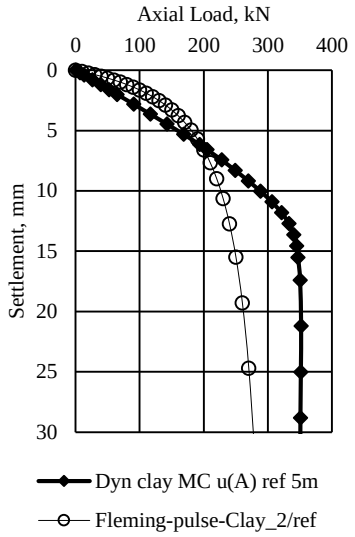

(c)

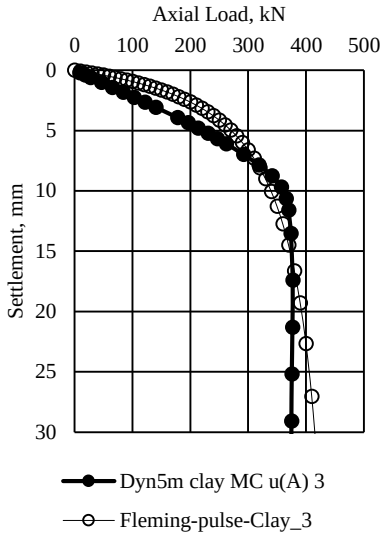

(d)

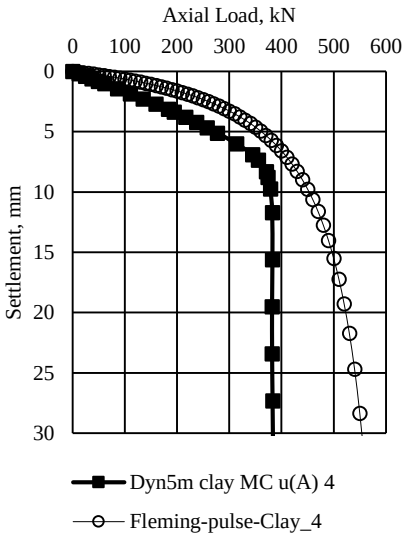

(e)

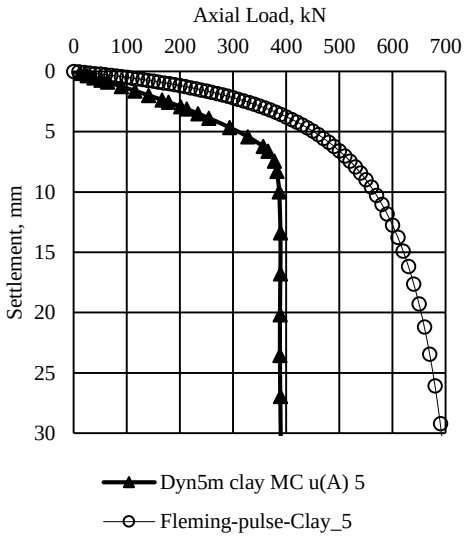

(f)

Figure 9-16 – Load settlement curves: Pulse pile performance in fine grained soils by Fleming method (*Ms*=0.01) and calculated in Plaxis: (a) soil case 0, (b) soil case 1, (c) soil case 2/ref, (d) soil case 3, (e) soil case 4, (f) soil case 5

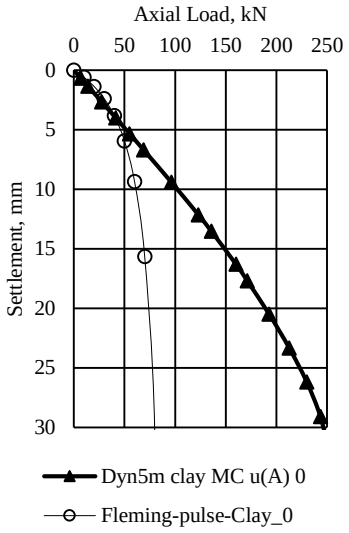
Axial Load, kN
0 50 100 150 200 250
Settlement, mm
0 5 10 15 20 25 30
Dyn5m clay MC u(A) 0
Fleming-pulse-Clay_0

(a)

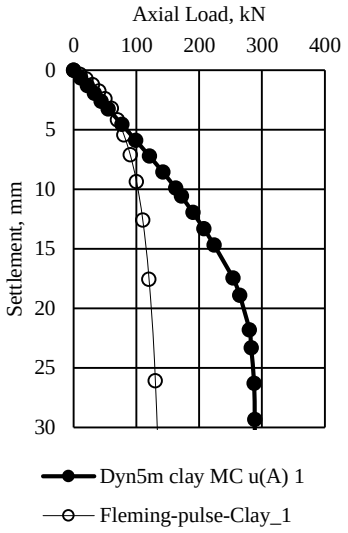
Axial Load, kN
0 100 200 300 400
Settlement, mm
0 5 10 15 20 25 30
Dyn5m clay MC u(A) 1
Fleming-pulse-Clay_1

(b)

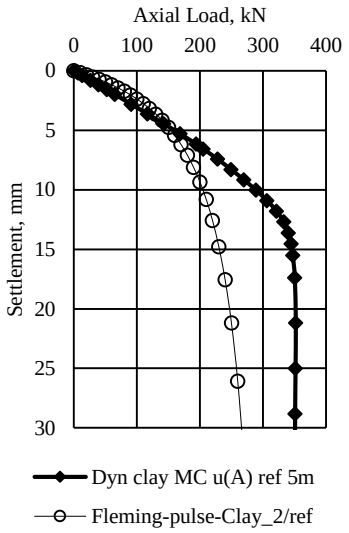
Axial Load, kN
0 100 200 300 400
Settlement, mm
0 5 10 15 20 25 30
Dyn clay MC u(A) ref 5m
Fleming-pulse-Clay_2/ref

(c)

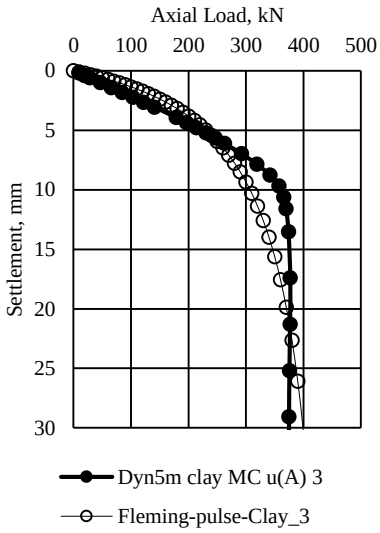
Axial Load, kN
0 100 200 300 400 500
Settlement, mm
0 5 10 15 20 25 30
Dyn5m clay MC u(A) 3
Fleming-pulse-Clay_3

(d)

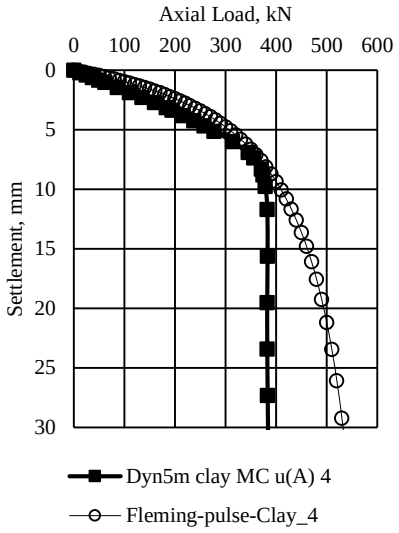

(e)

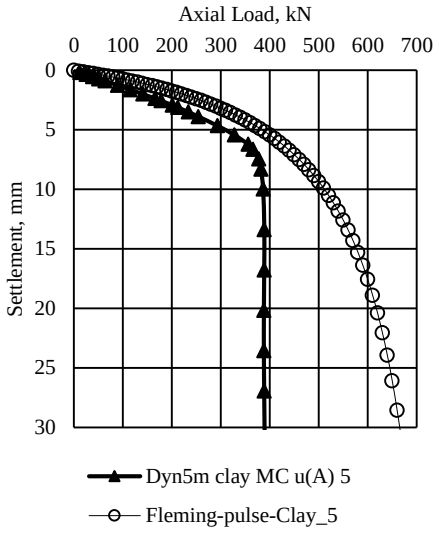

(f)

Figure 9-17 – Load settlement curves: Pulse pile performance in fine grained soils by Fleming method (*Ms*=0.015) and calculated in Plaxis: (a) soil case 0, (b) soil case 1, (c) soil case 2/ref, (d) soil case 3, (e) soil case 4, (f) soil case 5

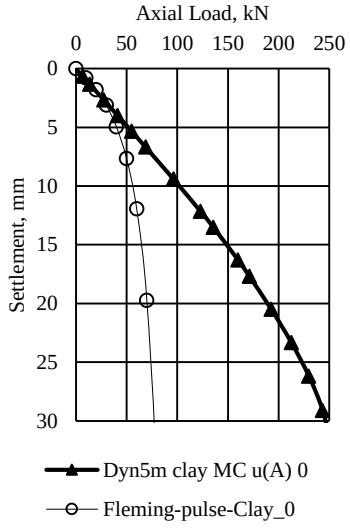

(a)

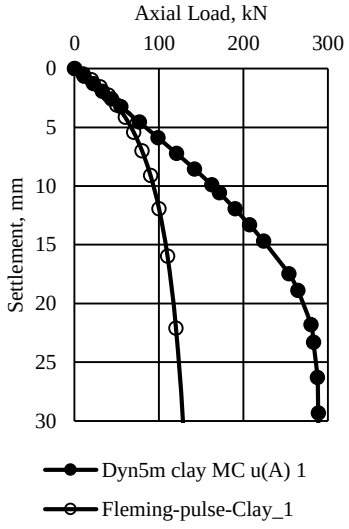

(b)

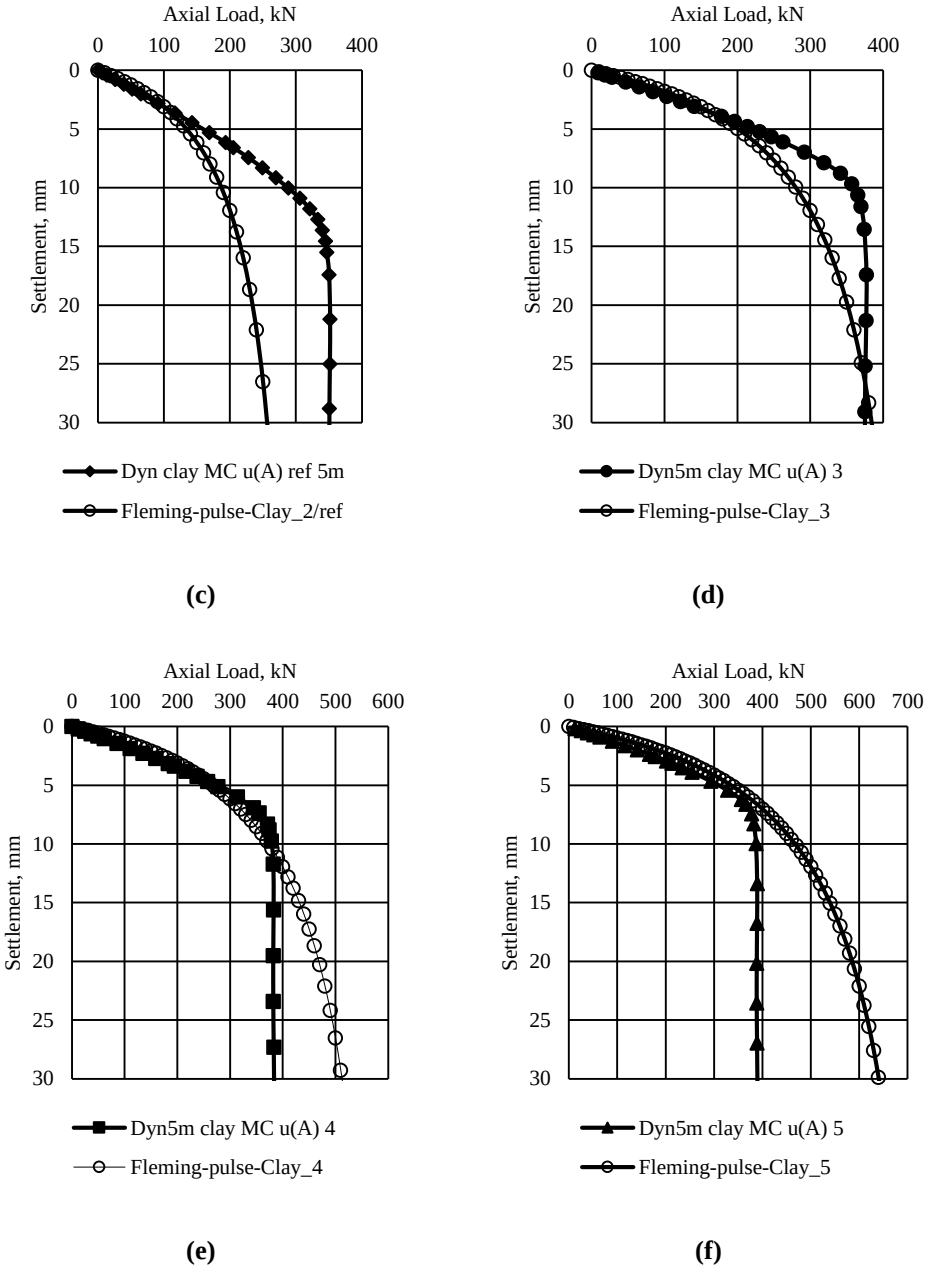

Figure 9-18 – Load settlement curves: Pulse pile performance in fine grained soils by Fleming method (*Ms*=0.02) and calculated in Plaxis: (a) soil case 0, (b) soil case 1, (c) soil case 2/ref, (d) soil case 3, (e) soil case 4, (f) soil case 5

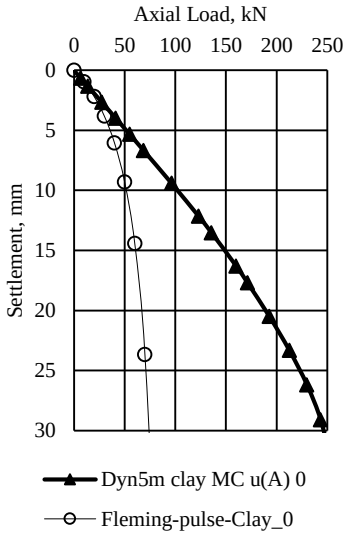
Axial Load, kN
0 50 100 150 200 250
Settlement, mm
0 5 10 15 20 25 30
Dyn5m clay MC u(A) 0
Fleming-pulse-Clay_0

(a)

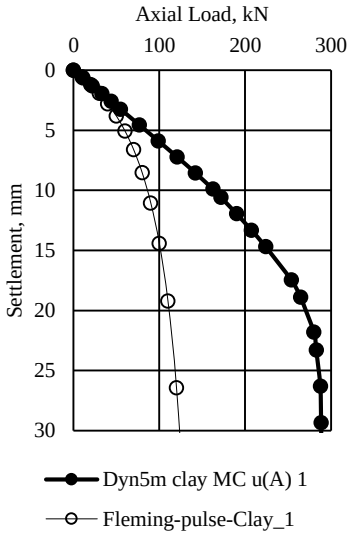
Axial Load, kN
0 100 200 300
Settlement, mm
0 5 10 15 20 25 30
Dyn5m clay MC u(A) 1
Fleming-pulse-Clay_1

(b)

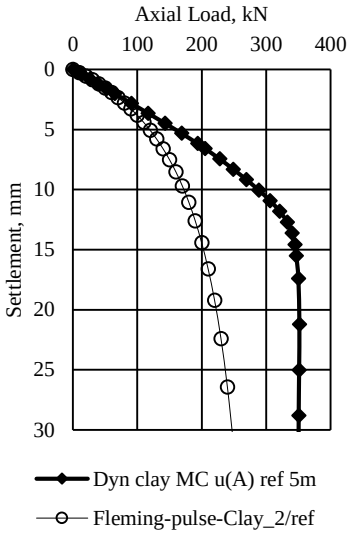
Axial Load, kN
0 100 200 300 400
Settlement, mm
0 5 10 15 20 25 30
Dyn clay MC u(A) ref 5m
Fleming-pulse-Clay_2/ref

(c)

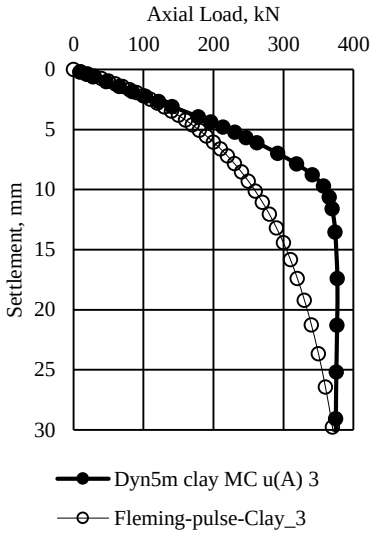
Axial Load, kN
0 100 200 300 400
Settlement, mm
0 5 10 15 20 25 30
Dyn5m clay MC u(A) 3
Fleming-pulse-Clay_3

(d)

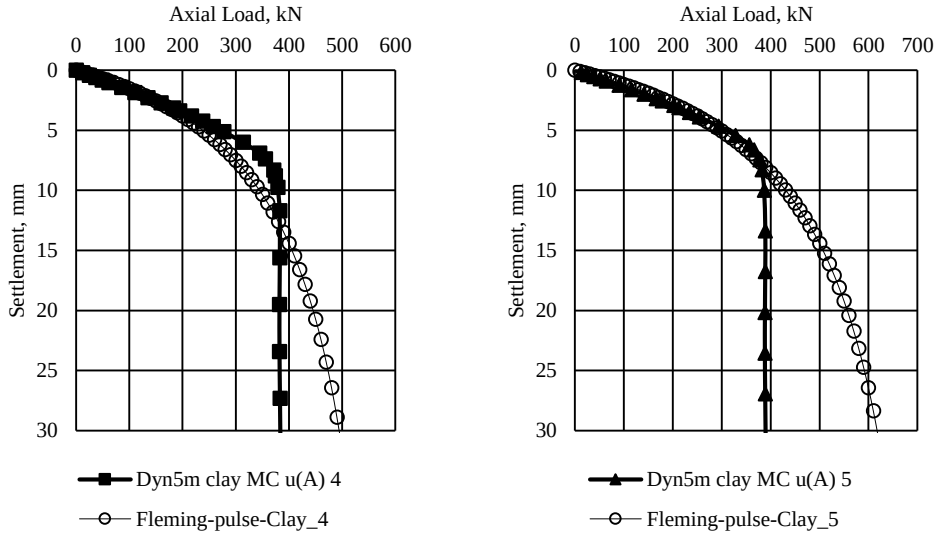

(e) **(f)**

Figure 9-19 – Load settlement curves: Pulse pile performance in fine grained soils by Fleming method (*Ms*=0.025) and calculated in Plaxis: (a) soil case 0, (b) soil case 1, (c) soil case 2/ref, (d) soil case 3, (e) soil case 4, (f) soil case 5